Issue 2 2024 | Volume 20

The Journal on Advanced Studies in Theoretical and Experimental Physics, including Related Themes from Mathematics

PROGRESS IN PHYSICS

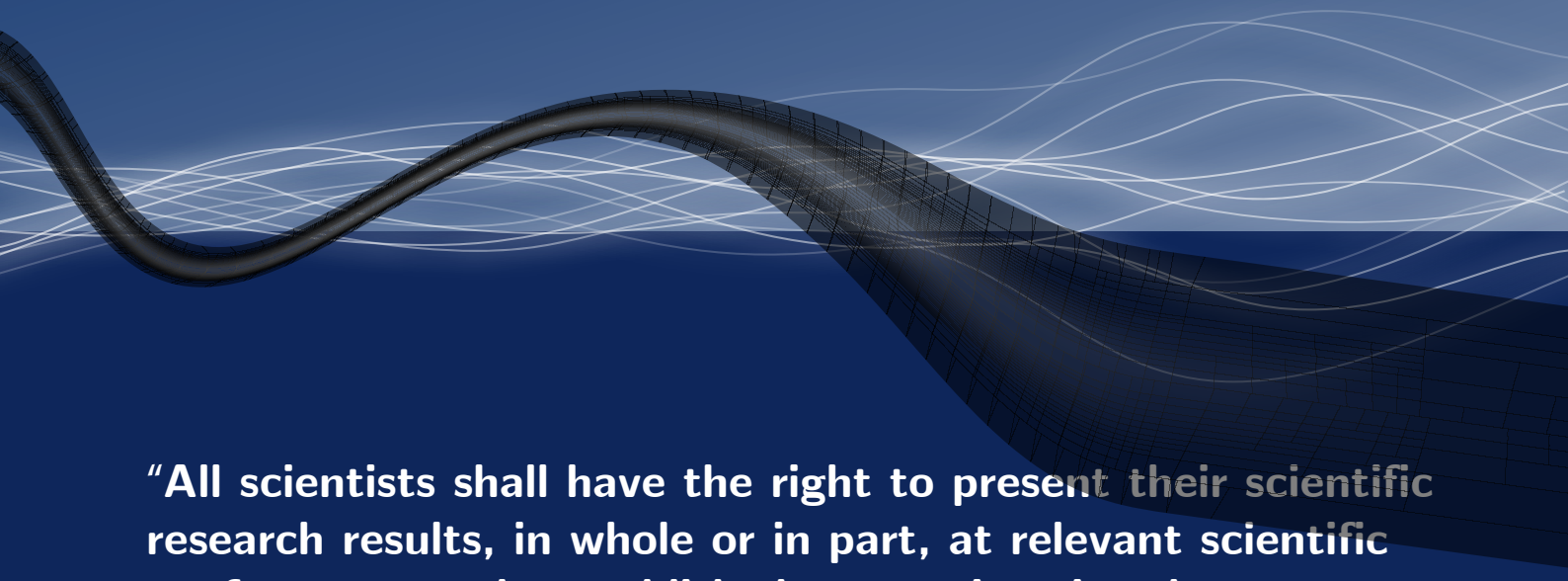

"All scientists shall have the right to present their scientific research results, in whole or in part, at relevant scientific conferences, and to publish the same in printed scientific journals, electronic archives, and any other media." — Declaration of Academic Freedom, Article 8

ISSN 1555-5534

PROGRESS IN PHYSICS

A Scientific Journal on Advanced Studies in Theoretical and Experimental Physics, including Related Themes from Mathematics. This journal is registered with the Library of Congress (DC, USA).

Electronic version of this journal:
https://www.progress-in-physics.com

Postal Address

Department of Mathematics and Science,
University of New Mexico,
705 Gurley Ave., Gallup, NM 87301, USA

ISSN: 1555-5534 (print)
ISSN: 1555-5615 (online)

Standard Address Number: 297-5092
Printed in the United States of America

December 2024 **Vol. 20, Issue 2**

CONTENTS

Information for Authors

Progress in Physics has been created for rapid publications on advanced studies in theoretical and experimental physics, including related themes from mathematics and astronomy. All submitted papers should be professional, in good English, containing a brief review of a problem and obtained results.

All submissions should be designed in LaTeX format using *Progress in Physics* template. This template can be downloaded from *Progress in Physics* home page http://www.ptep-online.com

Preliminary, authors may submit papers in PDF format. If the paper is accepted, authors can manage LaTeXtyping. Do not send MS Word documents, please: we do not use this software, so unable to read this file format. Incorrectly formatted papers (i.e. not LaTeXwith the template) will not be accepted for publication. Those authors who are unable to prepare their submissions in LaTeXformat can apply to a third-party payable service for LaTeX typing. Our personnel work voluntarily. Authors must assist by conforming to this policy, to make the publication process as easy and fast as possible.

Abstract and the necessary information about author(s) should be included into the papers. To submit a paper, mail the file(s) to the Editor-in-Chief.

All submitted papers should be as brief as possible. Short articles are preferable. Large papers can also be considered. Letters related to the publications in the journal or to the events among the science community can be applied to the section *Letters to Progress in Physics*.

All that has been accepted for the online issue of *Progress in Physics* is printed in the paper version of the journal. To order printed issues, contact the Editors.

Authors retain their rights to use their papers published in *Progress in Physics* as a whole or any part of it in any other publications and in any way they see fit. This copyright agreement shall remain valid even if the authors transfer copyright of their published papers to another party.

Electronic copies of all papers published in *Progress in Physics* are available for free download, copying, and re-distribution, according to the copyright agreement printed on the titlepage of each issue of the journal. This copyright agreement follows the *Budapest Open Initiative* and the *Creative Commons Attribution-Noncommercial-No Derivative Works 2.5 License* declaring that electronic copies of such books and journals should always be accessed for reading, download, and copying for any person, and free of charge.

Consideration and review process does not require any payment from the side of the submitters. Nevertheless the authors of accepted papers are requested to pay the page charges. *Progress in Physics* is a non-profit/academic journal: money collected from the authors cover the cost of printing and distribution of the annual volumes of the journal along the major academic/university libraries of the world. (Look for the current author fee in the online version of *Progress in Physics*.)

Galileo's Principle and the Origin of Gravitation According to General Relativity

Larissa Borissova and Dmitri Rabounski

Puschino, Moscow Region, Russia
E-mail: rabounski@yahoo.com, lborissova@yahoo.com

Using the chronometrically invariant notation of General Relativity (chronometric invariants are the physically observable projections of four-dimensional quantities onto the time line and the three-dimensional space of an observer), we deduce Galileo's principle and Newton's law of gravitation as a particular case of the chr.inv.-formula for the gravitational inertial force acting in the four-dimensional pseudo-Riemannian space (space-time of General Relativity). This is a "mathematical bridge", connecting the empirical laws of Newton's theory of gravitation with the purely geometric laws of General Relativity. We also show that the origin of the gravitational field in the space of the Schwarzschild mass-point metric is a spherical surface that surrounds any mass-point at a very small radius, equal to the gravitational radius calculated for the mass. There, on the spherical surface, a breaking of the three-dimensional observable space takes place, and the observer's physical observable time stops. It is not possible to get these results using the general covariant notation of General Relativity, because physically observable quantities in the general covariant notation are not mathematically defined.

We dedicate this article to Prof. Kyril Stanyukovich (1916–1989), our long friendly conversations with whom in the 1980s formed the basis of this study 40 years later and prompted us to write this article.

1 Problem statement

Our closest colleague, patron and friend over decades was Prof. Kyril Stanyukovich (1916–1989). In addition to his groundbreaking works on gas dynamics and super-powerful non-nuclear ammunition, he was also a prominent researcher in the field of General Relativity; see [1–4] and References therein. Over many years in the 1980s, he repeatedly focused our attention onto a still unsolved problem: in the framework of Riemannian geometry (which is the basis of General Relativity), the fundamental laws of Newtonian classical mechanics have not yet been mathematically deduced as an unambiguous special case of the purely geometric laws of General Relativity.

This problem was also pointed out earlier by Alexei Petrov (1910–1972), the outstanding scientist in the field of General Relativity, who in 1950 introduced an algebraic classification of the spaces (and the gravitational fields) known in the framework of General Relativity [5–8]. This classification is called the Petrov classification of Einstein spaces thanks to his monograph *Einstein Spaces* [7], first published in 1961.

In our personal opinion, the fundamental laws of Newtonian classical mechanics have not yet been deduced as a special case of the geometric laws of General Relativity only because the researchers, who worked on this problem earlier, used the *general covariant notation* of General Relativity. In the framework of the general covariant notation, physically observable quantities are not mathematically determined. As a result, there is no clear mathematical transition from the four-dimensional quantities of General Relativity to the three-dimensional quantities of Newton's theory, which are measurable in experiment.

In this paper, we will solve the mentioned problem using the *chronometrically invariant notation* of General Relativity, i.e., the mathematical apparatus of chronometric invariants, which are mathematically determined as physically observable quantities in the four-dimensional pseudo-Riemannian space (space-time). To do this, we compare the mathematical basis of Newton's theory of gravitation with the mathematical basis of General Relativity. This comparison will allow us to consider the fundamental laws of Newton's theory as the three-dimensional spatial projections of the four-dimensional (space-time) laws of General Relativity.

2 The mathematical basis of Newton's theory of gravitation and that of Einstein's theory of relativity

It is well known that Newton's theory of gravitation and Einstein's theory of relativity are based on different mathematical foundations. The bases of both theories are sets, each of which has its own method of measuring infinitely small distances ds between its elements (points). Such sets are called *metric spaces*, and the quantity ds^2 is called the *space metric*. Metric spaces play a huge rôle in topology, geometry, and in the sections of theoretical physics where we study the structure of space and time.

Newton's fundamental laws, including the Law of Universal Gravitation, are formulated in the framework of the three-dimensional flat, homogeneous and isotropic (Euclidean) space E_3. Such a space allows the existence of *inertial reference frames*: in an inertial reference frame, free bodies

either travel uniformly and rectilinearly or are at rest relative to the observer. In any inertial reference frame, time is homogeneous, and space is homogeneous and isotropic. The homogeneity of time means uniformity of its pace. The homogeneity of a space means the equality of all its points, and the isotropy of a space means the equality of all directions in it. The homogeneity and isotropy of space follow from Newton's first law (the law of inertia), which says: "if in the region, where inertial reference frames exist, no forces act on a body, or all forces acting on the body balance each other, then the body is either at rest or travels rectilinearly and uniformly".

In a three-dimensional flat space E_3 (Euclidean space), the square of the length of an elementary three-dimensional interval ds, characterizing the distance between two infinitely close points of the space, in the Cartesian coordinates x, y, z has the form

$$ds^2 = dx^2 + dy^2 + dz^2, \tag{1}$$

where the numerical value of ds^2 can only be *positive* and, hence, the three-dimensional interval ds is always a *substantional quantity*. The metric (1) is called *positive definite*, and the space E_3 described by it is *properly Euclidean*. Here the word "properly" means that all basis vectors of E_3 have substantional lengths. The three-dimensional curvature of the space E_3 is zero. For this reason, the space E_3 is flat. The condition $ds^2 = 0$ is satisfied only in the coordinate origin $x = y = z = 0$.

The laws of Newtonian classical mechanics, including Newton's law of gravitation, are formulated in the framework of a flat three-dimensional (Euclidean) space E_3.

Einstein's theory of relativity was created to describe space and time as a single entity, which is "space-time". The necessary prerequisites for Einstein's theory were obtained in the works of several other scientists, mainly in the works authored by Hermann Minkowski and Henri Poincaré. The basis of the theory is the four-dimensional curved pseudo-Riemannian space V_4. The prefix "pseudo" in this case indicates the fundamental difference between the mathematical basis of Newton's theory and the mathematical basis of Einstein's theory: this prefix means that one coordinate basis vector (time basis vector) has an imaginary length, and three other three-dimensional (spatial) basis vectors have substantional lengths (or vice versa, which is the same).

Initially, Einstein created the Special Theory of Relativity, the mathematical basis of which is the flat four-dimensional pseudo-Euclidean space E_4, later called the *Minkowski space*. The Minkowski space is a simplest particular case of four-dimensional pseudo-Riemannian spaces, which is homogeneous and isotropic, while its four-dimensional curvature is zero: the three-dimensional subspace of the Minkowski space may be non-uniform and anisotropic in one reference frame, but these factors in the Minkowski space depend on the observer's reference frame and, therefore, they can be reduced to zero simply by choosing another different reference frame. Bodies that are not affected by external forces travel uniformly and rectilinearly in the Minkowski space.

The Minkowski space is described by the metric

$$ds^2 = -(dx^0)^2 + (dx^1)^2 + (dx^2)^2 + (dx^3)^2, \tag{2}$$

where $x^0 = ct$ is the time coordinate, in which c is the velocity of light, t is the ideal (uniform) coordinate time, and $x^1 = x$, $x^2 = y$, $x^3 = z$ are the Cartesian three-dimensional (spatial) coordinates. In this notation, each of the three-dimensional spatial basis vectors e^i (where $i = 1, 2, 3$) has a substantional unit length, and the time basis vector e^0 has an imaginary unit length $(e^0)^2 = -1$ or vice versa, depending on the choice for the space signature $(-+++)$ as in (2) above or $(+---)$ as is most commonly used in General Relativity.

The basic space (space-time) of the General Theory of Relativity is the curved four-dimensional pseudo-Riemannian space V_4 — the generalization of the flat four-dimensional pseudo-Euclidean (Minkowski) space E_4, which can be inhomogeneous, anisotropic, etc. per se, i.e., independently of the choice of the observer's reference frame. The laws of General Relativity are formulated in the framework of the curved four-dimensional pseudo-Riemannian space V_4.

The square of the elementary distance ds between two infinitely close points (i.e., the space metric) in V_4 is expressed as follows

$$\begin{aligned} ds^2 &= g_{\alpha\beta}\, dx^\alpha dx^\beta = \\ &= g_{00}\, dx^0 dx^0 + 2\, g_{0i}\, dx^0 dx^i + g_{ik}\, dx^i dx^k, \end{aligned} \tag{3}$$

where $\alpha, \beta = 0, 1, 2, 3$ are the space-time (four-dimensional) indices, $i, k = 1, 2, 3$ are the spatial (three-dimensional) indices, and $g_{\alpha\beta}$ is the fundamental metric tensor of the space (it is a symmetric tensor, i.e., $g_{\alpha\beta} = g_{\beta\alpha}$). In the pseudo-Riemannian space, the time basis vector e^0 has the length dependent on the gravitational field potential, and the lengths of the three-dimensional spatial basis vectors e^i depend on the inhomogeneity and anisotropy of space, i.e., they are not unit length vectors, in contrast to the four-dimensional pseudo-Euclidean (Minkowski) space. The factors that deviate the lengths of the space basis vectors from unit are determined by the components of the fundamental metric tensor $g_{\alpha\beta}$ (while in the Minkowski space we can always find an inertial reference frame, in which the diagonal components of $g_{\alpha\beta}$ are units, and its non-diagonal components are zero). The time component g_{00} characterizes the gravitational field potential, the spatial components g_{ik} characterize the inhomogeneity and anisotropy of the observer's three-dimensional space, and the mixed (space-time) components g_{0i} characterize the angle of inclination of his three-dimensional space to the lines of time (the spaces in which this inclination takes place are called *non-holonomic spaces*; see Section 3, where we explain the basics of the theory of physically observable quantities in the space-time of General Relativity). In particular,

the physically observable time of the observer depends on the magnitude of the gravitational potential at the place of observation, and also on the magnitude and direction of the rotation speed of his three-dimensional physical space (its inclination to the time line).

As a result of the aforementioned absolute factors of $g_{\alpha\beta}$, which cannot vanish by choosing an inertial reference frame in the pseudo-Riemannian space (in contrast to the pseudo-Euclidean space of Special Relativity), we formulate Newton's first law (the law of inertia) in General Relativity as follows: "a body can be at rest or travelling rectilinearly and uniformly only in the absence of the gravitational field, inhomegeneity and isotropy of space and its rotation (the latter means the absence of the inclination of the three-dimensional space to the time lines)".

3 Physically observable quantities in the space-time of General Relativity

Before comparing the mathematical foundations of Newton's theory of gravitation and Einstein's theory of relativity, we must explain the basics of the theory of physically observable quantities in the four-dimensional pseudo-Riemannian space (which are also known as the Zelmanov chronometric invariants).

This mathematical apparatus that uniquely determines physically observable quantities in the space-time of General Relativity was created in 1944 by Abraham Zelmanov [9–11], who was our teacher. In addition to Zelmanov's original publications, which were very concise, this mathematical apparatus was explained in detail by us in a special Chapter given in each of our three research monographs, originally published in 2001 [12, 13] and 2013 [14]. The most comprehensive survey of Zelmanov's mathematical apparatus was published by us in 2023, in the special paper [15], where we collected everything (or almost everything) that we know about this mathematical apparatus personally from Zelmanov and on the basis of our own research studies.

Over the past decades, the following problems of General Relativity have been solved using the mathematical apparatus of chronometric invariants:

— The theory of non-quantum teleportation in the space-time of General Relativity [12, 16, 17], the basics of which were first outlined in 2001 in our book [12] and then developed in all necessary details in 2022 [17];

— The theory of the direct and opposite flow of time, and also the three kinds of particles in the space-time of General Relativity, published in 2001, in the book [12];

— The theory of frozen/stopped light according to General Relativity, which explained the frozen light experiment (2000). This theory was first drafted in 2001, in the 1st edition of our book [12], then in 2011 published in all necessary details in our paper [18] and since 2012 added to all subsequent editions of the book [12];

— The cosmological mass-defect — a new effect of General Relativity, predicted in 2011 [19], according to which the observed masses of cosmic bodies depend on their distance from the observer if they are at cosmological large-scale distances from him (depending on the specific metric of space);

— The non-linear cosmological redshift, deduced in 2012 [20] for various space metrics, including the Friedmann expanding universe and the de Sitter static universe. Three short papers [21–23] were then focused on specific aspects of the obtained solutions, and a final analysis of those of them that are most suitable for explaining the non-linear cosmological redshift observed by astronomers was given in 2013, in the paper [24];

— The deflection of light rays and mass-bearing particles, and also the length stretching and time dilation in the field of a rotating body — these are three new effects of General Relativity, deduced in 2023 [25, 26];

— The condensed matter model of the Sun, created in the framework of General Relativity, according to which the space breaking in the gravitational field of the Sun meets the maximum concentration of the asteroids in the Asteroid belt. This study was first published in 2009–2010 [27, 28];

— The theory of the internal constitution of stars and the sources of stellar energy according to General Relativity, which was first published in 2013, in the book [14];

— The exact solutions, obtained in 2005 to the equations of deviating geodesics for solid-body and free-mass gravitational wave detectors [29, 30] (different from the approximate solutions presumed in 1961 by Joseph Weber). Since 2008, this study was added to all subsequent editions of our book [12]. The obtained solutions are based on the comprehensive theoretical study of gravitational waves performed during a decade in 1968–1978 [31–33];

— "Zitterbewegung" of travelling electrons, explained in 2023 by Pierre Millette [34] on the basis of the theory of spin-particles in General Relativity, published in 2001 [13, Chapter 4].

For a complete list of the published research studies performed using the mathematical apparatus of chronometric invariants as of January 2023, see Bibliography in our comprehensive paper on this subject [15].

In short, the essence of Zelmanov's mathematical apparatus of chronometric invariants (known also as the chronometrically invariant formalism) is as follows. Zelmanov unambiguously determined physically observable quantities in the space-time of General Relativity as the projections of four-dimensional tensor quantities onto the time line and the three-dimensional spatial section of the space-time, which are associated with an observer. Such projections remain invariant

throughout the three-dimensional spatial section associated with the observer (his observable three-dimensional physical space), i.e., they are "chrono-metric invariants" in the physical reference frame of the observer and depend on the physical and geometric properties of his space, such as the gravitational potential, rotation, curvature, etc., which are determined by the respective components of the fundamental metric tensor $g_{\alpha\beta}$ and their derivatives.

The "chronometrically invariant" projections of any four-dimensional tensor quantity onto the time line and the three-dimensional spatial section associated with an observer are calculated using the Zelmanov operators of projection, which take the physical and geometric properties of the observer's space into account (see our comprehensive survey [15] of the chronomerically invariant formalism for detail).

As a result, the square of the four-dimensional (space-time) interval $ds^2 = g_{\alpha\beta}\,dx^\alpha dx^\beta$, expressed with chronometrically invariant (physically observable) quantities, has the form

$$ds^2 = c^2 d\tau^2 - d\sigma^2, \tag{4}$$

where $d\tau$ is the chr.inv.-time interval (physically observable time interval), obtained as the chr.inv.-projection of the four-dimensional displacement vector dx^α onto the observer's time line

$$d\tau = \sqrt{g_{00}}\,dt - \frac{1}{c^2}\,v_i dx^i, \qquad \sqrt{g_{00}} = 1 - \frac{\mathrm{w}}{c^2}, \tag{5}$$

and $d\sigma^2$ is the square of the chr.inv.-spatial interval (physically observable three-dimensional spatial interval)

$$d\sigma^2 = h_{ik}\,dx^i dx^k, \tag{6}$$

created using the chr.inv.-metric three-dimensional tensor h_{ik}

$$h_{ik} = -g_{ik} + \frac{1}{c^2}\,v_i v_k, \qquad h^{ik} = -g^{ik}, \qquad h^i_k = \delta^i_k, \tag{7}$$

which is the chr.inv.-projection of the fundamental metric tensor $g_{\alpha\beta}$ onto the observer's three-dimensional space (the spatial section of the space-time, which is associated with him). So forth, w is the physically observable chr.inv.-potential of the gravitational field that fills the observer's space, and v_i is the three-dimensional vector of the linear velocity of rotation of the observer's space

$$\mathrm{w} = c^2\,(1 - \sqrt{g_{00}}), \qquad v_i = -\frac{c\,g_{0i}}{\sqrt{g_{00}}}, \tag{8}$$

dx^i is the elementary interval of the three-dimensional spatial coordinates ($i = 1, 2, 3$), and $\mathrm{v}^i = dx^i/d\tau$ is the chr.inv.-velocity vector (physically observable three-dimensional velocity), which is different from the three-dimensional coordinate velocity vector $u^i = dx^i/dt$.

If all g_{0i} of a four-dimensional (space-time) metric ds^2 are zero, then such space-time is *holonomic*. In this case the three-dimensional spatial section associated with the observer (his observed three-dimensional space) is everywhere orthogonal to the time lines $x^0 = ct = const$ that pierce it. If at least one of the components g_{0i} of the four-dimensional metric is different from zero, then such space-time is *non-holonomic*. In such a (non-holonomic) space-time, the observer's three-dimensional spatial section $x^0 = const$ is inclined to the time lines. In this case, at different points the observed three-dimensional space can be inclined to the time lines at different angles depending on the local geometric structure of the particular four-dimensional space-time.

The formula for the physically observable time interval $d\tau$ (5) can therefore be re-written as

$$d\tau = \left(1 - \frac{\mathrm{w} + v_i u^i}{c^2}\right) dt, \tag{9}$$

where $v_i u^i$ is the scalar product of the linear rotational velocity of the observer's space v_i and the three-dimensional coordinate velocity vector u^i

$$v_i u^i = |v_i|\,|u^i| \cos\,(v_i u^i), \tag{10}$$

which means that if the vectors v_i and u^i are orthogonal to each other, then their scalar product $v_i u^i = 0$. In this case, the rotation of the three-dimensional reference space does not contribute to the change in the observer's physically observable time τ. If the vectors v_i and u^i are inclined to each other, then their mutual orientation in space affects the physically observable time τ, as well as its direction to the future or to the past: in the case, where the vector of the linear rotational velocity of the observer's reference space v_i is inclined in the same direction as the velocity motion vector of his reference body u^i (i.e., $v_i u^i > 0$), the observer's physical time τ flows faster; in the case, where the vectors v_i and u^i are inclined in opposite directions ($v_i u^i < 0$), the observed time τ flows slower. This purely theoretical conclusion was confirmed by the Hafele and Keating experiment (1971, repeated in 2005), in which they compared the readings of atomic clocks installed on board a jet airplane flying along a parallel around the globe with the readings of atomic clocks left on the surface of the Earth [35–39]. Thus, it was proven that the observed time on our planet depends on the following physical factors: 1) the magnitude of the gravitational field potential at the place of observation; 2) the speed of the Earth's rotation around its own axis (diurnal rotation); 3) the speed of the observer's motion relative to the Earth's rotation. For detail, see our recent publication on this subject [26].

In the theory of chronometric invariants, there are physically observable (chronometrically invariant) analogues of the quantities known in Newtonian classical mechanics. This fact will help us to find a connexion between Newton's theory of gravitation and General Relativity.

So, the physical reference space of a real observer (which is his physical reference frame) is characterized by the following physically observable chr.inv.-quantities. These are

the chr.inv.-vector of the physically observable gravitational inertial force F_i acting in the observer's space, the first (gravitational) term of which is created by the gradient of the gravitational potential w and the second (inertial) term is created by the centrifugal force of inertia

$$F_i = \frac{1}{\sqrt{g_{00}}}\left(\frac{\partial \mathrm{w}}{\partial x^i} - \frac{\partial v_i}{\partial t}\right), \quad \sqrt{g_{00}} = 1 - \frac{\mathrm{w}}{c^2}, \qquad (11)$$

the antisymmetric chr.inv.-tensor A_{ik} of the physically observable three-dimensional angular velocity of rotation of the observer's space

$$A_{ik} = \frac{1}{2}\left(\frac{\partial v_k}{\partial x^i} - \frac{\partial v_i}{\partial x^k}\right) + \frac{1}{2c^2}\left(F_i v_k - F_k v_i\right), \qquad (12)$$

the symmetric chr.inv.-tensor D_{ik} of the physically observable deformation rate of the space

$$\left.\begin{aligned} D_{ik} &= \frac{1}{2}\frac{{}^{*}\partial h_{ik}}{\partial t}, & D^{ik} &= -\frac{1}{2}\frac{{}^{*}\partial h^{ik}}{\partial t} \\ D &= h^{ik}D_{ik} = \frac{{}^{*}\partial \ln\sqrt{h}}{\partial t}, & h &= \det \| h_{ik} \| \end{aligned}\right\}, \qquad (13)$$

the chr.inv.-Christoffel symbols of the 1st rank $\Delta_{jk,m}$ and the 2nd rank Δ^i_{nk} (they are the coefficients of the physically observable inhomogeneity of the observer's space)

$$\Delta^i_{nk} = h^{im}\Delta_{nk,m} = \frac{1}{2}\,h^{im}\left(\frac{{}^{*}\partial h_{nm}}{\partial x^k} + \frac{{}^{*}\partial h_{km}}{\partial x^n} - \frac{{}^{*}\partial h_{nk}}{\partial x^m}\right), \qquad (14)$$

and the physically observable chr.inv.-curvature of the observer's space, which is expressed with the chr.inv.-curvature tensor C_{lkij} that has all properties of the Riemann-Christoffel curvature tensor throughout the entire three-dimensional spatial section associated with the observer, whereas its subsequent contractions produce the chr.inv.-curvature scalar C

$$\begin{aligned} C_{lkij} &= \frac{1}{4}\left(H_{lkij} - H_{jkil} + H_{klji} - H_{iljk}\right) = \\ &= H_{lkij} - \frac{1}{2}\left(2A_{ki}D_{jl} + A_{ij}D_{kl} + A_{jk}D_{il} + \right. \\ &\qquad \left. + A_{kl}D_{ij} + A_{li}D_{jk}\right), \end{aligned} \qquad (15)$$

$$C_{lk} = C_{lki}^{\cdots i} = H_{lk} - \frac{1}{2}\left(A_{kj}D^j_l + A_{lj}D^j_k + A_{kl}D\right), \qquad (16)$$

$$C = h^{lk}C_{lk} = h^{lk}H_{lk}, \qquad (17)$$

where it is denoted, for brevity and a better association with the Riemann-Christoffel curvature tensor,

$$H_{lki}^{\cdots j} = \frac{{}^{*}\partial\Delta^j_{il}}{\partial x^k} - \frac{{}^{*}\partial\Delta^j_{kl}}{\partial x^i} + \Delta^m_{il}\Delta^j_{km} - \Delta^m_{kl}\Delta^j_{im}, \qquad (18)$$

and the operators

$$\frac{{}^{*}\partial}{\partial t} = \frac{1}{\sqrt{g_{00}}}\frac{\partial}{\partial t}, \qquad \frac{{}^{*}\partial}{\partial x^i} = \frac{\partial}{\partial x^i} + \frac{v_i}{c^2}\frac{{}^{*}\partial}{\partial t} \qquad (19)$$

are the chr.inv.-operators of derivation with respect to time t and the spatial coordinates x^i.

It should be noted that the physically observable chr.inv.-curvature of the observer's space is depended on not only the space inhomogeneity (Christoffel symbols), but also on the rotation A_{ik} and deformation D_{ik} of the space, and, therefore, does not vanish in the absence of the gravitational field.

Since the task here is to find a connexion between Einstein's theory of relativity and Newton's theory of gravitation, in which space-time is static (non-deforming) and flat, we will not consider the deformation and curvature of space (i.e., we will assume that $D_{ik} = 0$ and $C_{lkij} = 0$). In addition, if in this particular case the three-dimensional observable space does not rotate or if its rotation velocity does not depend on time, then the gravitational inertial force F_i depends only on the numerical value of the gravitational potential w and its spatial derivatives. We will therefore consider this particular case in the next Section to deduce Galileo's principle and Newton's law of gravitation as consequences of the purely geometric laws of General Relativity.

4 Galileo's principle and Newton's law of gravitation in the framework of General Relativity

According to the biography of Galileo, in 1589 he conducted his famous experiments with bodies falling from the Leaning Tower of Pisa to the surface of the Earth. Galileo wanted to prove his case in a correspondence dispute with Aristotle, who, in turn, about 2000 years before Galileo, in 360–330 B.C., argued that the motion speed of falling bodies depends on the magnitude of their masses: he argued the greater the mass of a falling body, the faster it falls down.

In contrast to Aristotle, Galileo made a supposition that the fall time of bodies does not depend on their masses. In support of his hypothesis, Galileo dropped down balls of different masses from the Leaning Tower of Pisa. With this experiment, Galileo established that bodies of different masses, dropped down to the surface of the Earth simultaneously from the same altitude above the Earth's surface, access the ground simultaneously. Since the Tower's height h is much less than the radius of the Earth ($h \ll R_\oplus$), it can be assumed that any body located at a small altitude above the Earth's surface is attracted to the centre of the Earth with a force proportional to the numerical value of the body's mass. In fact, Galileo had discovered that the fall time of the body does not depend on the numerical value of its mass. Therefore, he had arrived at the conclusion that is now called *Galileo's principle*:

> All bodies, regardless of the numerical values of their masses, fall to the surface of the Earth with the same acceleration, called the *free-fall acceleration*.

Later, in 1666, Isaac Newton formulated the Law of Universal Gravitation. According to this law, the force of attraction F between two material points with masses m_1 and m_2, located at a distance r from each other, acts along the line

connecting their centres. This force is formulated as

$$F = -\frac{Gm_1m_2}{r^2}, \tag{20}$$

where $G = 6.67\times10^{-8}$ cm^3/gram sec^2 is the Newton gravitational constant. From the above formula (20) it follows that in a flat (Euclidean) space E_3 the gravitational force of attraction F is determined only by the numerical values of the interacting masses and the distance between them, and does not depend on the size of the bodies. Such an interaction is called *point interaction*. Thus, in Newton's theory of gravitation, the gravitational interaction between two bodies is "point-like", i.e., it is carried out between the gravitating centres of these bodies (material points).

Applying (20) to the gravitational interaction between the Earth and a body of mass m falling to the Earth's surface, we obtain

$$F = -\frac{GmM_\oplus}{R_\oplus^2} = -mg, \tag{21}$$

where $g = GM_\oplus/R_\oplus^2$ is the free-fall acceleration due to the Earth's gravitation, $M_\oplus = 5.97\times10^{27}$ gram is the mass of the Earth, $R_\oplus = 6.37\times10^8$ cm is the radius of the Earth, and m is the mass of the body falling down to the Earth's surface. Formula (4.2) explains the results of Galileo's experiments under the condition that the bodies fall on the surface of the Earth from a small altitude $h \ll R_\oplus$. In this case, it is easy to calculate the magnitude of the free-fall acceleration on the Earth's surface: $g = 981$ cm/sec^2.

Formula (21) is the mathematical expression of Galileo's principle in the framework of Newton's theory of gravitation.

Let us now deduce Galileo's principle and Newton's law of gravitation in the framework of the four-dimensional space (space-time) of General Relativity. To do this, we consider Schwarzschild's mass-point metric. This metric is an exact solution of Einstein's field equations, which describes a spherically symmetric gravitational field created in an empty space (space-time) by a spherical island of substance, the mass of which is M, and which is approximated by a mass-point. The Schwarzschild mass-point metric in the spherical coordinates r, θ, φ has the form

$$ds^2 = \left(1-\frac{r_g}{r}\right)c^2dt^2 - \frac{dr^2}{1-\frac{r_g}{r}} - r^2\left(d\theta^2+\sin^2\theta d\varphi^2\right), \tag{22}$$

where $r_g = 2GM/c^2$ is the so-called *gravitational radius* calculated here for a spherical body of the mass M (which we approximate by a mass-point). The polar coordinate angle θ is measured from the North pole to the equator.

Since, according to the chronometrcally invariant formalism, the component g_{00} in a general case is expressed with the gravitational field potential w as

$$g_{00} = \left(1-\frac{\mathrm{w}}{c^2}\right)^2, \tag{23}$$

and according to the Schwarzschild mass-point metric (22) we have

$$g_{00} = 1-\frac{r_g}{r}, \tag{24}$$

then in the space of the Schwarzschild mass-point metric the gravitational field potential $\mathrm{w} = c^2(1-\sqrt{g_{00}})$ has the form

$$\mathrm{w} = c^2\left(1-\sqrt{1-\frac{r_g}{r}}\right) = c^2\left(1-\sqrt{1-\frac{2GM}{c^2r}}\right), \tag{25}$$

which in the quasi-Newtonian approximation ($r_g \ll r$), where the ratio r_g/r takes small numerical values and, therefore,

$$\sqrt{1-\frac{2GM}{c^2r}} \simeq 1-\frac{GM}{c^2r}, \tag{26}$$

takes the form

$$\mathrm{w} = c^2\left(1-\sqrt{1-\frac{2GM}{c^2r}}\right) \simeq \frac{GM}{r}, \tag{27}$$

which coincides with the gravitational field potential according to Newton's theory of gravitation.

So forth, looking at the Schwarzschild mass-point metric (22), we realize that it is static, since all components of its fundamental metric tensor $g_{\alpha\beta}$ do not depend on the time coordinate $x^0 = ct$. This means that the space of the Schwarzschild mass-point metric does not deform ($D_{ik} = 0$). In addition, since all space-time components of the fundamental metric tensor of the metric are zero ($g_{0i} = 0$), such a space does not rotate ($v_i = 0$, $A_{ik} = 0$). As a result of the above, the physically observable time interval $d\tau$ in the Schwarzschild mass-point field has the form

$$d\tau = \sqrt{g_{00}}\,dt - \frac{1}{c^2}v_i\,dx^i = \sqrt{g_{00}}\,dt = \left(1-\frac{\mathrm{w}}{c^2}\right)dt = \\ = \sqrt{1-\frac{r_g}{r}}\,dt = \sqrt{1-\frac{2GM}{c^2r}}\,dt, \tag{28}$$

which means that the flow of the physically observable time τ in the Schwarzschild mass-point field is determined only by the numerical value of the gravitational field potential w.

Since the space of the Schwarzschild mass-point metric is static ($D_{ik} = 0$) and does not rotate ($v_i = 0$, $A_{ik} = 0$), the components of the chr.inv.-vector of the physically observable gravitational inertial force F_i (11) that acts on a unit mass in such a space take the form

$$F_1 = \frac{1}{\sqrt{g_{00}}}\frac{\partial \mathrm{w}}{\partial r}, \quad F_2 = 0, \quad F_3 = 0, \tag{29}$$

where $\mathrm{w} = c^2(1-\sqrt{g_{00}})$ is the gravitational field potential. Therefore, in terms of the gravitational radius $r_g = 2GM/c^2$ calculated for the mass M, the solely non-zero component of the physically observable gravitational inertial force acting in

the space of the Schwarzschild mass-point metric is

$$F_1 = -\frac{c^2}{2g_{00}}\frac{\partial g_{00}}{\partial r} = -\frac{c^2}{2\left(1-\frac{r_g}{r}\right)}\frac{r_g}{r^2}. \qquad (30)$$

Apply the obtained formula (30) to a body having a mass m (different from unit mass) and located on the Earth's surface ($r = R_\oplus$) or at a small altitude h above it ($h \ll R_\oplus$). Since the radius of the Earth is $R_\oplus = 6.37\times10^8$ cm, and its gravitational radius is $r_g = 0.89$ cm, the ratio $r_g/R_\oplus$ on the Earth's surface takes a very small numerical value $r_g/R_\oplus = 1.4\times10^{-9}$ that can be neglected. In this case, the formula for the gravitational force F_1 (30), which we have obtained in the framework of General Relativity, takes the following form

$$\Phi_1 = mF_1 = -\frac{c^2}{2\left(1-\frac{r_g}{r}\right)}\frac{mr_g}{r^2} = -\frac{GmM_\oplus}{R_\oplus^2} = -mg, \quad (31)$$

which coincides with the formula (21), which, in turn, is the mathematical expression of Galileo's principle in the framework of Newton's theory of gravitation.

This means that, according to General Relativity, all bodies located on the surface of the Earth or at a small altitude above it are attracted to the centre of the Earth with the same acceleration, equal to the free-fall acceleration $g = GM_\oplus/R_\oplus^2$ = 981 cm/sec^2 (which is a conclusion, analogous to Galileo's principle in Newton's theory of gravitation).

In fact, using the chronometrically invariant notation of General Relativity, we have just deduced the following:

> Both Galileo's principle and Newton's law of gravitation (empirical laws of classical mechanics) are direct consequences of the geometric structure of the four-dimensional pseudo-Riemannian space (space-time of General Relativity), since the force of gravity, which attracts material bodies to the Earth, is the chr.inv.-vector of the physically observable gravitational inertial force acting in the space (gravitational field) of the Schwarzschild mass-point metric.

This cannot be shown using the general covariant notation of General Relativity, because it does not include physical observable quantities. This is why there is no unambiguous mathematical transition from General Relativity to Newton's theory of gravitation in the framework of the general covariant notation of General Relativity.

5 The origin of the gravitational field according to General Relativity

Let us now consider the origin of gravitation using the chronometrically invariant notation of General Relativity.

In the space of the Schwarzschild mass-point metric, on a spherical surface of the radius $r = r_g$ from the coordinate origin (which is the centre of the gravitating body approximated by a mass-point), the time component g_{00} of the fundamental metric tensor is zero ($g_{00} = 0$), and the radial component g_{11} becomes infinitely large ($g_{11} \to \infty$)

$$r = r_g, \quad g_{00} = 1 - \frac{r_g}{r} = 0, \quad g_{11} = \frac{1}{1-\frac{r_g}{r}} \to \infty, \qquad (32)$$

and, since the Schwarzschild space does not rotate ($v_i = 0$), hence the radial component h_{11} of the chr.inv.-metric tensor $h_{ik} = -g_{ik} + \frac{1}{c^2}v_iv_k$ becomes also infinite ($h_{11} \to -\infty$).

This means that on the spherical surface $r = r_g$ that surrounds any mass-point (located at the coordinate origin in the space of the Schwarzschild mass-point metric) the following conditions take place:

1) The three-dimensional observable space (and the gravitational field of the mass-point, which fills the space) has a space breaking ($g_{11} \to \infty$, $h_{11} \to -\infty$);
2) The physically observable time τ of the observer stops ($d\tau = 0$) on this surface

$$d\tau = \sqrt{g_{00}}\,dt - \frac{1}{c^2}v_i dx^i = \sqrt{g_{00}}\,dt = 0. \qquad (33)$$

That is, there on the surface of the gravitational radius $r = r_g$, which surrounds the centre of gravity inside any material body, the physically observable time stops ($d\tau = 0$), and the observable three-dimensional space is expanded infinitely in the radial direction $x^1 = r$ since the three-dimensional physically observable chr.inv.-interval $d\sigma$ that is determined as $d\sigma^2 = h_{ik}\,dx^i dx^k$ (6) on such a surface is

$$d\sigma = \sqrt{h_{11}\,x^1x^1} = \frac{dr}{\sqrt{1-\frac{r_g}{r}}} \to \infty. \qquad (34)$$

Equating $d\tau$ in the Schwarzschild mass-point field, which is $d\tau = \left(1-\frac{\mathrm{w}}{c^2}\right)dt$ (28), to zero (since $d\tau = 0$ on the surface of the gravitational radius), we obtain

$$E = M\mathrm{w} = Mc^2, \qquad (35)$$

i.e., the energy $E = M\mathrm{w}$ of the gravitational field, created by a body having a non-unit mass M, on the surface of the gravitational radius $r = r_g$ (which surrounds the centre of gravity inside any material body) is the same as the total energy of the body $E = Mc^2$.

We therefore arrive at the following conclusion:

> The gravitational field of any body is originated in the surface of the gravitational radius $r = r_g$, which is surrounding the centre of gravity inside the body.

This is the origin of the gravitational field according to General Relativity. Since the gravitational radius of an ordinary body is incomparably smaller than its physical radius, the conclusion we have obtained in the framework of General Relativity is completely consistent with Newton's theory of gravitation, according to which the gravitational field of any

body is originated in its center of gravity (which coincides with its geometric center in the case, where the body has a spherically symmetrical shape).

For example, the surface of the gravitational radius, which is surrounding the centre of gravity of the planet Earth, is the origin of the Earth's gravitational field attracting to this surface near the centre of the planet everything that is underground, grows on the Earth's surface, moves along it and above it (in the Earth's atmosphere and in the cosmos). Trees indicate this fact: their trunks are always directed from the centre of the Earth, and not at an angle to this direction. This is especially clearly seen in cases, where the ground on which the tree grows lies at an angle to a flat surface, for example, on a mountain slope: in this case, the tree does not grow perpendicular to the slope, but its trunk is oriented strictly in the direction from the centre of the Earth.

From the above conclusion about the origin of the gravitational field it also follows that a *collapse surface* (in terms of General Relativity, this is a surface on which $g_{00} = 0$ and, as a result, the physically observable time stops $d\tau = 0$) is not exclusively the surface of a black hole (gravitational collapsar) — a body, the substance of which is compressed to such a super-dense state that it is concentrated under its gravitational radius. Indeed, ordinary bodies are not in the state of gravitational collapse, since almost all mass of an ordinary body is located above its gravitational radius (which is very small compared to its physical radius). However, the tiny sphere of the gravitational radius that takes place at the centre of every ordinary body is also a *collapse surface*, because the physically observable time stops and the spatial metric has a breaking on this tiny sphere, just like on the surface of a black hole (gravitational collapsar).

The same conclusion about the origin of the gravitational field follows from the geodesic equations (equations of motion of free particles) in the space of the Schwarzschild mass-point metric. "Free" here means that the moving particle is affected only by the forces, the source of which is the geometric structure of the space itself (i.e., in the absence of extraneous fields).

The geodesic equations in the chronometrically invariant notation are a system of the chr.inv.-projections onto the time line (the chr.inv.-scalar projection) and onto the three-dimensional space (the chr.inv.-vector projection) associated with a particular observer. They have the following form (see References to the Zelmanov chronometric invariants)

$$\frac{dm}{d\tau} - \frac{m}{c^2} F_i \mathrm{v}^i + \frac{m}{c^2} D_{ik} \mathrm{v}^i \mathrm{v}^k = 0 , \tag{36}$$

$$\frac{d(m\mathrm{v}^i)}{d\tau} - mF^i + 2m\left(D^i_k + A^{i\cdot}_{\cdot k}\right)\mathrm{v}^k + m\Delta^i_{nk}\mathrm{v}^n\mathrm{v}^k = 0 , \tag{37}$$

where m is the relativistic mass of the particle, τ is the physically observable time of its motion, $\mathrm{v}^i = dx^i/d\tau$ is its physically observable chr.inv.-velocity, F_i is the chr.inv.-vector of the gravitational inertial force, A_{ik} is the chr.inv.-tensor of the angular velocity of rotation of the observer's space, D_{ik} is the chr.inv.-tensor of the rate of its deformation, and Δ^i_{nk} are the chr.inv.-Christoffel symbols of the 2nd rank (which are the coefficients of the physically observable inhomogeneity of the observer's space).

The chr.inv.-geodesic equations (36, 37) are simplified in the space of the Schwarzschild mass-point metric

$$\frac{dm}{d\tau} - \frac{m}{c^2} F_i \mathrm{v}^i = 0 , \tag{38}$$

$$\frac{d(m\mathrm{v}^i)}{d\tau} - mF^i + m\Delta^i_{nk}\mathrm{v}^n\mathrm{v}^k = 0 , \tag{39}$$

since such a space does not rotate or deform (see above). Here $\mathrm{v}^1 = dr/d\tau$, $\mathrm{v}^2 = d\theta/d\tau$, $\mathrm{v}^3 = d\varphi/d\tau$. In addition, only the radial component F_1 of the gravitational inertial force F_i is non-zero. According to (29), it is

$$F_1 = \frac{1}{\sqrt{g_{00}}}\frac{\partial \mathrm{w}}{\partial r} = \frac{c^2}{c^2 - \mathrm{w}}\frac{\partial \mathrm{w}}{\partial r} , \tag{40}$$

where $\mathrm{w} = c^2(1 - \sqrt{g_{00}})$ is the potential of the gravitational field (created by a massive body, approximated by a mass-point), in which the particle travels. Therefore, the scalar geodesic equation (38) takes the form

$$\frac{dm}{m} = \frac{1}{c^2} F_1 \, dr , \tag{41}$$

which can be re-written as

$$\frac{dm}{m} = -\frac{d(c^2 - \mathrm{w})}{c^2 - \mathrm{w}} , \tag{42}$$

which is the same as

$$d(\ln m) = -d\left[\ln(c^2 - \mathrm{w})\right] . \tag{43}$$

Integrating (43), we obtain the solution

$$mc^2 - m\mathrm{w} = C , \tag{44}$$

where C in the integration constant. Since $\mathrm{w} = c^2(1 - \sqrt{g_{00}})$, $g_{00} = 1 - r_g/r$, and $r_g = 2GM/c^2$, then $C = 0$ under the condition $g_{00} = 0$, which satisfies at the spherical surface of the gravitational radius $r = r_g$ (where $\mathrm{w} = c^2$).

From the obtained solution (44) we see that a particle of mass m, which travels in the gravitational field of a mass M, has a maximum energy $m\mathrm{w} = mc^2$ under the condition $g_{00} = 0$, which satisfies on the surface of the gravitational radius $r = r_g = 2GM/c^2$ from this mass-point (on which the physically observable time stops $d\tau = 0$, and the space and the gravitational field have a breaking $g_{11} = -h_{11} \to \infty$).

In particular, the above solution is applicable to the Earth, planets, the Sun, stars, galaxies and generally any bodies in the Universe.

In conclusion, we note that Riemannian spaces are non-degenerate by definition: the determinant $g = \det \| g_{\alpha\beta} \|$ of the fundamental metric tensor satisfies the condition $g < 0$. In addition, Zelmanov had obtained a relation connecting the determinants of the four-dimensional metric tensor $g_{\alpha\beta}$ and the three-dimensional chr.inv.-metric tensor h_{ik}

$$h = -\frac{g}{g_{00}}\,, \tag{45}$$

where $h = \det \| h_{ik} \|$, $g = \det \| g_{\alpha\beta} \|$, and g_{00} is the time component of the four-dimensional Riemannian metric.

These quantities in the space of the Schwarzschild mass-point metric (22) are

$$h = \frac{r^4 \sin^2\theta}{1 - \frac{r_g}{r}}\,, \quad g_{00} = 1 - \frac{r_g}{r}\,, \quad g = -\, r^4 \sin^2\theta\,. \tag{46}$$

From this we see that the numerical values of h and g depend on the location of the observer with respect to the polar coordinate θ (which is opposite to the geographic latitude, because it is measured from the North pole to the equator). At the North and South poles, where $\theta = 0^\circ$ and 180°, respectively, the space-time of the Schwarzschild mass-point metric is *completely degenerate*, since in this case $g = 0$. The observable three-dimensional space is also degenerate ($h = 0$) at the North and South poles. In addition, the radial component h_{11} becomes infinite over the entire surface of the gravitational radius $r = r_g$ that means a breaking in the space (and the gravitational field) on this surface.

It should be noted that the complete degeneration of the four-dimensional space-time and the three-dimensional observable space takes place in the Schwarzschild mass-point field not only on the spherical surface of the gravitational radius $r = r_g$ (around the centre of gravity of the mass-point), but also everywhere along the radial coordinate r directed to North and South. But even with a tiny deviation from the polar direction $\theta = 0^\circ$ or $\theta = 180^\circ$ (i.e., from the polar axis of the coordinate frame) the space is already non-degenerate.

The above conclusion means that the surface of the gravitational radius $r = r_g$ is not only the origin of the gravitational field of any body, which spreads outside and inside the surface, but is also the special space-time "membrane" separating the external space (gravitational field) of the body, where $r > r_g$, from its internal space (gravitational field), where $r < r_g$. Since both the space-time metric and the spatial metric are degenerate inside the "membrane", the space (space-time) inside the "membrane" is different from the ordinary pseudo-Riemannian space (space-time) and is a completely degenerate space-time.

6 Conclusion

So, using the chronometrically invariant notation of General Relativity (chronometric invariants are the physically observable projections of four-dimensional quantities onto the time line and the three-dimensional space of an observer), we have deduced Galileo's principle and Newton's law of gravitation as a particular case of the chr.inv.-formula for the gravitational inertial force acting in the four-dimensional pseudo-Riemannian space (space-time of General Relativity).

In fact, by doing this, we have created a "mathematical bridge", connecting Newton's theory of gravitation with General Relativity. This "mathematical bridge" is important for theoretical physics, since no one earlier than us had derived the empirical laws of Newton's theory of gravitation as a particular case of the purely geometric laws of General Relativity.

We have also showed that on the spherical surface that surrounds any mass-point at a very small radius, equal to the gravitational radius calculated for the mass, a space breaking takes place in the gravitational field of the mass-point (and in its three-dimensional observable space), and the observer's physical observable time stops. That is, the gravitational field of any mass-point extends both inward from the mentioned spherical surface to the coordinate origin (which coincides with the mass-point), and outward from the mentioned surface into the surrounding space to infinity, but is absent on the surface itself. This theoretical result leads us to the conclusion that the origin of the gravitational field in the space of the Schwarzschild mass-point metric is a spherical surface that surrounds any mass-point at the gravitational radius calculated for the mass.

The above results were obtained only thanks to the chronometrically invariant notation of General Relativity, which provides an unambiguous mathematical definition of physically observable quantities in the four-dimensional pseudo-Riemannian space (space-time). It would be impossible to get these results using the conventional general covariant notation of General Relativity, because physically observable quantities in the general covariant notation are not mathematically defined.

Submitted on July 21, 2024

References

1. Stanyukovich K. P. The gravitational field and elementary particles. Science Press, Moscow, 1965.
2. Stanyukovich K. On the problem of the existence of stable particles in the Metagalaxy. *The Abraham Zelmanov Journal*, 2008, v. 1, 99–110 (translated from *Problemy Teorii Gravitazii i Elementarnykh Chastiz*, v. 1, Atomizdat, Moscow, 1966, 267–279).
3. Stanyukovich K. On increasing entropy in an infinite universe. *The Abraham Zelmanov Journal*, 2008, v. 1, 111–117 (translated from the extended draft of the publication in *Doklady Akademii Nauk SSSR*, 1949, v. LXIX, no. 6, 793–796).
4. Stanyukovich K. On the evolution of the fundamental physical constants. *The Abraham Zelmanov Journal*, 2008, v. 1, 118–126 (translated from the presentation held on May 12, 1971, in Kiev, at the seminar on General Relativity maintained by Alexei Z. Petrov in the Institute of Theoretical Physics).
5. Petrov A.Z. On the spaces determining the gravitational fields. *Doklady Academii Nauk USSR*, 1951, v. XXXI, 149–152.

6. Petrov A. The classification of spaces determining the fields of gravitation. *The Abraham Zelmanov Journal*, 2008, v. 1, 81–98 (translated from *Uchenye Zapiski Kazanskogo Gosudarstvennogo Universiteta*, 1954, v. 114, book 8, 55–69).
7. Petrov A.Z. Einstein Spaces. Pergamon Press, Oxford, 1969 (translated from the 1st Russian edition, Moscow, 1961).
8. Rabounski D. Biography of Alexei Petrov (1910–1972). *The Abraham Zelmanov Journal*, 2008, v. 1, xxvii–xxix.
9. Zelmanov A. L. Chronometric Invariants. Translated from the 1944 PhD thesis, American Research Press, Rehoboth, New Mexico, 2006.
10. Zelmanov A. L. Chronometric invariants and accompanying frames of reference in the General Theory of Relativity. *Soviet Physics Doklady*, 1956, v. 1, 227–230 (translated from *Doklady Academii Nauk USSR*, 1956, v. 107, issue 6, 815–818).
11. Zelmanov A. L. On the relativistic theory of an anisotropic inhomogeneous universe. *The Abraham Zelmanov Journal*, 2008, vol. 1, 33–63 (translated from the thesis of the *6th Soviet Conference on the Problems of Cosmogony*, USSR Academy of Sciences Publishers, Moscow, 1957, 144–174).
12. Rabounski D. and Borissova L. Particles Here and Beyond the Mirror. The 4th revised edition, New Scientific Frontiers, London, 2023 (the 1st edition was issued in 2001).
Rabounski D. et Larissa Borissova L. Particules de l'Univers et au delà du miroir. La 2ème édition révisée en langue française, New Scientific Frontiers, Londres, 2023.
13. Borissova L. and Rabounski D. Fields, Vacuum, and the Mirror Universe. The 3rd revised edition, New Scientific Frontiers, London, 2023 (the 1st edition was issued in 2001).
Borissova L. et Rabounski D. Champs, Vide, et Univers miroir. La 2ème édition révisée en langue française, New Scientific Frontiers, Londres, 2023.
14. Borissova L. and Rabounski D. Inside Stars. The 3rd edition, revised and expanded, New Scientific Frontiers, London, 2023 (the 1st edition was issued in 2013).
15. Rabounski D. and Borissova L. Physical observables in General Relativity and the Zelmanov chronometric invariants. *Progress in Physics*, 2023, v. 19, issue 1, 3–29.
16. Borissova L. and Rabounski D. On the possibility of instant displacements in the space-time of General Relativity. *Progress in Physics*, 2005, v. 1, issue 1, 17–19.
17. Rabounski D. and Borissova L. Non-quantum teleportation in a rotating space with a strong electromagnetic field. *Progress in Physics*, 2022, v. 18, issue 1, 31–49.
18. Rabounski D. and Borissova L. A theory of frozen light according to General Relativity. *The Abraham Zelmanov Journal*, 2011, v. 4, 3–27.
19. Rabounski D. Cosmological mass-defect — a new effect of General Relativity. *The Abraham Zelmanov Journal*, 2011, v. 4, 137–161.
20. Rabounski D. Non-linear cosmological redshift: the exact theory according to General Relativity. *The Abraham Zelmanov Journal*, 2012, v. 5, 3–30.
21. Rabounski D. On the exact solution explaining the accelerate expanding Universe according to General Relativity. *Progress in Physics*, 2012, v. 8, issue 2, L1–L6.
22. Borissova L. and Rabounski D. Cosmological redshift in the de Sitter stationary Universe. *Progress in Physics*, 2018, v. 14, issue 1, 27–29.
23. Rabounski D. and Borissova L. On the lambda term in Einstein's equations and its influence on the cosmological redshift. *Progress in Physics*, 2024, v. 20, issue 2, 4–12.
24. Rabounski D. and Borissova L. Cosmological redshift: which cosmological model best explains it? *Progress in Physics*, 2024, v. 20, issue 2, 13–20.
25. Rabounski D. and Borissova L. Deflection of light rays and mass-bearing particles in the field of a rotating body. *Progress in Physics*, 2022, v. 18, issue 1, 50–55.
26. Rabounski D. and Borissova L. Length stretching and time dilation in the field of a rotating body. *Progress in Physics*, 2022, v. 18, issue 1, 62–65.
27. Borissova L. The gravitational field of a condensed matter model of the Sun: the space breaking meets the Asteroid strip. *The Abraham Zelmanov Journal*, 2009, v. 2, 224–260.
28. Borissova L. The Solar System according to General Relativity: the Sun's space breaking meets the Asteroid strip. *Progress in Physics*, 2010, v. 6, issue 2, 43–47.
29. Borissova L. Gravitational waves and gravitational inertial waves in the General Theory of Relativity: A theory and experiments. *Progress in Physics*, 2005, no. 2, 30–62.
30. Rabounski D. and Borissova L. Exact theory of a gravitational wave detector. New experiments proposed. *Progress in Physics*, 2006, v. 2, issue 2, 31–38.
31. Borissova L. B. Relative oscillations of test particles in comoving reference frames. *Soviet Physics Doklady*, 1976, v. 20, 816–819 (translated from *Doklady Acad. Nauk SSSR*, 1975, v. 225, no. 4, 786–789).
32. Borissova L. B. Quadrupole mass-detector in field of weak plane gravitational fields. *Russian Physics Journal*, 1978, v. 21, no. 10, 1341–1344 (translated from *Izvestiia Vysshikh Uchebnykh Zavedenii*, *Fizika*, 1978, no. 10, 109–114).
33. Borissova L. Gravitational waves and gravitational inertial waves according to the General Theory of Relativity. *The Abraham Zelmanov Journal*, 2010, v. 3, 25–70.
34. Millette P. A. Zitterbewegung and the non-holonomity of pseudo-Riemannian spacetime. *Progress in Physics*, 2023, v. 19, issue 1, 66–72.
35. Hafele J. Performance and results of portable clocks in aircraft. *PTTI 3rd Annual Meeting*, November 16–18, 1971, 261–288.
36. Hafele J. and Keating R. Around the world atomic clocks: predicted relativistic time gains. *Science*, July 14, 1972, v. 177, 166–168.
37. Hafele J. and Keating R. Around the world atomic clocks: observed relativistic time gains. *Science*, July 14, 1972, v. 177, 168–170.
38. Demonstrating relativity by flying atomic clocks. *Metromnia*, *the UK's National Measurement Laboratory Newsletter*, issue 18, Spring 2005.
39. Rabounski D. and Borissova L. In memoriam of Joseph C. Hafele (1933–2014). *Progress in Physics*, 2015, v. 11, issue 2, 136.

Introducing the Space Metric of a Rotating Massive Body and Four New Effects of General Relativity

Dmitri Rabounski
Puschino, Moscow Region, Russia. E-mail: rabounski@yahoo.com

This paper introduces and proves the space metric of a rotating spherical body (approximated by a mass-point). This is a new metric to General Relativity, which is an extension and replacement of Schwarzschild's mass-point metric (since all cosmic bodies rotate). Physically observable characteristics of such a space are calculated, including the curvature of space and others. It is shown that the curvature of such a space has two components: a component created by the gravitational field (it decreases with distance from the body) and a constant curvature component created by the rotation of space (it does not depend on distance). Using Einstein's equations, the Riemannian conditions are calculated under which the introduced metric is valid (with the conditions, the Einstein equations vanish). Four new effects of General Relativity are calculated: the deflection of light rays and mass-bearing particles near a rotating body, a length-stretching effect along the geographical longitudes, a time-loss effect in the clocks co-moving with the Earth's rotation (to the East) and a time increment when moving to the West.

1 Introduction

This is the fourth paper in the series of papers on the effects of the space curvature, caused by the rotation of space.

The first [1] of these studies, besides many other scientific results obtained in it, showed that the rotation of space makes it curved. Then, two subsequent studies [2, 3] predicted four new effects of General Relativity, the origin of which is the space curvature caused by the rotation of space.

The first two effects are the deflection of light rays and mass-bearing particles in the field of a rotating body [2].

When a body rotates, the space around it curves towards the direction of its rotation and the centre of the body (around which it rotates), thereby creating a "slope of the hill" descending "down" along the equator in the direction, in which the body rotates, and also to the centre of the body. Therefore, when a particle travels freely to a rotating body, it "rolls down" the slope of the space curvature along the equator in the direction, in which the body rotates, as well as to the centre of the body. As a result, the following two effects should occur in the field of a rotating body:

1. A particle travelling freely to a rotating body should be deflected slightly from its radial trajectory in the equatorial direction, in which the body rotates, i.e., along the geographical longitudes;
2. The particle should gain a small increase of its velocity, and its path should become physically "stretched" for a little, causing the particle to reach the body with a delay in time compared to if the body did not rotate.

That is, light rays and mass-bearing particles should be deflected near a rotating body due to the curvature of space caused by its rotation. These two effects should take place both for mass-bearing particles and for light rays (massless light-like particles such as photons).

The other two effects are the length stretching and time loss/gain, expected in the field of a rotating body due to the curvature of its space, caused by its rotation [3]:

3. Since the diurnal rotation of the Earth around its axis curves the Earth's space making it "stretched" along the geographical longitudes, then the measured length of a standard rod should be greater when the rod is installed in the longitudinal direction;
4. Due to the same reason, there should be a time loss on board an airplane flying to the East (the direction in which the Earth's space rotates), and also a time increment when flying in the opposite direction, to the West.

Both of the effects are maximum at the equator (where the curvature of the Earth's space caused by its rotation is maximum and, therefore, space is maximally "stretched") and decrease towards the North and South Poles.

The above four effects, namely — the deflection of light rays and mass-bearing particles in the field of a rotating body, and also the length stretching and time loss/gain in the field of a rotating body — are new fundamental effects of the General Theory of Relativity, which were predicted "au bout d'un stylo". These four effects can be considered as an addition to the well-known Einstein effect of the deflection of light rays in the field of a gravitating body (which does not take the rotation of space into account).

2 Problem statement

When calculating the mentioned four new effects in the field of a rotating body, our task was to deduce the effects in their "pure form", i.e., without any other factors taken into account. To do this, the simplest metric was used, which described the four-dimensional space (space-time) of a rotating body, the mass of which is so small that the gravitational field it creates

can be neglected.

This space metric is easy to deduce. Consider the metric of an empty space, which does not rotate or deform

$$ds^2 = c^2dt^2 - dr^2 - r^2\left(d\theta^2 + \sin^2\theta\, d\varphi^2\right), \qquad (1)$$

where and below, in terms of the spherical coordinates, r is the radial coordinate, dr is the elementary segment length along the radial r-axis, θ is the polar coordinate angle measured from the North Pole to the equator, $r\,d\theta$ is the elementary arc length along the θ-axis (along the geographical latitudes), φ is the geographical longitude (equatorial coordinate axis), and $r\sin\theta\, d\varphi$ is the elementary arc length along the equatorial φ-axis.

Assume that the space rotates along the equatorial axis φ, i.e., along the geographical longitudes, with the linear velocity $v_3 = \omega r^2\sin^2\theta$, where $\omega = const$ is the angular velocity of this rotation. Since by definition of v_i (13)

$$v_3 = \omega r^2\sin^2\theta = -\frac{c\,g_{03}}{\sqrt{g_{00}}} \qquad (2)$$

then we have

$$g_{03} = -\frac{1}{c}\,v_3\sqrt{g_{00}} = -\frac{\omega r^2\sin^2\theta}{c}, \qquad (3)$$

and the metric of such a rotating empty space has the form

$$ds^2 = c^2dt^2 - 2\omega r^2\sin^2\theta\, dt\, d\varphi - \\ - dr^2 - r^2\left(d\theta^2 + \sin^2\theta\, d\varphi^2\right). \qquad (4)$$

As you can see, the non-zero components of the fundamental metric tensor $g_{\alpha\beta}$ of this metric are

$$\left.\begin{array}{lll} g_{00} = 1, & g_{03} = -\dfrac{\omega r^2\sin^2\theta}{c} & \\ g_{11} = -1, & g_{22} = -r^2, & g_{33} = -r^2\sin^2\theta \end{array}\right\}, \qquad (5)$$

where $g_{00} = 1$ means that the space is free of gravitational fields or such fields can be neglected: with $g_{00} = 1$ the gravitational field potential w, the general formula of which for any space metric is $w = c^2(1 - \sqrt{g_{00}})$ (12), is either equal to zero $w = 0$ or approaches zero $w \to 0$.

The deflection of light rays and mass-bearing particles in the field of a rotating body [2], and also the length stretching and time loss/gain in the field of a rotating body [3] were obtained in the space of the above metric (4). Thanks to the above approximation, expressed with the simplest metric (4) describing a rotating empty space, it was possible to obtain the mentioned effects of the space curvature created by the rotation of space in their "pure form", without adding any other geometric or physical factors.

But real experiments conducted in an Earth-bound laboratory must take the gravitational field of the Earth into account. From this follows the problem statement for this paper:

Problem statement

Our task now is to re-calculate the space curvature effects caused by the rotation of space — the deflection of light rays and mass-bearing particles, and also the length stretching and time loss/gain in the field of a rotating body — for the case, where the gravitational field of the rotating body is taken into account.

To do this, we need the metric of such a space. We deduce it from Schwarzschild's mass-point metric, which describes a spherically symmetric space filled with the gravitational field created in emptiness by a spherical massive island of substance (approximated by a mass-point)

$$ds^2 = \left(1 - \frac{r_g}{r}\right)c^2dt^2 - \frac{dr^2}{1 - \frac{r_g}{r}} - r^2\left(d\theta^2 + \sin^2\theta\, d\varphi^2\right), \qquad (6)$$

where r is the radial distance from the centre of the massive island, $r_g = 2GM/c^2$ is its gravitational radius, calculated for its mass M, and the non-zero components of the fundamental metric tensor $g_{\alpha\beta}$ are

$$\left.\begin{array}{ll} g_{00} = 1 - \dfrac{r_g}{r}, & g_{11} = -\dfrac{1}{1 - \frac{r_g}{r}} \\ g_{22} = -r^2, & g_{33} = -r^2\sin^2\theta \end{array}\right\}. \qquad (7)$$

As before, we assume that the space rotates along the equatorial axis φ (along the geographical longitudes) with the linear velocity $v_3 = \omega r^2\sin^2\theta$, where $\omega = const$ is the angular velocity of this rotation. Since by definition of v_i (13)

$$v_3 = \omega r^2\sin^2\theta = -\frac{c\,g_{03}}{\sqrt{g_{00}}}, \qquad (8)$$

and, hence,

$$g_{03} = -\frac{1}{c}\,v_3\sqrt{g_{00}} = -\frac{\omega r^2\sin^2\theta}{c}\sqrt{1 - \frac{r_g}{r}} \neq 0, \qquad (9)$$

then we obtain the desired metric

$$ds^2 = \left(1 - \frac{r_g}{r}\right)c^2dt^2 - 2\omega r^2\sin^2\theta\sqrt{1 - \frac{r_g}{r}}\, dt\, d\varphi - \\ - \frac{dr^2}{1 - \frac{r_g}{r}} - r^2\left(d\theta^2 + \sin^2\theta\, d\varphi^2\right), \qquad (10)$$

which describes a spherically symmetric space, which is filled with the gravitational field created in emptiness by a rotating spherical island of matter (approximated by a mass-point) and rotates together with this body.

It is the metric (10), in the space of which we are going to re-calculate the space curvature effects, created due to the rotation of space.

We will do this in the following steps. First, we need to give a short description of the mathematical formalism we are

using — the mathematical apparatus of chronometric invariants, which are physically observable quantities in the space-time of General Relativity.

Second, we calculate the physically observable chr.inv.-characteristics of the space of a rotating mass-point, which is the space of the metric (10).

Third, it is not a fact that the space described by the introduced metric of a rotating mass-point (10) is Riemannian. By definition, a Riemannian space is such one, the metric of which has the Riemannian square form $ds^2 = g_{\alpha\beta}\,dx^\alpha dx^\beta$, determined by the Riemann fundamental metric tensor $g_{\alpha\beta}$, is invariant $ds^2 = inv$ everywhere in the space, and also satisfies Einstein's field equations, which are the specific relation between the Ricci curvature tensor, the fundamental metric tensor multiplied by the curvature scalar, and the energy-momentum tensor of the "space filler" (the latter targets non-empty Riemannian spaces filled with distributed matter). The above three requirements are specific to the family of Riemannian spaces.

Finding a metric that satisfies the first two conditions is easy, but satisfying the third condition (Einstein's field equations) is problematic. This is why, until now, only a small number of space metrics have been proven to be Riemannian and used in the General Theory of Relativity.

A space metric satisfies the field equations, if the components of the fundamental metric tensor $g_{\alpha\beta}$ (specific to this metric) and the components of the energy-momentum tensor of the medium (that fills the space), substituted into the field equations, make the left-hand and right-hand sides of the equations identical (the field equations vanish). In an empty Riemannian space, the left-hand side of the field equations itself after the above substitution must become zero (since in this case the energy-momentum tensor of distributed matter on the right-hand side is zero).

Most likely, the introduced metric of the space of a rotating mass-point (10) does not satisfy the field equations. For this reason, at our third step, we will substitute the $g_{\alpha\beta}$ components from the introduced metric (10) into the left-hand terms of the field equations (the right-hand side of the equations is zero, since the space of a rotating mass-point we are considering is not filled with distributed matter). The relations (particular conditions) that vanish the resulting field equations are *Riemannian conditions*, under which the introduced metric (10) is Riemannian and, therefore, can be used in the framework of General Relativity.

At our fourth step, we will deduce formulae for the space curvature effects in the field of a rotating massive body, i.e., in the space of the metric (10), which is the final task of this research.

3 Chronometrically invariant quantities

We use the mathematical apparatus of chronometric invariants, which uniquely determines physically observable quantities in the four-dimensional pseudo-Riemannian space (space-time of General Relativity). This mathematical formalism was created in 1944 by Abraham Zelmanov.

In addition to the publications by Zelmanov [4–6], which were very concise, an extended review of the chronometrically invariant formalism was given in each of our three research monographs (together with L. Borissova), originally published in 2001 [7, 8] and 2013 [9]. In 2023 we published the most comprehensive survey of the Zelmanov formalism [10], where we collected almost everything that we know in this field personally from Zelmanov and based on our own research studies. The most complete list of the research studies performed using the chronometrically invariant formalism as of January 2023 can be found in the Bibliography to our survey [10].

In short, Zelmanov unambiguously determined physically observable quantities in the space-time of General Relativity as the projections of four-dimensional tensor quantities onto the time line and the three-dimensional spatial section, associated with an observer. Such projections remain invariant throughout the observer's three-dimensional spatial section (his observable three-dimensional physical reference space), i.e., they are "chrono-metric invariants" in his reference frame and depend on the properties of his physical reference space, such as the gravitational potential, rotation, deformation, curvature, etc.

The chronometrically invariant projections of any four-dimensional tensor quantity are calculated using operators of projection, which take the physical properties and geometric structure of the observer's space into account. For detail, see the References to chronometric invariants, e.g., the most detailed survey [10].

Below you can find only the necessary minimum of this mathematical formalism, which is necessary for understanding and reproducing the results obtained in this study.

Projecting the four-dimensional displacement vector dx^α ($\alpha = 0, 1, 2, 3$) onto the time line of an observer gives the physically observable chr.inv.-time interval $d\tau$

$$d\tau = \sqrt{g_{00}}\,dt - \frac{1}{c^2}\,v_i dx^i, \quad i = 1, 2, 3, \tag{11}$$

where g_{00} is expressed with the chr.inv.-potential w (physically observable potential) of the gravitational field that fills the space of the observer as

$$\mathrm{w} = c^2\,(1 - \sqrt{g_{00}}\,), \qquad \sqrt{g_{00}} = 1 - \frac{\mathrm{w}}{c^2}\,, \tag{12}$$

and v_i is the three-dimensional vector of the linear velocity of rotation of the observer's space

$$v_i = -\,\frac{c\,g_{0i}}{\sqrt{g_{00}}}\,, \quad v^i = -\,c\,g^{0i}\sqrt{g_{00}}\,, \quad v_i = h_{ik}\,v^k. \tag{13}$$

Projecting dx^α onto the observer's three-dimensional spatial section gives the three-dimensional chr.inv.-displacement

vector dx^i (which coincides with the three-dimensional coordinate displacement vector). As a result, $d\tau$ distinguishes the chr.inv.-velocity vector $\mathrm{v}^i = dx^i/d\tau$ (physically observable three-dimensional velocity) from the three-dimensional coordinate velocity vector $u^i = dx^i/dt$.

The three-dimensional chr.inv.-spatial interval $d\sigma$ (physically observable three-dimensional interval) is determined

$$d\sigma^2 = h_{ik}\, dx^i dx^k, \tag{14}$$

using the three-dimensional chr.inv.-metric tensor h_{ik}

$$h_{ik} = -g_{ik} + \frac{1}{c^2}\, v_i v_k\,, \quad h^{ik} = -g^{ik}, \quad h^i_k = \delta^i_k\,, \tag{15}$$

which is the chr.inv.-projection of the fundamental metric tensor $g_{\alpha\beta}$ onto the observer's spatial section and possesses all properties of $g_{\alpha\beta}$ throughout the spatial section (the observer's three-dimensional space).

The square of the four-dimensional (space-time) interval $ds^2 = g_{\alpha\beta}\, dx^\alpha dx^\beta$ is therefore expressed with chronometrically invariant (physically observable) quantities as

$$ds^2 = c^2 d\tau^2 - d\sigma^2. \tag{16}$$

Thanks to the splitting of space-time into three-dimensional spatial sections pierced by time lines, which is specific to the chronometrically invariant formalism, we can reveal the true nature of three-dimensional rotations. When $v_i \neq 0$, i.e., the reference body of an observer rotates (together with his reference space), then this rotation cannot be vanished by a coordinate transformation (by moving the observer to another reference frame within his three-dimensional spatial section). This happens because the rotation speed v_i (13) is determined by the mixed (space-time) components g_{0i} of the fundamental metric tensor $g_{\alpha\beta}$, and not by its three-dimensional spatial components g_{ik} dependent on time (as it is considered in classical mechanics, where time is just a parameter, and not the fourth coordinate). Since the components of $g_{\alpha\beta}$ are cosines of the angles between the respective coordinate lines, then three-dimensional rotations are due to the *non-holonomity* of space-time, which means that time lines are not orthogonal to three-dimensional spatial sections.

If all g_{0i} are zero, then such space-time is *holonomic*. In this case the three-dimensional spatial section is everywhere orthogonal to the time lines that pierce it. If at least one of the components g_{0i} is different from zero, then such space-time is *non-holonomic*, and the spatial section $x^0 = const$ is inclined to the time lines (at different points it can be inclined to the time lines at different angles depending on the local geometric structure of the particular four-dimensional space-time).

In general, the physical reference space of a real observer can be filled with a gravitational field, rotate, deform, be inhomogeneous and curved.

The chr.inv.-vector of the gravitational inertial force F_i, where the first (gravitational) term is created by the gradient of the gravitational potential w and the second (inertial) term is created by the centrifugal force of inertia, is

$$F_i = \frac{1}{\sqrt{g_{00}}}\left(\frac{\partial \mathrm{w}}{\partial x^i} - \frac{\partial v_i}{\partial t}\right), \qquad \sqrt{g_{00}} = 1 - \frac{\mathrm{w}}{c^2}\,. \tag{17}$$

The antisymmetric chr.inv.-tensor A_{ik} of the angular velocity of rotation of space is

$$A_{ik} = \frac{1}{2}\left(\frac{\partial v_k}{\partial x^i} - \frac{\partial v_i}{\partial x^k}\right) + \frac{1}{2c^2}\,(F_i v_k - F_k v_i), \tag{18}$$

which is related to F_i by two identities

$$\frac{{}^*\partial A_{ik}}{\partial t} + \frac{1}{2}\left(\frac{{}^*\partial F_k}{\partial x^i} - \frac{{}^*\partial F_i}{\partial x^k}\right) = 0, \tag{19}$$

$$\frac{{}^*\partial A_{km}}{\partial x^i} + \frac{{}^*\partial A_{mi}}{\partial x^k} + \frac{{}^*\partial A_{ik}}{\partial x^m} + \\ + \frac{1}{2}\,(F_i A_{km} + F_k A_{mi} + F_m A_{ik}) = 0, \tag{20}$$

where asterisk denotes the chr.inv.-derivation operators

$$\frac{{}^*\partial}{\partial t} = \frac{1}{\sqrt{g_{00}}}\,\frac{\partial}{\partial t}, \qquad \frac{{}^*\partial}{\partial x^i} = \frac{\partial}{\partial x^i} + \frac{1}{c^2}\, v_i\, \frac{{}^*\partial}{\partial t}\,. \tag{21}$$

Antisymmetric chr.inv.-tensors can be used to create the corresponding chr.inv.-pseudovectors (marked with an asterisk) using the antisymmetric chr.inv.-discriminant tensor

$$\varepsilon^{ikm} = \frac{e^{ikm}}{\sqrt{h}}\,, \qquad \varepsilon_{ikm} = e_{ikm}\sqrt{h}, \tag{22}$$

where $h = \det \| h_{ik} \|$. This tensor is the chr.inv.-analogy of the Levi-Civita antisymmetric unit tensor e^{ikm} (the components of e^{ikm} are either $+1$ or -1 depending on the transposition of its indices).* For example, the antisymmetric chr.inv.-tensor A_{ik} of the angular velocity of rotation of space has the corresponding chr.inv.-pseudovector Ω^{*i} of this rotation

$$\left.\begin{aligned} &\Omega^{*i} = \frac{1}{2}\,\varepsilon^{ikm} A_{km}\,, \qquad \Omega_{*i} = \frac{1}{2}\,\varepsilon_{imn} A^{mn} \\ &\varepsilon^{ipq}\,\Omega_{*i} = \frac{1}{2}\,\varepsilon^{ipq}\varepsilon_{imn} A^{mn} = \\ &\qquad = \frac{1}{2}\left(\delta^p_m \delta^q_n - \delta^q_m \delta^p_n\right) A^{mn} = A^{pq} \end{aligned}\right\}. \tag{23}$$

The symmetric chr.inv.-tensor D_{ik} of the deformation rate of space is formulated as

$$\left.\begin{aligned} &D_{ik} = \frac{1}{2}\,\frac{{}^*\partial h_{ik}}{\partial t}\,, \qquad\qquad D^{ik} = -\frac{1}{2}\,\frac{{}^*\partial h^{ik}}{\partial t} \\ &D = h^{ik} D_{ik} = \frac{{}^*\partial \ln\sqrt{h}}{\partial t}\,, \quad h = \det \| h_{ik} \| \end{aligned}\right\}. \tag{24}$$

*For detail, see pages 14–16 in our comprehensive survey of the Zelmanov chronometric invariants [10], or §2.3 in our monograph [8].

The chr.inv.-Christoffel symbols of the 1st rank $\Delta_{jk,m}$ and the 2nd rank Δ^i_{nk} (their physical sense is the coefficients of inhomogeneity of space) are

$$\Delta^i_{nk} = h^{im}\Delta_{nk,m} = \frac{1}{2}\,h^{im}\left(\frac{{}^*\partial h_{nm}}{\partial x^k} + \frac{{}^*\partial h_{km}}{\partial x^n} - \frac{{}^*\partial h_{nk}}{\partial x^m}\right). \quad (25)$$

The physically observable curvature of space is expressed with the chr.inv.-curvature tensor C_{lkij} that possesses all properties of the Riemann-Christoffel curvature tensor throughout the three-dimensional spatial section associated with the observer. Its subsequent contractions give the chr.inv.-Ricci curvature tensor C_{ik} and the chr.inv.-scalar curvature C

$$C_{lkij} = \frac{1}{4}\left(H_{lkij} - H_{jkil} + H_{klji} - H_{iljk}\right) = \\ = H_{lkij} - \frac{1}{2}\left(2A_{ki}D_{jl} + A_{ij}D_{kl} + A_{jk}D_{il} + \right. \\ \left. + A_{kl}D_{ij} + A_{li}D_{jk}\right), \quad (26)$$

$$C_{lk} = C^{\cdots i}_{lki\cdot} = H_{lk} - \frac{1}{2}\left(A_{kj}D^j_l + A_{lj}D^j_k + A_{kl}D\right), \quad (27)$$

$$C = h^{lk}C_{lk} = h^{lk}H_{lk}, \quad (28)$$

where, for a better association with the Riemann-Christoffel curvature tensor, we denote

$$H^{\cdots j}_{lki\cdot} = \frac{{}^*\partial\Delta^j_{il}}{\partial x^k} - \frac{{}^*\partial\Delta^j_{kl}}{\partial x^i} + \Delta^m_{il}\Delta^j_{km} - \Delta^m_{kl}\Delta^j_{im}. \quad (29)$$

From the above definitions we see that the physically observable curvature of space depends on not only the gravitational inertial force (hidden in the second chr.inv.-derivatives of the chr.inv.-metric tensor), but also the rotation, deformation and inhomogeneity of space and, therefore, does not vanish in the absence of the gravitational field.

By analogy with absolute (general covariant) derivatives, the corresponding chr.inv.-derivatives are introduced

$${}^*\nabla_i Q_k = \frac{{}^*\partial Q_k}{dx^i} - \Delta^l_{ik}Q_l, \quad (30)$$

$${}^*\nabla_i Q^k = \frac{{}^*\partial Q^k}{dx^i} + \Delta^k_{il}Q^l, \quad (31)$$

$${}^*\nabla_i Q_{jk} = \frac{{}^*\partial Q_{jk}}{dx^i} - \Delta^l_{ij}Q_{lk} - \Delta^l_{ik}Q_{jl}, \quad (32)$$

$${}^*\nabla_i Q^k_j = \frac{{}^*\partial Q^k_j}{dx^i} - \Delta^l_{ij}Q^k_l + \Delta^k_{il}Q^l_j, \quad (33)$$

$${}^*\nabla_i Q^{jk} = \frac{{}^*\partial Q^{jk}}{dx^i} + \Delta^j_{il}Q^{lk} + \Delta^k_{il}Q^{jl}, \quad (34)$$

$${}^*\nabla_i Q^i = \frac{{}^*\partial Q^i}{\partial x^i} + \Delta^j_{ji}Q^i, \qquad \Delta^j_{ji} = \frac{{}^*\partial \ln\sqrt{h}}{\partial x^i}, \quad (35)$$

$${}^*\nabla_i Q^{ji} = \frac{{}^*\partial Q^{ji}}{\partial x^i} + \Delta^j_{il}Q^{il} + \Delta^l_{li}Q^{ji}, \quad \Delta^l_{li} = \frac{{}^*\partial \ln\sqrt{h}}{\partial x^i}, \quad (36)$$

which, in particular, exhibit some properties of the chr.inv.-metric tensor h_{ik} and the chr.inv.-discriminant tensor ε_{ijk} (used further in calculations)

$${}^*\nabla_i h_{jk} = 0, \quad {}^*\nabla_i h^k_j = 0, \quad {}^*\nabla_i h^{jk} = 0, \quad (37)$$

$${}^*\nabla_l \varepsilon_{ijk} = 0, \qquad {}^*\nabla_l \varepsilon^{ijk} = 0, \quad (38)$$

Einstein's field equations, having the well-known general covariant (four-dimensional) form

$$R_{\alpha\beta} - \frac{1}{2}\,g_{\alpha\beta}R = -\varkappa\,T_{\alpha\beta} + \lambda g_{\alpha\beta} \quad (39)$$

can also be presented in chr.inv.-form, i.e., in the form of their physically observable chr.inv.-projections.

Note, that the Zelmanov formalism uses $\varkappa = \frac{8\pi G}{c^2}$, but not $\varkappa = \frac{8\pi G}{c^4}$ as Landau and Lifshitz did in their *The Classical Theory of Fields* [11]. This is because, since Ricci's tensor $R_{\alpha\beta}$ has the dimension [cm^{-2}] and the energy-momentum tensor $T_{\alpha\beta}$ has the dimension of mass density [gram/cm^3], if we used $\varkappa = \frac{8\pi G}{c^4}$ on the right-hand side of the field equations, then we would not use the energy-momentum tensor $T_{\alpha\beta}$ itself, but $c^2T_{\alpha\beta}$ as Landau and Lifshitz did (which is not correct at all from the point of view of physical sense and physically observable quantities).

To understand the chr.inv.-Einstein equations that below, we should note that any tensor or tensor equation of the 2nd rank has three chr.inv.-projections: the time projection, the space-time (mixed) projection and the spatial projection; for detail, see [10]. So, the energy-momentum tensor $T_{\alpha\beta}$ of a distributed matter has the following chr.inv.-projections

$$\varrho = \frac{T_{00}}{g_{00}}, \qquad J^i = \frac{c\,T^i_0}{\sqrt{g_{00}}}, \qquad U^{ik} = c^2T^{ik}, \quad (40)$$

where ϱ is the observable mass density of the distributed matter, J^i is its observable momentum density, and U^{ik} is the observable stress-tensor of the matter field.

The general covariant Einstein field equations (39) also have three chr.inv.-projections, which are called the chr.inv.-Einstein equations

$$\frac{{}^*\partial D}{\partial t} + D_{jl}D^{jl} + A_{jl}A^{lj} + {}^*\nabla_j F^j - \frac{1}{c^2}F_jF^j = \\ = -\frac{\varkappa}{2}\left(\varrho c^2 + U\right) + \lambda c^2, \quad (41)$$

$${}^*\nabla_j\left(h^{ij}D - D^{ij} - A^{ij}\right) + \frac{2}{c^2}F_jA^{ij} = \varkappa J^i, \quad (42)$$

$$\frac{{}^*\partial D_{ik}}{\partial t} - \left(D_{ij} + A_{ij}\right)\left(D^j_k + A^{\cdot j}_{k\cdot}\right) + DD_{ik} + 3A_{ij}A^{\cdot j}_{k\cdot} - \\ - \frac{1}{c^2}F_iF_k + \frac{1}{2}\left({}^*\nabla_iF_k + {}^*\nabla_kF_i\right) - c^2C_{ik} = \\ = \frac{\varkappa}{2}\left(\varrho c^2h_{ik} + 2U_{ik} - Uh_{ik}\right) + \lambda c^2h_{ik}. \quad (43)$$

With the above mathematical tools, we now have everything we need to consider the space of a rotating massive body using the chronometrically invariant formalism.

4 Physically observable characteristics of the space of a rotating massive body

Consider a space of the rotating Schwarzschild metric, which we have introduced (10). It has the form

$$ds^2 = \left(1 - \frac{r_g}{r}\right) c^2 dt^2 - 2\,\omega r^2 \sin^2\theta \sqrt{1 - \frac{r_g}{r}}\, dt\, d\varphi - \\ - \frac{dr^2}{1 - \frac{r_g}{r}} - r^2\left(d\theta^2 + \sin^2\theta\, d\varphi^2\right). \quad (44)$$

Such a space rotates in the equatorial plane along the geographical longitudes φ with an angular velocity $\omega = const$. The linear velocity of this rotation is $v_3 = \omega r^2 \sin^2\theta$

$$v_3 = \omega r^2 \sin^2\theta = -\frac{c\, g_{03}}{\sqrt{g_{00}}}, \qquad v_1 = v_2 = 0, \quad (45)$$

hence, non-zero components of the fundamental metric tensor of the above space metric are

$$\left.\begin{aligned} g_{00} &= 1 - \frac{r_g}{r}, & g_{03} &= -\frac{\omega r^2 \sin^2\theta}{c}\sqrt{1 - \frac{r_g}{r}} \\ g_{11} &= -\frac{1}{1 - \frac{r_g}{r}}, & g_{22} &= -r^2, \quad g_{33} = -r^2\sin^2\theta \end{aligned}\right\}. \quad (46)$$

Respectively, the chr.inv.-metric tensor $h_{ik} = -g_{ik} + \frac{1}{c^2} v_i v_k$ (15) of a rotating Schwarzschild space has only the following non-zero components

$$\left.\begin{aligned} h_{11} &= \frac{1}{1 - \frac{r_g}{r}}, & h_{22} &= r^2 \\ h_{33} &= r^2\sin^2\theta\left(1 + \frac{\omega^2 r^2 \sin^2\theta}{c^2}\right) \end{aligned}\right\}, \quad (47)$$

and, respectively, calculating the determinant of the chr.inv.-metric tensor h_{ik}, we obtain

$$h = \det\| h_{ik}\| = h_{11} h_{22} h_{33} = \\ = \frac{r^4 \sin^2\theta}{1 - \frac{r_g}{r}}\left(1 + \frac{\omega^2 r^2 \sin^2\theta}{c^2}\right), \quad (48)$$

$$\sqrt{h} = \frac{r^2 \sin\theta}{\sqrt{1 - \frac{r_g}{r}}}\sqrt{1 + \frac{\omega^2 r^2 \sin^2\theta}{c^2}}. \quad (49)$$

As is seen from the above formulae, the matrix h_{ik} is strict diagonal: all of its non-diagonal components h_{ik} $(i \neq k)$ are zero. Therefore, the upper-index components of h_{ik} are obtained just like the invertible matrix components to any diagonal matrix as $h^{ik} = (h_{ik})^{-1}$. They are

$$\left.\begin{aligned} h^{11} &= 1 - \frac{r_g}{r}, & h^{22} &= \frac{1}{r^2} \\ h^{33} &= \frac{1}{r^2\sin^2\theta\left(1 + \frac{\omega^2 r^2 \sin^2\theta}{c^2}\right)} \end{aligned}\right\}. \quad (50)$$

In particular, as a result, the square of the linear velocity, with which the space rotates $v^2 = v_i v^i = v_i h^{ik} v_k$ (13) is

$$v^2 = v_3 h^{33} v_3 = \frac{\omega^2 r^2 \sin^2\theta}{1 + \frac{\omega^2 r^2 \sin^2\theta}{c^2}}. \quad (51)$$

As is seen from (47), the obtained chr.inv.-metric tensor h_{ik} does not depend on time. This means that the chr.inv.-tensor of the deformation rate of space D_{ik} (24) is zero

$$D_{ik} = \frac{1}{2}\frac{{}^*\partial h_{ik}}{\partial t} = 0, \quad (52)$$

i.e., a rotating Schwarzschild space does not deform.

Taking into account that the linear velocity $v_3 = \omega r^2 \sin^2\theta$ with which the space rotates does not depend on time

$$\frac{\partial v_3}{\partial t} = 0 \quad (53)$$

and also that the gravitational field potential $\mathrm{w} = c^2(1 - \sqrt{g_{00}})$ in the present case is

$$\mathrm{w} = c^2\left(1 - \sqrt{1 - \frac{r_g}{r}}\right), \quad (54)$$

we obtain the components of the chr.inv.-vector of the gravitational inertial force F_i (17). They are

$$F_1 = \frac{1}{\sqrt{g_{00}}}\frac{\partial \mathrm{w}}{\partial r} = -\frac{c^2 r_g}{2r^2}\frac{1}{1 - \frac{r_g}{r}}, \quad F_2 = F_3 = 0, \quad (55)$$

$$F^1 = h^{11} F_1 = -\frac{c^2 r_g}{2r^2}, \qquad F^2 = F^3 = 0. \quad (56)$$

Since the gravitational inertial force in the present case is a radially acting force F_1 that depends only on $x^1 = r$, i.e.

$$\frac{{}^*\partial F_k}{\partial x^i} = 0, \qquad i \neq k, \quad (57)$$

then according to the 1st Zelmanov identity (19) we have

$$\frac{{}^*\partial A_{ik}}{\partial t} = 0, \quad (58)$$

i.e., the rotation of the space of the rotating Schwarzschild metric is stationary.

According to the definition of the chr.inv.-tensor of the angular velocity of rotation of space A_{ik} (18), only the following components of it are non-zero in the space of the rotating Schwarzschild metric: $A_{13} \neq 0$, $A_{31} \neq 0$, $A^{13} \neq 0$, $A^{31} \neq 0$,

$A_{23} \neq 0$, $A_{32} \neq 0$, $A^{23} \neq 0$, $A^{32} \neq 0$. Using the definition of A_{ik} (18), after some algebra we obtain

$$A_{13} = \frac{1}{2}\frac{\partial v_3}{\partial r} + \frac{1}{2c^2} F_1 v_3 = \omega r \sin^2\theta - \frac{\omega r_g \sin^2\theta}{4\left(1 - \frac{r_g}{r}\right)}, \quad (59)$$

$$A_{31} = -A_{13} = -\omega r \sin^2\theta + \frac{\omega r_g \sin^2\theta}{4\left(1 - \frac{r_g}{r}\right)}, \quad (60)$$

$$A^{13} = h^{11} h^{33} A_{13} = \\ = \frac{\left(1 - \frac{r_g}{r}\right)\omega}{r\left(1 + \frac{\omega^2 r^2 \sin^2\theta}{c^2}\right)} - \frac{\omega r_g}{4r^2\left(1 + \frac{\omega^2 r^2 \sin^2\theta}{c^2}\right)}, \quad (61)$$

$$A^{31} = -A^{13} = \\ = -\frac{\left(1 - \frac{r_g}{r}\right)\omega}{r\left(1 + \frac{\omega^2 r^2 \sin^2\theta}{c^2}\right)} + \frac{\omega r_g}{4r^2\left(1 + \frac{\omega^2 r^2 \sin^2\theta}{c^2}\right)}, \quad (62)$$

$$A_{23} = \frac{1}{2}\frac{\partial v_3}{\partial \theta} = \omega r^2 \sin\theta\cos\theta, \quad (63)$$

$$A_{32} = -A_{23} = -\omega r^2 \sin\theta\cos\theta, \quad (64)$$

$$A^{23} = h^{22} h^{33} A_{23} = \frac{\omega \cot\theta}{r^2\left(1 + \frac{\omega^2 r^2 \sin^2\theta}{c^2}\right)}, \quad (65)$$

$$A^{32} = -A^{23} = -\frac{\omega \cot\theta}{r^2\left(1 + \frac{\omega^2 r^2 \sin^2\theta}{c^2}\right)}. \quad (66)$$

Find the physically observable scalar angular velocity Ω, with which the space rotates. Its square is calculated as

$$\Omega^2 = \Omega_{*i}\Omega^{*i} = \Omega_{*1}\Omega^{*1} + \Omega_{*2}\Omega^{*2} = \\ = h_{11}\Omega^{*1}\Omega^{*1} + h_{22}\Omega^{*2}\Omega^{*2}. \quad (67)$$

In the space of the rotating Schwarzschild metric, which we are considering, we have

$$\Omega^{*1} = \frac{1}{2}\varepsilon^{1km} A_{km} = \frac{e^{1km}}{2\sqrt{h}} A_{km} = \frac{e^{123}}{2\sqrt{h}} A_{23} + \frac{e^{132}}{2\sqrt{h}} A_{32} \quad (68)$$

and, taking into account that $e^{123} = +1$ and $e^{132} = -1$, and also $A_{32} = -A_{23}$, we obtain

$$\Omega^{*1} = \frac{e^{123}}{2\sqrt{h}} A_{23} + \frac{e^{123}}{2\sqrt{h}} A_{23} = \frac{e^{123}}{\sqrt{h}} A_{23} = \frac{A_{23}}{\sqrt{h}}. \quad (69)$$

In the same way, we obtain

$$\Omega^{*2} = \frac{1}{2}\varepsilon^{2km} A_{km} = \frac{e^{2km}}{2\sqrt{h}} A_{km} = \\ = \frac{e^{213}}{2\sqrt{h}} A_{13} + \frac{e^{231}}{2\sqrt{h}} A_{31} = \frac{e^{213}}{\sqrt{h}} A_{13} = -\frac{A_{13}}{\sqrt{h}}. \quad (70)$$

Finally, substituting A_{13} (59), A_{23} (63), $h = \det \| h_{ik} \|$ (48), h_{11} and h_{22} (47) into Ω^2 (67), we obtain the physically observable scalar angular velocity Ω of the rotation of space

$$\Omega = \sqrt{\Omega_{*i}\Omega^{*i}} = \frac{\omega}{\sqrt{1 + \frac{\omega^2 r^2 \sin^2\theta}{c^2}}} \times \\ \times \sqrt{1 - \frac{3 r_g \sin^2\theta}{2r} + \frac{r_g^2 \sin^2\theta}{16 r^2\left(1 - \frac{r_g}{r}\right)}}. \quad (71)$$

If there is no mass ($M = 0$), then the gravitational radius is $r_g = 2GM/c^2 = 0$. In this case, $g_{00} = 1 - \frac{r_g}{r} = 1$ and the formulae for h_{ik} (47–50), A_{ik} (59–66) and Ω (71) we have obtained in the space of the rotating Schwarzschild metric transform into the corresponding formulae in the spherically symmetric rotating space without the gravitational field, which we have obtained earlier; see page 43 in the previous paper [1].

To calculate the chr.inv.-Einstein equations in the space of the rotating Schwarzschild metric, we need the chr.inv.-Ricci curvature tensor C_{ik} containing in the third, tensor chr.inv.-Einstein equation (43). The chr.inv.-Ricci tensor C_{ik} (27) consists of the chr.inv.-derivatives of the chr.inv.-Christoffel symbols Δ^i_{nk} and the products of Δ^i_{nk} with each other. In turn, Δ^i_{nk} (25) are the re-combination of the chr.inv.-derivatives of the chr.inv.-metric tensor h_{ik} (47). Therefore, at first we calculate the non-zero chr.inv.-derivatives of h_{ik}

$$\frac{{}^*\partial h_{11}}{\partial r} = -\frac{r_g}{\left(1 - \frac{r_g}{r}\right)^2 r^2}, \quad (72)$$

$$\frac{{}^*\partial h_{22}}{\partial r} = 2r, \quad (73)$$

$$\frac{{}^*\partial h_{33}}{\partial r} = 2r\sin^2\theta\left(1 + \frac{2\omega^2 r^2 \sin^2\theta}{c^2}\right), \quad (74)$$

$$\frac{{}^*\partial h_{33}}{\partial \theta} = 2r^2 \sin\theta\cos\theta\left(1 + \frac{2\omega^2 r^2 \sin^2\theta}{c^2}\right). \quad (75)$$

The chr.inv.-Christoffel symbols Δ^i_{nk} (25) in the rotating Schwarzschild metric space have the non-zero components

$$\left.\begin{array}{ll} \Delta^1_{11} = \frac{1}{2} h^{11}\frac{{}^*\partial h_{11}}{\partial r}, & \Delta^1_{22} = \frac{1}{2} h^{11}\frac{{}^*\partial h_{22}}{\partial r} \\ \Delta^1_{33} = -\frac{1}{2} h^{11}\frac{{}^*\partial h_{33}}{\partial r}, & \Delta^2_{12} = \frac{1}{2} h^{22}\frac{{}^*\partial h_{22}}{\partial r} \\ \Delta^2_{21} = \frac{1}{2} h^{22}\frac{{}^*\partial h_{22}}{\partial r}, & \Delta^2_{33} = -\frac{1}{2} h^{22}\frac{{}^*\partial h_{33}}{\partial \theta} \\ \Delta^3_{13} = \frac{1}{2} h^{33}\frac{{}^*\partial h_{33}}{\partial r}, & \Delta^3_{23} = \frac{1}{2} h^{33}\frac{{}^*\partial h_{33}}{\partial \theta} \\ \Delta^3_{31} = \frac{1}{2} h^{33}\frac{{}^*\partial h_{33}}{\partial r}, & \Delta^3_{32} = \frac{1}{2} h^{33}\frac{{}^*\partial h_{33}}{\partial \theta} \end{array}\right\}. \quad (76)$$

After some algebra using the obtained formulae for the non-zero components of h^{ik} (50) and the chr.inv.-derivatives of the non-zero components of h_{ik} (72–75), we obtain

$$\Delta^1_{11} = -\frac{r_g}{2r^2\left(1-\frac{r_g}{r}\right)}, \tag{77}$$

$$\Delta^1_{22} = -r, \tag{78}$$

$$\Delta^1_{33} = -r\sin^2\theta\left(1+\frac{2\omega^2r^2\sin^2\theta}{c^2}\right), \tag{79}$$

$$\Delta^2_{12} = \Delta^2_{21} = \frac{1}{r}, \tag{80}$$

$$\Delta^2_{33} = -\sin\theta\cos\theta\left(1+\frac{2\omega^2r^2\sin^2\theta}{c^2}\right), \tag{81}$$

$$\Delta^3_{13} = \Delta^3_{31} = \frac{1}{r\left(1+\frac{\omega^2r^2\sin^2\theta}{c^2}\right)}\left(1+\frac{2\omega^2r^2\sin^2\theta}{c^2}\right), \tag{82}$$

$$\Delta^3_{23} = \Delta^3_{32} = \frac{\cot\theta}{1+\frac{\omega^2r^2\sin^2\theta}{c^2}}\left(1+\frac{2\omega^2r^2\sin^2\theta}{c^2}\right). \tag{83}$$

The non-zero contracted chr.inv.-Christoffel symbols Δ^i_{i1} and Δ^i_{i2} are calculated from their definition based on the determinant $h = \det\| h_{ik}\|$; see (35) or (36). Using the formulae for h (48) and its square root (49) obtained in the space of the rotating Schwarzschild metric, we obtain

$$\Delta^i_{i1} = \frac{{}^*\partial\ln\sqrt{h}}{\partial r} = \frac{2}{r\left(1+\frac{\omega^2r^2\sin^2\theta}{c^2}\right)}\left(1+\frac{3\omega^2r^2\sin^2\theta}{2c^2}\right) - \\ - \frac{r_g}{2r^2\left(1-\frac{r_g}{r}\right)}, \tag{84}$$

$$\Delta^i_{i2} = \frac{{}^*\partial\ln\sqrt{h}}{\partial\theta} = \frac{\cot\theta}{1+\frac{\omega^2r^2\sin^2\theta}{c^2}}\left(1+\frac{2\omega^2r^2\sin^2\theta}{c^2}\right). \tag{85}$$

Based on the above formulae, we calculate the non-zero chr.inv.-derivatives of the contracted chr.inv.-Christoffel symbols Δ^i_{i1} and Δ^i_{i2}. After some algebra, we obtain

$$\frac{{}^*\partial\Delta^i_{i1}}{\partial r} = -\frac{2}{r^2\left(1+\frac{\omega^2r^2\sin^2\theta}{c^2}\right)^2} - \frac{3\omega^2\sin^2\theta}{c^2\left(1+\frac{\omega^2r^2\sin^2\theta}{c^2}\right)^2} - \\ - \frac{3\omega^4r^2\sin^4\theta}{c^4\left(1+\frac{\omega^2r^2\sin^2\theta}{c^2}\right)^2} + \frac{r_g}{r^3\left(1-\frac{r_g}{r}\right)^2}\left(1-\frac{r_g}{2r}\right), \tag{86}$$

$$\frac{{}^*\partial\Delta^i_{i1}}{\partial\theta} = \frac{2\omega^2r\sin\theta\cos\theta}{c^2\left(1+\frac{\omega^2r^2\sin^2\theta}{c^2}\right)^2}, \tag{87}$$

$$\frac{{}^*\partial\Delta^i_{i2}}{\partial r} = \frac{2\omega^2r\sin\theta\cos\theta}{c^2\left(1+\frac{\omega^2r^2\sin^2\theta}{c^2}\right)^2} = \frac{{}^*\partial\Delta^i_{i1}}{\partial\theta}, \tag{88}$$

$$\frac{{}^*\partial\Delta^i_{i2}}{\partial\theta} = -\frac{1}{\sin^2\theta\left(1+\frac{\omega^2r^2\sin^2\theta}{c^2}\right)} - \\ - \frac{2\omega^2r^2\sin^2\theta}{c^2\left(1+\frac{\omega^2r^2\sin^2\theta}{c^2}\right)^2} - \frac{2\omega^4r^4\sin^2\theta}{c^4\left(1+\frac{\omega^2r^2\sin^4\theta}{c^2}\right)^2}. \tag{89}$$

Now, using the quantities calculated above, we calculate the chr.inv.-Ricci curvature tensor C_{ik} in the space of the rotating Schwarzschild metric. Since the space we are considering does not deform ($D_{ik} = 0$), then in this case the general formula for $C_{lk} = C^{\cdots i}_{lki\cdot}$ (27) is simplified to

$$C_{lk} = H_{lk} = H^{\cdots i}_{lki\cdot} = \\ = \frac{{}^*\partial\Delta^i_{il}}{\partial x^k} - \frac{{}^*\partial\Delta^i_{kl}}{\partial x^i} + \Delta^m_{il}\Delta^i_{km} - \Delta^m_{kl}\Delta^i_{im}, \tag{90}$$

which, according to the non-zero chr.inv.-Christoffel symbols calculated in the space of the rotating Schwarzschild metric (see above), has the following non-zero components

$$C_{11} = \frac{{}^*\partial\Delta^i_{i1}}{\partial r} + \Delta^2_{21}\Delta^2_{12} + \Delta^3_{31}\Delta^3_{13} - \\ - \frac{{}^*\partial\Delta^1_{11}}{\partial r} + \Delta^1_{11}\Delta^1_{11} - \Delta^1_{11}\Delta^i_{i1}, \tag{91}$$

$$C_{12} = \frac{{}^*\partial\Delta^i_{i1}}{\partial\theta} + \Delta^3_{31}\Delta^3_{23} - \Delta^2_{21}\Delta^i_{i2}, \tag{92}$$

$$C_{21} = \frac{{}^*\partial\Delta^i_{i2}}{\partial r} + \Delta^3_{32}\Delta^3_{13} - \Delta^2_{12}\Delta^i_{i2}, \tag{93}$$

$$C_{22} = \frac{{}^*\partial\Delta^i_{i2}}{\partial\theta} - \frac{{}^*\partial\Delta^1_{22}}{\partial r} + \\ + 2\Delta^2_{12}\Delta^1_{22} + \Delta^3_{32}\Delta^3_{23} - \Delta^1_{22}\Delta^i_{i1}, \tag{94}$$

$$C_{33} = -\frac{{}^*\partial\Delta^1_{33}}{\partial r} - \frac{{}^*\partial\Delta^2_{33}}{\partial\theta} + \\ + 2\Delta^3_{13}\Delta^1_{33} + 2\Delta^3_{23}\Delta^2_{33} - \Delta^1_{33}\Delta^i_{i1} - \Delta^2_{33}\Delta^i_{i2}. \tag{95}$$

To calculate these components, we calculate the unknown derivatives contained in them. We obtain

$$\frac{{}^*\partial\Delta^1_{11}}{\partial r} = \frac{r_g}{r^3\left(1-\frac{r_g}{r}\right)^2}\left(1-\frac{r_g}{2r}\right), \tag{96}$$

$$\frac{{}^*\partial\Delta^1_{33}}{\partial r} = -\sin^2\theta\left(1+\frac{6\omega^2r^2\sin^2\theta}{c^2}\right), \tag{97}$$

$$\frac{{}^*\partial\Delta^2_{33}}{\partial\theta} = \sin^2\theta + \frac{2\omega^2r^2\sin^4\theta}{c^2} - \\ - \cos^2\theta - \frac{6\omega^2r^2\sin^2\theta\cos^2\theta}{c^2}. \tag{98}$$

Substituting the non-zero necessary chr.inv.-Christoffel symbols and their chr.inv.-derivatives into these general for-

mulae (91–95), after some algebra and non-trivial transformations we obtain formulae for the non-zero components of the chr.inv.-Ricci tensor in the space of the rotating Schwarzschild metric. They have the form

$$C_{11} = \frac{3\omega^2\sin^2\theta}{c^2\left(1+\frac{\omega^2r^2\sin^2\theta}{c^2}\right)} - \frac{\omega^4r^2\sin^4\theta}{c^4\left(1+\frac{\omega^2r^2\sin^2\theta}{c^2}\right)^2} + \\ + \frac{r_g}{r^3\left(1-\frac{r_g}{r}\right)\left(1+\frac{\omega^2r^2\sin^4\theta}{c^2}\right)}\left(1+\frac{3\omega^2r^2\sin^2\theta}{2c^2}\right), \quad (99)$$

$$C_{12} = \frac{3\omega^2r\sin\theta\cos\theta}{c^2\left(1+\frac{\omega^2r^2\sin^2\theta}{c^2}\right)} - \frac{\omega^4r^3\sin^3\theta\cos\theta}{c^4\left(1+\frac{\omega^2r^2\sin^2\theta}{c^2}\right)^2}, \quad (100)$$

$$C_{21} = \frac{3\omega^2r\sin\theta\cos\theta}{c^2\left(1+\frac{\omega^2r^2\sin^2\theta}{c^2}\right)} - \frac{\omega^4r^3\sin^3\theta\cos\theta}{c^4\left(1+\frac{\omega^2r^2\sin^2\theta}{c^2}\right)^2}, \quad (101)$$

$$C_{22} = \frac{3\omega^2r^2\cos^2\theta}{c^2\left(1+\frac{\omega^2r^2\sin^2\theta}{c^2}\right)} - \frac{\omega^4r^4\sin^2\theta\cos^2\theta}{c^4\left(1+\frac{\omega^2r^2\sin^2\theta}{c^2}\right)^2}, \quad (102)$$

$$C_{33} = \frac{3\omega^2r^2\sin^2\theta}{c^2} - \frac{\omega^4r^4\sin^4\theta}{c^4\left(1+\frac{\omega^2r^2\sin^2\theta}{c^2}\right)}, \quad (103)$$

where $C_{12} = C_{21}$ means that the space of the rotating Schwarzschild metric has a certain curvature symmetry.

Using the obtained components of the chr.inv.-Ricci tensor C_{ik} (99–103) and the upper-index components h^{ik} (50) of the chr.inv.-metric tensor, we calculate the physically observable chr.inv.-scalar curvature $C = h^{ik}C_{ik}$ (28) of the space of the rotating Schwarzschild metric. Since only h^{11}, h^{22}, h^{33} are non-zero in such a space, then $C = h^{11}C_{11} + h^{22}C_{22} + h^{33}C_{33}$. After some algebra, we obtain

$$C = \frac{6\omega^2}{c^2\left(1+\frac{\omega^2r^2\sin^2\theta}{c^2}\right)} - \frac{2\omega^4r^2\sin^2\theta}{c^4\left(1+\frac{\omega^2r^2\sin^2\theta}{c^2}\right)^2} + \\ + \frac{r_g}{r^3\left(1+\frac{\omega^2r^2\sin^2\theta}{c^2}\right)} \times \\ \times \left(1 - \frac{3\omega^2r^2\sin^2\theta}{2c^2} + \frac{\omega^4r^4\sin^4\theta}{c^4}\right), \quad (104)$$

where the first two terms are due only to the rotation of space, and the third term (in the second and third lines of the formula) is due to the combined action of the gravitational field and the rotation of space.

This is the *physically observable chr.inv.-scalar curvature* of the three-dimensional space of a rotating massive body. It is this curvature of space that is registered in astronomical observations and laboratory measurements in the space near such rotating massive bodies as stars and planets.

In the absence of a massive island of substance producing the gravitational field ($M = 0$, $r_g = 2GM/c^2 = 0$), the obtained formula (104) transforms into the formula

$$C = \frac{6\omega^2}{c^2\left(1+\frac{\omega^2r^2\sin^2\theta}{c^2}\right)} - \frac{2\omega^4r^2\sin^2\theta}{c^4\left(1+\frac{\omega^2r^2\sin^2\theta}{c^2}\right)^2}, \quad (105)$$

obtained recently in a rotating spherically symmetric space without a gravitational field; see page 45 in the first paper [1] of this series of papers.

At small speeds of rotation, the obtained formula for the chr.inv.-scalar curvature (104) takes the simplified form

$$C = \frac{6\omega^2}{c^2} + \frac{r_g}{r^3}. \quad (106)$$

From the obtained simplified formula for C (106), we see that the rotation of a massive body at slow rotations creates a constant curvature field that does not depend on distance from its source (the rotating body), whereas the gravitational field of the body creates a curvature that decreases inversely proportional to r^3 from it.

If the massive body approximated by a mass-point does not rotate ($\omega = 0$), then the space metric of a rotating massive body (10), which we have introduced and considered here, transforms into the Schwarzschild mass-point metric (6). In this case the obtained formula for the physically observable chr.inv.-scalar curvature (104) transforms into

$$C = \frac{r_g}{r^3}, \quad (107)$$

which is the same as the three-dimensional scalar curvature of a spherically symmetric gravitational field, which Landau and Lifshitz give in their *The Classical Theory of Fields* [11]; see page 325 of §100 in the 4th final English edition, or pages 378–379 of §97 in the 3rd French edition. The only difference is that their curvature has a negative sign. This is because in the years, when they wrote their book (the 1st edition was issued in 1939), Zelmanov's chronometrically invariant formalism had not yet been created. Therefore, Landau and Lifshitz believed that the three-dimensional components g_{ik} of the fundamental metric tensor $g_{\alpha\beta}$ create an observable metric tensor. On the contrary, the chronometrically invariant formalism clearly proves that the physically observable metric tensor that possesses all properties of the fundamental metric tensor throughout the three-dimensional spatial section associated with an observer (his observable three-dimensional space) is $h_{ik} = -g_{ik} + \frac{1}{c^2}v_iv_k$ (15). This is why their curvature of a non-rotating centrally symmetric gravitational field is negative, and the truly physically observable chr.inv.-curvature (107), which we have just deduced using the chronometrically invariant formalism, has a positive sign, as it should be according to the physical sense of this quantity.

Consider a few typical numerical examples of the curvature of space caused by rotating cosmic bodies.

The first typical example is the Sun: $r_\odot \simeq 7.0\times10^{10}$ cm, $M_\odot \simeq 2.0\times10^{33}$ gram, $r_{g\odot} = 2GM_\odot/c^2 \simeq 3.0\times10^5$ cm, $\omega_\odot \simeq$ $\simeq 2.87\times10^{-6}$ sec^{-1} (we are considering the Carrington rotation of the Sun at the equator with a sidereal period of 25.38 days). According to the obtained formula (106), the expected constant curvature of space due to the proper rotation of the Sun is $C = 6\,\omega_\odot^2/c^2 \simeq 5.6\times10^{-32}$ cm^{-2}, while the variable curvature of space due to the gravitational field of the Sun at a distance of one solar radius $r_\odot$ from its centre (i.e., on the Sun's surface) is 4 orders of magnitude greater: $C = r_{g\odot}/r_\odot^3 \simeq$ $\simeq 8.8\times10^{-28}$ cm^{-2}.

Since the curvature of space due to the Sun's rotation is constant, and the curvature due to its gravitational field decreases inversely proportional to r^3 from it, then there is a spherical surface in the cosmos on which these curvatures are equal to each other: $C = r_g/r^3 = 6\,\omega^2/c^2$. For the Sun, this is a spherical surface surrounding the Sun at a distance of

$$r = \sqrt[3]{\frac{c^2 r_{g\odot}}{6\,\omega_\odot^2}} \simeq 1.8\times10^{12}\text{ cm} \simeq 25\,r_\odot\,. \qquad (108)$$

Starting from the distance $r \simeq 1.8\times10^{12}$ cm $\simeq 25\,r_\odot$ from the centre of the Sun, the contribution of the Sun's rotation to the observable curvature of space (it remains constant with distance) exceeds the contribution of the Sun's gravitational field (since it decreases inversely proportional to r^3). For comparison: Mercury, the closest planet to the Sun, orbits the Sun at a distance of $r = 57.9$ mln km $= 82.7\,r_\odot$.

For the Earth ($r_\oplus = 6.37\times10^8$ cm, $M_\oplus = 5.97\times10^{27}$ gram, $r_{g\oplus} = 0.884$ cm, $\omega_\oplus = 7.27\times10^{-5}$ sec^{-1}), the constant curvature of space caused by the Earth's rotation is $C = 6\,\omega_\oplus^2/c^2 \simeq$ $\simeq 3.5\times10^{-29}$ cm^{-2} that is 3 orders of magnitude greater than the constant curvature $C = 6\,\omega_\odot^2/c^2 \simeq 5.6\times10^{-32}$ cm^{-2} caused by the rotation of the Sun. The curvature of space caused by the Earth's gravitational field on the Earth's surface ($r = r_\oplus$) is $C = r_{g\oplus}/r_\oplus^3 \simeq 3.4\times10^{-27}$ cm^{-2}.

At a distance of

$$r = \sqrt[3]{\frac{c^2 r_{g\oplus}}{6\,\omega_\oplus^2}} \simeq 2.93\times10^9\text{ cm} \simeq 29\,300\text{ km} \simeq 4.6\,r_\oplus \qquad (109)$$

from the centre of the Earth (or at an altitude of $h = r - r_\oplus \simeq$ $\simeq 23\,000$ km $\simeq 3.6\,r_\oplus$ above the Earth's surface) the contributions of the Earth's rotation and its gravitational field to the curvature of space become equal to each other. At higher altitudes, the contribution of the Earth's rotation to the curvature of space, since it remains constant with altitude, is greater than the contribution of the Earth's gravitational field (the latter becomes comparatively negligible, since it decreases inversely proportional to r^3).

For our Galaxy ($r \simeq 30\,000$ pc $\simeq 10^{23}$ cm, $M \simeq 2\times10^{11} M_\odot$, $r_g \simeq 6\times10^{16}$ cm, $T \simeq 200$ mln years, $\omega = 2\pi/T \simeq 10^{-15}$ sec^{-1}), the constant curvature of space caused by its rotation is $C =$ $= 6\,\omega^2/c^2 \simeq 7\times10^{-51}$ cm^{-2}, while the curvature caused by its gravitational field at its edge ($r \simeq 30\,000$ pc $\simeq 10^{23}$ cm) is 2 orders of magnitude weaker: $C = r_g/r^3 \simeq 6\times10^{-53}$ cm^{-2}. The distance from the Galactic centre, at which the contribution of the rotation of the Galaxy to the curvature of space becomes equal to the contribution of its gravitational field is

$$r = \sqrt[3]{\frac{c^2 r_g}{6\,\omega^2}} \simeq 2.1\times10^{22}\text{ cm} \simeq 7\,000\text{ parsec}. \qquad (110)$$

The observed frequencies of radio-pulsars are in the range from $\omega_{\min} = 0.53$ to $\omega_{\max} = 4501$ sec^{-1}. Therefore, the constant curvature of space caused by pulsars is in the range of magnitudes from $C \simeq 1.9\times10^{-21}$ to $C \simeq 1.4\times10^{-13}$ cm^{-2}.

	$^*C = \frac{r_g}{r^3}$, cm^{-2}	$^\dagger C = \frac{6\,\omega^2}{c^2}$, cm^{-2}	$^\ddagger r = \sqrt[3]{\frac{c^2 r_g}{6\,\omega^2}}$
Galaxy	6×10^{-53}	7×10^{-51}	7 000 pc
Sun	8.8×10^{-28}	5.6×10^{-32}	$25\,r_\odot$
Earth	3.4×10^{-27}	3.5×10^{-29}	$4.6\,r_\oplus$
Pulsars (min)		1.9×10^{-21}	
Pulsars (max)		1.4×10^{-13}	

*The variable (decreasing) curvature of space caused by the gravitational field of the cosmic body at a distance equal to its radius from its centre.

†The constant curvature of space caused by the rotation of the cosmic body.

‡The distance from the centre of the cosmic body at which the contribution of its rotation to the curvature of space becomes equal to the contribution of its gravitational field.

As a result of the above calculation, we arrive at the following conclusion:

Conclusion on the background curvature of space

The curvature of space caused by the gravitational field of rotating massive bodies decreases inversely proportional to r^3 and, therefore, becomes negligibly small already in the immediate vicinity of these bodies, at a distance of a few of their radii from them. However, the rotation of these bodies creates a constant curvature field, which is much weaker than the curvature caused by their gravitational fields near these bodies, but does not depend on the distance to them. Moreover, such rapidly rotating cosmic objects as pulsars create strong fields of a constant curvature, the magnitude of which is many orders greater than the constant curvature fields caused by other rotating stars and Galaxies.

It seems that the space of the entire Universe is filled with a constant curvature field that is the superposition of the constant curvature fields caused by rapidly rotating cosmic bodies such as pulsars. This is the basis for considering the background space of our Universe as a *constant curvature space*.

This is a very interesting theoretical discovery that requires further study and analysis by astronomers.

5 Einstein's field equations in the space of a rotating massive body

As mentioned on page 81, Einstein's equations are one of the necessary conditions for a space to be Riemannian. Therefore, the considered space metric of a rotating massive body (10) is Riemannian under some particular conditions (*Riemannian conditions*) by which the Einstein equations for this space metric vanish. Now our task is to find out the Riemannian conditions for the space metric (10).

As we showed above (52), the space of a rotating massive body, which we are considering, does not deform ($D_{ik}=0$), and is not filled with any distributed matter such as gas, dust, electromagnetic fields, etc. The latter means that the energy-momentum tensor of distributed matter is zero ($T_{\alpha\beta}=0$) and, hence, the entire right-hand side of the Einstein field equations is zero. With taking the above into account, the chr.inv.-Einstein equations (41–43) take the simplified form

$$A_{jl}A^{lj} + {}^*\nabla_j F^j - \frac{1}{c^2}F_jF^j = 0\,, \tag{111}$$

$${}^*\nabla_j A^{ij} - \frac{2}{c^2}F_jA^{ij} = 0\,, \tag{112}$$

$$2A_{ij}A^{\cdot j}_{k\cdot} - \frac{1}{c^2}F_iF_k + \frac{1}{2}\left({}^*\nabla_i F_k + {}^*\nabla_k F_i\right) - c^2C_{ik} = 0\,. \tag{113}$$

The *1st Riemannian condition* for the space metric of a rotating massive body (10), which we are considering, follows from the obtained scalar chr.inv.-Einstein equation (111). Since $A_{jl}A^{lj} = -A_{jl}A^{jl}$ is the square of the chr.inv.-tensor A_{jl} of the angular velocity of the rotation of space, taken with the opposite sign, and the Zelmanov operator of the chr.inv.-physical divergence (marked with a tilde)

$${}^*\widetilde{\nabla}_j = {}^*\nabla_j - \frac{1}{c^2}F_j\,, \tag{114}$$

gives a divergence that is physically registered by the observer, for instance, ${}^*\widetilde{\nabla}_j F^j$ according to (31) is

$${}^*\widetilde{\nabla}_j F^j = \frac{{}^*\partial F^j}{dx^j} + \Delta^j_{jl}F^l - \frac{1}{c^2}F_jF^j = {}^*\nabla_j F^j - \frac{1}{c^2}F_jF^j, \tag{115}$$

then the scalar chr.inv.-Einstein equation (111) gives:

The 1st Riemannian condition

In the space of a rotating massive body, the physically observable rotation of space is always balanced by the physically observable divergence of the acting gravitational inertial force:

$$A_{jl}A^{jl} = {}^*\widetilde{\nabla}_j F^j, \tag{116}$$

or, which is the same,

$$2\Omega^2 = {}^*\widetilde{\nabla}_j F^j. \tag{117}$$

P.S. The alternative form (117) of the 1st Riemannian condition (116) is obtained using the components of A_{jl} (59–66) that we have calculated earlier in the space of a rotating massive body, after which we have

$$A_{jl}A^{jl} = \frac{2\omega^2}{1+\frac{\omega^2r^2\sin^2\theta}{c^2}} - \frac{3\omega^2 r_g\sin^2\theta}{r\left(1+\frac{\omega^2r^2\sin^2\theta}{c^2}\right)} + \frac{\omega^2 r_g^2\sin^2\theta}{8r^2\left(1+\frac{\omega^2r^2\sin^2\theta}{c^2}\right)\left(1-\frac{r_g}{r}\right)} = 2\Omega^2, \tag{118}$$

where Ω^2 is the square of the physically observable scalar angular velocity Ω (71) with which the space rotates.

The *2nd Riemannian condition* for the space metric of a rotating massive body follows from the obtained vector chr. inv.-Einstein equation (112):

The 2nd Riemannian condition

In the space of a rotating massive body, the physically observable divergence of the rotation of space is always and everywhere equal to zero:

$${}^*\widetilde{\nabla}_j A^{ij} = 0\,, \tag{119}$$

which means that the physically observable rotation of such a space is *homogeneous* (i.e., such a space rotates always and everywhere homogeneously).

P.S. And here is why. Using the definition of the operator of the chr.inv.-physical divergence ${}^*\widetilde{\nabla}_j$ (114) that is physically registered by the observer, we calculate the chr.inv.-physical divergence of the contravariant tensor of the angular velocity of rotation of space A^{ij}. According to the general formula for the chr.inv.-derivative ${}^*\nabla_j$ of an arbitrary contravariant tensor of the 2nd rank (36), we obtain

$${}^*\widetilde{\nabla}_j A^{ij} = \frac{{}^*\partial A^{ij}}{\partial x^j} + \Delta^i_{jl}A^{jl} - \frac{1}{c^2}F_jA^{ij} + \Delta^l_{lj}A^{ij} - \frac{1}{c^2}F_jA^{ij} = {}^*\nabla_j A^{ij} - \frac{2}{c^2}F_jA^{ij}, \tag{120}$$

which completely coincides with the left-hand side of the obtained vector chr.inv.-Einstein equation (112), while the right-hand side of the equation is zero.

The *3rd and 4th Riemannian conditions* for the space metric of a rotating massive body follow from the obtained tensor chr.inv.-Einstein equation (113), re-written in the expanded component notation

$$2A_{1j}A^{\cdot j}_{1\cdot} - \frac{1}{c^2}F_1F_1 + {}^*\nabla_1 F_1 - c^2C_{11} = 0\,, \tag{121}$$

$$2A_{1j}A^{\cdot j}_{2\cdot} - c^2C_{12} = 0\,, \tag{122}$$

$$2A_{2j}A^{\cdot j}_{2\cdot} - c^2C_{22} = 0\,, \tag{123}$$

$$2A_{3j}A^{\cdot j}_{3\cdot} - c^2C_{33} = 0\,, \tag{124}$$

in accordance with the non-zero components of A_{ij}, F_i and C_{ik}, which we have calculated earlier (see above).

So, the *3rd Riemannian condition* follows from the first component (124). It says:

The 3rd Riemannian condition

In the space of a rotating massive body, the physically observable curvature of space in the radial direction $x^1 = r$ from the body is caused by both the physically observable rotation of space (the first term of the equation) and the physically observable divergence of the gravitational inertial force acting in the same radial direction (the second term):

$$2A_{13}A^{\cdot 3}_{1\cdot} + {}^{*}\widetilde{\nabla}_1 F_1 = c^2 C_{11}\,. \tag{125}$$

The *4th Riemannian condition* follows from the rest three non-zero components (122–124) of the tensor chr.inv.-Einstein equation:

The 4th Riemannian condition

In the space of a rotating massive body, the physically observable curvature of space in all other directions from the body, except for the radial direction $x^1 = r$ (in which the gravitational-inertial force acts), is caused only by the physically observable rotation of space:

$$\left.\begin{aligned} &2A_{13}A^{\cdot 3}_{2\cdot} = c^2 C_{12} \\ &2A_{23}A^{\cdot 3}_{2\cdot} = c^2 C_{22} \\ &2\left(A_{31}A^{\cdot 1}_{3\cdot} + A_{32}A^{\cdot 2}_{3\cdot}\right) = c^2 C_{33} \end{aligned}\right\}. \tag{126}$$

P.S. It should be noted that the components A_{13} and A^{31} (59–62) of the chr.inv.-tensor of the angular velocity of rotation of space A_{ij} contain both terms determined only by the rotation of space and terms dependent on $r_g = 2GM/c^2$ (which includes the mass M of the attracting body). This is because the chr.inv.-tensor A_{ij} (18) by definition takes into account the effect of the acting gravitational inertial force F_i onto the tensor A_{ij}, thereby making A_{ij} a truly physically observable quantity dependent on the physical properties of space.

Therefore, when we say a "physically observable rotation of space" or a "physically observable quantity" in general, we mean a chronometrically invariant physical quantity, actually registered by the observer in his real measurements and, therefore, dependent on the physical properties of space.

Finally, summing up the results obtained in this Section of the present work, we can state the following:

Conclusion

Under the four Riemannian conditions deduced above, the space metric of a rotating massive body (10) that we have introduced and studied in this paper satisfies Einstein's field equations (thereby turning them into zero identities) and is therefore proven to be Riemannian and can be used in General Relativity.

The above conclusion has great significance for General Relativity, cosmology and astrophysics. This is because the introduced (and now proven) space metric of a rotating spherical body, approximated by a mass-point, is not only a new metric to General Relativity, which is an extension and replacement of the classical Schwarzschild mass-point metric (which does not take into account the rotation of space). The introduced space metric is the *main space metric in the Universe*, characterizing the physically observable field of any real cosmic body, be it a planet, star, galaxy or something else (since all real cosmic bodies rotate).

6 Deflection of light rays and mass-bearing particles in the space of a rotating massive body

In the previous study [2], we considered massless (light-like) and mass-bearing particles moving in the space of a rotating body, where the gravitational field created by the body was so weak that its influence on the moving particles could be neglected. The solutions obtained for the chronometrically invariant equations of motion of free massless and free mass-bearing particles in the space of a rotating body showed that their physically observable motion should deviate from a straight line due to the curvature of space caused by the rotation of space. In other words, the trajectories of light rays and mass-bearing particles should be deflected near a rotating body due to the curvature of space caused by its rotation.

These are two new fundamental effects of General Relativity, in addition to the deflection of light rays in the field of a gravitating body (known in Einstein's theory from the very beginning).

In the paper [2], the mentioned two new effects were calculated in the space metric of a rotating body, where $g_{00} = 1$, i.e., the gravitational potential is zero $\mathrm{w} = c^2\left(1 - \sqrt{g_{00}}\right) = 0$, in order to show these effects of the rotation of space in their "pure form" (i.e., in the absence of the gravitational field).

Now we are going to calculate these two new effects of General Relativity anew, now in the space of a rotating massive body, the metric of which (10) takes the gravitational field of the rotating body into account: the gravitational potential is $\mathrm{w} \neq 0$ and, hence, $g_{00} < 1$; for details, see the space metric (10) that we are considering. This, in contrast to the abstract case considered in the previous work [2], is a *real physical case*, since all real cosmic bodies in the Universe such as planets, stars, galaxies and something else not only rotate, but also have their own gravitational field.

So, let us begin. The chr.inv.-equations of motion are the physically observable chr.inv.-projections of the general covariant four-dimensional equations of motion onto the time line and the three-dimensional spatial section associated with a particular observer. Such projections are invariant throughout the spatial section of the observer (his physically observable three-dimensional space) and are expressed through the physical properties of his local reference space. A detailed

derivation of the chr.inv.-equations of motion can be found in the monographs [7, 8], the first of which is devoted to free (geodesic) motion of particles, while the second is a study of non-geodesic motion.

The chr.inv.-equations of motion of a free mass-bearing particle have the form

$$\frac{dm}{d\tau} - \frac{m}{c^2} F_i \mathrm{v}^i + \frac{m}{c^2} D_{ik} \mathrm{v}^i \mathrm{v}^k = 0, \tag{127}$$

$$\frac{d(m\mathrm{v}^i)}{d\tau} + 2m\left(D^i_k + A^{\cdot i}_{k\cdot}\right)\mathrm{v}^k - mF^i + m\Delta^i_{nk}\mathrm{v}^n\mathrm{v}^k = 0, \tag{128}$$

and the chr.inv.-equations of motion of a free massless (light-like) particle have the form

$$\frac{d\omega}{d\tau} - \frac{\omega}{c^2} F_i c^i + \frac{\omega}{c^2} D_{ik} c^i c^k = 0, \tag{129}$$

$$\frac{d(\omega c^i)}{d\tau} + 2\omega\left(D^i_k + A^{\cdot i}_{k\cdot}\right)c^k - \omega F^i + \omega\Delta^i_{nk} c^n c^k = 0, \tag{130}$$

where the first (scalar) chr.inv.-equation of motion is the projection of the general covariant equations of motion onto the observer's time line, and the second (vector) chr.inv.-equation of motion is the projection onto his spatial section (his three-dimensional space).

Here m is the relativistic mass of the mass-bearing particle, ω is the relativistic frequency of the massless (light-like) particle, the physically observable time interval $d\tau$ (11) is expressed through the gravitational potential w (12) and the linear velocity of the rotation of space v_i (13) as

$$d\tau = \left(1 - \frac{\mathrm{w}}{c^2}\right)dt - \frac{1}{c^2} v_i dx^i, \tag{131}$$

and the chr.inv.-vector of the physically observable velocity of the particle has the form

$$\mathrm{v}^i = \frac{dx^i}{d\tau}, \qquad \mathrm{v}_i\mathrm{v}^i = h_{ik}\mathrm{v}^i\mathrm{v}^k = \mathrm{v}^2,$$

which, in the case of massless (light-like) particles, transforms into the chr.inv.-vector of the physically observable velocity of light, for which $c_i c^i = h_{ik} c^i c^k = c^2 = const$ (despite the fact that its individual components c^i are variables depending on the properties of space).

Since the space of a rotating massive body, which we are considering, does not deform ($D_{ik} = 0$), then the chr.inv.-equations of motion simplify by vanishing D_{ik}. For a free mass-bearing particle they take the form

$$\frac{dm}{d\tau} - \frac{m}{c^2} F_i \mathrm{v}^i = 0, \tag{132}$$

$$\frac{d(m\mathrm{v}^i)}{d\tau} + 2mA^{\cdot i}_{k\cdot}\mathrm{v}^k - mF^i + m\Delta^i_{nk}\mathrm{v}^n\mathrm{v}^k = 0, \tag{133}$$

while for a massless (light-like) particle they become

$$\frac{d\omega}{d\tau} - \frac{\omega}{c^2} F_i c^i = 0, \tag{134}$$

$$\frac{d(\omega c^i)}{d\tau} + 2\omega A^{\cdot i}_{k\cdot} c^k - \omega F^i + \omega\Delta^i_{nk} c^n c^k = 0. \tag{135}$$

6.1 Solving the chr.inv.-scalar equation of motion

Since the rotating massive body we are considering is not a gravitational collapsar, i.e., its physical radius r is much greater than its gravitational radius ($r \gg r_g$), then according to the formulae for F_i (55) and F^i (56) obtained for the field of a rotating massive body we have

$$F_1 = F^1 = -\frac{c^2 r_g}{2r^2} = -\frac{GM}{r^2}. \tag{136}$$

With this fact taken into account, the scalar equation of motion of a free mass-bearing particle (132), in the case when it travels along the radial direction $x^1 = r$ from the rotating massive body, takes the form

$$\frac{dm}{m} = -\frac{GM}{c^2}\frac{dr}{r^2}, \tag{137}$$

which is a simple differential equation $\frac{dy}{y} = -a\frac{dx}{x^2}$ or, which is the same, $d\ln m = -a\frac{dx}{x^2}$. It solves as $y = Ce^{a/x}$, where the integration constant C in this case is $C = m_{(r=r_0=0)} = m_0$. As a result, we obtain that the scalar equation of motion of a free mass-bearing particle (132) solves as

$$m = m_0 e^{\frac{GM}{c^2 r}} \simeq m_0\left(1 + \frac{GM}{c^2 r}\right). \tag{138}$$

For example, according to the obtained solution, the mass of a body located on the Earth's surface ($M_\oplus = 5.97\times10^{27}$ gram, $r_\oplus = 6.37\times10^8$ cm) is greater than its mass, measured when the body was located at a distance of the Moon's orbit from the Earth ($r = 3.0\times10^{10}$ cm) by a value of $1.5\times10^{-11}\, m_0$ due to the greater magnitude of the Earth's gravitational field potential on the Earth's surface.

The scalar equation of motion of a free massless (light-like) particle (134), when it radially travels in space, solves in the same way. Its solution has the form

$$\omega = \omega_0 e^{\frac{GM}{c^2 r}} \simeq \omega_0\left(1 + \frac{GM}{c^2 r}\right). \tag{139}$$

This solution means that photons gain an additional energy (and frequency) from the gravitational field. For example, a photon with a frequency ω_0 at the moment of emission from the surface of a star has a lower frequency $\omega < \omega_0$ (and energy) when it moves away from this star at some distance. The greater the gravitational field potential (i.e., the closer the photon is to the source of the gravitational field), the more the photon's frequency is redshifted. According to the above so-

lution, the photon's redshift z in the field of a rotating massive body is determined as (where $r_0 < r_1$)

$$z = \frac{\omega_0 - \omega}{\omega} = e^{\frac{GM}{c^2 r_0} - \frac{GM}{c^2 r_1}} - 1 \simeq \frac{GM}{c^2 r_0} - \frac{GM}{c^2 r_1}. \quad (140)$$

So, by solving the chr.inv.-scalar equation of free mass-bearing and massless (light-like) particles we have deduced two effects. First, we have deduced the well-known relativistic effect of the decrease in the mass of a body with height above the Earth's surface (138). Second, we have deduced the gravitational redshift (140), which is also the effect of General Relativity, known from the very beginning and first registered in the spectra of white dwarfs.

Landau and Lifshitz derived these effects from the conservation of energy of a free particle travelling in a stationary gravitational field; for example, see [11, §88]. Zelmanov followed the same way of derivation. However, the new derivation method presented here, based on the integration of the chr.inv.-scalar geodesic equation, allows us to represent the mentioned effects as something not specifically related to the stationary gravitational field, but as general effects of General Relativity that can be calculated in any metric space.

Note that the chr.inv.-scalar equation of motion does not take the rotation of space into account. Therefore, the obtained solutions of the equation (and the effects following from them) coincide with the solutions in a space of the Schwarzschild's mass-point field (which does not rotate).

6.2 Solving the chr.inv.-vector equation of motion

Let us now solve the chr.inv.-vector equation of motion. For a free mass-bearing particle, radially travelling in the space of a rotating massive body, this is the equation (133), while for a massless particle this is the equation (135).

Since the chr.inv.-vector equation of motion depends on the tensor of the angular velocity of rotation of space A_{ik}, we expect that its solution will reveal new effects of General Relativity, previously unknown in the framework of the non-rotating Schwarzschild mass-point metric.

The chr.inv.-vector equations of motion are unsolvable in their general form (133) and (135), because they require substitution of the solutions for the particle's mass m (138) and frequency ω (139) obtained from the chr.inv.-scalar equations of motion, which in turn contain an exponential function of distance r (as a result, each term of the vector equations of motion would contain this complicated function).

Therefore, we will solve the chr.inv.-vector equations of motion in an approximation that the mass-bearing particle's mass m and the massless (light-like) particle's frequency ω remain constant during the travel. This approximation can be used in problems of motion near planets and stars, because, as shown above, the mass m_0 of a body located on the surface of the Earth is only $1.5 \times 10^{-11} m_0$ greater than its mass measured when the body was at the distance of the Moon.

In addition to the assumed approximations $m = const$ and $\omega = const$, we assume, as well as when we solved the scalar equations of motion above, that the rotating massive body that is the source of the gravitational field is not a gravitational collapsar ($r \gg r_g$), so the acting gravitational inertial force is expressed in the simplified form (136).

Moreover, to further simplify the vector equations of motion, we assume that the particle travels at a very high radial velocity v_1 in the equatorial plane along the radial axis $x^1 = r$ towards the origin of the coordinates (the body's centre). For example, it could be a particle falling from the near-Earth space in the equatorial plane onto the Earth's surface. In this case: a) the polar angle is $\theta = \frac{\pi}{2}$ and, therefore, $\cos\theta = 0$ and $\sin\theta = 1$, b) the velocities v^2 and v^3, with which the particle is deflected along the geographical latitudes and longitudes, are negligible compared to its radial velocity v^1.

Finally, we assume that the body that is the source of the field rotates (synchronously with its entire space) with slow linear velocities compared to the velocity of light.

Now we substitute into the chr.inv.-vector equations of motion (133) and (135) the components of the gravitational inertial force F_i (136), the tensor of the angular velocity of rotation of space A_{ik} (59–66), and also the inhomogeneity coefficients of space, a.k.a. the Christoffel symbols Δ^i_{nk} (77–83), which we have calculated above in this paper in accordance with the space metric of a rotating massive body. As a result, after using the above approximations, we obtain the vector equations of motion in component notation.

The resulting chr.inv.-vector equation of motion of a free mass-bearing particle, in component notation derived after some algebra, has the form

$$\left.\begin{aligned} &\frac{d\mathrm{v}^1}{d\tau} - 2\omega r\,\mathrm{v}^3 - r\,\mathrm{v}^2\mathrm{v}^2 - r\,\mathrm{v}^3\mathrm{v}^3 + \frac{GM}{r^2} = 0 \\ &\frac{d\mathrm{v}^2}{d\tau} + \frac{2}{r}\,\mathrm{v}^1\mathrm{v}^2 = 0 \\ &\frac{d\mathrm{v}^3}{d\tau} + \frac{2\omega}{r}\,\mathrm{v}^1 + \frac{2}{r}\,\mathrm{v}^1\mathrm{v}^3 = 0 \end{aligned}\right\}. \quad (141)$$

and for a massless (light-like) particle the resulting chr.inv.-vector equation of motion has the components

$$\left.\begin{aligned} &\frac{dc^1}{d\tau} - 2\omega r c^3 - r c^2 c^2 - r c^3 c^3 + \frac{GM}{r^2} = 0 \\ &\frac{dc^2}{d\tau} + \frac{2}{r}\,c^1 c^2 = 0 \\ &\frac{dc^3}{d\tau} + \frac{2\omega}{r}\,c^1 + \frac{2}{r}\,c^1 c^3 = 0 \end{aligned}\right\}. \quad (142)$$

As can be seen from the equations, the gravitational field of a rotating body makes a contribution in the form of only the last term in the first equation, i.e., it affects the motion of the particle only along the radial direction $x^1 = r$. On the

contrary, the rotation field of this body makes a contribution to the motion of the particle both along the radial axis r and along the equatorial (longitudinal) coordinate axis φ and the latitudinal coordinate axis θ.

As is seen, the vector equations of motion for a mass-bearing particle and a massless (light-like) particle are identical. The only difference is that the equations for a massless (light-like) particle contain the physically observable velocity of light c^i instead of the mass-bearing particle's physically observable velocity v^i. For this reason, we will solve only the equation of motion of a mass-bearing particle (the solution for a massless particle will coincide).

The problem is that this system of differential equations is unsolvable even when considered in the above simplified form. Therefore, we will solve them using the *small parameter method*.

Namely, — we assume that the radially travelling particle gains only a very small increment or decrement α' to its initial numerical value v^1. This allows us to set $\mathrm{v}^1 = const$ in the third equation of the system, which is the equation of motion along the equatorial (longitudinal) axis φ, and in the second equation that is the equation of motion along the latitudinal axis θ. Then, using the obtained solutions of the third and second equations, we will solve the first equation (the equation of motion along the radial axis r) with respect to $\mathrm{v}^1 + \alpha'$, i.e., with respect to the small parameter α.

But even now, without solving the vector equations of motion, but only based on their general form given above, we see that three effects are possible, namely:

1. The deflection of a radially travelling particle along the geographic longitudes due to the influence of the rotation of space (the third equation);
2. The deflection of a radially travelling particle along the geographic latitudes due to the influence of the rotation of space (the second equation);
3. The acceleration or braking of a radially travelling particle in the radial direction due to both the gravitational field and the rotation of space (the first equation).

6.2.1 Solving the third vector equation of motion

The third equation is an equation of motion along the equatorial axis φ. This is a differential equation of the form

$$y' + ay + b = 0, \tag{143}$$

or, which is the same,

$$\varphi'' + a\varphi' + b = 0, \tag{144}$$

where the variable y and the constants used are

$$y = \mathrm{v}^3 = \frac{d\varphi}{d\tau}, \tag{145}$$

$$a = \frac{2}{r}\,\mathrm{v}^1 = const, \quad b = \frac{2\omega}{r}\,\mathrm{v}^1 = const. \tag{146}$$

The above equations (143) and (144) solve as

$$y = \frac{C}{e^{ax}} - \frac{b}{a}, \qquad \varphi = \frac{C_1}{e^{ax}} - \frac{bx}{a} + C_2. \tag{147}$$

Substituting the integration constants, calculated from the initial conditions $x = x_0 = 0$ and $y = y_0 = 0$,

$$C = \frac{b}{a} = \omega, \tag{148}$$

$$C_1 = -\frac{b}{a^2} = -\frac{\omega r}{2\,\mathrm{v}^1}, \quad C_2 = -C_1 = \frac{\omega r}{2\,\mathrm{v}^1}, \tag{149}$$

below we represent the above solutions of the equations (143) and (144) in their final form.

As a result, the obtained solution of the equation (143), which is the physically observable velocity $y = \mathrm{v}^3$ of the radially travelling particle along the equatorial axis φ at the point of arrival on the surface of the rotating body (onto which the particle was falling down from the cosmos along the radial direction r), takes the final form

$$\mathrm{v}^3 = -\omega + \omega e^{-\frac{2}{r}\mathrm{v}^1\tau}. \tag{150}$$

The first term here is the basic equatorial velocity of the particle, the cause of which is the shift of its equatorial coordinate φ towards negative numerical values due to the turn of the rotating massive body during the time of the particle's travel to the body's surface.

The second term is absent in the classical theory. This additional term reveals an additional velocity gained by the free falling mass-bearing particle along the equatorial coordinate φ (geographical longitudes) of the rotating massive body in the direction, opposite to its rotation.

In turn, the obtained solution for the equatorial coordinate φ of the particle's point of arrival, which is the solution of the equation (144), takes the final form as follows

$$\varphi = \varphi_0 - \omega\tau + \frac{\omega r}{2\,\mathrm{v}^1}\left(1 - e^{-\frac{2}{r}\mathrm{v}^1\tau}\right). \tag{151}$$

The first and second terms of the solution are known in the classical theory.

The third, additional term of this solution, unknown in the classical theory, reveals a deflection of the free falling mass-bearing particle along the equatorial coordinate φ (geographical longitudes) of the rotating massive body in the direction, opposite to its rotation.

Respectively, the solutions of the third vector equation of motion for a massless (light-like) particle, such as a photon, have the same form

$$c^3 = -\omega + \omega e^{-\frac{2}{r}c^1\tau}, \tag{152}$$

$$\varphi = \varphi_0 - \omega\tau + \frac{\omega r}{2c^1}\left(1 - e^{-\frac{2}{r}c^1\tau}\right), \tag{153}$$

where the mass-bearing particle's velocity is replaced with the physically observable velocity of light.*

These solutions show another new effect of the rotation of space, which is absent in the classical theory and is revealed by the second term of the solution (152) and the third term of the solution (153). This is an additional deflection of a light ray travelling towards the surface of a rotating massive body, which occurs along the equatorial coordinate φ (geographical longitudes) of the body in the direction, in which the body rotates.

Note that the solutions of the third vector equation of motion, which we have derived above in the field of a rotating massive body with a significant gravitational field, coincide with those derived earlier [2] in the field of a rotating body, the gravitational field can be neglected (i.e., in the absence of the gravitational field). This is because the acting gravitational force takes effect on only the first vector equation of motion (along the radial axis r), but is not included into the second and third vector equations of motion (along the latitudinal polar coordinates θ and the equatorial longitudinal coordinates φ).

For this reason, the numerical examples of the solutions will be identical to those calculated in the previous paper [2] in the absence of the gravitational field. Therefore, we now reproduce the examples here in short from [2].

Thus, the curvature of space caused by the rotation of the Earth around its axis ($\omega_\oplus = 1$ rev/day $= 1.16\times10^{-5}$ rev/sec, $r_\oplus = 6.37\times10^8$ cm) deflects a light ray arriving at the Earth's surface from the Moon ($\tau = 1$ sec) along the geographical longitudes φ in the direction of the Earth's rotation. The angle of deflection of the light ray is†

$$\Delta\varphi = \frac{\omega_\oplus r_\oplus}{2c^1}\left(1 - e^{-\frac{2}{r}c^1\tau}\right) \simeq 1.2\times10^{-7}\,\text{rev} \simeq 0.16'', \quad (154)$$

where the deflection of the light ray is mainly due to the first term, and the second term, depending on the travel time τ, is equal to 1.5×10^{-41} and, therefore, can be neglected.

The magnitude of this effect increases with the radius and rotation velocity of the cosmic body. Thus, a light ray arriving at the Sun ($\omega_\odot = 4.5\times10^{-7}$ rev/sec, $r_\odot = 7.0\times10^{10}$ cm) is deflected by the curvature of space caused by the Sun's rotation by an angle, the numerical value of which is

$$\Delta\varphi \simeq 5.3\times10^{-7}\,\text{rev} \simeq 0.68'', \quad (155)$$

the value of which is much larger in the case of a rapidly rotating star, such as Wolf-Rayet stars or neutron stars.

*Note that, despite the components of the physically observable velocity of light are variables depending on the properties of space, its square remains constant $c_i\,c^i = h_{ik}\,c^i c^k = c^2 = const$).

†In this case, the physically observable velocity of light has a negative numerical value of $c^1 = -3\times10^{10}$ cm/sec, since the velocity of light vector is directed towards the Earth, i.e., opposite to the radial coordinates r measured from the centre of the Earth.

6.2.2 Solving the second vector equation of motion

The second vector equation of motion is an equation of motion along the geographical latitudes, where the latitudinal coordinate θ (polar angle) is measured from the North Pole. This is a differential equation of the form

$$y' + ay = 0, \quad (156)$$

or, with respect to the latitudinal coordinates θ,

$$\theta'' + a\theta' = 0, \quad (157)$$

where the variable y and the constant a are

$$y = \mathrm{v}^2 = \frac{d\theta}{d\tau}, \qquad a = \frac{2}{r}\,\mathrm{v}^1 = const. \quad (158)$$

These equations solve as

$$y = \frac{C}{e^{ax}}, \qquad \theta = \frac{C_1}{e^{ax}} + C_2, \quad (159)$$

where the integration constants are calculated from the initial conditions $x = x_0 = 0$ and $y = y_0 = 0$. They are $C = 0$, $C_1 = 0$ and $C_2 = \theta_0$.

Thus, the final solutions of the second vector equation of motion have the following form

$$\mathrm{v}^2 = 0, \qquad \theta = \theta_0, \quad (160)$$

which means that a particle travelling radially towards the surface of a massive rotating body is not deflected along the geographical latitudes.

6.2.3 Solving the first vector equation of motion

The first vector equation of motion is an equation of motion along the first (radial) coordinate axis r.

This equation contains contributions from both the rotation of space (the second term) and the gravitational field (the last term of the equation). Therefore, its solution will differ from the solution of the first equation of motion in the field of a rotating body, the gravitational field of which can be neglected (i.e., in the absence of the gravitational field).

Assume that the particle's velocity in the radial direction gains only a very small increment or decrement α' to its initial numerical value v^1. In other words, we assume $\mathrm{v}^1 = const$ and, therefore, solve the first vector equation of motion with respect to the sum $\mathrm{v}^1 + \alpha'$, i.e., with respect to the small parameter α.

Taking the obtained solutions $\mathrm{v}^3 = -\omega$ and $\mathrm{v}^2 = 0$ into account, the first vector equation of motion is reduced to

$$\frac{d\,\mathrm{v}^1}{d\tau} + \omega^2 r + \frac{GM}{r^2} = 0, \quad (161)$$

where r is the radius of the rotating body, and M is its mass. This is a differential equation having the form

$$y' + b = 0, \quad (162)$$

or, with respect to the small parameter α,

$$\alpha'' + b = 0, \tag{163}$$

where the variable y and the constant b are

$$y = \alpha', \qquad b = \omega^2 r + \frac{GM}{r^2} = const. \tag{164}$$

The above equations (162) and (163) solve as

$$y = C - bx, \qquad \alpha = -\frac{bx^2}{2} + C_2 x + C_1, \tag{165}$$

where the integration constants, calculated from the initial conditions $x = x_0 = 0$, $\alpha = \alpha_0 = 0$ and $y = y_0 = 0$, are zero. As a result, the solutions of the equations (162) and (163) take their final form

$$\alpha' = -\omega^2 r\tau - \frac{GM}{r^2}\tau, \qquad \alpha = -\frac{\omega^2 r}{2}\tau^2 - \frac{GM}{2r^2}\tau^2. \tag{166}$$

The second terms in the solutions are the contribution of the gravitational field, created by the rotating massive body, which is the well-known effect of the classical theory. The terms reveal, respectively, the additional radial velocity gain by the falling particle (in the solution for α') and also the reduction of the distance travelled by the particle (in the solution for α), all due to the influence of the gravitational field attracting the particle to the rotating body.

However, the first terms in the solutions are absent in the classical theory. They show, respectively, the additional negative radial velocity (in the solution for α') and the stretching in the distance travelled by the particle (in the solution for α) due to the influence of the rotation of space of the gravitating body onto which the particle falls.

We see that here only the rotation of space produces a new effect of General Relativity in addition to the classical theory (i.e., the gravitational field of the rotating body does not produce a new additional effect).

In the absence of the gravitational field, the obtained solutions (166) coincide with those obtained in the previous paper [2] for a particle travelling towards a rotating body, the gravitational field of which can be neglected.

In fact, the new effect revealed by the first terms of the solutions (166) means that a mass-bearing particle or a light ray reaches a rotating massive body later due to the "stretching" of its path of travel due to the curvature of space caused by the rotation of space of the body, i.e., the mass-bearing particle or the light ray arrives at the rotating body with a time delay compared if the body did not rotate.

These new effects are the same for both mass-bearing and massless (light-like) particles. For example, the increment of the path length travelled by a light ray from the Moon to the Earth, and also the delay in its travel time are

$$\alpha = -\frac{\omega_\oplus^2 r_\oplus}{2}\tau^2 \simeq -1.7 \text{ cm}, \tag{167}$$

$$\Delta\tau = \frac{\alpha}{c^1} \simeq 5.7 \times 10^{-11} \text{ sec}, \tag{168}$$

and for a light ray that travelled from the Earth to the Sun the increment of the travelled path length and the delay in its travel time are

$$\alpha = -\frac{\omega_\odot^2 r_\odot}{2}\tau^2 \simeq -6.6 \times 10^4 \text{ cm}, \tag{169}$$

$$\Delta\tau = \frac{\alpha}{c^1} \simeq 2.2 \times 10^{-6} \text{ sec}, \tag{170}$$

which are the same as those calculated in the previous paper [2] in the field of a rotating body, the gravitational field of which can be neglected.

6.2.4 Conclusion

In concluding this Section of the present paper, let us formulate the two new effects of General Relativity calculated here in the field of a rotating massive body:

The 1st new effect of General Relativity

A mass-bearing particle radially falling onto the surface of a rotating body gains an additional velocity, directed along the equatorial coordinate φ (geographical longitudes) of the body in the opposite direction of its rotation, thereby causing a deflection of the particle in the longitudinal direction φ.

In addition, the radially falling mass-bearing particle arrives at the rotating body with a time delay compared if the body did not rotate.

This happens due to the "stretching" of the rotating body's space along the equatorial coordinate φ (along the geographical longitudes) and the radial direction r (towards the body) as a result of the curvature of space, caused by its rotation (together with the body).

The 2nd new effect of General Relativity

A light ray radially spreading towards the surface of a rotating body acquires an additional deflection upon arrival along the equatorial latitudinal coordinate φ of the body in the direction, in which the body rotates.

In addition, the radially spreading light ray arrives at the rotating body with a time delay compared if the body did not rotate.

This deflection of the light ray and the delay in its arrival at the rotating body occurs due to the "stretching" of the rotating body's space along the equatorial coordinate φ (along the geographical longitudes) and the radial direction r (towards the body), which are the result of the curvature of space, caused by its rotation (together with the body).

The physical origin of the new effects is obvious from our above calculation of the curvature of space, which we found to be caused by not only the gravitational field but also the rotation of space:

On the origin of the new effects

As has been found, the rotation of any body curves space in the direction of its rotation and to the centre of this body (the centre of rotation), thereby creating a "slope of the hill" slowing "down" along the equator in the direction, in which this body rotates, and also to the centre of this body.

In addition, the gravitational field created by the rotating body also curves space, making its own contribution in the form of the curvature of space towards the body's centre.

As a result, due to the created curvature of space, a mass-bearing particle or a light ray freely travelling towards a rotating massive body "rolls down the curvature hill" of space along the equator of the body in the direction of the body's rotation (the contribution of the rotation of space), and also "rolls" towards the centre of the body (the combined contribution of the rotation of space and the gravitational field).

7 Length stretching and time loss/gain in the space of a rotating massive body

According to the chronometrically invariant formalism, the three-dimensional physically observable chr.inv.-interval $d\sigma$ (14) and the physically observable time interval $d\tau$ (11)

$$d\sigma^2 = h_{ik}\,dx^i dx^k, \quad d\tau = \left(1 - \frac{\mathrm{w}}{c^2}\right)dt - \frac{1}{c^2}\,v_i\,dx^i \quad (171)$$

depend on the chr.inv.-metric tensor $h_{ik} = -g_{ik} + \frac{1}{c^2}\,v_i v_k$ (15), the gravitational field potential w (12) and the linear velocity of the rotation of space v_i (13). Thus, we can calculate $d\sigma$ and $d\tau$ in the space of any particular metric, for which we have previously calculated the quantities h_{ik}, w and v_i.

Let us now calculate the length of a rigid rod and the time interval in the field of a rotating massive body.

7.1 Length stretching

Let us substitute into the formula for $d\sigma$ the non-zero components h_{ik} (47) that we have calculated according to the space metric of a rotating massive body (10).

Thus, we obtain the physically observable length dl of a rigid rod, installed in stages along each of the coordinates

$$dl_r = \sqrt{h_{11}\,dr^2} = \frac{dr}{\sqrt{1 - \frac{r_g}{r}}} = \frac{dl_0}{\sqrt{1 - \frac{r_g}{r}}}, \quad (172)$$

$$dl_\theta = \sqrt{h_{22}\,d\theta^2} = r\,d\theta = dl_0, \quad (173)$$

$$dl_\varphi = \sqrt{h_{33}\,d\varphi^2} = \sqrt{1 + \frac{\omega^2 r^2 \sin^2\theta}{c^2}}\; r\sin\theta\,d\varphi = \sqrt{1 + \frac{\omega^2 r^2 \sin^2\theta}{c^2}}\; dl_0, \quad (174)$$

where $dr = dl_0$ is the length of an elementary segment along the radial axis r, $r\,d\theta = dl_0$ is the length of an elementary arc along the latitudinal axis θ (the polar angle θ is measured from the North Pole), and $r\sin\theta\,d\varphi = dl_0$ is the length of an elementary arc along the equatorial latitudinal axis φ.

As is seen from the above calculation, a rigid rod located in the field of a rotating massive body (say, in the field of the Earth or the Sun) retains its original physically observable length dl_0, when installed along the geographical latitudes ($dl_\theta = dl_0$).

In contrast, when the rod installed in the position along the radial coordinate r, i.e., in the direction towards the centre of the rotating massive body (along its radius), its physically observable length dl_r is greater than its original length dl_0 by a small value δl_r

$$dl_r = \sqrt{h_{11}\,dr^2} = \frac{dl_0}{\sqrt{1 - \frac{r_g}{r}}} \simeq \left(1 + \frac{r_g}{2r}\right)dl_0, \quad (175)$$

$$\delta l_r \simeq \frac{r_g}{2r}\,dl_0 \simeq \frac{1}{2}\,C\,r^2 dl_0, \quad (176)$$

which is determined by the curvature of space $C = \frac{r_g}{r^3}$ caused by the gravitational field of the rotating body. See the second term in the formula for the physically observable curvature C (106) of the space of a rotating massive body, which we have derived above in this paper.

And also, when the rod is installed in the position along the equatorial coordinate φ, i.e., in the direction along the geographical longitudes along which the massive body (say, the Earth or the Sun) rotates around its own axis, its physically observable length dl_φ is greater than its original length dl_0 by a small value δl_φ

$$dl_\varphi = \sqrt{1 + \frac{\omega^2 r^2 \sin^2\theta}{c^2}}\; dl_0 \simeq \left(1 + \frac{\omega^2 r^2 \sin^2\theta}{2c^2}\right)dl_0, \quad (177)$$

$$\delta l_\varphi \simeq \frac{\omega^2 r^2 \sin^2\theta}{2c^2}\,dl_0 \simeq \frac{1}{12}\,C\,r^2 \sin^2\varphi\,dl_0, \quad (178)$$

determined by the curvature of space $C = \frac{6\omega^2}{c^2}$ created by its rotation (together with the massive body) and is expressed with the first term in the formula for the physically observable curvature C (106), which we have derived in this paper.

As a result of the above derivation, we obtain the 3rd new effect of General Relativity:

The 3rd new effect of General Relativity

A rigid rod installed along the radial coordinate in the field of a rotating massive body (i.e., in the direction to the body's centre) acquires an additional length. This additional length is determined by the curvature of the body's space caused by its gravitational field.

In addition, if the rod is installed along the equatorial coordinate φ (i.e., along the geographical longi-

tudes of the body), then its length acquires an additional length determined by the curvature of the body's space caused by its rotation.

This effect of length stretching of a rod in the field of a rotating massive body is due to the "stretching" of the body's space along the radial direction r (towards the body) caused by its gravitational field, and along the equatorial coordinate φ (along the geographical longitudes), caused by the rotation of the body's space (together with the body).

In other words, a rod in the field of a rotating massive body is "stretched" together with the "stretching" of the coordinate grid of space in the radial and equatorial directions. The "stretching" of the grid of space in the radial direction occurs due to the curvature of the body's space (the funnel of space) in this direction, caused by its gravitational field. Whereas the "stretching" of the coordinate grid of space along the equatorial coordinates is caused by the curvature of the body's space due to its rotation in this direction.

For example, the length stretching of a rod installed at the equator of the Earth ($\omega_\oplus = 1$ rev/day $= 7.27 \times 10^{-5}$ sec^{-1}, $r_\oplus = 6.37 \times 10^8$ cm) in the direction along the longitudinal axis φ, i.e., along the equator, has a numerical value of

$$\delta l_\varphi \simeq \frac{\omega_\oplus^2 r_\oplus^2 \sin^2\theta}{2c^2}\, dl_0 \simeq 1.2 \times 10^{-12}\, dl_0 \qquad (179)$$

of the original length dl_0 of the rod.

The length stretching of a rod installed vertically on the Earth's surface, has a numerical value of

$$dl_r \simeq \frac{r_{g\oplus}}{2r_\oplus}\, dl_0 \simeq 7.0 \times 10^{-10}\, dl_0\,. \qquad (180)$$

This length stretching effect is maximum at the equator, where the curvature and "stretching" of the Earth's space caused by the Earth's gravitational field are maximum (since the Earth is oblate towards the equator), and the curvature and "stretching" of the Earth's space caused by the Earth's rotation are also maximum. This length stretching effect decreases towards the geographical poles, where the length stretching caused by the rotation of the Earth's space vanishes (since $\sin\theta = 0$ at the poles), and the length stretching caused by the gravitational field is a little lesser than at the equator.

7.2 Time loss/gain

Let us now substitute into the general formula for the physically observable interval $d\tau$ the gravitational potential w (54) and the linear velocity of the rotation of space $v_3 = \omega r^2 \sin^2\theta$ (45) that we have calculated above in this paper among the other characteristic of the space metric of a rotating massive body (10).

Thus, we obtain the physically observable time interval $d\tau$, which will be registered by an observer travelling along the equatorial direction φ (i.e., along the geographical longitudes) in the space of a rotating massive body

$$d\tau = \sqrt{1 - \frac{r_g}{r}}\, dt - \frac{1}{c^2}\, v_3\, u^3\, dt = \\ = \sqrt{1 - \frac{r_g}{r}}\, dt - \frac{\omega r^2 \sin^2\theta}{c^2}\, u^3\, dt\,, \qquad (181)$$

where $u^3 = \frac{d\varphi}{dt}$ is the coordinate velocity of the observer in the equatorial direction $x^3 = \varphi$, along which he travels.

The first term in this formula determines the known effect of time loss due to the curvature of the body's space $C = \frac{r_g}{r^3}$ caused by its the gravitational field: the stronger the gravitational field (the closer the observer is to a massive body), the shorter the time intervals registered by him

$$d\tau = \sqrt{1 - \frac{r_g}{r}}\, dt \simeq \left(1 - \frac{r_g}{2r}\right) dt\,, \qquad (182)$$

$$\delta\tau \simeq -\frac{r_g}{2r}\, dt \simeq -\frac{1}{2}\, C r^2 dt\,. \qquad (183)$$

In other words, this is the known effect of the classical theory: the higher the observer is above the surface of a massive body, the weaker the curvature of the body's space and, consequently, the shorter the time intervals that the observer records.

However, the second term of (181) is absent in the classical theory. This term reveals the increment of the physically observable time, which is due to the curvature of the body's space $C = \frac{6\omega^2}{c^2}$ caused by its rotation (together with the massive body itself)

$$\delta\tau = -\frac{\omega r^2 \sin^2\theta}{c^2}\, u^3 dt = -\frac{C r^2 \sin^2\theta}{6\omega}\, u^3 dt\,. \qquad (184)$$

The sign of this effect depends on the direction, in which the observer travels with respect to the rotation of space, i.e., on the sign of the observer's coordinate velocity u^3 (he travels along the equatorial axis $x^3 = \varphi$).

As a result, based on the second term in the obtained solution, we obtain the 4th new effect of General Relativity in addition to those three explained above. This effect says:

The 4th new effect of General Relativity

A clock on board an airplane (or a spacecraft) flying in the field of a rotating massive body in the same direction in which the body's space rotates (together with the body itself) should register a time loss depending on the airplane's (or a spacecraft's) velocity and the rotation velocity of the body's space.

In contrast, a clock on board an airplane (or a spacecraft) flying in the direction, opposite to the body's space rotation should register a time increment, as well depending on the airplane's (or a spacecraft) velocity and the velocity, with which the body's space rotates.

This effect of time loss/gain in the field of a rotating massive body is due to the "stretching" of the body's space along the equatorial direction φ (along the geographical longitudes), caused by the rotation of the body's space along this axis. When, say, an airplane flies towards the Earth's rotation, the magnitude of the total rotation of space registered on its board is less than the proper rotation of the Earth's space at the point of departure/arrival and, therefore, the "stretching" (and curvature) of space registered on board the airplane is also less. In contrast, when an airplane flies backwards the Earth's space rotation, the clock on its board registers a time increment due to the greater magnitude of the total rotation and, therefore, greater "stretching" (and curvature) of space.

For example, consider a typical commercial flight travelling at 10 000 m along the Earth's equator ($\omega_\oplus = 1$ rev/day $= 7.27 \times 10^{-5}$ sec^{-1}, $r_\oplus = 6.37 \times 10^8$ cm) at a typical cruising speed of 800 km/hour, which means a flight time around the globe of $t \simeq 1.8 \times 10^5$ sec. Since the planet Earth rotates from West to East, the above 800 km/hour mean that the airplane's velocity is $u^3 = +3.5 \times 10^{-5}$ sec^{-1} when flying Eastward and $u^3 = -3.5 \times 10^{-5}$ sec^{-1} when flying Westward.

Then, according to the second term (184) in the obtained solution for $d\tau$ (181) we have obtained in the field of a rotating massive body, a clock installed on board the airplane should register a time loss of

$$\delta\tau_{\text{East}} = -\frac{\omega_\oplus r_\oplus^2 \sin^2\theta}{c^2}\, u^3 t \simeq -210 \text{ nanosec}, \qquad (185)$$

when flying to the East (i.e., in the same direction, in which the Earth's space rotates), and also a time increment

$$\delta\tau_{\text{West}} = +\frac{\omega_\oplus r_\oplus^2 \sin^2\theta}{c^2}\, u^3 t \simeq +210 \text{ nanosec}, \qquad (186)$$

when flying to the West (i.e., oppositely to the rotation of the Earth's space).*

This effect is maximum at the equator (where the curvature of the Earth's space caused by its rotation is maximum and, therefore, space is maximally "stretched") and decreases towards the poles, where $\sin\theta = 0$ and, therefore, this effect vanishes.

This effect was first registered in the "around-the-world-clock experiment", conducted in 1971 by Joseph C. Hafele and Richard E. Keating [12–14] and then repeated in 2005 by the UK's National Measurement Laboratory [15], despite the fact that they did not know about the chronometrically invariant formalism and the effects caused by the rotation of space; I discussed this issue in extensive friendly correspondence with Joseph C. Hafele in the last years of his life, before he passed away in 2014 [16]. Their flights took place in the Northern Hemisphere (not at the equator) and at different altitudes. In addition, the results of their measurements were affected by the relativistic addition of the airplane's velocity to the Earth's rotation velocity when flying Eastward (and subtraction when flying Westward), as well as the decrease in the Earth's gravitational potential with flight altitude. That is their measurement results were not purely the effect of the rotation of space. The total effect registered in the Hafele-Keating experiment was a time loss of -59 ± 10 nanoseconds when flying Eastward and a time increment of $+273 \pm 7$ nanoseconds when flying Westward, which fits well with our above calculation of the new effect due to the rotation of space, if we take into account the relativistic addition of the airplane's velocity to the Earth's rotation velocity when flying Eastward and subtraction when flying Westward.

*The calculated numerical values are the same as those calculated in the previous paper [3] in the absence of the gravitational field, since the gravitational field produces an individual effect, expressed by the first term of the obtained solution for $d\tau$ (181).

8 Conclusion

The main contribution of this paper is introducing and proving the space metric of a rotating massive body, approximated by a mass-point. This is a new space metric to General Relativity, the main purpose of which is to be a modern extension and replacement of the classical Schwarzschild mass-point metric (since in the space of the Schwarzschild metric a massive body creating gravitational field does not rotate).

We have proven that the introduced space metric of a rotating massive body satisfies Einstein's field equations, and also derived the Riemann conditions under which this occurs. Therefore, the introduced metric can be legitimately used in General Relativity.

We have calculated all known physically observable properties of space determined by the introduced metric of a rotating massive body, including the physically observable curvature of space. And here is what is especially interesting: we have found that the curvature of space is caused not only by the gravitational field filling it, but also by the rotation of space (together with the massive body). Based on this theoretical discovery, we have predicted and calculated four new effects of General Relativity:

1. Deflection along the equatorial coordinate and time delay of mass-bearing particles falling onto a rotating massive body, which is due to the "stretching" (curvature) of space, caused by its rotation (together with the body itself);
2. Deflection along the equatorial coordinate and time delay of light rays spreading to a rotating massive body, which is due to the "stretching" (curvature) of space, caused by its rotation;
3. Length stretching of a rod installed along the radial and equatorial coordinates in the field of a rotating massive body due to the "stretching" (curvature) of space in these directions, caused by its rotation;

4. The loss of time in a clock travelling in the direction of the body's space rotation, which is due to the increase in the "stretching" (curvature) of space in the direction of its rotation, and accordingly the increment of time when the clock travels oppositely to the rotation of space.

All real cosmic bodies in the Universe rotate. Therefore, the introduced and proved space metric is the *main space metric in the Universe*, characterizing the field of any real cosmic body, be it a planet, star, galaxy or something else.

Feel free to use this new metric instead of the classical Schwarzschild metric to solve problems in General Relativity and astrophysics, if you have the necessary mathematical skills and wishes to do so, of course.

Submitted on September 28, 2024

References

1. Rabounski D. and Borissova L. Non-quantum teleportation in a rotating space with a strong electromagnetic field. *Progress in Physics*, 2022, v. 18, issue 1, 31–49.
2. Rabounski D. and Borissova L. Deflection of light rays and mass-bearing particles in the field of a rotating body. *Progress in Physics*, 2022, v. 18, issue 1, 50–55.
3. Rabounski D. and Borissova L. Length stretching and time dilation in the field of a rotating body. *Progress in Physics*, 2022, v. 18, issue 1, 62–65.
4. Zelmanov A. L. Chronometric Invariants. Translated from the 1944 PhD thesis, American Research Press, Rehoboth, New Mexico, 2006.
5. Zelmanov A. L. Chronometric invariants and accompanying frames of reference in the General Theory of Relativity. *Soviet Physics Doklady*, 1956, v. 1, 227–230 (translated from *Doklady Academii Nauk USSR*, 1956, v. 107, issue 6, 815–818).
6. Zelmanov A. L. On the relativistic theory of an anisotropic inhomogeneous universe. *The Abraham Zelmanov Journal*, 2008, vol. 1, 33–63 (translated from the thesis of the *6th Soviet Conference on the Problems of Cosmogony*, USSR Academy of Sciences Publishers, Moscow, 1957, 144–174).
7. Rabounski D. and Borissova L. Particles Here and Beyond the Mirror. The 4th revised edition, New Scientific Frontiers, London, 2023 (the 1st edition was issued in 2001).
   Rabounski D. et Larissa Borissova L. Particules de l'Univers et au delà du miroir. La 2ème édition révisée en langue française, New Scientific Frontiers, Londres, 2023.
8. Borissova L. and Rabounski D. Fields, Vacuum, and the Mirror Universe. The 3rd revised edition, New Scientific Frontiers, London, 2023 (the 1st edition was issued in 2001).
   Borissova L. et Rabounski D. Champs, Vide, et Univers miroir. La 2ème édition révisée en langue française, New Scientific Frontiers, Londres, 2023.
9. Borissova L. and Rabounski D. Inside Stars. The 3rd edition, revised and expanded, New Scientific Frontiers, London, 2023 (the 1st edition was issued in 2013).
10. Rabounski D. and Borissova L. Physical observables in General Relativity and the Zelmanov chronometric invariants. *Progress in Physics*, 2023,v. 19, issue 1, 3–29.
11. Landau L. D. and Lifshitz E. M. The Classical Theory of Fields. First published in 1939 in Russian, and then in 1951 in English (Pergamon Press, Oxford). The section and page references are given here from the final, 4th, twice expanded and revised English edition (1979, Butterworth-Heinemann, Oxford).
    Landau L. et Lifchitz E. Théorie des champs. Première édition en français, Éditions MIR, Moscou, 1964. Publié pour la première fois en 1939 en russe. Les références des sections et pages sont données à partir de la dernière 3ème édition française, révisée et augmentée deux fois (1970, Éditions MIR, Moscou).
12. Hafele J. Performance and results of portable clocks in aircraft. PTTI 3rd Annual Meeting, November 16–18, 1971, 261–288.
13. Hafele J. and Keating R. Around the world atomic clocks: predicted relativistic time gains. *Science*, July 14, 1972, v. 177, 166–168.
14. Hafele J. and Keating R. Around the world atomic clocks: observed relativistic time gains. *Science*, July 14, 1972, v. 177, 168–170.
15. Demonstrating relativity by flying atomic clocks. *Metromnia*, the UK's National Measurement Laboratory Newsletter, issue 18, Spring 2005.
16. Rabounski D. and Borissova L. In memoriam of Joseph C. Hafele (1933–2014). *Progress in Physics*, 2015, v. 11, issue 2, 136.

Galaxy Clusters: Quantum Celestial Mechanics (QCM) Rescues MOND?

Franklin Potter

Sciencegems, 8642 Marvale Drive, Huntington Beach, CA, USA. E-mail: frank11hb@yahoo.com

Although the MOND radial acceleration $g = \sqrt{g_N a_0}$ for the acceleration of objects in a low acceleration environment less than $a_0 = -1.2 \times 10^{-10}\,\mathrm{m/s^2}$ has been extremely successful for single galaxies, the much higher mass clusters of galaxies do not have enough baryonic mass to comply. We consider the possibility that the MOND a_0 value, instead of being a universal constant, actually depends upon both the total baryonic mass of the gravitationally bound system and its total angular momentum, as derived by Quantum Celestial Mechanics (QCM) from the general relativistic Hamilton-Jacobi equation. If the total angular momentum of the galaxy cluster is less than expected, then the MOND radial acceleration expression can remain valid.

1 Introduction

Galaxy rotation velocities do not match Newton's Law of Universal Gravitation, $g = -GM/r^2$, for stars experiencing low gravitational radial accelerations [1]. The stars at all large orbital radii where the radial acceleration is less than about 10^{-10} m/s^2 are moving at nearly identical velocities instead of decreasing to the lower velocity values predicted by Newton's Law.

Initial attempts to alter Newton's Law failed, so the dark matter hypothesis became the alternative explanation with the consequence that Newton's Law could apply once again [2]. However, two important challenges to dark matter continue to exist: (1) no predicted dark matter particle has ever been detected in at least 50 years of experimental searches [3, 4], and (2) a modification of gravitation called MOND (MOdified Newtonian Dynamics) exists and agrees extremely well with single galaxy rotation curves [5] and has predicted many other physical properties that have been found to hold true for single galaxies and other gravitationally bound systems [6,7].

Even though fitting the rotation curves of single galaxies is remarkably successful, MOND does not fit the radial acceleration values for clusters of galaxies [8,9]. There is a significant disagreement with the MOND gravitational acceleration expression

$$g = \sqrt{g_N a_0}\,, \tag{1}$$

where the MOND acceleration constant $a_0 = -1.2 \times 10^{-10}$ m/s^2 and $g_N = -GM(< r)/r^2$ is the Newtonian acceleration for enclosed baryonic mass M. This gravitational expression using the a_0 value has been shown to hold true for all single galaxies and is assumed to be true for clusters of galaxies.

However, the measurements for galaxy clusters reveal that the observed acceleration g_{obs} is greater than the acceleration value g predicted by this MOND expression at the low radial acceleration environments where the expression should be true. Fig. 1 shows the discrepancy between the dynamic mass and all the observed mass of the baryons in the gas and the stars within the cluster, with the data from [8]. Some clusters need as much as a factor of 5 more baryonic mass for the MOND expression to hold true, i.e., be at the straight line where the dynamic mass and the observed mass values agree.

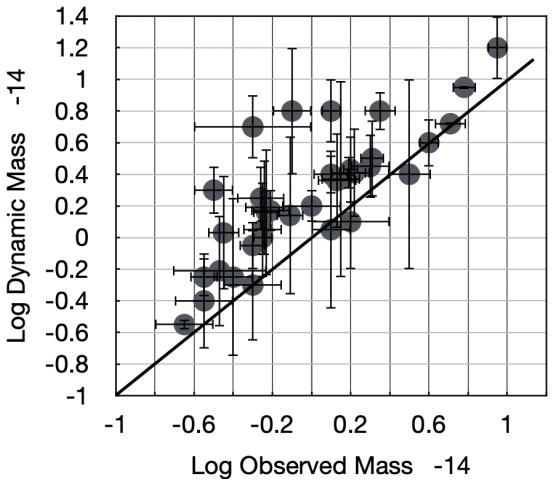

Fig. 1: Log scales around 10^{14} solar masses for galaxy clusters. If MOND is to prevail with its constant a_0 value, all the clusters should be at the straight line. Data is a representative selection from Sanders (2003).

This discrepancy between g_{obs} and the MOND predicted g has been attributed to missing baryonic mass M in the cluster, but several searches have not found any more mass than already determined. Consequently, to fit the actual observed radial accelerations for all galaxy clusters, a distribution of dark matter has been proposed so that Newton's Law applies to galaxy clusters.

We propose a different explanation for the acceleration discrepancy, one that allows the MOND acceleration expression $g = \sqrt{g_N a_0}$ to be correct for galaxy clusters as well as for single galaxies. In 2003, H. G. Preston and I investigated [10] an approach to gravitation that we called quantum celestial mechanics (QCM) in which the general relativistic Hamilton-Jacobi equation is converted into a new scalar gravitational wave equation (GWE). In different metrics the GWE allows

us to propose some new explanations for specific types of gravitational behavior.

In the Schwarzschild metric the GWE leads to the quantization of angular momentum *per unit mass* because both Newtonian gravitational attraction and a QCM gravitational repulsion exists for orbiting bodies. All confirmed planetary systems, including the Solar System, have been shown to agree with this QCM prediction [11], i.e. the orbital planetary equilibrium radii of the multi-planetary systems are only at the QCM predicted subset of all possible equilibrium radii that are allowed by Newton's Law.

We also derived the above MOND gravitational expression, which revealed that the MOND acceleration a_0 will have slightly different values in different single galaxies depending on the total baryonic mass M_T of the gravitationally bound system and its total angular momentum L_T,

$$a_0 = \frac{G^3 M_T^7}{n^4 L_T^4}\,, \tag{2}$$

with n an integer.

This dependency of a_0 upon both M_T and L_T will allow us to re-interpret the MOND expression for g so that clusters of galaxies, as well as single galaxies, satisfy $g_{obs} = g$ without the need for dark matter.

2 Derivation of QCM and MOND, a brief review

From the general relativistic Hamilton-Jacobi equation,

$$g^{\alpha\beta}\,\frac{\partial S}{\partial x^\alpha}\,\frac{\partial S}{\partial x^\beta} - \mu^2 c^2 = 0 \tag{3}$$

the transformation

$$\Psi = e^{iS'/\mu cH} \tag{4}$$

introduces a wave function Ψ, with S the action, μ the mass of the orbiting object, and $S' = S/\mu c$ so that the equivalence principle is obeyed. For a detailed derivation, see [10]. Here we have defined a system scale length H by

$$H = \frac{L_T}{M_T c} \tag{5}$$

for the total gravitationally bound system mass M_T having total angular momentum L_T and c being the speed of light in vacuum.

Following through with the mathematical steps produces a scalar gravitational wave equation (GWE)

$$g^{\alpha\beta}\,\frac{\partial^2\Psi}{\partial x^\alpha \partial x^\beta} + \frac{\Psi}{H^2} = 0\,. \quad \text{(GWE)} \tag{6}$$

Expressing the GWE in the Schwarzschild metric, a separation of variables leads to differential equations in coordinates (t, r, θ, ϕ) that produce quantization conditions. The angular parts dictate the quantization of angular momentum *per unit mass* for orbital angular momentum L as

$$\frac{L}{\mu} = mcH \tag{7}$$

for integer m. The radial equation leads to the quantization of energy per unit mass

$$E_n = -\mu c^2\,\frac{r_g^2}{8n^2H^2} \tag{8}$$

for integer n.

Using the virial theorem and E_n, we obtain the velocity v in terms of the Schwarzschild radius r_g and H,

$$v = \frac{r_g c}{2nH}\,. \tag{9}$$

Whence, with the radial acceleration $g = v^2/r$, we derive the MOND acceleration expression from

$$g = \frac{r_g^2 c^2}{4n^2H^2 r} = \sqrt{\frac{GM}{r^2}\left(\frac{G^3M_T^7}{n^4L_T^4}\right)}. \tag{10}$$

Therefore, the MOND acceleration a_0 is not a universal constant but is determined to be

$$a_0 = \frac{G^3 M_T^7}{n^4 L_T^4}\,, \tag{11}$$

explicitly expressing its dependency upon both the total mass M_T of the system and its total angular momentum L_T.

3 Discussion

We have begun with the successful MOND espression $g = \sqrt{g_N a_0}$ using $a_0 = -1.2\times10^{-10}$ m/s^2, with a_0 having this value for all single galaxies. But if we assume that a_0 has this same value for galaxy clusters, then the baryonic mass discrepancy shown in Fig. 1 arises.

According to QCM, there can be two possible causes for the discrepancy between the observed radial acceleration g_{obs} and the predicted MOND value g in the galaxy clusters, the values of total baryonic mass value M_T and the total angular momentum L_T. All the baryonic mass M_T in the gas and stars, etc., has been identified. However, we do not know the total angular momentum L_T of any galaxy cluster.

QCM predicts that the a_0 value depends upon the ratio M_T^7/L_T^4. We already know the baryonic M_T for the clusters, but there are no published values of L_T for any cluster. Therefore, we must estimate the L_T values for different galaxy clusters if the MOND $g = g_{obs}$ is to hold true.

In some clusters of galaxies the dynamical mass M_{dyn} has been determined to be as much as a factor of 5 larger than the actual observed mass M_{obs} of the hot gas and the stellar content. Therefore, the ratio M_T^7/L_T^4 for a_0 in these galaxy clusters must be up to 5 times larger than for single galaxies in order to have $g_{obs} = \sqrt{g_N a_0}$.

We assume that the expected L_T value is the one that makes the MOND $a_0 = -1.2\times10^{-10}$ m/s^2. Then in the general case, if there is a factor f reduction in the baryonic mass

M_T, QCM requires

$$fa_0 = \frac{G^3 M_T^7}{n^4 L_T^4} \tag{12}$$

which, for n = 1 and $M_{obs} = M_T/f$, means

$$L_T^4 = \frac{G^3 M_{obs}^7}{f^8 a_0}\,. \tag{13}$$

For example, if $f = 2$, the L_T value would be 4 times smaller than expected for the M_{obs}. This L_T value then makes the product $g_N a_0$ guarantee $g = g_{obs}$. Thus. each galaxy cluster could have a unique a_0 value.

There exists several possible sources of a lower angular momentum total than expected:

1. the intracluster (IC) gas that comprises about 90% of the baryonic mass of the cluster could, in part or as a whole, have a slower rotation speed than gas in single galaxies,
2. the IC stars are known to rotate slower than many stars,
3. the angular momentum vectors of the galaxies in the cluster may have a greater variety of directions than expected, thereby decreasing their vector sum.

Whether any or all of these possible sources of lower angular momentum are the cause of the different a_0 values for the galaxy clusters has yet to be determined.

4 Conclusion

Recent measurements have verified that there is not enough baryonic mass for the successful MOND gravitational acceleration expression for single galaxies

$$g = \sqrt{g_N a_0} \tag{14}$$

to be true for clusters of galaxies, where g_N is the Newtonian gravitational radial acceleration and the MOND $a_0 = -1.2 \times 10^{-10}$ m/s^2 is assumed to be a universal constant.

However, a_0 may not be a universal constant as originally proposed. We briefly reviewed the quantum celestial mechanics (QCM) derivation of a_0 from the general relativistic Hamilton-Jacobi equation to obtain the acceleration

$$g = \frac{r_g^2 c^2}{4n^2 H^2 r} = \sqrt{\frac{GM}{r^2}\left(\frac{G^3 M_T^7}{n^4 L_T^4}\right)}. \tag{15}$$

Therefore, QCM dictates

$$a_0 = \frac{G^3 M_T^7}{n^4 L_T^4}\,, \tag{16}$$

showing that a_0 depends upon both the total baryonic mass M_T and its total angular momentum L_T of any gravitationally bound system obeying the Schwarzschild metric. For single galaxies, this QCM expression for a_0 varies less than a few percent and therefore a_0 can be assumed universal.

However, in more massive gravitationally bound systems such as clusters of galaxies, a_0 could have different values in order to satisfy the MOND expression $g = \sqrt{g_N a_0}$. If galaxy clusters possess significantly less angular momentum than is expected for the measured total baryonic mass, this MOND expression can be satisfied still. Several possible reasons for the lesser total angular momentum values were suggested.

We await total angular momentum estimates for galaxy clusters in the near future to establish whether the MOND acceleration a_0 has a different value for galaxy clusters and whether the MOND expression $g = \sqrt{g_N a_0}$ continues to hold true.

Acknowledgements

We thank Sciencegems for continued support and encouragement to investigate various challenges in gravitation.

Received on September 26, 2024

References

1. Rubin V. C., Ford W. K. Jr., Thonnard N. Rotational properties of 21 SC galaxies with a large range of luminosities and radii, from NGC 4605 (R=4kpc) to UGC 2885 (R=122kpc). *Astrophysical J.*, 1980, v. 238, 471–487.
2. Navarro J. F., Frenk C. S., White S. D. M. The Structure of Cold Dark Matter Halos. *The Astrophysical J.*, 1996, v. 462, 563–575.
3. Chen C-Y, Hwang C-Y. Six spiral galaxies lacking dark matter. *Scientific Reports*, 2024, v. 14, 17268.
4. Das A., Kurinsky N., Leane R. K. Dark Matter Induced Power in Quantum Devices. *Phys. Rev. Lett.*, 2024, v. 132, 121801.
5. Mistele T., McGaugh S., Lelli F., Schombert J., Li P. Indefinitely Flat Circular Velocities and the Baryonic Tully-Fisher Relation from Weak Lensing. *ApJL.*, 2024, v. 969 (1), L3.
6. Milgrom M. A modification of the Newtonian dynamics: implications for galaxy systems. *Astrophysical J.*, 1983, v. 270, 384–389.
7. Sanders R. H., McGaugh S. S. Modified Newtonian Dynamics as an Alternative to Dark Matter. *Annual Rev. of Astronomy and Astrophysics*, 2002, v. 40, 263–317.
8. Sanders R. H. Clusters of galaxies with modified Newtonian dynamics. *Monthly Notice of the Royal Astronomical Society*, 2003, v. 342 (3), 901-908.
9. Li P., Tian Y., *et al*. Measuring galaxy cluster mass profiles into the low acceleration regime with galaxy kinematics. arXiv: astro-ph/2303.10175v2.
10. Preston H. G., Potter F. Exploring large-scale gravitational quantization without $\hbar$ in planetary systems, galaxies, and the Universe. arXiv: gr-qc/0303112.
11. Potter F. Multi-planetary exosystems all obey orbital angular momentum quantization per unit mass as predicted by Quantum Celestial Mechanics (QCM). *Prog. in Phys.*, 2013, v. 9 (3), 29–30.

On the Possibility of a Scientific Prognosis of the Weather with the Introduction of Galactic Impacts into Analysis

Nikolai A. Morozov*

In this paper the author gives a preliminary information of his research study concerning cosmic influences on the weather. For this purpose, solar time was converted into sidereal (stellar) time for many thousands of meteorological data taken from the meteorological yearbooks published by meteorological observatories of the world. The resulting more than 200 diagrams identify interesting dependencies indicating a significant influence of the Galactic Centre and some other Galactic sources on the weather.

*Translated from *Bulletin de L'Académie des Sciences de L'URSS*, *Série Géographique et Géophysique*, 1944, t. VIII, no. 2–3, 63–71.

Nikolai A. Morozov, 1910

Nikolai A. Morozov (1854–1946) was the first child of a Russian millionaire and his freed female slave (slavery in Russia was abolished only 7 years later in 1861). He was a polymath and also a political figure who, while living in Genève, became the main theorist and one of the leaders of the 1881 Russian Bourgeois Revolution: they dreamed of a parliament, constitution, free capitalism, human rights and "liberté, égalité, fraternité" in the sense of Robespierre and Marat, but ended by the assassination of Alexander II, Emperor of Russia, which was not supported by mass people. After returning to Russia in 1881, Morozov was sentenced to life in solitary confinement in the Schlüsselburg Fortress near St. Petersburg, where he spent the next 24 years of his life (1881–1905) in a solitary confinement cell.

After the royal amnesty in 1905, Morozov devoted himself entirely to continuing the theoretical scientific research he had begun before the jail and then continued while in prison. He was immediately elected Professor of chemistry at the Lesgaft Research Institute in St. Petersburg, and then headed the entire Institute, where he remained Director until his death in 1946. His main research works were in the fields of chemistry, physics, astrophysics, meteorology, linguistics and world history. After the fall of the royal regime in Russia, he was elected to the Russian Academy of Sciences.

Being already an old man, in order to conduct experiments necessary for his scientific work, Morozov flew into the stratosphere in a stratospheric balloon. His original periodic table of chemical elements (an alternative to the generally accepted Mendeleev table) extends to elementary particles. In 1919, he conducted a series of original experiments testing the effects of Special Relativity. "Linguistic spectra" he introduced to identify true authors are now widely used in cryptography.

In the first half of the last [19th] century, attempts were made to scientifically process the old folk belief about the connexion between weather changes and the combination of the Sun and Moon, especially with new moons. Indeed, there was much in this belief that deserved attention: due to solar heating, ascending air currents occur, and thanks to them, descending air currents with the formation of cumulus and thunderclouds of local origin, as well as trade winds and non-trade wind air currents, and also cold polar layers that mix air with the warmer layers of the Earth's temperate zones.

Due to the tidal action of the Moon and the Sun, there must inevitably be ebbs and flows not only in the seas, but also in the atmosphere, and the ebbs and flows of the atmosphere due to the attraction of the Sun, running into the lunar ebbs and flows lagging behind them, must, depending on the time of year, cause various cyclones (the main factors of weather instability on the Earth), depending on the geographical place of their origin.

All this seemed so clear that many astronomers and meteorologists, beginning with the famous François Arago, put a lot of effort into testing the aforementioned idea on a huge number of daily records in meteorological observatories throughout the world. But no matter how they combined these records, bringing them into connexion with the combinations of the positions of the Sun and the Moon, they always came to the same thing: 60 percent of the predictions came true, and 40 percent did not, showing that in addition to the Sun and the Moon, some other cosmic factors influence weather changes, since from a natural-scientific point of view no natural phenomenon can be causeless. Many years ago I also studied this subject. At that time, I had the idea that the missing third fac-

In December 1942, at the age of 88, Morozov volunteered for military service as a sniper and scored a number of confirmed hits, but was demobilized one month later due to health reasons. He died from pneumonia at the age of 92 in 1946 in his mansion, which he inherited from his father.

The presented paper is a preliminary communication outlining the results of his extensive monograph on this subject (unpublished since he passed away in 1946). The staff of the Astronomy Department of the Lesgaft Research Institute, where he was Director, assisted him over many years in the 1930s in calculations and the construction of hundreds of graphs (necessary for this study) based on data from meteorological yearbooks for the entire history of regular meteorological observations over the past 150 years (until the 1940s). — Editor's remark.

tor in weather changes could and even should be our entire Galactic cosmos, i.e., the entire set of our disk-shaped cluster of stars and, in particular, the centre of their rotation.

But to clarify such an influence and determine its magnitude, it was necessary to re-calculate the records of all meteorological yearbooks from our usual solar time, according to which they are kept, to sidereal (stellar) time, the day of which is 4 minutes shorter than the solar day. And this recalculation of hundreds of thousands of meteorological observations, necessary to obtain some specific conclusion, would be such a huge job that the work of hundreds of calculators would be required for more than many years.

Only seven years ago, after much research on this subject, I succeeded in finding a new method of conversion, using which in one evening it is possible to convert from solar time to sidereal time such a number of meteorological records, which by the method that has existed up to now would have required at least a month. And I immediately set to work. Taking from the library of the [Russian] Academy of Sciences and the library of the Pulkovo Observatory the meteorological yearbooks of the Paris, London, Bombay, Batavian on Java, Leningrad, Moscow, Tbilisi, Cape Town and other observatories over the past few years, I personally made several thousand such conversions. Then, having instructed my assistants [from the Astronomy Department], I continued this work, as a result of which the calculation results were presented in the form of more than 200 diagrams.

Looking at these diagrams, I immediately found that for the sidereal-daily influences of our entire star cluster, clearly expressed diagrammatic configurations of the same type as the configurations of solar influences, only of a different magnitude, were obtained. Among the hundreds of thousands of data calculated, there was not even a single contradictory case in Europe, Asia, Africa, America, or Australia. All my tables and diagrams testified to the same thing: the influences of our entire star cluster cannot be ignored in any way when forecasting the weather.

It turned out to be possible to determine even the places [on the sky] from which the hitherto missing cosmic influences on the weather originate. All the discovered maxima and minima of the sidereal-daily influences on the air temperature unanimously showed that behind the constellation Argo Navis [now divided into Carina, Puppis and Vela], around the VIII-XI hour of right ascension, there is a gigantic accumulation of high-temperature matter, the radiation of which, like a gigantic furnace invisible at night, increases the air temperature above the horizon of any place during its highest ascent by more than one-seventh of the solar heating (Table I).

As this source rises above the horizon, the relative humidity of the air, i.e., its saturation with water gas, also increases. By designating 100% as the saturation at which water gas begins to be released in the form of fog or rain, we obtain very regular diametric arcs for both solar and Galactic influences (Table II), with the magnitude of the arc of Galactic influence reaching up to half the magnitude of the solar arc in the Earth's temperate climate zones.

Table I: Two examples of [air] temperature increase due to solar diurnal period action and galactic action (sidereal-daily period).

Northern Hemisphere: Tbilisi (42° N), average for 1913.	Southern Hemisphere: Batavia on Java (−7° S), average for 1866–1868.

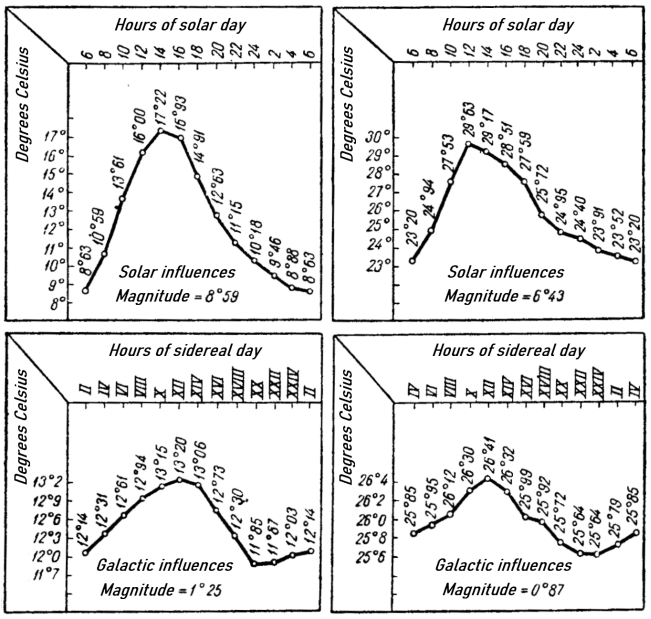

The increase in [air] temperature due to solar action reaches its maximum 2 hours after the Sun passes through the celestial meridian (at 14 solar hours). Similarly, the increase in temperature due to Galactic impact should reach its maximum 2 hours after the X celestial hour passes through the celestial meridian (the Galactic heat emitter is located near the X celestial hour). This Galactic heat emitter is located in the Southern Hemisphere of the sky, since its radiant heat, for example, in Batavia is equal to 1/3 of the solar radiant heat, and in Tbilisi — only 1/6 of the solar.

The rate of evaporation of the water surface (Table III, left) due to the influence of the rays of this Galactic centre reaches one third of the solar influence. This influence increases by the XII sidereal hour similarly to how the solar influence increases by 14 hours of the solar day, i.e., it occurs from the place of intersection of the XII-hour wing of the starry sky with the Milky Way, where there is a cluster of small stars and several "coal sacks" near the constellation Argo Navis.

Directly related to the evaporation rate, absolute humidity (the same Table III, on the right) has in the tropical zone of the Earth (probably due to the residual accumulation of evaporation) a less sharp peak in the curve of solar influence, so that the maximum of water gas remains undiminished from 14 to 20 hours of solar time. As for Galactic influences, their maximum effect on absolute humidity also falls at approximately the XX hour of sidereal time, but its growth and fall

Table II: Two examples of relative humidity changes due to solar influences by hours of the solar day, and two examples of galactic influences by hours of the sidereal day.

Northern Hemisphere: near Moscow (about 55° N), average for 1927.

Southern Hemisphere: Batavia on Java (−7° S), average for 1866–1868.

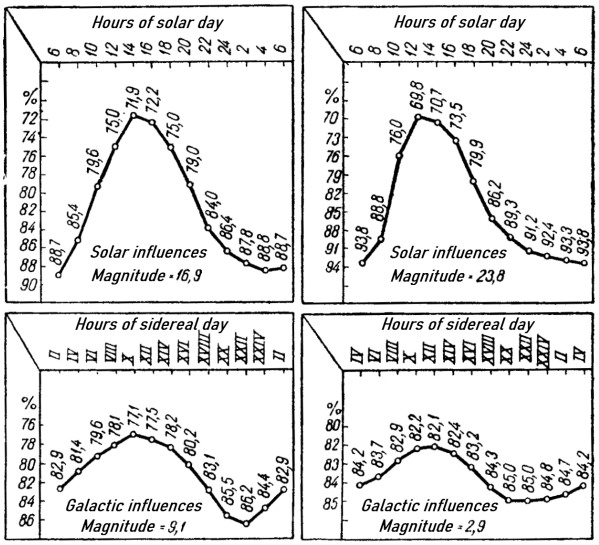

Solar influence reaches its maximum 2 hours after the Sun passes through the local celestial meridian (at about 14 solar hours). Similarly, Galactic influences should also reach their maximum 2 hours after [its source] passes through the meridian of the X sidereal hour, near which the centre of Galactic radiation is located. In Batavia, the magnitude of its influence is 0.12 of the solar influence, and near Moscow — 0.54 of the solar.

occur more smoothly (Table III, on the right).

Assuming that the main maximum of Galactic influence (under the XVIII–XX hours at the end of Table III) is delayed like the solar maximum by 8 hours after its passage through the celestial meridian, we find that the source of Galactic influence is also located [on the celestial sphere] at the X hour of right ascension (XVIII − 8 = X), that is, in the same constellation Argo Navis. The maximum of a smaller magnitude under the II sidereal hour corresponds to the influence from the XVIII sidereal hour, at the intersection of which with the Milky Way there is another huge cluster of small stars and "coal sacks" in the tail of the constellation Scorpio. The third maximum on the same diagram under the XII sidereal hour corresponds, according to the same calculation (XVIII − 8 = X), to the VI sidereal hour on the celestial sphere, where there is nothing special against the background of the Milky Way, but next to it is the giant Orion Nebula with a "coal sack" inside and two main star clusters visible to the naked eye: the Pleiades and the Hyades. However, it is still premature to claim that the secondary maximums (under the II and XVIII sidereal hours on the celestial sphere) are their influence, since on other diagrams that I have studied, simple

Table III: Example of solar and galactic influences on the rate of evaporation of water surfaces and on the amount of water gas in the atmosphere (absolute humidity). Solar-diurnal periods and sidereal-diurnal periods.

Evaporation rate: Tbilisi (42° N), average for 1913.

Absolute humidity: Batavia on Java (−7° S), average for 1866–1868.

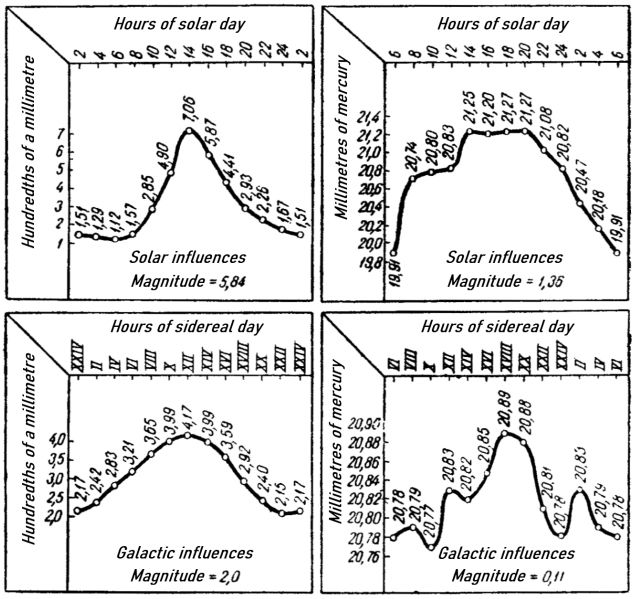

The rate of evaporation due to solar influence reaches its maximum 2 hours after the Sun passes through the celestial meridian (at 12 o'clock solar time), and the rate of evaporation due to galactic influence reaches its maximum 2 hours after the constellation Argo Navis passes through the celestial meridian (at X o'clock stellar time). Absolute humidity reaches its maximum due to solar influence 6–8 hours after the Sun passes through the celestial meridian, and due to galactic influence — VI–VIII hours after the constellation Argo Navis passes through the meridian.

arc-shaped configurations are also obtained.

Generally speaking, absolute humidity (i.e., the amount of water gas in the atmosphere at the observation site), expressed through partial pressure, varies in an average annual distribution very capriciously over the course of solar and sidereal days, although when non-periodic deviations are taken into account and eliminated, this dependence retains its arc-shaped form.

And this shows that in addition to the air pressure and its own temperature and speed of motion, as well as the direct impact of the Sun's rays in clear weather, there is another powerful cause. And it can already be expected a priori that the action of electromagnetic forces is involved here, because the artificial induction of rain by scattering electrified dust from airplanes at a sufficient height in the Earth's troposphere clearly shows the influence of this factor on the entire water regime of our atmosphere. For example, Table IV shows the distribution of rainfall due to solar influence and due to Galac-

Table IV: Example of average annual distribution of rainfall (by hours of the day) due to solar influence and Galactic influence.

Batavia on Java (−7° S), average for 1866–1868.

Tbilisi (42° N), average for 1913.

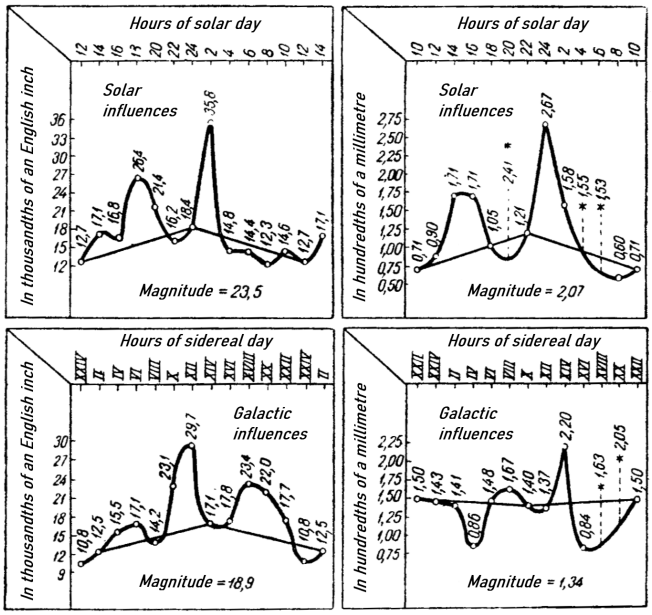

The irregular bends and jumps of these diagrammatic curves, especially — Tbilisi (asterisk) — show that rains depend not only on temperature and barometric pressure drops, but also on the electromagnetic effects of the Sun and the Galactic Centre, and that even more powerful electromagnetic storms than on the Sun permanently occur at this Centre.

Table V: Examples of solar influences on solar-diurnal variations of the magnetic and electric field strengthes and examples of similar galactic influences on the sidereal-diurnal period.

Magnetic field: Val Joyeux, Paris (about 49° N), average for 1933.

Electric field: Tashkent (about 42° N), average for 1930.

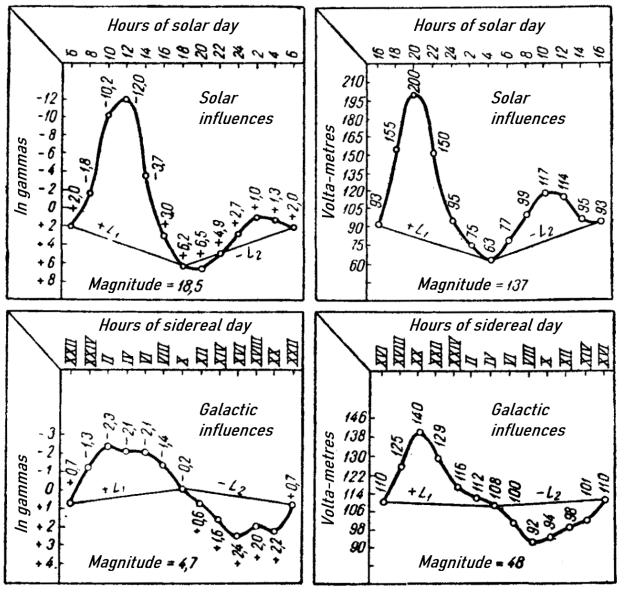

Magnetic Galactic influences from the constellation Argo Navis lag behind solar influences by 8 hours. If they were lagging by 12 hours, this would mean that the magnetic axes of the Sun and the Galactic Centre under study in the constellation Navis Argo are oriented opposite to each other. The lag of 8 hours shows that both of these axes are inclined to each other (as seen from the Earth) at an angle of about 120°.

tic influences by the hours of the sidereal day. On the left it is given for Batavia on Java (−7° S) and on the right — for Tbilisi in the Caucasus (42° N).

The two main maxima generated after the solar action (at 2 and 24 o'clock in the morning), as well as the evening actions (at 18 and 16 o'clock in the afternoon) show here that the solar actions in Tbilisi are generally the same as in Batavia, although they are delayed by 2 hours compared to Batavia. But why in Tbilisi in 1913 in the 20th, 4th and 6th solar hours the amount of rainfall (they are marked with asterisks) jumped out of the norm so much (see Table IV, upper right), that if I had not excluded them, they would have made the configuration of this diagrammatic curve completely disordered and having nothing in common with Batavia? Why do we see the same thing below in the Galactic influences? Here again we have only one way out: to admit that the distribution of rainfall depends not only on changes in temperature and barometric pressure, but also to a large extent on electromagnetic storms, constantly occurring not only on the Sun, but also on the Galactic Centre now being studied in the constellation Argo Navis. It is even possible that such storms on the Sun are only a resonance of Galactic storms, which must be repeated simultaneously on the Earth, and on the Moon, and on all the planets. Otherwise, it would be difficult to imagine why the jumps shown by the stars on our diagrams are repeated not only at midday, when the given horizon is turned toward the Sun, but also at different hours of the day, and why they are distributed in the same way among various sidereal hours. It even turns out that it is as if each stroke of cosmic lightning and protuberances on some Galactic centre is accompanied by multiple echoes on the others. In any case, thunderstorms, constantly accompanied by showers, sufficiently indicate a connexion between these two meteorological manifestations. Therefore, it is appropriate to dedicate a few lines to them in this preliminary message.

In Table V on the right I give an example of solar and Galactic influences on the oscillations of the electric field in Tashkent, and in the same place I give an example of the magnetic influences of the Sun in Val Joyeux near Paris (Table V on the left).

The necessity of brevity of this message of mine enforces me to give here, as an example of the substantiation of my theory, only one example of the most important sidereal-daily influences of the Galaxy, excluding its sidereal-annual influ-

ences. But in my working manuscripts, beginning in 1932, when I first began to study this subject systematically, there are hundreds of such re-calculations based on the systematic records of many geophysical and meteorological observatories of the world, and above all, the two Spitsbergen stations (in Horn Sound and Treyrenberg), the Sondakull station in Iceland, the Pavlovsk (now Slutsk) station, the Main Physical Observatory (in Leningrad), Sverdlovsk, Wilhelmshaven, Greenwich, Val Joyeux (near Paris), Budapest, Petrovsko-Razumovskaya (in Moscow), Cheltenham near Washington, Barcelona, Tbilisi, Tashkent, Caesarea in Lebanon, Tucson in Arizona, Beijing, Hong Kong, Alibag near Bombay, and Singapore.

For the Southern Hemisphere, I had at my disposal the records of the observatories at Batavia on Java, on the Island of St. Helena, at Antananarivo in Madagascar, at Buenos Aires, at Christchurch (New Zealand), and on the South Polar Continent [Antarctic] at the observatories at Cape Royds and Cape Evans.

All these observatories are known to every specialist, and their yearbooks that I have indicated are available in the libraries of the [Russian] Academy of Sciences, the Pulkovo Astronomical Observatory, and the Main Physical Observatory (in Leningrad). And all the hundreds of summary recalculations for sidereal time compiled by me and my coworkers from these publications, and all the diagrams constructed from the calculations unanimously show that the influence of the Galaxy on the meteorological and geophysical processes of the Earth is of a regular nature and so great that without introducing them into the calculations one cannot even dream of a scientific forecasting of the weather even for a month ahead.

Here, first of all, a cycle of 521 Julian years is manifested, since only after this period do the previous combinations of the Sun, Moon and Galaxy repeat for each specific place on the globe. Such a long period does not, of course, provide any practical help for [weather] forecasting, since during most of it there were no meteorological records. However, another period of 19 years manifests itself, but only according to this period it turns out that a cyclone that, for example, swept over Leningrad today, will sweep in 19 years later somewhere over Irkutsk, then over Tokyo, then over San Francisco, and so forth and so on. And another cyclone that will come to Leningrad will be the one that was 19 years ago somewhere over London, and 38 years ago near New York, etc.

It is impossible not to mention here also the dendrochrochronological period of 11.35 years, determined by the alternation of the thickness of tree rings and coinciding with the same period of sunspots, with the proviso that this [dendrochronological] period itself can only be explained by the effect on the Sun (and with it of course on the Earth) of the radiation of some luminary rotating around its axis in 11.35 years. There can be no other rational explanation here, just as there can be no 280-year cycle consisting of almost 25 of the same (exactly 11.35-year) cycles repeating quite regularly on the rings of giant Californian pines Sequoia Gigantea, for example, on the pine "Mark Twain", a section of which is kept in the New York Museum of Natural History (this pine was 1341 years old when it was cut down*).

And this period cannot be explained by anything except the fact that in the Galactic space there is an even more powerful centre rotating around its axis in 280 years (± a few years).

All this shows that for an absolutely accurate weather forecast it is necessary to determine not only the motion of the Moon, the Sun and Galactic centres above the horizon of the observation point, but also which side of their surface the latter are facing the Earth at that moment.

Of great help in using reference points to determine upcoming weather changes in a specific geographic area should be the already existing predictions of solar and lunar eclipses. Adding to them, Galactic influences will undoubtedly eliminate all cases of failure of predictions based on solar and lunar influences alone, but this requires the work of not one person or group of people, but the work of many meteorological institutions using the entire network of meteorological records throughout the globe.

November 4, 1940

*See A. E. Douglass and Waldo S. Glock, *Carnegie Institution of Washington Supplementary Publications*, July 1934, no. 9, and also, in the same place, *News Service Bulletin*, 1937, v. IV, no. 20.

Yang-Mills Theory in the Framework of General Relativity

Patrick Marquet

Calais, France. E-mail: patrick.marquet6@wanadoo.fr

In our recent publication, we derived a solution that allows the coupling between the Yang-Mills theory and the space-time curvature; Progr. Phys., 2021, v.18, 97–102 [1]. This result was achieved by considering a specific manifold which we named the Weyl-Einstein manifold spanned by the connection coefficients displaying a 4-vector. We then deduced a Weyl-Einstein tensor, which was found to be conserved. The Weyl-Einstein 4-vector was directly identified with the Yang-Mills gauge field vectors as described in the Minkowski space tangent to the Weyl-Einstein manifold. In the present work, we investigate further this topic, and we examine how this coupling fits into the field equations.

Notations

Throughout this text, we assume the Einstein summation, whereby a repeated index implies summation over all values of this index.
4-tensor or 4-vector: small Latin indices $a, b, \ldots = 0, 2, 3, 4$.
3-tensor or 3-vector: small Greek indices $\alpha, \beta, \ldots = 1, 2, 3$.
Signature of the space-time metric: $(+---)$.
Ordinary derivative: $\partial_a U$.
Riemannian covariant derivative on $(\mathrm{M}, \boldsymbol{g})$: ∇_a or $(;)$.

1 The Weyl-Einstein field equations

1.1 The Weyl-Einstein tensor

Following Lichnerowicz [2] we defined the semi-metric manifold $(\mathrm{M_w}, \boldsymbol{g})$ spanned by the Weyl-Einstein connexion coefficients expressed here with the metric connexion

$$W^c_{ab} = \frac{1}{2}\, g^{cd}\,(\partial_b\, g_{da} + \partial_a\, g_{db} - \partial_d\, g_{ab}) - \\ - \frac{1}{2}\, g^{cd}\,(J_b\, g_{da} + J_a\, g_{db} - J_d\, g_{ab})\,, \tag{1.1}$$

$$W^c_{ac} = \frac{1}{2}\, g^{cd}\,(\partial_a\, g_{cd} - J_a\, g_{cd})\,, \tag{1.2}$$

where J_a is referred to as the Weyl-Einstein 4-vector.

The Einstein-Weyl-curvature tensor is assumed to keep its original form

$$(R^c{}_{adb})_{\mathrm{w}} = \partial_b\, W^c_{ad} - \partial_d\, W^c_{ab} + W^c_{eb} W^e_{ad} - W^c_{ed} W^e_{ab}\,. \tag{1.3}$$

Setting

$$(\Gamma^c_{ab})_J = \frac{1}{2}\, g^{cd}\,(J_b\, g_{da} + J_a\, g_{db} - J_d\, g_{ab}) \tag{1.4}$$

and using the Riemannian covariant derivatives, we found

$$(R_{ab})_{\mathrm{w}} = R_{ab} + \nabla_c(\Gamma^c_{ab})_J - \nabla_b(\Gamma^c_{ac})_J + \\ + (\Gamma^d_{ab})_J(\Gamma^c_{dc})_J - (\Gamma^d_{ae})_J(\Gamma^e_{db})_J\,, \tag{1.5}$$

$$R_{\mathrm{w}} = R - \left(\nabla_a\, J^a + \frac{1}{2}\, J^2\right). \tag{1.6}$$

With these, we derived the Weyl-Einstein tensor as

$$(G_{ab})_{\mathrm{w}} = (R_{ab})_{\mathrm{w}} - \frac{1}{2}\,(g_{ab} R_{\mathrm{w}} - 2\, J_{ab})\,, \tag{1.7}$$

where

$$J_{ab} = (\Gamma^d_{ab})_J(\Gamma^c_{dc})_J - (\Gamma^d_{ae})_J(\Gamma^e_{db})_J\,.$$

The Weyl-Einstein tensor was shown to be conserved.

1.2 Massive source

The Weyl-Einstein field equations are now expressed by

$$(G_{ab})_{\mathrm{w}} = \varkappa\, T_{ab}\,. \tag{1.8}$$

Using the Riemannian covariant derivatives, the Weyl-Einstein tensor conservation law reads

$$\nabla_a (G^a_b)_{\mathrm{w}} = 0\,. \tag{1.9}$$

The right hand side of (1.8) should also verify

$$\nabla_a\, T^a_b = 0$$

or

$$\partial_a\, \boldsymbol{T}^a_b = 0 \tag{1.10}$$

with the tensor density $\boldsymbol{T}^a_b = \sqrt{-g}\, T^a_b$.

However, inspection shows that

$$\partial_a\, \boldsymbol{T}^a_b = \frac{1}{2}\, \boldsymbol{T}^{ca}\, \partial_b\, g_{ca} \tag{1.11}$$

or equivalently

$$\partial_a\, \boldsymbol{T}^a_b = \frac{1}{2}\, \boldsymbol{T}^{ca}\,(\partial_b\, g_{ca} - J_b\, g_{ca})\,.$$

Thus the condition (1.10) is never satisfied in a general coordinates system. This circumstance results from the fact that the *global* conservation should hold for the 4-momentum of *both* the matter and its gravitational field.

To keep the equation (1.10) consistent with (1.9), we must look for a solution of the form

$$\partial_a \left(\boldsymbol{T}^a_b + \boldsymbol{t}^a_b \right) = 0 \,, \tag{1.12}$$

where $\boldsymbol{t}^{ab}$ is the given tensor's density.

Let us compute

$$d\boldsymbol{g}^{ab} = d\left(\sqrt{-g}\, g^{ab}\right) = \sqrt{-g}\left(dg^{ab} + \frac{1}{2}\, g^{ab} g^{ed}\right) dg_{ed} =$$

$$= \sqrt{-g}\left(-g^{ae} g^{bd} + \frac{1}{2}\, g^{ab} g^{ed}\right) dg_{ed} \,,$$

therefore

$$(R_{ab})_{\mathrm{w}}\, d\boldsymbol{g}^{ab} = \sqrt{-g}\left(-R^{ce}_{\mathrm{w}} + \frac{1}{2}\, g^{ce} R_{\mathrm{w}}\right) dg_{ce} = -\varkappa\, \boldsymbol{T}^{ce} dg_{ce} \,.$$

Taking into account the Lagrangian form of the Weyl-Einstein Ricci tensor

$$(R_{ab})_{\mathrm{w}} = \partial^e \left[\frac{\boldsymbol{L}_{\mathrm{w}}}{\partial\left(\partial_e\, \boldsymbol{g}^{ab}\right)} \right] - \frac{\partial \boldsymbol{L}_{\mathrm{w}}}{\partial \boldsymbol{g}^{ab}} \,,$$

where the effective Weyl-Einstein Lagrangian is now

$$\boldsymbol{L}_{\mathrm{w}} = g^{ab}\, \sqrt{-g}\, (W^e_{ab} W^d_{de} - W^d_{ae} W^e_{bd}) \tag{1.13}$$

one obtains

$$-\varkappa\, \boldsymbol{T}^{ab}\, dg_{ab} = \left(\partial_c \frac{\partial \boldsymbol{L}_{\mathrm{w}}}{\partial_c\, \boldsymbol{g}^{ab}} - \frac{\partial \boldsymbol{L}_{\mathrm{w}}}{\partial \boldsymbol{g}^{ab}} \right) d\boldsymbol{g}^{ab} =$$

$$= \partial_c \left(d\boldsymbol{g}^{ab} \frac{\partial \boldsymbol{L}_{\mathrm{w}}}{\partial_c\, \boldsymbol{g}^{ab}} \right) - d\boldsymbol{L}_{\mathrm{w}} \,,$$

$$-\varkappa\, \boldsymbol{T}^{ab}\, \partial_d\, g_{ab} = \partial_c \left(\partial_d\, \boldsymbol{g}^{ab} \frac{\partial \boldsymbol{L}_{\mathrm{w}}}{\partial\left(\partial_c \boldsymbol{g}^{ab}\right)} - \delta^c_d \boldsymbol{L}_{\mathrm{w}} \right) = 2\varkappa\, \partial_c\, \boldsymbol{t}^c_d \,.$$

From the last equation we find

$$\partial_c\, \boldsymbol{T}^c_a = \frac{1}{2}\, \boldsymbol{T}^{dc}\, \partial_a\, g_{dc} = -\partial_c\, \boldsymbol{t}^c_a \,.$$

In order to satisfy the conservation law (1.12), one clearly sees that the gravitational field energy-momentum tensor density should be described by the Weyl-Einstein extension of the *Einstein-Dirac pseudo-tensor* [3, p.61]

$$\boldsymbol{t}^c_d = \frac{1}{2}\, \varkappa \left[\partial_d\, \boldsymbol{g}^{ab}\, \frac{\partial \boldsymbol{L}_{\mathrm{w}}}{\partial(\partial_c\, \boldsymbol{g}^{ab})} - \delta^c_d \boldsymbol{L}_{\mathrm{w}} \right] \tag{1.14}$$

the quantities $\boldsymbol{t}^{ab}$ are called "pseudo-tensor density" since they can be transformed away by a suitable choice of the reference frame and they are not irreducible [4]. This is why the classical theory stipulates that a (free) gravitational energy cannot be *localizable*.

In the classical General Relativity, the non symmetric tensor $\boldsymbol{t}_{ab}/\sqrt{-g}$ is symmetrized through the Belinfante procedure [5] to suit the standard symmetric Einstein tensor. The relevant symmetric tensor is denoted t_{ab}.

Unfortunately, the Einstein field equations whatever their transcriptions, are yet unbalanced since they do not exhibit a full real tensor as a source. To remedy this problem, we showed that a slightly variable cosmological term Λ-term induces a stress-energy tensor of vacuum, which restores a true gravitational tensor on the right-hand side of equation (1.6) as it should be [6, 7].

This real tensor is given by

$$(t_{ab})_{\mathrm{vac}} = -\frac{1}{2\varkappa}\, \Lambda\, g_{ab} \,. \tag{1.15}$$

The Λ-term was found to be [8]

$$\Lambda = \nabla_a K^a = \theta^2, \tag{1.16}$$

where K^a is a 4-vector and

$$\theta = X^a_{;a} \tag{1.17}$$

is the space-time volume scalar expansion characterizing the vacuum stress-energy tensor $(t_{ab})_{\mathrm{vac}}$, and X^a is a congruence of non intersecting unit time lines $X^a X_a = 1$

$$X^a_{;a} = h^{ab} \theta_{ab} \,, \tag{1.18}$$

while θ_{ab} stands for the expansion tensor and $h_{ab} = g_{ab} - X_a X_b$ is the projection tensor.

Due to the form of (1.16), the Lagrangian (1.13) differs only from a divergence and varying its action generates the same field equations. The real tensor $(t_{ab})_{\mathrm{vac}}$ which corresponds to the vacuum stress-energy tensor can be added to t_{ab} without affecting the Weyl-Einstein Lagrangian.

With this definition the Weyl-Einstein field equations can be finally written as

$$(G_{ab})_{\mathrm{w}} = (R_{ab})_{\mathrm{w}} - \frac{1}{2}\, (g_{ab} R_{\mathrm{w}} - 2 J_{ab}) =$$

$$= \varkappa \left[\rho c^2 u_a u_b + \frac{\boldsymbol{t}_{ab}}{\sqrt{-g}} + (t_{ab})_{\mathrm{vac}} \right]. \tag{1.19}$$

Here the symmetrization procedure is evaded, because the quantity $\boldsymbol{t}_{ab}/\sqrt{-g}$ is genuinely antisymmetric.

When gravity is weak and velocities are low compared to c, we have the Newtonian approximation where the massive tensor in (1.19) reduces to

$$T^0_0 = \rho c^2.$$

Inspection then shows that

$$(R^0_0)_{\mathrm{w}} = R^0_0 = \frac{1}{c^2}\, \frac{\partial^2 \varphi}{\partial^2_\beta}$$

with $g_{00} = 1 + \varphi/c^2$, from which we find the well-known Poisson equation

$$\Delta\varphi = 4\pi G\rho\,,$$

where G is Newton's constant.

1.3 Electromagnetic contribution

The field equations are expressed by

$$(R_{ab})_{\mathrm{w}} - \frac{1}{2}\,(g_{ab}R_{\mathrm{w}} - 2J_{ab}) = \\ = \varkappa\,\frac{1}{4\pi}\left(-\partial_a A^c F_{bc} + \frac{1}{4}\,g_{ab}F_{cd}F^{cd}\right), \tag{1.20}$$

$$F_{ab} = \partial_a A_b - \partial_b A_a\,.$$

The source tensor is antisymmetric. Its form is derived from the canonical equation

$$(t_a^b)_{\mathrm{elec}} = \frac{\partial_a A_c\,\partial L}{\partial(\partial_b A_c)} - \delta_a^b L\,,$$

where $L = -\frac{1}{16\pi}F_{bc}F^{bc}$.

If the Weyl part is neglected, the term $\frac{1}{4\pi}\partial_c A^c F_{bc}$ is classically added so that when charge is absent, holds the relation

$$\frac{1}{4\pi}\,\partial_c A_a F_b^c = \frac{1}{4\pi}\,\partial_c\left(A_a F_b^c\right).$$

This eventually yields the well-known symmetric energy-momentum tensor of the electromagnetic field

$$\tau_{ab} = \frac{1}{4\pi}\left(-F_a^c F_{bc} + \frac{1}{4}\,g_{ab}F^{cd}F_{cd}\right).$$

1.4 Charged matter

The Weyl-Einstein field equations are

$$(R_{ab})_{\mathrm{w}} - \frac{1}{2}\,(g_{ab}R_{\mathrm{w}} - 2J_{ab}) = \\ = \varkappa\left[\rho c^2 u_a u_b + \frac{\boldsymbol{t}_{ab}}{\sqrt{-g}} + (t_{ab})_{\mathrm{vac}} + \right. \\ \left. + \frac{1}{4\pi}\left(-\partial_a A^c F_{bc} + \frac{1}{4}\,g_{ab}F_{cd}F^{cd}\right)\right]. \tag{1.21}$$

We easily check that the right hand side of the equations is conserved.

2 Relation to the Yang-Mills gauge fields

We first write the Minkowskian line element ds and the Weyl-Einstein line element ds_{w}, then we set

$$dJ = dA\left(1 + \mathrm{Log}\,\frac{ds_{\mathrm{w}}}{ds}\right) \tag{1.22}$$

with the following one-forms

$$dJ = J_a\,dx^a,$$
$$dA = A_a\,dx^a.$$

The above 4-vector A_a is a generic gauge vector of the Yang-Mills field defined in the flat space tangent to the Weyl-Einstein manifold.

2.1 Weak interaction SU(2) symmetry

Let us now examine the rôle of the Weyl-Einstein tensor in the field equations. We write the group element of SU(2) as

$$\mathrm{U} = \exp\left[-i\,\mathrm{T}^\beta \mathrm{k}_\beta\right],$$

where k is the group parameter with the generators

$$\mathrm{T}^\beta = \frac{1}{2}\,\sigma^\beta,$$

(here σ^β are the 2×2 Pauli spin matrices) with the coupling constant h, the gauge field transforms as

$$B_a \to B_a - \mathrm{T}^\beta\,\partial_a \mathrm{k}^a(x) + i\,\mathrm{h}\mathrm{k}^a(x)\left[\mathrm{T}^\beta, B_a(x)\right].$$

Here, the Weyl-Einstein field equations (1.19) apply with the correspondence

$$J_a \to B_a\,.$$

2.2 The electromagnetic symmetry U(1)

This symmetry group is the abelian group U(1) with a single commuting generator $\mathrm{T}_1 = \mathrm{Q}$ satisfying

$$[\mathrm{T}_1, \mathrm{T}_1] = 0\,,$$

where Q is the quantity of the charges of the field $\Phi(x)$ proportional to the fundamental charge unit e. Under the phase rotation

$$\Phi(x) \to \Phi(x)\exp\left[-i\,\mathrm{k}\mathrm{Q}(x)\right]$$

the vector field $A_a(x)$ transforms as

$$A_a(x) \to A_a(x) + \partial_a \mathrm{k}\,.$$

Within the Weyl-Einstein field equations (1.20), we have the correspondence

$$J_a \to A_a\,.$$

2.3 Combined symmetry U(1) × SU(2)

Here the Weyl-Einstein field equations for charged matter (1.21) are used, where we simply have

$$J_a \to A_a + B_a\,,$$

where A_a is the electromagnetic vector field gauge field and B_a is the gauge vector field of the weak interaction.

Other combinations implying for example strong interaction SU(3) could be derived in the same way.

3 Conclusion

What have we achieved? Our theory relies on the specific form of the connexion coefficients which displays a 4-vector. This connexion form was first considered by H. Weyl by relating this vector to the "segment curvature" next to the Riemann curvature and zero torsion, with the aim to unify electricity and gravitation in a non trivial way [9]. Although we kept the name Weyl-Einstein connexion, the extra segment curvature is not introduced here. On the contrary, we have exploited the Weyl-Einstein 4-vector to connect the Yang-Mills gauge fields through an extended field equations set where both the left and right sides are still conserved. In doing so, such field equations can now display the type of interactions that is considered thus informing us between either electromagnetic field or weak and strong interactions of matter which was basically impossible with the standard field equations.

Submitted on October 8, 2024

References

1. Marquet P. How to couple the space-time curvature with the Yang-Mills Theory. *Progress in Physics*, 2022, v.18, no.2, 97–102.
2. Lichnerowicz A. Les espaces variationnels généralisés. *Annales scientifiques de l'Ecole Normale Supérieure*, *série 3*, 1945, t.62, 339–384.
3. Dirac P.A.M. General Theory of Relativity. Princeton University Press, 2nd edition, 1975.
4. Landau L. et Lifchitz E. Théorie des champs. Éditions MIR, Moscou, 1964.
5. Rosenfeld L. Sur le tenseur d'impulsion-énergie. *Acad. Roy. de Belgique*, *Mémoires de Classes de Sciences*, t.18, 1940.
6. Marquet P. The gravitational field: a new approach. *Progress in Physics*, 2013, v.9, no.3, 62–66.
7. Marquet P. Vacuum background field in General Relativity. *Progress in Physics*, 2016, v.12, no.4, 314–316.
8. Marquet P. Some insights on the nature of the vacuum background field in General Relativity. *Progress in Physics*, 2016, v.12, no.4, 366–367.
9. Weyl H. Gravitation und Elektrizität. *Sitzungsberichte der Königlich Preussischen Akademie der Wissenschaften zu Berlin*, 1918, 465–480.

On a Plausible Solution to the Hubble Tension via the Hypothesis of Cosmologically Varying Fundamental Natural Constants

G. G. Nyambuya

National University of Science and Technology, Faculty of Applied Sciences — Department of Applied Physics, Fundamental Theoretical and Astrophysics Group, P. O. Box 939, Ascot, Bulawayo, Republic of Zimbabwe.
E-mail: physicist.ggn@gmail.com

We herein present what we propose could be a plausible solution to the current, interesting and topical problem in cosmology — the *Hubble Tension*. This problem of the Hubble tension seems to have thrown all of cosmology into a crisis. By employing the seemingly temarious hypothesis of varying *Fundamental Natural Constants* (FNCs), namely Planck's constant, $\hbar$, we demonstrate that for the case where the cosmological Interstellar Medium (ISM) is a perfect *vacuo* with a refractive index of unity, the supernovae derived $\mathcal{H}_0$-value can be brought down from its current lofty height of: $\mathcal{H}_0^{\rm SNe} = 73.30 \pm 1.03\,{\rm km\,s^{-1}\,Mpc^{-1}}$, down to a more humble and modest value of: $68.70 \pm 0.30\,{\rm km\,s^{-1}\,Mpc^{-1}}$, and within the margins of error, this new value is in agreement with the Tip of the Red Giant Branch (TRGB) derived $\mathcal{H}_0$-value, namely: $\mathcal{H}_0^{\rm TRGB} = 69.80 \pm 2.20\,{\rm km\,s^{-1}\,Mpc^{-1}}$, and this is much closer to the CMB-derived $\mathcal{H}_0$-value: $\mathcal{H}_0^{\rm CMB} = 67.40 \pm 0.50\,{\rm km\,s^{-1}\,Mpc^{-1}}$. At a 2.2σ-level of statistical significance in discrepancy, this new $\mathcal{H}_0$-value reduces the tension by 88%, and this surely is a most welcome development. On the other hand, if the ISM is assumed to be homogeneous and isotropic with a slightly varying, if not near constant refractive index, $n_r^{\rm ISM}$, for most photon wavelengths, then, a refractive index value of: $n_r^{\rm ISM} = 1.010 \pm 0.006$, does bring the new SNe-derived $\mathcal{H}_0$-value into complete and total concordance with the CMB-derived $\mathcal{H}_0$-value, thus resolving the tension altogether. The final concordance $\mathcal{H}_0$-value that matches or resolves both measurements after a final correction of the ISM's refractive index is found to be: $\mathcal{H}_0 = 68.00 \pm 0.90\,{\rm km\,s^{-1}\,Mpc^{-1}}$.

> Cosmology is peculiar among the sciences for it is both the oldest and the youngest. From the dawn of civilization man has speculated about the nature of the starry heavens and the origin of the world, but only in the present century has physical cosmology split away from general philosophy to become an independent discipline.
>
> Gerald James Whitrow (1912–2000)*

1 Introduction

Without an *iota* of doubt, the Hubble constant, denoted by the symbol $\mathcal{H}_0$, is an all important constant in all of modern cosmology and astrophysics [1–4]. It, amongst others, measures the expansion rate of the Universe and is pivotal in the measurement of the age of the Universe [1–4]. Since the theoretical discovery [5] of the expansion of the Universe by the Belgian Catholic priest, theoretical physicist, mathematician, astronomer, and then professor of physics at the Catholic University of Louvain, Georges Henri Joseph Édouard Lemaître (1894–1966), and the subsequent observational confirmation [6] of this hypothetical expansion by the great American astronomer, Edwin Powell Hubble (1889–1953), a great many efforts have been made to measure this constant with the highest and optimum possible precision available at the time. The importance of this parameter in cosmology cannot be overstated. Hence, accurate knowledge of this constant is not only a *sine qua non*, but very important as all of cosmology and the cosmological models thereof, depend on it.

Rather worrisomely, initial measurements of this constant in the past century were marred by serious scattering with the resultant values thereof ranging from: $\sim 40\,{\rm km\,s^{-1}\,Mpc^{-1}}$ to $\sim 100\,{\rm km\,s^{-1}\,Mpc^{-1}}$ [4]. However, recent 21st century advances in science and technology have made it all possible to obtain very accurate measurements of this constant using at least three different methods — which methods measure the Hubble constant on two different evolutionary epochs of the Universe, namely the early-and-late Universe. Values of $\mathcal{H}_0$ from the early Universe are typically referred to as global measurements of $\mathcal{H}_0$, while those from the late Universe are commonly referred to as local values of $\mathcal{H}_0$. Global $\mathcal{H}_0$ values measure the Hubble constant in the early Universe (distant past) while the local $\mathcal{H}_0$ values measure this constant in our local neighbourhood which is the present epoch in the Universe.

According to the widely accepted Standard ΛCDM cosmology model that is used to describe the Universe, $\mathcal{H}_0$ must be the same for any evolutionary epochs of the Universe — be it in early or late Universe, it does not matter, the value of $\mathcal{H}_0$ aught to be the same. To the chagrin and against the desideratum of the cosmologically searching mind, the local and global values of $\mathcal{H}_0$ seem to not be in agreement — each yielding at a 4.9σ-level of statistical significance [10], two

*In "Theories of the Universe" (1958)

Table 1: Critical Measurements of the Hubble Constant

Group	Cosmic Epoch	Measurement Type	$\mathcal{H}_0$ ($\mathrm{km\,s^{-1}\,Mpc^{-1}}$)	Reference
Supernova Cosmology (SCG)	Late Universe	Far Local	73.30 ± 1.04	[7]
Carnegie-Chicago Hubble Project (CCHP)	Late Universe	Near Local	69.80 ± 2.20	[8]
Planck Collaboration (PC)	Early Universe	Global	67.40 ± 0.50	[9]

different values that are not only $\sim 10\%$ apart, but also outside of the provinces of their error margins. This interesting and topical problem or discrepancy in the local and global measurements of the Hubble constant has come to be known as the *Hubble tension* and has thrown cosmology into a serious crisis.

From a fundamental theoretical stand point, before suspecting that there possibly may be errors in the measurements and/or systematics thereof, one needs to first trust that — those that have made these measurements have done so meticulously with due and requisite diligence, and with the best precision at hand. Of course, one cannot rule out errors in the measurements and/or systematics — we are human after all, we err. Be that as it may, as our point of departure, we shall assume that these measurements are flawless. With that having been said, we must say that there are three main popular and common techniques used to measure $\mathcal{H}_0$:

1. Supernovae Type Ia (SNe Ia) method;
2. Tip-of-the-Red-Giant-Branch (TRGB) method;
3. Cosmic Microwave Background (CMB) radiation method.

We shall discuss in detail these techniques in §4. Our interest in taking a deeper look into these methods is to unravel their dependence on FNCs because it is in these FNCs that we believe the source of our error in the determination of the Hubble constant may lay.

For further clarity, as already aforementioned, we shall elaborate that the methods to measure the Hubble constant fall into two classes: a) *Local* measurements, and, b) *Global* measurements, i.e.:

1. Local $\mathcal{H}_0$ measurements: measure $\mathcal{H}_0$ in the present (local) evolutionary epoch of the Universe. The present epoch is the late Universe, hence, these type of measurements are also referred to as late Universe measurements.
2. Global $\mathcal{H}_0$ measurements: are all-sky measurements of $\mathcal{H}_0$, measuring the Hubble constant across the entire sky, hence, they being referred to as global $\mathcal{H}_0$ measurements. These measurements typically measure, $\mathcal{H}_0$, in the very early Universe hence they also being referred to as early Universe measurements.

The TRGB and SNe Ia measurements are classified as local $\mathcal{H}_0$ measurements as they measure $\mathcal{H}_0$ in the present (and not past) evolutionary epoch of the Universe. The TRGB method measures $\mathcal{H}_0$-values in galaxy systems much closer to us (yielding: $\mathcal{H}_0^{\mathrm{TRGB}} = 69.80 \pm 2.20\,\mathrm{km\,s^{-1}\,Mpc^{-1}}$ [8]), while the SNe Ia measurement $\mathcal{H}_0$-values in galaxy systems relatively far in the local Universe (yielding: $\mathcal{H}_0^{\mathrm{SNe}} = 73.30 \pm 1.04\,\mathrm{km\,s^{-1}\,Mpc^{-1}}$ [7]). We shall say that the TRGB method measures $\mathcal{H}_0$-values in the near-local Universe, while, the SNe Ia methods measures $\mathcal{H}_0$-values in the far-local Universe. The near and far-local $\mathcal{H}_0$-values do not agree ($69.80 \pm 2.20\,\mathrm{km\,s^{-1}\,Mpc^{-1}}$ [8] and $73.30 \pm 1.04\,\mathrm{km\,s^{-1}\,Mpc^{-1}}$ [7], respectively), thus, giving raise to yet another tension within an already existing tension.

On the other hand, the CMB $\mathcal{H}_0$ measurements are classified as a global $\mathcal{H}_0$ measurements as these measurements are all-sky measurements of $\mathcal{H}_0$ measuring the Hubble constant across the entire sky, hence, they being referred to as a global $\mathcal{H}_0$ measurements. The CMB method is a state-of-the-art precision method of global $\mathcal{H}_0$ measurements by Aghanim *et al.* [9] and this has yielded: $\mathcal{H}_0^{\mathrm{CMB}} = 67.40 \pm 0.50\,\mathrm{km\,s^{-1}\,Mpc^{-1}}$. A summary of these key measurements is presented in self-explanatory Table 1.

Since Lemaître [5] and Hubble [6]'s initial estimates, there has been numerous measurements of the Hubble constant. For our purposes here, the above three measurements (presented in [7–9], which are summarised in a clear and succinct manner in Table 1) shall constitute our focal point in all the $\mathcal{H}_0$ measurements as these three important measurements sufficiently capture the morass substance contained in our current musings and at the same time — they drive our point home regarding this important tropical issue of the Hubble tension.

Astronomers, astrophysicists and cosmologists are hard at work to figure out why the discrepancy in the values of $\mathcal{H}_0$ from the two different methods as a number have wondered if this discrepancy is heralding some hitherto yet unknown physics [3, 11, 12] or there might be some serious, albeit subtle, error in our methods and analysis? We herein present a suggestion to this problem and this suggestion is to the effect that varying Fundamental Natural Constants (FNCs) may be the cause of this tension. As will be demonstrated, a simple hypothesis regarding the nature of the said variation on the FNCs seem to deliver a bold solution to this problem.

In closing this introductory section, we shall give a synopsis of the reminder of this article, i.e.: the reminder of this article is arranged as follows: for no other than smoothness,

completeness and self-containment purpose, we present in the next §2, a pedestrian derivation of the distance modulus formula used in astronomy, astrophysics and cosmology. Thereafter in §3, we discuss distances in cosmology with emphasis on how the luminosity and Light travel distances are used in the distance modulus formula in order to derive the Hubble constant and having done this, in §4, we discuss the three common and popular methods to measure the Hubble constant. In §5, we present what we believe is the source of the problem in our endeavour to compute the Hubble constant leading to the current tension in the measurement of this constant using the two major methods. In §6, we justify the idea of variable fundamental natural constants. It is this idea that our proposed solution to the Hubble tension is to be found, hence there is need to justify the idea. In §7, we present our proposed solution and application of this solution to real data in §8. Lastly, in §10 and §11, we present a general discussion and the conclusion drawn thereof.

2 Distance modulus

In this section, we are going to go through some necessary trivialities and this is for no other purpose other than for self-containment and smooth flow of the paper thereof. As is well known, in astronomy, astrophysics and cosmology, the distance modulus, denoted by the symbol μ, is a way of expressing distances to stellar objects. It is a measure of the difference between the apparent (m) and absolute magnitude (M), of an astronomical object, i.e.: $\mu = m - M$. For a star (or any stellar body of radius, R, mean temperature, T, and, with surface emissivity, ϵ) whose luminosity: $L = 4\pi R^2 \epsilon \sigma_0 T^4$ (where: σ_0 is the Stefan-Boltzmann constant), with a total flux of: $F(d_L)$, and with this flux reaching at the arbitrary distance, d_L, away from the star — the flux received at the said arbitrary distance d_L, obeys the following inverse square law:

$$F(d_L) = \frac{L}{4\pi d_L^2} \,. \tag{1}$$

The absolute magnitude is by definition defined as follows:

$$M = -2.5 \log_{10} F(d_L) \,, \tag{2}$$

while the apparent magnitude is by definition defined:

$$m = -2.5 \log_{10} F(10\,\mathrm{pc}) \,, \tag{3}$$

where: $F(10\mathrm{pc}) = L/4\pi(10\,\mathrm{pc})^2$ is the flux of the given stellar object at a distance: $d_L = 10\,\mathrm{pc}$, away. Hence:

$$\begin{aligned} \mu_L &= m - M \,, \\ &= -2.5 \log_{10}\left(\frac{F(d_L)}{F(10\,\mathrm{pc})}\right) \,, \\ &= -2.5 \log_{10}\left(\frac{10\,\mathrm{pc}}{d_L}\right)^2 \,. \end{aligned} \tag{4}$$

This further simplifies to:

$$\mu_L = 5 \log_{10}\left(\frac{d_L}{10\,\mathrm{pc}}\right) \,, \tag{5}$$

In cosmology, one often works with distances in mega-parsec (Mpc), so, it is convenient to write (5) with, d_L, in Mpc and not in in units of 10pc. Written in the units of Mpc, (5) becomes:

$$\mu_L = 5 \log_{10}\left(\frac{d_L}{\mathrm{Mpc}}\right) + 25 \,. \tag{6}$$

Now, (6) applies in the case where the flux does not experience attenuation as a result of interstellar material along its path — i.e., in the case where there is no extinction of the flux.

In the case were there is extinction, the flux undergoes attenuation. Let, τ, be the optical depth of the Interstellar Medium (ISM) along the intervening spaces along the path of the photons reaching our telescopes and let, F_0, be the flux at the surface of the star (or stellar body). Then, the flux at distance d_L away is such that:

$$F(d_L) = F_0\left(\frac{4\pi R^2}{4\pi d^2}\right) e^{-\tau} \,. \tag{7}$$

For the absolute magnitude, we need the flux, $F(10\mathrm{pc})$, at a distance of 10 parsecs as this is to be evaluated without extinction, i.e.:

$$F(10\mathrm{pc}) = F_0\left(\frac{4\pi R^2}{4\pi(10\mathrm{pc})^2}\right) \,. \tag{8}$$

Therefore, from (7) and (8), it follows that:

$$\frac{F(d_L)}{F(10\mathrm{pc})} = \frac{(10\mathrm{pc})^2}{d_L^2} e^{-\tau} \,, \tag{9}$$

hence:

$$\mu_{L^\tau} = 5 \log_{10}\left(\frac{d_{L^\tau}}{10\,\mathrm{pc}}\right) + A_\tau \,, \tag{10}$$

where:

$$A_\tau = -2.5 \log_{10}(e^{-\tau}) = 5 \log_{10}(e^{0.5\tau}) \,, \tag{11}$$

is the extinction correction term to the distance modulus, and: μ_{L^τ}, is the extinction-corrected distance modulus. With, d_L, expressed in Mpc, the above can be written as follows:

$$\mu_{L^\tau} = 5 \log_{10}\left(\frac{d_{L^\tau}}{\mathrm{Mpc}}\right) + 25 \,, \tag{12}$$

where:

$$d_{L^\tau} = e^{0.5\tau} d_L \,, \tag{13}$$

is the extinction-corrected luminosity distance. Eq. (12) is what is used in cosmology in the study of supernovae to estimate the distance to the Cepheid variables that are resident in the Host galaxy of supernovae.

In closing this section, allow us to say that we are very much aware that we have presented an elementary and textbook derivation of the distance modulus formula. We want to rest assure our reader that this has been done for a very good reason and the reason is that there is an esoteric subtlety associated with this derivation that we want to *exegetically* unmask (point out) and "correct", all this in the hope that this may be one of the problems from which the discrepancy in the measurement of the Hubble constant might lie. Therefore, we kindly ask our reader for their due indulgence as we unpack this esoteric subtlety.

3 Distances in cosmology

If we get our distances wrong in astronomy, astrophysics and cosmology, so is our interpretation of the results — they will be wrong as well. So, the importance of the measures that we use to obtain these distances cannot be overstated. Different distance measures are used in astronomy, astrophysics and physical cosmology. These distance measures give a natural notion of the distance between two objects or events in the Universe. They are often used to tie some observable quantity to another quantity that is not directly observable, but is more convenient for calculations such as the comoving coordinates of quasars, galaxy, *etc*. The observable quantities in question are quantities such as the luminosity of a distant star (or quasar), the redshift of a distant galaxy, or the angular size of the acoustic peaks in the CMB power spectrum. For low redshift objects, these distance measures reduce to the common notion of Euclidean distance. Of particular interest in our present expedition are the luminosity and Light travel distances.

3.1 Light travel distance

Herein denoted by the symbol d_{LT}, the *Light Travel Distance*, is a cosmological concept that refers to the distance Light travels from one point (A) to the other (B), in particular, the distance Light could travel say from one galaxy to our own telescope at the time of observation. The Light travel distance can be important for understanding phenomenon such as the age of the Universe, its expansion rate and the spatial size of the observable Universe for example. Wholly within the framework of Einstein [13–15]'s General Theory of Relativity (GTR), the Light travel distance is calculated with respect to proper time $d\tau$, i.e.:

$$d_{LT} = \int_{\tau_e}^{\tau_r} c\, d\tau = \int_{\tau_e}^{\tau_r} \left(\frac{c_0}{n_r}\right) d\tau\,, \tag{14}$$

where in this case: n_r, is the refractive index of the Interstellar Medium (ISM). In most considerations in the definition and calculation of the Light travel distance, the refractive index does not appear in the formulae, the meaning of which is that, the ISM is, in the said cases, being assumed to be a perfect *vacuo* with a refractive index of unity. In the present expedition, we shall be meticulous and exercise equanimity by not assuming a perfect *vacuo* for the ISM. This is going to help us in our effort to explain the remaining discrepancy in the resulting Hubble constant after the correction of the FNCs has been made.

From the homogeneous and isotropic metric tensor of Friedmann (1924) [16], Lemaître (1933) [17], Robertson (1935, 1933a,b,c) [18–20] and Walker (1937) [21] (hereafter, FLRW-metric), which is what is used in the ΛCDM cosmology model — by setting the proper time in this metric to equal zero for the propagation of Light in an FLRW-Universe — one can show from it that, the Light travel distance, d_{LT}, defined in (14), is such that:

$$d_{LT} = \frac{d_{\rm H}}{n_r} \int_0^z \frac{dz}{(1+z_\lambda)\, n_r \sqrt{\Omega}} = d_{\rm H} f(z_\lambda)\,, \tag{15}$$

where off cause:

$$f(z_\lambda) = \int_0^{z_\lambda} \frac{dz_\lambda}{(1+z_\lambda)\,\sqrt{\Omega}}\,, \tag{16}$$

and: $d_{\rm H} = c_0/\mathcal{H}_0$, is what is called the Hubble distance with:

$$\Omega = \frac{1}{\mathcal{H}_0^2}\frac{\dot{\mathfrak{a}}^2}{\mathfrak{a}^2} = \Omega_{\rm m} + \Omega_\Lambda + \Omega_k\,. \tag{17}$$

The Ω's appearing in (17) are the usual Ω-parameters used in cosmology, with Ω, being the total Ω-parameter; while, $\Omega_{\rm m}$, is the Ω-matter parameter; Ω_Λ, is the Ω-vacuum parameter for the Λ-cosmological field; and, Ω_k is the Ω-curvature parameter.

Now as is the usual case, using the Light travel distance, d_{LT}, one can calculate from it the corresponding distance modulus, μ_{LT}, of the given supernovae, it is given by:

$$\mu_{LT} = 5\log_{10}\left(\frac{d_{LT}}{\rm Mpc}\right) + 25\,. \tag{18}$$

Inserting (15) into (18), we obtain:

$$\mu_{LT} = 5\log_{10}\left[f(z_\lambda)\right] + K\,, \tag{19}$$

where:

$$K = 25 + 5\log_{10}\left(\frac{c_0}{\rm Mpc}\right) - 5\log_{10}\left(n_r\mathcal{H}_0\right)\,. \tag{20}$$

It is from the value of, K, as given in (20), that one is able to calculate the Hubble constant.

3.2 Luminosity distance

We have already met the concept of luminosity distance in our derivation of the distance modulus in §2, which distance we have denoted by the symbol, $d_{\rm L}$. There are two concepts relating to luminosity distance that we shall call the observationally derived luminosity distance and the redshift derived luminosity distance. The former is what we have met. We shall discuss these two concepts below:

1. *Observationally Derived Luminosity Distance*: The observationally derived luminosity, is the luminosity distance that is defined as the distance at which an object would need to be located in order for its observed (apparent) luminosity to match its intrinsic (absolute) luminosity. This is the distance, $d_{\rm L}$, as defined in (1). That is to say, the luminosity distance, $d_{\rm L}$, is related to the observed (apparent) flux (F) from the given object and its intrinsic (absolute) luminosity (L) through (1). At the instance of (8) leading to (13), the luminosity distance has been corrected for extinction and the extinction-corrected luminosity distance has been denoted by the symbol, d_{L^τ}. We will argue in §5 that our understanding of the luminosity may need to be updated if FNCs are variable over cosmic epochs. It is this dearth and paucity of knowledge in our understanding of the luminosity distance that may very well be the cause of the Hubble tension.
2. *Redshift Derived Luminosity Distance*: The redshift derived luminosity distance, $d_L(z_\lambda)$, depends on cosmology under probe and is given by:

$$\frac{d_L(z_\lambda)}{d_{\rm H}} = \frac{1+z_\lambda}{a_0}\int_0^{z_\lambda}\frac{dz_\lambda}{\sqrt{\Omega}}\,, \tag{21}$$

where: $d_{\rm H} = c_0/\mathcal{H}_0$, is the Hubble distance and Ω is the total Ω-parameter already defined in (17). The cosmology is defined by the total Ω-parameter.

What happens in the supernovae determinations of the Hubble constant is that two distance moduli are constructed and equated and the resulting equation, the Hubble constant is determined. That is to say, from the observationally derived luminosity distance, d_{L^τ}, the distance modulus, μ_{L^τ}, is constructed as given in (12). From (21), one constructs the corresponding the redshift derived distance modulus:

$$\mu_L(z_\lambda) = 5\log_{10}\left(\frac{d_L(z_\lambda)}{\rm Mpc}\right) + 25\,. \tag{22}$$

Now, from the equation: $\mu_{L^\tau} = \mu_L(z_\lambda)$, the Hubble constant is determined.

4 Measuring the Hubble constant

The Hubble constant, can be determined through several different methods, each with its own advantages, disadvantages, and limitations. Here are some of the primary methods:

1. The *Distance Ladder Method* makes use of standard candles such as Cepheid variable stars and type Ia supernovae and from these standard candle distance measures and the the corresponding redshift, one can infer the Hubble constant.
2. The *Cosmic Microwave Background* observations from missions like the Planck satellite provide a measurement of the Hubble constant based on the early Universe's conditions.
3. The *Tip-of-the-Red-Giant Method* makes use of stars at the tip of the red giant branch on a IV-color-color diagram. These stars have known fixed intrinsic brightness, hence, they are standard candles. Using this fact other with their redshift, one can infer the Hubble constant.
4. The *Baryon Acoustic Oscillations (BAO) Method* uses the distribution of galaxies to infer distances and hence the expansion rate of the Universe.
5. The *Gravitational Lensing Method* uses the bending of light from distant objects by massive foreground objects as this can be analyzed to estimate the Hubble constant.
6. The *Time Delay Measurements Method* in systems with multiple images of the same astronomical event (like a supernova), the time delays in these systems can be used to calculate the Hubble constant.
7. The *Tying to Local Measurements Method* links the Hubble constant to local measurements in the Solar System, such as the motion of nearby galaxies.
8. The *Galaxy Cluster Dynamics Method* utilizes the motion of galaxies within clusters providing insights into the expansion rate.

In the next two subsections [i.e., §4.1 and §4.2], we shall give an *exegetic exposition* of the first two methods, namely the *Distance Ladder Method* and the *CMB-Method*. The exegesis that we institute is meant to pinpoint the plausible sources of error that may need to be corrected so as to bring about concordance in the $\mathcal{H}_0$-values derived from these two state-of-the-art methods.

4.1 SNe Ia distance ladder method

In the SNe Ia method, three things are necessary:

1. A type Ia supernovae and its redshift, z_λ.
2. A host galaxy for the given supernova.
3. A Cepheid variable star or Cepheid variable stars in the supernovae host galaxy.

Cepheids are stars that vary periodically in brightness in a predictable way, and their brightness can be used to determine their distance from Earth. The Cepheid distances are then used to calibrate type Ia supernova luminosities, whose luminosities are then applied to SN Ia out into the far-field to measure $\mathcal{H}_0$ [22]. With the distance to the supernova known, the distance modulus, μ_{L^τ}, corrected for extinction is known. From the calibrated supernova luminosity, the redshift of the supernova is known. With the redshift of the supernova now known, the theoretically derived redshift dependent luminosity distance, $d_L(z_\lambda)$, is then calculated and the value of, $\mathcal{H}_0$, is deduced from the equation: $\mu_{L^\tau} = \mu_{L^{z_\lambda}}$.

4.2 CMB method

BAO experiments essentially measure two quantities, one parallel to the line-of-sight:

$$\beta_\parallel = \mathcal{H}(z) r_s(z_\star)\,, \tag{23}$$

and the other perpendicular to the line-of-sight:

$$\beta_\perp = \frac{r_s(z_\star)}{D_A(z)} = \theta_s(z_\star)\,, \tag{24}$$

where $\mathcal{H}(z)$ is the Hubble parameter, $r_s(z_\star)$ is the comoving sound horizon at recombination (i.e., the standard ruler) and $D_A(z)$ is the comoving angular distance to the observation redshift, z. The latter is computed as:

$$D_A(z) = d_{\rm H} \int_0^z \frac{dz}{\sqrt{\Omega}} \,. \tag{25}$$

The standard ruler $r_s(z_\star)$ is well constrained by CMB experiments. For the shape of $\mathcal{H}(z)$, one needs to assume some model (such as ΛCDM). Thus, by fitting the theoretical predictions for $\beta_\parallel$ and $\beta_\perp$ to the BAO data, we get indirect constraints on the expansion history of the Universe, $\mathcal{H}(z)$, and thus on the Hubble constant $H_0 = H(z = 0)$. In a similar way to other probes of the early Universe (as the CMB), this method gives a value of H_0 that is in tension with the direct measurement in the local Universe (using the cosmic distance ladder). Note that even if BAO observations are made in the late Universe (by looking at the large-scale distribution of galaxies), it is considered as an early probe because it provides a constraint on $r_s(z_\star)$, that gives information about the primordial plasma.

To determine, $\mathcal{H}_0$, from the CMB data one calculates a *Monte Carlo Markov Chain* (MCMC) which involves evaluation of the likelihood of parameter values and their associated spectra at tens to hundreds of thousands of points in the parameter space, and then one uses this chain to infer the posterior density of, $\mathcal{H}_0$, or any other cosmological parameter of interest [12, 23]. Apart from laying down the method leading to the calculation of, $\mathcal{H}_0$, what we want at the end of this section is a generic formula of how one proceeds to calculate $\mathcal{H}_0$.

The Hubble constant is inferred from CMB temperature anisotropies measurements. That is, measurements of temperature anisotropies in the CMB have revealed a series of (damped) acoustic peaks [12, 23]. These acoustic peaks constitute the esoteric fingerprint of the early Universe's BAO during the era of the pre-recombination plasma — i.e.: sound waves propagating in the baryon-photon plasma prior to photon decoupling, set up by the interplay between gravity and radiation pressure [24–28]. The first acoustic peak is set up by an oscillation mode which had exactly the time to compress once before freezing as photons decoupled shortly after recombination and this peak is precisely determined at: $\theta_s = 1^\circ$.

The first acoustic peak of the CMB carries the indelible imprint of the comoving sound horizon at last scattering $r_s(z_\star)$, given by the following:

$$r_s(z_\star) = \int_0^{z_\star} \frac{c_s(z_\lambda) dz_\lambda}{\mathcal{H}(z_\lambda)} = \frac{c_0}{\mathcal{H}_0} \int_0^{z_\star} \frac{c_s(z_\lambda) dz_\lambda}{c_0 \sqrt{\Omega}} \,, \tag{26}$$

where: $z_\star \sim 1100$, denotes the redshift of last scattering, $\mathcal{H}(z_\lambda)$ denotes the expansion rate, and $c_s(z_\lambda)$ is the sound speed of the photon-baryon fluid. For most of the expansion history prior to last scattering, $c_s(z_\lambda)/c_0 \simeq 1/\sqrt{3}$, before dropping rapidly when matter starts to dominate.

On the other hand, the spatial temperature fluctuations at last scattering are projected to us as anisotropies on the CMB sky. As a consequence, the first acoustic peak actually carries information on the angular scale θ_s (usually referred to as the angular scale of the first peak), given by:

$$\theta_s(z_\star) = \frac{r_s(z_\star)}{D_A(z_\star)} \,, \tag{27}$$

where: $D_A(z_\star)$, is the angular diameter distance to the surface of last scattering, given by:

$$\begin{aligned} D_A(z_\star) &= \frac{c_0}{1 + z_\star} \int_0^{z_\star} \frac{dz_\lambda}{\mathcal{H}(z_\lambda)} \\ &= \frac{c_0}{\mathcal{H}_0 \, (1 + z_\star)} \int_0^{z_\star} \frac{dz_\lambda}{\sqrt{\Omega}} \,, \end{aligned} \tag{28}$$

From this, one can determine the CMB-derived Hubble constant, $\mathcal{H}_0^{\rm CMB}$, from the following:

$$\mathcal{H}_0^{\rm CMB} = \frac{\theta_s(z_\star)}{r_s(z_\star)} \left(\frac{c_0}{1 + z_\star} \int_0^{z_\star} \frac{dz_\lambda}{\sqrt{\Omega}} \right) . \tag{29}$$

According (*e.g.*) to Vagnozzi (2020) [12], measurements of anisotropies in the temperature of the CMB, and in particular the position of the first acoustic peak (which appears at a multipole $\ell \simeq \pi/\theta_s$), accurately fix θ_s, therefore, any modification to the standard cosmological model aimed at solving the Hubble tension should not modify θ_s in the process.

In (29), we see that the CMB-derived redshift is not affected by the variation of FNCs. Apart from, $\mathcal{H}_0$, the only other FNC in the CMB $\mathcal{H}_0$ determination is the speed of Light and in-accordance with the very strong reservations laid down by [29] and [30], we are not going to vary this. The sound speed, c_0, in the pre-recombination plasma medium is the only quantity that can depend on FNC *via* the radiation density term, that is to say, the sound speed is such that: $c_s = c_0/\sqrt{3(1 + \varrho_b/\varrho_\gamma)}$, where: ϱ_b and ϱ_γ, are the densities of baryonic matter and radiation in this plasma, respectively. Because during the plasma era, radiation dominated the Universe, hence, it is generally assumed that: $\varrho_b/\varrho_\gamma \lll 1$, so that the sound speed in this cosmic plasma medium is approximately equal to $c_0/\sqrt{3}$. Hence, the CMB measurements of, $\mathcal{H}_0$, are not affected by the variation of FNCs.

5 Problem

So what is the problem? We are of the strong view that the problem with the discrepancy leading to the Hubble tension may arise from an underestimate of the distance modulus (μ_L) from its determination using the luminosity distance and this underestimate may be a result of the variation of the FNCs:

most probably Planck's constant, $\hbar^*$. We will show in §7, that if indeed FNCs are to vary with cosmological time, then, this variation will introduce a form of "dark extinction" that is not accounted for in the typical calibrations leading to the Hubble constant and this is so for the case of the cosmic distance ladder method. The reason for this omission is that at present, the idea of a variable FNCs is not taken with the seriousness it so deserves despite observations [31–39] of the FSC strongly pointing to this possibility.

The two distance moduli, μ_{L^τ} and μ_{LT}, are determined and then compared (i.e.: $\mu_{L^\tau} = \mu_{LT}$), with μ_{L^τ} being determined from the brightness of the Cepheids resident in the supernovae galaxy, while, μ_{LT}, is determined from the supernova's redshift and in addition to the redshift, it relays on the chosen parameters of the Friedmann model. It is in this comparison: $\mu_{L^\tau} = \mu_{LT}$, that the Hubble constant, $\mathcal{H}_0$, is determined. One thing that one can immediately deduce without fail from this comparison is that $d_{L^\tau} \neq d_{LT}$. That is to say, from (12) and (18), we have that:

$$\mu_{L^\tau} = 5\log_{10}\left(\frac{d_{L^\tau}}{\text{Mpc}}\right) + 25\,, \tag{30a}$$

$$\mu_{LT} = 5\log_{10}\left(\frac{d_{LT}}{\text{Mpc}}\right) + 25\,, \tag{30b}$$

and from (30), it is not difficult to deduce that the said comparison of μ_{L^τ} and μ_{LT} ($\mu_{L^\tau} = \mu_{LT}$) implies that:

$$d_{L^\tau} = d_{LT}\,. \tag{31}$$

So, the luminosity and Light travel distances are generally not equal and are only equal in the case of the ISM having a vanishing optical depth. Now, before we deliver our suggested solution, we shall first motivate for our working model on the variation of FNCs.

6 Variable fundamental natural constants

If we blindly were to go by their verbatim name, then *Fundamental Natural Constants* (FNCs) aught to be what is purported or suggested by their very name "Fundamental", "Natural" and "Constant".

1. Fundamental — meaning intrinsic, inherent and foundational in all reality where they are involved;
2. Natural — meaning that these FNCs must arise naturally in our theories and are not imposed by our finite and limited *intellect*, *whim*, *will* or *desideratum*;
3. Constant — meaning they are sacrosanct and unchanging throughout the entire evolution of the Universe.

Pristinely and succinctly stated, the term *Fundamental Natural Constant* expresses a somewhat "divine" notion of the sacrosanctity of these seemingly immutable and divinely imposed physical quantities.

How far true is this assumption of sacrosanctity, immutability and constancy of these FNCs? For all we know, physics is an experimental human endeavour where answers to the questions that we pause regarding the inner and outer workings of Nature are to be sought by way of physical enquiry *via* ponderable measurements. That is to say, only measurements can decisively and conclusively answer this deep and very interesting question about the possible variation the FNCs. Fortunately, this question of the possible variation of FNCs is now a question capable of being answered from both experimental and observational science — thanks to the capabilities of modern state-of-the-art precision technology that has made this a reality.

The path to the road of inquiry into the possible variation of the FNCs began sometime in 1935 and 1937 with the great British theoretical physicists Edward Arthur Milne (1896-1950) and Paul Adrian Maurice Dirac (1902-1984). That is to say, Milne [40, 41] and Dirac [42] were perhaps the first (in the recorded scientific literature) to question this *status quo* by suggesting that this long held assumption that Newton's supposed universal constant of gravitation, G, was a sacrosanct and sacred constant of Nature that has remained constant since the Universe came into being.

To that end, if current observations [31–39] indicating the cosmological variation of the *Fine Structure Constant* (FSC) stand up to the most ruthless scientific scrutiny, then Milne [40, 41] and Dirac [42] may have been right after all, albeit not on the possible variation of Newton's constant G, but the cosmological variation of the FSC which involves four FNCs, namely: the electronic charge, $e = 1.602176634 \times 10^{-19}$ C; the permittivity of free space, $\varepsilon_0 = 8.8541878128(13) \times 10^{12}$ F m^{-1}; Planck's constant, $h = 6.62607015 \times 10^{-34}$ J s; and, the speed of Light in *vacuo*, $c_0 = 299792458 \times 10^8$ m s^{-1} (2022, CODATA Values).

The dimensionless FSC, denoted by the symbol α_0, is such that:

$$\alpha_0 = \frac{e^2}{4\pi\varepsilon_0\hbar c_0} = \frac{1}{137.035999074(44)}\,, \tag{32}$$

hence:

$$\frac{\Delta\alpha}{\alpha_0} = 2\left(\frac{\Delta e}{e}\right) - \frac{\Delta\varepsilon_0}{\varepsilon_0} - \frac{\Delta\hbar}{\hbar} - \frac{\Delta c}{c_0}\,, \tag{33}$$

that is to say, a cosmological variation in α_0, directly points to a variation in any one, or any possible combination, of the four FNCs: $e, \varepsilon_0, \hbar$, and, c_0.

At present, there exists no properly constituted and fairly accepted theory that explains why any of the supposed FNCs must vary. Most theories that do make the endeavour to explain the possibility of the variation of the FSC are speculative theories based on exotic and exogenous ideas [43–48] and some of these theories are yet to make contact with experience such as string and string-related theories.

*Typically, $\hbar$ is referred to as the reduced or normalized Planck constant. Fully cognisant of this fact, we shall however refer to this constant $\hbar$, simply as Planck's constant.

Following Dirac [42] on the variation of the Newtonian gravitational constant that it must vary in proportional to the age of the Universe, which also translates to a variation with respect to the cosmological scale factor $\mathfrak{a} = \mathfrak{a}(t)$, we shall assume that the expansion of the Universe is what is responsible for the variation of FNCs. That is to say, if for example, K, is some arbitrary FNC, then, its variation will scale in proportion to the scale factor, $\mathfrak{a}$, that is to say: $K \propto \mathfrak{a}^{\beta_K}$, and as a mathematical equation, this can be written as follows:

$$K = K_H \mathfrak{a}^{\beta_K} = K_H (1 + z_\lambda)^{-\beta_K} , \tag{34}$$

where: K_H, is the value of this constant at the beginning of time where: $t = \tau_P$, and β_K, is the proportionality index for this constant and $\mathfrak{a}_0$, is the scale factor of the Universe while, $\mathfrak{a}$, is the scale factor of the Universe at the time of emission of the photon whose redshift we measure with our telescopes today. We hypothesize that the Universe began when the cosmic clock was reading one Planck second $\tau_P = \sqrt{G\hbar/c_0^5}$. From this, it follows that:

1. If: $\beta_K > 0$, then, the FNC in question increases with time, i.e., its value gets larger as the Universe gets older.
2. If: $\beta_K < 0$, then, the FNC in question decreases with time, i.e., its value gets smaller as the Universe gets older.
3. If: $\beta_K = 0$, then, the FNC in question is indeed a true constant of Nature.

In the present exploration of ideas, we shall assume that one of, or all of, or any possible combination of the four FNCs $(e, \varepsilon_0, \hbar, c_0)$ making up the FSC will vary with cosmological time, i.e.:

$$e = e_H \mathfrak{a}^{\beta_e} = e_H (1 + z_\lambda)^{-\beta_e} , \tag{35a}$$

$$\varepsilon_0 = \varepsilon_{0H} \mathfrak{a}^{\beta_{\varepsilon_0}} = \varepsilon_{0H} (1 + z_\lambda)^{-\beta_{\varepsilon_0}} , \tag{35b}$$

$$\hbar = \hbar_H \mathfrak{a}^{\beta_\hbar} = \hbar_H (1 + z_\lambda)^{-\beta_\hbar} , \tag{35c}$$

$$c_0 = c_{0H} \mathfrak{a}^{\beta_{c_0}} = c_{0H} (1 + z_\lambda)^{-\beta_{c_0}} , \tag{35d}$$

where: $e_H, \varepsilon_{0H}, \hbar_H$ and c_{0H}, are the values of the fundamental electronic charge, the permittivity of free space, Planck's constant and the speed of Light in *vacuo* at the beginning of time and: $\beta_e, \beta_{\varepsilon_0}, \beta_\hbar$, and, β_{c_0}, are the corresponding indices of the variation of these FNCs, respectively.

We want to be clear to our reader in that we are not proposing that all the four FNCs $e, \varepsilon_0, \hbar$, and, c_0, do vary with cosmic time. What we are saying is that the variation of the FSC allows us to entertain the possibility of the variation of at least one of these four constants. If we were asked our inclination regarding which of the four do we really think are varying, we would say, it is probably Planck's constant. We have our reasons, for we have pondered on this matter in our on-going ideas that we are still working on and are yet to be published; from the said ideas, we strongly holdfast that the speed of Light and as well the electronic charge must be true FNCs, thus leaving $\hbar$ and ε_0 as variables.

For our purpose here, it really does not matter as to which FNC is varying, as long just one of them is variable, this would lead to the Stefan-Boltzmann-Planck constant, σ_0, being a variable as it does depend on the Planck constant and the speed of Light in *vacuo*. That is to say, we know that:

$$\sigma_0 = \frac{2\pi^5 k_B^4}{15\hbar^3 c_0^2} = 5.670374419 \times 10^{-8} \,\mathrm{W\,m^{-2}\,K^{-4}} , \tag{36}$$

where: $k_B = 1.380649 \times 10^{-23} \,\mathrm{J\,K^{-1}}$ (2022, CODATA Value) is Boltzmann's constant. From (36), it follows that if say, $\hbar$, or, c_0, did vary with cosmological time, then, σ_0, will vary cosmologically as well, i.e.:

$$\sigma_0 = \sigma_{0H} \mathfrak{a}^{\beta_\sigma} , \tag{37}$$

where as before: σ_{0H}, is the Stefan-Boltzmann-Planck constant at the beginning of time and, $\beta_\sigma = 4\beta_{k_B} - 3\beta_\hbar - 2\beta_{c_0}$, is the corresponding index of the cosmological variation of σ_0. For our purposes here, following the strong advice of Ellis & Uzan [29,30], we shall assume that: $\beta_{c_0} = 0$, and also following our own intuition, we shall assume: $\beta_{k_B} = 0$; hence, we shall have: $\beta_\sigma = -3\beta_\hbar$ and this implies that the luminosity of a star, L, will vary with the scale factor as follows:

$$L \propto \mathfrak{a}^{-3\beta_\hbar} . \tag{38}$$

Equipped with this seemingly strange and exotic hypothetical idea of the cosmological variation of FNCs, we are going to suggest in the next section a plausible solution to the Hubble tension problem.

7 Proposed solution

From the thesis just laid down in the previous section, it is pristine clear that if FNCs are variable, then there aught to be a discrepancy in the values of early and late measurements of $\mathcal{H}_0$, and the reason is simple because these epochs have different values of these FNCs that drive the physics thereof. For example, late-type values are those from the local neighbourhood where the FNCs $(k_B, \hbar, c_0)$ in those galaxies are just about the same as in our own galaxy, whereas in the early-type $\mathcal{H}_0$-measurements, the FNCs are significantly different from our own, hence we are comparing two significantly different cosmological epochs. Thus, from the foregoing, it is clear that late-type $\mathcal{H}_0$-measurements aught to be the true and correct values of $\mathcal{H}_0$, whereas those from the early-type measurements are going to contain a hitherto intrinsic and inherent additional signal (term) which is not accounted for in contemporary measurements, hence the tension.

Now, in order to see how this variation of FNCs comes in, from (38), we now have the FNC variation term, $\mathfrak{a}^{-3\beta_\hbar}$, in the flux emitted by the source at distance, d, i.e.:

$$F(d_L) = F_0 \left(\frac{4\pi R^2}{4\pi d_L^2} \right) \mathfrak{a}^{-3\beta_\hbar} e^{-\tau} , \tag{39}$$

where in (39), we see that in comparison to (7), we have in addition to the traditional extinction term, $e^{-\tau}$, there now is supplemented a new extinction term $\mathfrak{a}^{-3\beta_\hbar}$. Our claim is that it is this term $\mathfrak{a}^{-3\beta_\hbar}$ that is not accounted for in contemporary cosmology models that do not embrace the variation of the FNCs.

Now, just as before for the absolute magnitude, we need the flux, $F(10\text{pc})$, at a distance of 10 parsecs as this is to be evaluated without any form extinction — either the optical (τ) term or the FNC-variation term ($\beta_\hbar$), i.e.:

$$F(10\text{pc}) = F_0\left(\frac{4\pi R^2}{4\pi(10\text{pc})^2}\right). \tag{40}$$

From (39) and (40), it follows that:

$$\frac{F(d_L)}{F(10\text{pc})} = \frac{(10\text{pc})^2}{d_L^2}\mathfrak{a}^{-3\beta_\hbar}e^{-\tau}, \tag{41}$$

hence, the *variation* of FNCs corrected-distance modulus, μ'_L, is given by:

$$\mu'_L = \overbrace{5\log_{10}\left(\frac{d_L}{\text{Mpc}}\right) + 25 + A_\tau}^{\mu_{L^\tau}} + \overbrace{5\log_{10}\left(\mathfrak{a}^{1.5\beta_\hbar}\right)}^{\mu_{\text{D}}}. \tag{42}$$
$$\text{Dark-Term}$$

That is to say, (42) reads: $\mu'_L = \mu_{L^\tau} + \mu_{\text{D}}$, where: μ_{D}, is a new emergent dark-term that arises from the variation of the Planck constant (if the Planck constant is not variable, then it must either be, k_{B}, and, c_0). Since: $\mu'_L = \mu_{LT}$, it follows that:

$$\overbrace{5\log_{10}\left(\frac{d_L}{\text{Mpc}}\right) + 25 + A_\tau}^{\mu_{L^\tau}} + \overbrace{5\log_{10}\left(\mathfrak{a}^{1.5\beta_\hbar}\right)}^{\mu_{\text{D}}} = \tag{43}$$
$$\text{Dark-Term}$$
$$= 5\log_{10}\left(\frac{d_{LT}}{\text{Mpc}}\right) + 25.$$

Taking the dark-term to the right hand-side of (43), we will have:

$$5\log_{10}\left(\frac{d_L}{\text{Mpc}}\right) + 25 + A_\tau = \tag{44}$$
$$= 5\log_{10}\left(\frac{d_{LT}}{\text{Mpc}}\right) + 25 - 5\log_{10}\left(\mathfrak{a}^{1.5\beta_\hbar}\right).$$

We can re-write (44), as follows:

$$\overbrace{\mu_{L^\tau} = 5\log_{10}\left(\frac{d_{L^\tau}}{\text{Mpc}}\right) + 25}^{\text{Flux-Dependent}} = \tag{45}$$
$$\text{Observationally Derived}$$
$$= \overbrace{5\log_{10}\left(\frac{d_{LT}^{\Delta\sigma_0}}{\text{Mpc}}\right) + 25 = \mu_{LT}^{\delta\hbar}}^{\text{Redshift-Dependent}},$$
$$\text{Theoretically Derived}$$

where:

$$d_{LT}^{\Delta\sigma_0} = \mathfrak{a}^{-1.5\beta_\hbar}d_{LT}, \tag{46}$$

is what we shall call the *FNC variation-corrected Light travel distance*, where in the present case, the FNC for which the Light travel distance has been corrected for, is the Planck constant because it is the particular FNC that we have chosen is variable, while the other two (k_{B}, c_0) have been held constant.

Now, given that in the ΛCDM cosmology model, the redshift, z_λ, and the scale factor, a, are related as follows: $1+z_\lambda = a_0/a$, i.e.:

$$a = \frac{a_0}{1+z_\lambda}, \tag{47}$$

where: a_0, is the present day scale factor of the Universe while, a, is the Universe's scale factor at the time of emission of the photon that we receive here on Earth. The present scale factor of the Universe is set: $a_0 = 1$. From this, it follows that if we are to insert this into (42), we will obtain:

$$d_{LT}^{\Delta\sigma_0} = (1+z_\lambda)^{1.5\beta_\hbar}\, d_{LT}. \tag{48}$$

Now, since: $d_{L^\tau} = d_{LT}^{\Delta\sigma_0}$, it follows that:

$$d_{L^\tau} = (1+z_\lambda)^{1.5\beta_\hbar}\, d_{LT} = d_{\text{H}}\,(1+z_\lambda)^{1.5\beta_\hbar}\, f(z_\lambda), \tag{49}$$

hence:

$$\mu_{L^\tau} = 5\log_{10}\left[(1+z_\lambda)^{1.5\beta_\hbar}\, f(z_\lambda)\right] + K, \tag{50}$$

where, K, is no longer as has been defined in (20), but is now defined as follows:

$$K = 25 + 5\log_{10}\left(\frac{c_0}{\text{Mpc}}\right) - 5\log_{10}\left(n_r\mathcal{H}_0\right). \tag{51}$$

This completes our theoretical exegesis on the plausible origins of the Hubble tension. What is now left is for us to calibrate this result (50) against real data. In order to to do this, there is need to first figure out what, $f(z_\lambda)$, is. This function, $f(z_\lambda)$, is dependent on the cosmology model that one adopts. In our present case, we shall adopt a cosmology for which the total Ω-parameter is identically equal to unity, i.e.: $\Omega \equiv 1$. That is to say, Ω, does not happen to be equal to unity in the present epoch of the Universe's evolution, but is eternally so for all times — i.e., from antiquity to eternity. If as declared: $\Omega \equiv 1$, it follows from (16), that:

$$f(z_\lambda) = \ln(1+z_\lambda), \tag{52}$$

hence:

$$\mu_{L^\tau} = 5\log_{10}\left[(1+z_\lambda)^{1.5\beta_\hbar}\ln(1+z_\lambda)\right] + K. \tag{53}$$

Thus, (53) is what we are going to test against observational evidence and we must hasten to say that (53) has not been *priori* designed to fit the observational data that it will excellently fit. It actually came as nothing short of a *non-posteriori* surprise that this model [(53)] agrees very well with empirical evidence.

8 Application of theory

We are now ready to apply our ideas onto some real and tangible data and for this, we are going to use the Supernova Cosmology Project (SCP) Union2.1 dataset spanning the redshift range: $0.015 \leq z_\lambda \leq 1.414$, [49]. This dataset is a compilation of 580 SNe type Ia drawn from 19 datasets [50–67]. We must say that this dataset may very well be the most comprehensive and most accurate SNe data available to date. Further, according to Suzuki *et al.* [49], all SNe were fitted using a single light-curve fitter (SALT2-1) and uniformly analyzed in blind-mode, i.e., without due consideration of a particular cosmology model. With 580 data points in the sufficiently large redshift range: $0.015 \leq z_\lambda \leq 1.414$, we certainly do have a statistically significant dataset to make a meaningful conclusion on the present model (53) of the plausible time variability of FNCs.

What we really want in this section is to test the proposed model presented in (53). We want to find the value of $\beta_\hbar$, and, K; and from the value of K, we can deduce $\mathcal{H}_0$. To that end, in Fig. 1, we have plotted the distance modulus, μ_{L^τ}, *vs* the redshift, z_λ, of the 580 SNe from the Union2.1 dataset and with this dataset, we perform a non-linear curve fitting on the data and from this non-linear curve fitting exercise, we obtain:

$$\beta_\hbar = +0.77 \pm 0.02\,, \tag{54a}$$

$$K = 43.20 \pm 0.01\,\text{mag}\,. \tag{54b}$$

From the value of K, obtained (43.20 ± 0.01 mag.), we find for the Hubble constant, the value:

$$\mathcal{H}_0 = \frac{68.70 \pm 0.30\,\text{km s}^{-1}\,\text{Mpc}^{-1}}{n_r} = \frac{\mathcal{H}_0^{\text{SNe}}}{n_r}\,. \tag{55}$$

If the ISM is a perfect *vacuo* (which it obviously is not), then:

$$\mathcal{H}_0 = \mathcal{H}_0^{\text{SNe}} = 68.70 \pm 0.30\,\text{km s}^{-1}\,\text{Mpc}^{-1}\,. \tag{56}$$

This value given (56) is the corrected *vacuo* SNe $\mathcal{H}_0$-value where the correction made is that hypothesised variation in the Planck constant and the tension in this value when compared with the CMB-value is significant at a 2.2σ-level (97%) of statistical significance.

Of this value, within the provinces of its own error margins, one can safely say that this rather unexpected result is in very good agreement (0.5σ-level of statistical significance in discrepancy) with that of Freedman *et al.* [8]'s TRGB-midpoint value: $\mathcal{H}_0 = 69.80 \pm 2.20\,\text{km s}^{-1}\,\text{Mpc}^{-1}$. Further, this value is in agreement with the *Wilkinson Microwave Anisotropy Probe* (*WMAP*) data for the CMB data — where: $\mathcal{H}_0 = 69.30 \pm 1.60\,\text{km s}^{-1}\,\text{Mpc}^{-1}$ [68, 69], and, the *Planck 2013* data — where: $\mathcal{H}_0 = 69.80 \pm 2.20\,\text{km s}^{-1}\,\text{Mpc}^{-1}$ [70]. In the $\mathcal{H}_0$ values of Anderson *et al.* [68], Mehta *et al.* [69] *&* Ade *et al.* [70], the BAO data has been admitted together with the CMB data, thus allowing Ω_k to be a free parameter [68, 70, 71], and this is unlike in Aghanim *et al.* [9]'s case were the curvature parameter has been tightly constrained to: $\Omega_k \sim 0$. Furthermore, applying the *WMAP &* CMB constraints to both BAO and SNe data together with the CMB, Blake *et al.* [72] obtained: $\mathcal{H}_0 = 68.70 \pm 1.90\,\text{km s}^{-1}\,\text{Mpc}^{-1}$, and Anderson *et al.* [68] obtained: $\mathcal{H}_0 = 69.60 \pm 1.70\,\text{km s}^{-1}\,\text{Mpc}^{-1}$. Within the margins of error — all these results are in very good agreement with our result: $\mathcal{H}_0 = 68.70 \pm 0.30\,\text{km s}^{-1}\,\text{Mpc}^{-1}$. While this is the case — that our derived value is an improvement in matching the two discontent $\mathcal{H}_0$-values, if at all possible, there is need to get a most perfect agreement between these two values and this can be done by considering the fact that the ISM is not a perfect *vacuo*, the meaning of which is that we need not assume a refractive index of unity for the ISM.

9 Concordance $\mathcal{H}_0$–value

As stated above, the two discontent $\mathcal{H}_0$-values ($\mathcal{H}_0^{\text{SNe}}$ and $\mathcal{H}_0^{\text{CMB}}$) can be brought into concordance by considering the fact that the ISM is not a perfect *vacuo*. That is to say, in the derivation of $\mathcal{H}_0^{\text{SNe}}$, leading to (55), the refractive index was taken into account but later in (56), it (refractive index) was then set to equal unity. We shall drop this assumption that the refractive index is unity. On the same pedestal, we must realize that this same assumption that the refractive index of ISM is unity is employed in the CMB-derivation of $\mathcal{H}_0^{\text{CMB}}$ in (29).

In order for us to take the refractive index into account in (29), what we need to do is to replace c_0 with c_0/n_r. So doing, we obtain:

$$\mathcal{H}_0^{\text{CMB}} = \frac{\theta_s(z_\star)}{r_s(z_\star)}\left(\frac{c_0/n_r}{1+z_\star}\int_0^{z_\star}\frac{dz_\lambda}{\sqrt{\Omega}}\right) = \frac{\mathcal{H}_0}{n_r}\,. \tag{57}$$

From (57), we obtain: $\mathcal{H}_0 = n_r\mathcal{H}_0^{\text{CMB}}$, and proceeding to substitute this into (55), we obtain:

$$\begin{aligned} n_r &= \sqrt{\frac{\mathcal{H}_0^{\text{SNe}}}{\mathcal{H}_0^{\text{CMB}}}}\,, \\ &= \sqrt{\frac{68.70 \pm 0.30\,\text{km s}^{-1}\,\text{Mpc}^{-1}}{67.40 \pm 0.50\,\text{km s}^{-1}\,\text{Mpc}^{-1}}}\,, \\ \therefore\ n_r^{\text{ISM}} &= 1.010 \pm 0.006\,. \end{aligned} \tag{58}$$

In all probity, this value ($n_r^{\text{ISM}} = 1.010 \pm 0.006$) is not at all in bad agreement with the measured refractive index ($n_r^{\text{ISM}} = 1.0001$ to 1.0003 [73–75]) of the ISM. With this ISM refractive index value (1.010 ± 0.006), the concordance $\mathcal{H}_0$-value is:

$$\mathcal{H}_0 = 68.00 \pm 0.90\,\text{km s}^{-1}\,\text{Mpc}^{-1}\,. \tag{59}$$

Within the margins of error, this concordance $\mathcal{H}_0$-value is in good agreement with Freedman *et al.* [8]'s TRGB $\mathcal{H}_0$-value. This good agreement can very well be understood from the fact that the TRGB stars, from which these measurement are inferred, are nearby stars and as a direct result

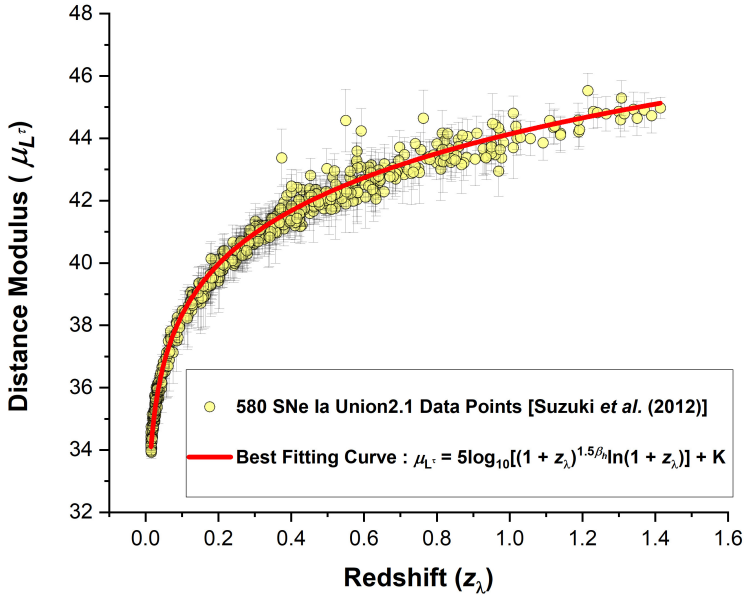

Fig. 1: Graph of Distance Modulus (μ_L) *vs* Redshift (z_λ) from the Union2.1 data of [49]. The Best Fit Graph (RED) is described by the non-linear curve: $\mu_{L^\tau} = 5\log_{10}\left[(1+z_\lambda)^{1.5\beta_\hbar}\ln(1+z_\lambda)\right] + K$, and, from it we obtain the following best parameter fittings: $\beta_\hbar = 0.77 \pm 0.02$, and, $K = 43.20 \pm 0.01$ mag. The R^2-value or Coefficient of Determination (COD) of the fit to data is: 99.49%. Assuming an ISM refractive index of unity — i.e.: $n_r^{\text{ISM}} \equiv 1$, the obtaining K-value leads to: $\mathcal{H}_0 = 68.70 \pm 0.30\,\text{km s}^{-1}\,\text{Mpc}^{-1}$. In order to bring the CMB and SNe Ia measurements into unity and harmony, an ISM refractive index of: $n_r^{\text{ISM}} = 1.010 \pm 0.006$, is needed and this leads to a concordance $\mathcal{H}_0$-value of: $\mathcal{H}_0 = 68.00 \pm 0.90\,\text{km s}^{-1}\,\text{Mpc}^{-1}$.

of this fact, the value of Planck's constant for these systems is pretty much the same as the value of Planck's constant here on Earth, hence, the correction of the variation of Planck's constant needed on these measurements may very well be negligible. Be that as it may, there is need to subject TRGB $\mathcal{H}_0$-measurements to the present idea of a variable Planck constant.

10 General discussion

We have herein suggested that cosmologically varying FNCs may very well present a viable and perdurable solution to the current crisis in cosmology, namely, the Hubble tension. That is to say, from the same SNe Ia data that usually produces values of the Hubble constant in the range ∼ 70–to–76 $\text{km s}^{-1}\,\text{Mpc}^{-1}$, we have downgraded this old value to the new concordance $\mathcal{H}_0$-value: $68.00 \pm 0.10\,\text{km s}^{-1}\,\text{Mpc}^{-1}$, and in the same exercise, the Planck collaboration value of: 67.40 $\pm 0.50\,\text{km s}^{-1}\,\text{Mpc}^{-1}$ has been upgraded to this concordance $\mathcal{H}_0$-value. This has required two major ideas to be evoked, namely, the:

1. Assumption of a cosmologically varying Planck constant, $\hbar$.
2. Adoption of a non-unity value for the refractive index of the ISM.

The assumption of a cosmologically varying Planck constant reduces the SNe Ia derived value of the Hubble constant from the: 70–to–76 $\text{km s}^{-1}\,\text{Mpc}^{-1}$, territory, to exactly: $68.70 \pm 0.30\,\text{km s}^{-1}\,\text{Mpc}^{-1}$. As pointed out in the penultimate of §4.2, this assumption of a cosmologically variable Planck constant does not apply to the derivation of the CMB-derived Hubble constant because none of the physical parameters that enter in the formulae leading to the $\mathcal{H}_0^{\text{CMB}}$ depend on $\hbar$. Effectively, what this means is that the tension in $\mathcal{H}_0^{\text{SNe}}$ and $\mathcal{H}_0^{\text{CMB}}$ is reduced and not resolved. The initial tension* (gap in the two values) is: $7.44\,\text{km s}^{-1}\,\text{Mpc}^{-1}$, and this is reduced to: $2.10\,\text{km s}^{-1}\,\text{Mpc}^{-1}$, and this is an 88% reduction. In order to "resolve" the tension completely, the fact that the ISM is not a perfect *vacuo* is taken into account and this fact affects both measurements — i.e., the CMB and SNe Ia measurement and is seen that a refractive index: $n_r = 1.010 \pm 0.006$, resolves the tension completely, leading to the concordance value: $\mathcal{H}_0 = 68.00 \pm 0.90\,\text{km s}^{-1}\,\text{Mpc}^{-1}$.

We candidly must say that our choice in the Planck constant, $\hbar$, as the likely culprit is informed by what we believe to

*By tension here we mean the difference within the margins of error between the two values: $\mathcal{H}_0^{\text{SNe}} = 68.00 \pm 0.10\,\text{km s}^{-1}\,\text{Mpc}^{-1}$, and, $\mathcal{H}_0^{\text{CMB}} = 67.40 \pm 0.50\,\text{km s}^{-1}\,\text{Mpc}^{-1}$. That is to say, the difference in: MIN($\mathcal{H}_0^{\text{SNe}}$) = $71.97\,\text{km s}^{-1}\,\text{Mpc}^{-1}$, and, MAX($\mathcal{H}_0^{\text{CMB}}$) = $67.90\,\text{km s}^{-1}\,\text{Mpc}^{-1}$. Clearly, this difference is equal to: $4.07\,\text{km s}^{-1}\,\text{Mpc}^{-1}$. Following the same line of thought and reasoning, the tension in the new variable-$\hbar$ corrected: $\mathcal{H}_0^{\text{SNe}} = 68.00 \pm 0.10\,\text{km s}^{-1}\,\text{Mpc}^{-1}$, and the old CMB-derived $\mathcal{H}_0$-value: $\mathcal{H}_0^{\text{CMB}} = 67.40 \pm 0.50\,\text{km s}^{-1}\,\text{Mpc}^{-1}$, is: $0.50\,\text{km s}^{-1}\,\text{Mpc}^{-1}$. Clearly, the percentage reduction in tension is: $(1 - 0.50\,\text{km s}^{-1}\,\text{Mpc}^{-1}/4.07\,\text{km s}^{-1}\,\text{Mpc}^{-1}) \times 100\% = 88\%$.

be our strong intuition rather than scientific objectivity. Because of a general lack or consensus on the variation of the FSC; without fail, we must say that ideas of variable FNCs are by their nature largely considered to be speculative and may very well be outside of the realm of the general support of contemporary scientific understanding because despite claims of a variable FSC [31–39], at present, there is no direct "incriminating" and invigorating evidence to suggest that the Planck constant could change over cosmic times [76–78].

The most widely considered FNCs to vary over cosmic times is the speed of Light [79–87] but we have our deep-seated reasons for holding back on taking this position*. We are not going to take a position simply because everyone is taking that position because we are aware that no amount of research on the candle would have led mankind to discover the Light bulb. To discover the Light bulb, it was needed to consider ideas alien to our common experience. We have here chosen to take the "road less travelled if not the road not travelled" and vary Planck's constant.

Because the Planck constant sets the scale for the quantum nature of particles and their interactions with its value determining the granularity of atomic energy levels and the scale at which quantum effects become significant — in a Universe with an increasing Planck constant such as the one that we are suggesting, over cosmic times, the behaviour of the Universe would tend to be more classical rather than quantum mechanical. From a quantum probability calculus view point, this means the initial state of the Universe must have been less probabilistic (i.e., highly unpredictable) and has been evolving into a more probabilistic state (i.e., more predictable). This evolutionary sequence of the Universe resonates well with the *Second Law of Thermodynamics* (SLT) as this implies that the Universe must have started in a state of lowest entropy and has been, and is, evolving into a state of highest entropy.

Further, if the Planck constant $\hbar$, were to vary as suggested here, it could help solve one of the outstanding problems in the Universe's expansion to do with the conservation of the photon's energy and the expansion of the spacetime. The problem is a simple one and is as follows. We know that the energy, E_γ, of a photon is related to the photon's wavelength, λ, as follows: $E_\gamma = 2\pi\hbar c_0/\lambda$. As a result of cosmic expansion, the wavelength of the photon increases. If $\hbar$, and, c_0, are to remain constant as the spacetime expands, it follows that the energy of the photon will diminish without any foreseeable compensation — i.e.: $\Delta E_\gamma \neq 0$, and this obviously violates the *Law of Conservation of Energy*.

*Completely in agreement with Ellis [29] and Ellis & Uzan [30], we are of the view that the speed of Light cannot be varied in a "part or portion of physics" but must be done wholesomely in a consistent manner at a most fundamental level. At the very least, this requires a complete and total rewrite of physics. Varying the speed of Light is unimaginable at the very least. We have held fast in the present exploration the idea of a sacrosanct and invariant speed of Light.

Where does the diminished energy go to? This is something that has bothered the desideratum of the foremost theoretical physicist since this issue was first noticed and to this day, it has not been resolved. In the advent of a time-variable Planck constant and an invariant Light speed c_0, one can postulate that the photon energy is conserved ($\Delta E_\gamma = 0$) and the compensation in the increase in its wavelength comes in the wake of an equal compensation in the increase of the Planck constant — i.e.:

$$z_\lambda = \frac{\Delta\lambda}{\lambda} = \frac{\Delta\hbar}{\hbar}\,. \tag{60}$$

What (60) means is that the redshift, z_λ, that we measure must be a measure in the change of the Planck constant.

Regarding the evidence of a varying Planck constant, there have been few direct references in the literature on the subject of a variable Planck constant [88–90]. [88, 89] approaches the subject from a laboratory view point while [90] does this on a purely speculative theoretical standpoint. Searches for a variable Planck constant have been under the guise of a variable FSC [31, 39] which amongst others also implies a variable electronic charge, the speed of Light and/or the permittivity of free space.

Hutchin [89] reports that a gradual and systematic drop has been observed in the decay rates of 8 radionuclides $\left[{}^{226}\mathrm{Ra},\ {}^{154}\mathrm{Eu},\ {}^{238}\mathrm{Pu},\ {}^{3}\mathrm{H},\ {}^{54}\mathrm{Mn},\ {}^{60}\mathrm{Co},\ {}^{90}\mathrm{Sr},\ {}^{36}\mathrm{Cl}\right]$ over a 20 year span by six organizations on three continents (German, American and Russian labs), including beta decay (weak interaction) and alpha decay (strong interaction) and in the search for a common cause, Hutchin [89] hypothesizes that small variations in Planck's constant might account for the observed synchronized variations in these strong and weak decays.

Hutchin [88] further suggests that this proposed variation of $\hbar$, may very well be a good candidate for the cause of the Casimir radiation and further proposes that if this Casimir radiation were emitted by stars *via* a changing $\hbar$, then:

> ... this could provide an alternative explanation for the Hubble constant, where the distant galaxies are redder simply because $\hbar$ is smaller back in time, making local time move more slowly. In contrast to the expanding model of the Universe, we could now consider whether our Universe might simply be static, where gravity is everywhere balanced on a large scale. Such a conclusion would end the search for dark energy since such a Universe is essentially static while the usual red shift would still be observed.

Unlike Hutchin [88], we do not believe that a variable $\hbar$ necessarily rules out "the expansion of the Universe and points to a *Static Universe*."

As apparent fissures in the standard model have been emerging, there are also indications that there may be cracks that need attention in the local distance scale as well. For example, the tip of the red giant branch (TRGB) method and the Cepheid distance scale result in differing values of $\mathcal{H}_0$ =

$69.60 \pm 1.90\ \mathrm{km\,s^{-1}\,Mpc^{-1}}$ [8,91] for the TRGB and $73.30 \pm 1.04, \mathrm{km\,s^{-1}\,Mpc^{-1}}$ [7], for the Cepheids. This divergence raises the question of whether the purported tension is being driven by yet-to-be-revealed systematic errors in the local Cepheid data, rather than in the cosmological models.

11 Conclusion

Assuming what has been presented herein is acceptable, we hereby present the following as the logical conclusion that can be drawn thereof:

1. We have shown that the Hubble tension can in principle be alleviated if we assume a cosmologically varying Planck constant and as well as a dispersive non-zero refractive index ISM.
2. Further — we have shown that the current supernovae derived $\mathcal{H}_0$-value can be brought down from its current lofty value: $\mathcal{H}_0^{\mathrm{SNe}} = 73.30 \pm 1.03\,\mathrm{km\,s^{-1}\,Mpc^{-1}}$, down to: $68.70 \pm 0.30\,\mathrm{km\,s^{-1}\,Mpc^{-1}}$, and this new value is not in dire disagreement with the CMB-derived $\mathcal{H}_0$-value: $\mathcal{H}_0^{\mathrm{CMB}} = 67.40 \pm 0.50\,\mathrm{km\,s^{-1}\,Mpc^{-1}}$. That is to say, at a 2.2σ-level of statistical significance in discrepancy, this new $\mathcal{H}_0$-value reduces the tension by 88%.
3. Furthermore — in order to "resolve" the tension completely, the fact that the ISM is not a perfect *vacuo* is taken into account and this fact affects both measurements — i.e., the CMB and SNe Ia measurement and it is seen that a refractive index: $n_r = 1.010 \pm 0.006$, resolves the tension completely, leading to the concordance value: $\mathcal{H}_0 = 68.00 \pm 0.90\,\mathrm{km\,s^{-1}\,Mpc^{-1}}$.
4. Additionally — apart from providing a viable solution to the Hubble tension problem, a time variable Planck constant has the potential to solve the problem of the conservation of the photon's energy in an expanding Universe if it is to be assumed that the photon's redshift, $\Delta\lambda/\lambda$, is compensated by a change in Planck's constant, $\Delta\hbar/\hbar$. Ultimately, the photon's redshift under this model emerges as a measure in the change in Planck's constant.
5. Lastly — as demonstrated herein, the idea of varying FNCs aught to be taken much more seriously than currently done as this has the potential to solve the darkenergy and darkmatter problem because if FNCs are really variable, this variation may bring in "dark" effects that might explain away darkenergy and darkmatter.

Dedication

This reading is dedicated to my friend *Anna Neff*.

Received on September 21, 2024

References

1. Verde L., Schöneberg N. and Gil-Marín H. A tale of many H_0. arXiv: 2311.13305.
2. Kamionkowski M. and Riess A. G. The Hubble tension and early dark energy. arXiv: 2211.04492.
3. Di Valentino E., Mena O., Pan S., *et al*. In the realm of the Hubble tension — a review of solutions. *Classical and Quantum Gravity*, 2021, v. 38 (15), 153001.
4. Huchra J. P. The Hubble constant. *Science*, 1992, v. 256 (5055), 321–325.
5. Lemaître G. Un univers homogène de masse constante et de rayon croissant rendant compte de la vitesse radiale des nébuleuses extragalactiques (A homogeneous universe of constant mass and increasing radius accounting for the radial velocity of extragalactic nebulae). *Annales de la Société Scientifique de Bruxelles*, 1927, v. A47, 49–59.
6. Hubble E. P. A relation between distance and radial velocity among extra-galactic nebulae. *Proceedings of the National Academy of Sciences*, 1929, v. 15 (3), 168–173.
7. Riess A. G., Yuan W., Macri L. M., *et al.* A comprehensive measurement of the local value of the Hubble constant with $1\,\mathrm{km\,s^{-1}\,Mpc^{-1}}$ uncertainty from the Hubble Space Telescope and the SH0ES team. *ApJL*, 2022, v. 934 (1), L7.
8. Freedman W. L., Madore B. F., Hatt D., *et al.* The Carnegie-Chicago Hubble Program. VIII. An independent determination of the Hubble constant based on the tip of the red giant branch. *ApJ*, 2019, v. 882 (1), 34.
9. Aghanim N., Akrami Y., Ashdown M., Aumont J. and The Planck Collaboration. Planck2018 Results: VI. Cosmological Parameters. *A&A*, 2020, v.641 (A6).
10. Freedman W. L. Measurements of the Hubble constant: tensions in perspective. *ApJ*, 2021, v. 919 (1), 16.
11. Di Valentino E., Anchordoqui L. A., Akarsu Ö., *at al.* Snowmass 2021 — Letter of interest cosmology intertwined II: the Hubble constant tension. *Astroparticle Physics*, 2021, v. 131, p.102605.
12. Vagnozzi, S. New physics in light of the H_0 tension: an alternative view. *Phys. Rev. D*, 2020, v. 102 (2), p.023518.
13. Einstein A. Kosmologische Betrachtungen zur allgemeinen Relativitätstheorie. *Preussische Akademie der Wissenschaften, Sitzungsberichte*, Bd. 1, 1917, 142–152.
14. Einstein A. Grundgedanken der allgemeinen Relativitätstheorie und Anwendung dieser Theorie in der Astronomie (Fundamental ideas of the General Theory of Relativity and the application of this theory in astronomy). *Preussische Akademie der Wissenschaften, Sitzungsberichte*, Bd. 1, 1915, 315.
15. Einstein A. Zur allgemeinen Relativitätstheorie (On the General Theory of Relativity). *Preussische Akademie der Wissenschaften, Sitzungsberichte*, Bd. 2, 1915, 778–786, 799–801.
16. Friedmann A. A. Über die Möglichkeit einer Welt mit konstanter negativer Krümmung des Raumes. *Zeitschrift für Physik*, 1924, v. 21 (1), 326–332.
17. Lemaître G. Über die Krümmung des Raumes. *Annales de la Société Scientifique de Bruxelles*, 1933, v. A53 (1), 51–85.
18. Robertson H. P. Kinematics and world-structure II. *AJ*, 1936, v. 83, 187–201.
19. Robertson H. P. Kinematics and world-structure III. *ApJ*, 1936, v. 83, 257–271.
20. Robertson H. P. Kinematics and world-structure. *ApJ*, 1935, v. 82, 284–301.
21. Walker A. G. On Milne's theory of world-structure. *Proceedings of the London Mathematical Society*, 1937, v. 42 (1), 90–127.
22. Anand G. S., Tully R. B., Rizzi L., Riess A. G. and Yuan W. Comparing tip of the red giant branch distance scales: an independent reduction of the Carnegie-Chicago Hubble Program and the value of the Hubble constant. *ApJ*, 2022, v. 932 (1), 15.
23. Knox L. and Millea M. Hubble Constant Hunter's Guide. *Phys. Rev. D*, 2020, v. 101 (4), 043533.
24. Bassett B. A. and Hlozek R. Baryon Acoustic Oscillations. 2009, 1–42.

25. Bond J. R. and Efstathiou G. The statistics of Cosmic Background Radiation fluctuations. *MNRAS*, 1987, v. 226 (3), 655–687.

26. Bond J. R. and Efstathiou G. Cosmic Background Radiation anisotropies in universes dominated by non-baryonic darkmatter. *ApJ*, 1984, v. 285, L4.

27. Peebles P. J. E. and Yu J. T. Primeval adiabatic perturbation in an expanding universe. *ApJ*, 1970, v. 162, 815.

28. Sunyaev R. A. and Zeldovich Ya. B. The interaction of matter and radiation in the hot model of the Universe, II. *Astrophys. & Space Sci.*, 1970, v. 7 (1), 20–30.

29. Ellis G. F. R. Note on varying speed of light cosmologies. *Gen. Rel. & Grav.*, 2007, v. 39 (4), 511–520.

30. Ellis G. F. R. and Uzan J. P. *c* is the speed of light, isn't it? *Am. J. Phys.*, 2005, 2005, v. 73 (3), 240–247.

31. King J. A., Webb J. K., Murphy M. T., *et al.* Spatial variation in the fine structure constant — new results from VLT/UVES. *MNRAS*, 2012, v. 422 (4), 3370–3414.

32. Webb J. K., King J. A., Murphy M. T., *et al.* Indications of a spatial variation of the fine structure constant. *Phys. Rev. Lett.*, 2011, v. 107, 191101.

33. Murphy M. T., Webb J. K. and Flambaum V. V. Keck constraints on a varying fine-structure constant: wavelength calibration errors. *Memorie della Società Astronomica Italiana*, 2009, v. 80 (H15), 833–841.

34. Murphy M. T., Webb J. K. and Flambaum V. V. Comment on "Limits on the Time Variation of the Electromagnetic Fine-Structure Constant in the Low Energy Limit from Absorption Lines in the Spectra of Distant Quasars". *Phys. Rev. Lett.*, 2007, v. 99, 239001.

35. Murphy M. T., Webb J. K. and Flambaum V. V. Revision of VLT/UVES constraints on a varying fine-structure constant. *Lect. Notes Phys.*, 2004, v. 648 (2), 131.

36. Murphy M. T., Webb J. K. and Flambaum V. V. Further evidence for a variable fine-structure constant from Keck/HIRES QSO absorption spectra. *MNRAS*, 2003, v. 345 (2), 609–638.

37. Murphy M. T., Webb J. K. and Flambaum V. V., *et al.* Possible evidence for a variable fine-structure constant from QSO absorption lines: motivations, analysis and results. *MNRAS*, 2001, v. 327 (4), 1208–1222.

38. Webb J. K., Murphy M. T., Flambaum, V. V., *et al.* Further evidence for cosmological evolution of the fine structure constant. *Phys. Rev. Lett.*, 2001, v. 87 (9), 091301.

39. Webb J. K., Flambaum V. V., Churchill C. W., *et al.* Search for time variation of the fine structure constant. *Phys. Rev. Lett.*, 1999, v. 82, 884–887.

40. Milne E. A. Relativity, gravitation and world-structure. *Nature*, 1935, v. 135 (3417), 635–636.

41. Milne E. A. Kinematics, dynamics, and the scale of time. *Proceedings of the Royal Society of London A: Mathematical, Physical and Engineering Sciences*, 1937, v. 158 (894), 324–348.

42. Dirac P. A. M. The cosmological constants. *Nature*, 1937, v. 139 (3512), 323–323.

43. Silva M. F. , Winther H. A., Mota D. F. and Martins C. J. A. P. Spatial variations of the fine-structure constant in symmetron models. *Phys. Rev. D*, 2014, v. 89, 024025.

44. Bamba K., Nojiri, S. and Odintsov S. D. Domain wall solution in $F(R)$ gravity and variation of the fine structure constant. *Phys. Rev. D*, 2012, v. 85, 044012.

45. Barrow J. D. and Lip S. Z. W. Generalized theory of varying alpha. *Phys. Rev. D*, 2012, v. 85, 023514.

46. Barrow J. D., Sandvik H. B. and Magueijo J. Behavior of varying-alpha cosmologies. *Phys. Rev. D*, 2002, v. 65(6), 063504.

47. Olive K. A., Peloso M. and Peterson A. J. Where are the walls? Spatial variation in the fine-structure constant. *Phys. Rev. D*, 2012, v. 86, 043501.

48. Calabrese E., Menegoni, Martins C. J. A. P., Melchiorri A., and Rocha G. Constraining variations in the fine structure constant in the presence of early dark energy. *Phys. Rev. D*, 2011, v. 84, 023518.

49. Suzuki N., Rubin D., Lidman C., *et al.* The Hubble Space Telescope cluster supernova survey: V. Improving the dark energy constraints above $z > 1$ and building an early-type-hosted supernova sample. *ApJ*, 2012, v. 746 (1), 85.

50. Amanullah R., Lidma C., Rubin, D., *et al.* Spectra and Hubble Space Telescope light curves of six Type Ia supernovae at $0.511 < z < 1.12$ and the Union2 compilation. *ApJ*, 2010, v. 716 (1), 712–738.

51. Amanullah R., Stanishev V., Goobar A., *et al.* Light curves of five Type Ia supernovae at intermediate redshift. *A&A*, 2008, v. 486 (2), 375–382.

52. Astier P., Guy J., Regnault N., *et al.* The supernova legacy survey: measurement of Ω_{M}, Ω_Λ and w from the first year data set. *A&A*, 2006, v. 447 (1), 31–48.

53. Barris B. J., Tonry J. L., Blondin S., *et al.* Twenty-three high-redshift supernovae from the Institute for Astronomy Deep Survey: doubling the supernova sample at $z > 0.7$. *ApJ*, 2004, v. 602 (2), 571–594.

54. Contreras C., Hamuy M, Phillips M. M., *et al.* The Carnegie Supernova Project: first photometry data release of low-redshift Type Ia supernovae. *AJ*, 2010, v. 139 (2), 519–539.

55. Hamuy M., Trager S. C., Pinto P. A., *et al.* A search for environmental effects on Type I[CLC]a[/CLC] supernovae. *AJ*, 2000, v. 120 (3), 1479–1486.

56. Hicken M., Challis P., Jha S., *et al.* CfA3: 185 Type Ia supernova light curves from the CfA. *ApJ*, 2009, v. 700 (1), 331–357.

57. Holtzman Jon A., Marriner J., Kessler R., *et al.* The Sloan Digital Sky Survey-II: photometry and Supernova IA light curves from the 2005 data. *AJ*, 2008, v. 136 (6), 2306–2320.

58. Jha S., Kirshner R. P., Challis P., *et al.* UBVRI light curves of 44 Type Ia supernovae. *AJ*, 2006, v. 131(1), 527–554.

59. Knop R. A., Aldering G., Amanullah R., *et al.* New constraints on Ω_{M}, Ω_Λ, and w from an independent set of 11 high-redshift supernovae observed with the Hubble Space Telescope. *ApJ*, 2003, v. 598 (1), 102–137.

60. Kowalski M., Rubin D., Aldering G., *et al.* Improved cosmological constraints from new, old, and combined supernova data sets. *ApJ*, 2008, v. 686 (2), 749–778.

61. Krisciunas K., Garnavich P. M., Challis P., *et al.* Hubble Space Telescope observations of nine high-redshift ESSENCE supernovae. *AJ*, 2005, v. 130 (6), 2453–2472.

62. Miknaitis G., Pignata G., Rest A., *et al.* The ESSENCE Supernova Survey: survey optimization, observations, and supernova photometry. *ApJ*, 2007, v. 666 (2), 674–693.

63. Perlmutter S., Aldering G., Goldhaber G., *et al.*, and The Supernova Cosmology Project. Measurements of ω and λ from 42 high-redshift supernovae. *ApJ*, 1999, v. 517 (2), 565–586.

64. Riess A. G., Strolger L. G., Casertano S., *et al.* New Hubble Space Telescope discoveries of Type Ia supernovae at $z \geq 1$: narrowing constraints on the early behavior of dark energy. *ApJ*, 2007, v. 659 (1), 98–121.

65. Riess A. G., Kirshner R. P., Schmidt B. P., *et al.* [ITAL]BVRI[/ITAL] light curves for 22 Type I[CLC]a[/CLC] supernovae. *AJ*, 1999, v. 117 (2), 707–724.

66. Riess A. G., Filippenko A. V., Challis P., *et al.* Observational evidence from supernovae for an accelerating universe and a cosmological constant. *ApJ*, 1998, v. 116 (3), 1009–1038.

67. Tonry J. L., Schmidt B. P., Barris B., *et al.* Cosmological results from high-z supernovae. *ApJ*, 2003, v. 594 (1), 1–24.

68. Anderson L., Aubourg E., Bailey S., Bizyaev D., and at al. The clustering of galaxies in the SDSS-III baryon oscillation spectroscopic survey: baryon acoustic oscillations in the data release 9 spectroscopic galaxy sample. *MNRAS*, 2012, v. 427 (4), 3435–3467.

69. Mehta K. T., Cuesta A. J., Xu X., Eisenstein D. J. and Padmanabhan K. A 2 percent distance to $z = 0.35$ by reconstructing baryon acoustic oscillations — III. Cosmological measurements and interpretation: A 2 percent distance to $z = 0.35$. *MNRAS*, 2012, v. 427 (3), 2168–2179.

70. Ade P. A. R., Aghanim N., Armitage-Caplan C., Arnaud M., Ashdown M., and the Planck Collaboration. Planck2013 Results. XVI. Cosmological parameters. *A&A*, 2014, v. 571 (A16).

71. Tegmark M., Eisenstein D. J., Strauss M. A., Weinberg D. H., at al. Cosmological constraints from the SDSS luminous red galaxies. *Phys. Rev. D*, 2006, v. 74 (12). 123507.

72. Blake C., Kazin E. A., Beutler F., *et al.* The WiggleZ Dark Energy Survey: mapping the distance-redshift relation with baryon acoustic oscillations: WiggleZ survey: BAOs in redshift slices. *MNRAS*, 2011, v. 418 (3), 1707–1724.

73. Saintonge A. and Catinella B. The cold interstellar medium of galaxies in the local Universe. *Ann. Rev. A&A*, 2022, v. 60 (1), 319–361.

74. Draine B. T. Physics of the Interstellar and Intergalactic Medium. Princeton series in astrophysics, Princeton University Press, Princeton, NJ, 2011. Formerly CIP UK. — Includes bibliographical references and index.

75. Rohlfs K. and Wilson T. L. Tools of Radio Astronomy. Springer, Berlin Heidelberg, 2004.

76. Levshakov S. A., Centurión M., Molaro P. and D'Odorico S. VLT/UVES constraints on the cosmological variability of the fine-structure constant. *A&A*, 2005, v. 434 (3), 827–838.

77. Chand H., Srianand R., Petitjean P., and Aracil B. Probing the cosmological variation of the fine-structure constant: results based on VLT-UVES sample. *A&A*, 2004, v. 417 (3), 853–871.

78. Srianand R., Chand H., Petitjean P. and Aracil B. Limits on the time variation of the electromagnetic fine-structure constant in the low energy limit from absorption lines in the spectra of distant quasars. *Phys. Rev. Lett.*, 2004, v. 92 (12), 121302.

79. Sanejouand Y. H. About some possible empirical evidences in favor of a cosmological time variation of the speed of light. *Europhys. Lett.*, 2009, v. 88 (5), 59002.

80. Unzicker A. A look at the abandoned contributions to cosmology of Dirac, Sciama, and Dicke. *Ann. der Physik*, 2009, v. 521 (1), 57–70.

81. Broekaert J. A spatially-VSL gravity model with 1-PN limit of GTR. *Found. Phys.*, 2008, v. 38 (5), 409–435.

82. Magueijo J. New varying speed of light theories. *Reports on Progress in Physics*, 2003, v. 66 (11), 2025–2068.

83. Barrow J. D. Cosmologies with varying light speed. *Phys. Rev. D*, 1999, v. 59 (4), 043515.

84. Moffat J. W. Superluminary universe: a possible solution to the initial value problem in cosmology. *Int. J. Mod. Phys. D*, 1993, V. 02 (03), 351–365.

85. Petit J. P. An interpretation of cosmological model with variable light velocity. *Mod. Phys. Lett. A*, 1988, v. 03 (16), 1527–1532.

86. Giere A. C. and Tan A. A derivation of Hubble's law. *Chinese J. Phys.*, 1986, v. 24 (3), 217–219.

87. Dicke R. H. Gravitation without a principle of equivalence. *Rev. Mod. Phys.*, 1957, v. 29 (3), 363–376.

88. Hutchin R. A. The physics behind the NASA flyby anomaly. *Optics and Photonics Journal*, 2022, v. 12 (03), 31–51.

89. Hutchin R. A. Experimental evidence for variability in Planck's constant. *Optics and Photonics Journal*, 2016, v. 6 (6), 124–137.

90. Dannenberg R. Planck's constant as a dynamical field and path integral. arXiv: 1812.02325.

91. Freedman W. L., Madore B. F., Hoyt T, *et al.* Calibration of the tip of the red giant branch. *ApJ*, 2020, v. 891 (1), 57.

I: Evidence for Phenomena, Including Magnetic Monopoles, Beyond 4-D Space-Time, and Theory Thereof

Richard Ellis
Corpus Christi College (Alumnus), Oxford OX1 4JF, UK
E-mail: r.ellis@physics.oxon.org

This phenomenology paper presents a framework to understand two little-known properties of light. Firstly Brittin and Gamow have shown that sunlight shining on the Earth's surface lowers the entropy level there because $T_s > T_e > T_{space}$. We have found evidence for this, presented separately, which shows it persists contrary to the second law. Secondly when ferromagnetic particles are strongly illuminated, they move as magnetic monopoles. Mikhailov made repeated measurements and determined that the monopole charge is quantized ($g = ng_D$, n = 1–5; $\bar{g} = (0.99 \pm 0.05)\, g_D$) as predicted by Dirac. But they cease to move as monopoles when the illumination is turned off, and so have been ignored. However, the results are reproducible and we deduce these Dirac monopoles are in another space-time. The chronometric invariant formalism of General Relativity (CIGR) predicts a more complex structure to space-time of 5D, with a second time dimension, mirror time, directed from the future to the past (3,2). We make the hypothesis that light, by lowering the entropy level via the Brittin and Gamow effect, can switch the arrow of time into that of the mirror world of CIGR to reveal phenomena there. We call this the "photo-mirror hypothesis". This reveals magnetic monopoles outside 4D but in mirror space-time, where they are less objective, but reproducible and so real. This explains why monopoles can be observed at low energies (because mirror mass is negative), and the infinite length of the Dirac string.

1 Introduction

Brittin and Gamow have used the quantum theory of radiation to derive an equation which predicts that sunlight shining on the Earth's surface, lowers the entropy level there, apparently contrary to the second law of thermodynamics — see equation (1) below [1]. As we investigated this further, we confirmed the violation of the second law. To explain this, we have found new physics which may help penetrate a number of other unsolved problems in quantum and particle physics, such as magnetic monopoles. However, there are several barriers blocking progress. We start with the theoretical barriers.

1. Murray Gell-Mann said at the Conference in Honour of his 80th birthday "I should like to emphasize particularly... the need to go against certain received ideas. Sometimes they are taken for granted all over the world... Often they have a negative character and they amount to prohibitions of thinking along certain lines... Now and then, however, the only way to make progress is to defy one of these prohibitions that are uncritically accepted without good reason" [2]. Such prohibitions often concern problems from the past. So it follows, contrary to the current view that references should be up-to-date, that some of the references below, are old ones. For example, another peculiar effect of light is the detection of magnetic monopoles only when strongly illuminated, in 1930 [3].

2. Secondly, theory is sometimes biased against experiment. True, it is accepted that experiment is the final arbiter of reality. However, important discoveries often get ignored, if the correct theoretical interpretation is not given. For example, parity violation was first observed in 1928, but was rejected as an "instrumental effect" [4]. In 1956 Lee and Yang suggested it could be violated theoretically, and Mme Wu "discovered" it shortly after that. Another example is that Irène Curie and Frédéric Joliot failed to discover the neutron because they did not believe Rutherford's neutron hypothesis. Chadwick realised that their January 18th 1932 results were not due to photons but evidence for neutrons, and so made the discovery a few months later. (The Joliot-Curies also failed to discover the positron, even though they had data for it before Anderson.) A fourth example is that the cosmic microwave background radiation from the Big Bang was first observed by A. McKellar in 1941, but misinterpreted [5]. The CMB was rediscovered at the Pulkovo Observatory by Soviet scientist T. A. Shmaonov in 1957 and published in his thesis, where he determined the temperature to be 4±3°K, but it was ignored [6]. Finally in 1964, Penzias and Wilson detected it a third time, and showed the results to Dicke at Princeton, who realised that this was the afterglow of the Big Bang. Finally the discovery was made.

Another example is the case of Felix Ehrenhaft who had the misfortune to make two such discoveries, firstly of fractional electric charges in 1910 onwards, and then magnetic monopoles in 1930, and get rejected for theoretical reasons twice! We go into magnetic monopoles in more detail below.

There is clearly a pattern here of unexpected experimental results being rejected, sometimes for decades, even indefinitely (e.g. Ehrenhaft). One possible explanation was given

by Einstein when he said to Heisenberg: "It is the theory which decides what we can observe" [7]. In effect it is theory which tells us what we can think. This is fine, when the theory is correct. However, experiment is the final arbiter of the truth, and so experimentalists are closer to Nature, and it is Nature which should tell us what to think. Therefore, when unusual experimental results are obtained, experimentalists should be encouraged to develop the theoretical explanation, especially when they can support their reasoning with mathematics already in the literature, as in this paper.

3. One of the prohibitions to thinking is the second law of thermodynamics. It is thought to be absolute, and to lead to the "heat death" of the Universe. This is in effect a classical physics "Theory of Everything". It is true that (superficially) there is almost overwhelming evidence that entropy tends to increase with time. However, the Universe is a big place and we now know that baryonic matter makes up only about 4% of the Universe. The other 96% consists of dark matter and dark energy; and we do not know what these are, *nor what laws they obey*. So it is illogical to assume that the second law applies to them — it may or it may not. So it is perfectly rational to look for processes which create order out of chaos.

The author has done some experiments on phenomena which apparently violate the second law of thermodynamics, and so are inexplicable [8]. It is the objective of this paper to present a phenomenological framework to understand these results. In the process, we find that this new framework also explains experiments on magnetic monopoles, and observations of fractional electric charges [9].

4. There are also experimental barriers to solving problems in quantum and particle physics. Firstly, particle physics has been re-branded "high energy physics", which is a technique, not a subject. Low energy particle physics is still an important and active area of research [10]. However, it does not get the support nor attention it deserves, because of high energy physics. High energy experiments are massive technological achievements, so low energy experiments can appear insignificant. It is the purpose of these papers to demonstrate the reverse. We present new approaches, both theoretical and experimental, into magnetic monopoles, quarks, preons, and possibly dark matter.

5. Furthermore, experimental physics is currently based upon determining *objective* facts in 4D space-time, for example, by controlled experiment. However, if one relies upon objective facts only, this assumes that the Universe can be reduced to objective facts, or at least if there are any non-objective aspects, they can be ignored. There is no proof of this, and it could lead to an infinite regression. (For example, if matter in the Universe is made from some fundamental objective substance S_A, then what is this made of? Either it is something non-objective, or it is another objective substance S_B, and so on.) So less-than-objective phenomena could be more fundamental than objective ones.

In order to bring experimental physics up to date and more in line with theoretical physics (which frequently incorporates other dimensions or space-times), *we propose that the requirement of objectivity should be relaxed*. For example, if one makes measurements in other spaces or dimensions then, assuming it is possible, *there is inevitably some reduction in control and/or objectivity*. It is currently not recognised that such less-objective results do occur occasionally, and so they tend to be rejected because they are not objective (i.e. not in 4-D space time). We argue that such results should be considered physically real *if they can be reproduced*. We have examined the literature and find that magnetic monopoles are an example of this. They are only detected under intense illumination and so may be linked to the Brittin and Gamow effect.

Our method to challenge these barriers, is to reason from experiment upwards, as opposed to that from theoretical principles downwards, *because it is experiment which can guide us to the true nature of reality*. Never-the-less, we include some mathematics when it is available and can help us understand the experiments.

2 Magnetic Monopoles

We present experimental evidence from the literature, for real ($\nabla \cdot \boldsymbol{B} \neq 0$) magnetic monopoles, as opposed to the pseudo-monopoles ($\nabla \cdot \boldsymbol{H} \neq 0$) sometimes observed in spin ices or other solid-state phenomena.

Over the last 70 years there have been numerous searches for real magnetic monopoles with mostly negative results. Compilations of these searches conclude that there is no reproducible evidence for magnetic monopoles [11, 12]. But there is an assumption behind this conclusion, namely that magnetic monopoles must be particles which can be detected objectively in 4-D space-time, because that is what controlled experiment is limited too. Firstly, in Dirac's theory there is a line connecting two monopoles which has to be *infinitely long*, and yet the universe is finite [13]. This infinite length of the Dirac string is normally explained away as an artefact of the calculation. However, it is there in the theory and implies that both monopoles are outside 4-D space-time, just as the Dirac equation implies the existence of antimatter. (In principle one monopole could be inside 4-D space-time and the other outside, but that would require preferential treatment for one monopole over another, which the theory does not provide. So we reject this.) If they are outside 4D space-time, then it would not be possible to detect them objectively by the normal methods of experimental physics (e.g. by controlled experiment). Therefore the conclusion of the above compilations is not strictly correct. It should read "there is no reproducible evidence for magnetic monopoles *in 4-D space-time*". However, this is not evidence for or against magnetic monopoles because they are not predicted to be in 4-D space-time.

Furthermore, if a phenomenon is not objective, then it is currently rejected by most physicists as *not* being physi-

cally real. Therefore, the above monopole surveys usually omit most, if not all, of the references to the following experiments which provide reproducible evidence for magnetic monopoles, but of a non-objective nature. They are non-objective because *these monopoles are only visible under intense illumination*. When the intense illumination is turned off, they disappear, in the sense that the particle being observed ceases to move as a monopole, and moves as a neutral particle or dipole. *Thus these monopoles do not seem to exist in their own right.* However, these results are reproducible, and so we argue they are physically real. Here is a summary of the published evidence.

2.1 Ehrenhaft

Ehrenhaft first reported observation of single magnetic charges, which were only detectable under intense illumination, in 1930 [3], before Dirac's paper in 1931 [13]. However, Dirac did not recognise Ehrenhaft's results [14, 15]. Not only were Ehrenhaft's results non-objective, but they were obtained at very low energies. So Dirac rejected them, not just because high energies imply objectiveness, but because he thought the very strong force between monopoles would require high energies to separate them. We explain how they can be separated at low energies below.

Dirac's rejection of Ehrenhaft's monopoles creates another problem, namely that there would be two different types of monopole: that predicted by Dirac's theory, and that observed by Ehrenhaft. This is unlikely.

The essence of Ehrenhaft's observations is that when microparticles of ferromagnetic substances (such as iron, nickel or cobalt) are suspended in a gas atmosphere and subjected *simultaneously* to a uniform magnetic field *and to intense illumination by light,* they move as objects carrying single magnetic charges. If the magnetic field $\boldsymbol{H}$ is reversed, then the direction of motion of the single magnetic charges is reversed (magnetic dipoles would not do this). This effect was confirmed by Benedict and Leng [16].

Ehrenhaft did a number of other experiments [17], and when he did not get the recognition he felt he deserved, he made more extreme claims, such as that "light magnetises matter" [18]. He was convinced that he had discovered free magnetic charges and should get the kind of recognition of someone such as Ampère or Faraday. He claimed he had created a magnetic current by causing the monopoles to move [19]. He also claimed to have discovered "magnetolysis", being the magnetic equivalent of electrolysis [20]. Many physicists were unconvinced that "light makes magnetism", suspected it could be due to surface effects, found the effect not objectively real, and so tended to ridicule the results [21]. Einstein took the observations seriously, but wanted a better explanation [22].

Kemple made a review of experimental searches for monopoles up to 1961, including not only the work of Ehrenhaft, but also by his contemporaries. He noted that other experimenters could not reproduce some of these results, and therefore concluded that this work is not evidence for magnetic monopoles [23]. However, this is not strictly correct, because even though some of the experiments may not have been confirmed, the basic observation of magnetic monopoles under intense illumination, was confirmed by Benedict and Leng [16].

2.2 Mikhailov

There the matter might have rested, had it not been that Mikhailov repeated Ehrenhaft's magnetic charge experiment with better technique, and confirmed the result [24–26]. In his first experiment, he used iron microparticles suspended in an atmosphere of argon, illuminated by a laser with power up to 1 kW/cm^2, and in the presence of crossed uniform electric and magnetic fields, which were switched by a square waveform with a frequency of a few Hertz. The particles were observed with a microscope, and moved under the influence of the crossed electric and magnetic fields ($\boldsymbol{E}$ and $\boldsymbol{H}$). By observing their motion, one could *select the signs of the electric and magnetic charges of the particles being observed, thereby confirming Ehrenhaft.*

The observed microparticles had a mass $M \leqslant 10^{-14}$ gram and size $r \leqslant 10^{-5}$ cm, and their motion was governed by Stokes' law. By making measurements on particles carrying both an electric and a magnetic charge, it was possible to measure the ratio g/q independently of the Stokes' coefficient, and hence of the size of the particle. From observations of 1200 such particles, Mikhailov found that *the magnetic charge is quantized*. But his initial value of g disagreed with Dirac's prediction. However, Akers pointed out that *Mikhailov had ignored components of the particle's velocity orthogonal to* $\boldsymbol{E}$ and $\boldsymbol{H}$, and so this interpretation of the result could be incorrect [27].

Mikhailov reanalysed his results and found that the magnetic charge in this experiment, is in fact the solution of a quadratic equation and so gives *two* possible values. One value is the one he had previously reported, the other being *that predicted by Dirac*. In order to distinguish between these two roots, Mikhailov redesigned the experiment to remove this ambiguity and also possible surface effects.

He condensed super-saturated vapour onto solid ferromagnetic particles in a diffusion chamber, which created a smooth surface round each particle and so eliminated surface effects. These ferromagnetic particles, surrounded by fluid, were allowed to drop through a beam of light, under the force of gravity in a magnetic field $\boldsymbol{H}$, which was periodically inverted. Under these conditions, particles exhibiting the magnetic charge effect, fall in a zig-zag path. He observed 428 such tracks with a mean magnetic charge of $\bar{g} = (2.5^{+1.6}_{-1.3}) \times 10^{-8}$ gauss $\times$ cm^2, which agrees with the value predicted by Dirac of $g_{\mathrm{D}} = 3.29 \times 10^{-8}$ gauss $\times$ cm^2 within

the errors. In this way, Mikhailov showed unambiguously that he was observing Dirac "monopoles", and furthermore, these were not due to surface effects on the particles [28].

He also repeated his previous experiment, choosing the correct root, and found that the ferromagnetic particles carried from 1 to 5 magnetic charges. The histogram of magnetic charges clearly shows 5 separate peaks corresponding to $g = ng_{\mathrm{D}}$, where $n = 1$ to 5, with the peaks being gaussian-like with some gaps in between [29]. This confirms that the magnetic charge is quantised as predicted by Dirac, and rules out Schwinger monopoles which have twice the magnetic charge ($g_{\mathrm{S}} = 2g_{\mathrm{D}}$) [30].

The microparticles measured by Mikhailov were composite ($M \leqslant 10^{-14}$ gram), so the monopoles could be composite pseudo-particles (instantons). However, the charge of these pseudo-particles would then not be quantised with the monopole charge predicted by Dirac [31].

He also reanalysed his previous experiments, selecting the correct root and dividing the data by n, and obtained a narrow bell-shaped distribution centred on $\bar{g} = (3.27 \pm 0.16) \times 10^{-8}$ gauss $\times$ cm^2 $= 0.99\, g_{\mathrm{D}}$ with an accuracy of $\pm 5\%$ [31]. Therefore, by these ingenious experiments, Mikhailov has observed Dirac monopoles, *but only when illuminated by light*. The problem is they are non-existent in their own right, because they cease to move as monopoles when the light is turned off. There has been no satisfactory explanation for this.

2.3 Discussion

These results are reproducible, because several experimentalists have observed more than 1600 single magnetic charges. Furthermore, they apparently obey gaussian statistics (e.g. the bell-shaped distribution) and are statistically significant. Therefore we argue, these single magnetic charges *should be considered a real physical phenomena.* However we have shown above that surveys of the objective methods of physics have failed to detect them, and concluded there is no evidence for them in 4-D space-time. *One possible explanation is that the monopoles observed only under intense illumination, are not in 4-D space-time but in another space-time,* as predicted by Dirac's theory.

Nevertheless, this is not a complete explanation. We also need a theory which predicts the existence of this second space-time, together with a mechanism which enables light to switch space-time into this second space-time. We now present such a combined theory.

3 Sunlight Shining on the Earth's Surface

We start with an existing theory of an unexpected property of light which does the switching, and then introduce a version of General Relativity which predicts a more complex structure to space-time. The basic idea is that light switches the direction of the flow of time into that of another space-time.

3.1 Brittin and Gamow's Theory

In a little-known theory, Brittin and Gamow have suggested that sunlight shining on the Earth, pumps entropy out into space, thereby allowing negentropy to accumulate on the Earth's surface. The Sun's radiation consists of high temperature photons coming from the surface at $T_{\mathrm{s}} \simeq 5{,}900^{\circ}$ K, which spreads out in space and becomes diluted. By the time it reaches the Earth's surface, it's energy density corresponds to a temperature of the Earth ($T_{\mathrm{e}} \simeq 300^{\circ}$ K), so these photons are not in thermodynamic equilibrium.

Brittin and Gamow use the quantum theory of radiation to show that the net entropy change when sunlight interacts with the Earth's surface is [1]:

$$\Delta S = \Delta S_s - \Delta S_e = \frac{4}{3}\,\Delta Q \left(\frac{1}{T_s} - \frac{1}{T_e}\right), \qquad (1)$$

which is negative because $T_{\mathrm{s}} > T_{\mathrm{e}}$. So the entropy at the Earth's surface is reduced. They reason that this is not contrary to the second law of thermodynamics because it is simply due to the temperature gradient $T_{\mathrm{s}} > T_{\mathrm{e}} > T_{\mathrm{space}}$, but see below. (Note this effect can also occur with light from an artificial source, such as an halogen lamp.) However, there is a hidden complication, independent of whether the source is natural or artificial.

The problem is that this mechanism enables negative entropy to build up on the Earth's surface, only if it can be stored. In the case of sunlight, they calculate that photosynthesis has an efficiency of about 10% for capturing this negative entropy. Brittin and Gamow suggest that this is the source of order for the food chain, which Schrödinger proposed to be a current of negative entropy [32, 33]. If this is the only mechanism for storage, then this is not a purely physical theory because it relies upon plants (and hence biochemistry) to capture the negentropy. However, we now show that there is a mechanism in physics to store the negentropy produced.

3.2 Discussion of Brittin and Gamow Effect

In classical thermodynamics, the entropy increases with the arrow of time [34]. What happens to time when a solar photon interacts with the Earth's surface, thereby lowering its entropy level? Is the direction of time reversed (e.g. locally), either momentarily or more persistently, when the photon lowers the entropy level? We conclude that it logically must be reversed, because otherwise Eddington's arrow of time would be violated, and the second law of thermodynamics also. Therefore what is missing from Brittin and Gamow's theory, is a theory of space-time with a second time dimension which is directed from the future to the past. (Experimental evidence for this reasoning is given in the following reference [8].)

There are a number of theories with two time dimensions, but these are compactified or otherwise unsuitable [35, 36]. However, Köhn has found a solution to the cosmological

problem using two time dimensions. The second time dimension is not compactified, but it is limited to a spacial scale of the Planck length [37]. Elsborg and Köhn have extended this theory to the problem of magnetic monopoles, and developed the theory of magnetic monopoles in this second time dimension [38]. They adopt the orthodox view noted above, that magnetic monopoles have not been observed [11, 12]. Therefore they continue the assumption from Köhn's first paper that the second time dimension only acts on the scale of the Planck length, so that monopoles cannot be observed experimentally at the macroscopic scales now present in the Universe. However, the above evidence for monopoles overrules this aspect of their approach, and requires the second time dimension to be macroscopic. Furthermore, it needs to be directed from the future to the past. Nevertheless, this an interesting paper which provides the mathematical analysis which shows that magnetic monopoles can exist in 5D (3,2) space-time.

There is, however, another theoretical approach. A little-known extension of the theory of General Relativity, has a second macroscopic time dimension directed from the future to the past.

4 General Relativity: Chronometric Invariants

In the 1930s, Landau and others realised that General Relativity is incomplete, because it does not correct for the reference frame of the Observer. As a result, what is observed in a specific reference frame, *is not well defined by the existing theory*. So without the Observer, General Relativity is *incomplete*. The case for including the Observer is thus compelling. Some progress was made by Landau and Lifshitz for specific cases [39]. Zelmanov developed the strict mathematical formalism to calculate the observable values for any tensor quantity in 1944. However this methodology for the general case, was not published until 1956 [40, 41]. The mathematical details of the theory are given in the references. We just present a short summary of the main points here.

Physically observable quantities are obtained by projecting four-dimensional quantities onto the time lines and three-dimensional space of the Observer's reference frame. *Physically observable quantities must be invariant with respect to transformations of time*, and so they are *chronometrically invariant quantities*. Thus the general case of the Observer was incorporated into General Relativity in Russia in the era of the Soviet Union. Cattaneo later obtained similar results [42–44].

This important extension of General Relativity is not well known in the West [45, 46]. Borissova and Rabounski, have developed this theory further. They find that the chronometric invariant equations of motion for mass-bearing particles into the past and into the future, are *asymmetric in time*. They conclude there is a fundamental asymmetry of the directions of time in the in-homogeneous space-time of General Relativity. They hold up a "mirror" to time and find that it does not reflect completely, and that there is a different world "beyond the mirror". The four-dimensional momentum vector for a particle with non-zero rest mass, m_0 is:

$$P^\alpha = m_0 \frac{dx^\alpha}{ds}, \quad P_\alpha P^\alpha = 1, \quad \alpha = 0, 1, 2, 3. \tag{2}$$

When a vector (or tensor) is projected onto the time line and spacial section of an observer, these projections give the physically observable quantities for that observer [40]. Using the properly observable time interval $d\tau = \sqrt{g_{00}}\, dt + \frac{g_{0i}}{c\sqrt{g_{00}}} dx^i$ [39, 40], the above four-dimensional momentum vector has two projections onto the time line, namely [47, 48]:

$$\frac{P_0}{\sqrt{g_{00}}} = \pm m, \quad \text{where } m = \frac{m_0}{\sqrt{1 - v^2/c^2}} \tag{3}$$

whereas it has only one spacial projection:

$$P^i = \frac{m}{c} v^i = \frac{1}{c} p^i, \text{ where } v^i = \frac{dx^i}{d\tau}, \ i = 1, 2, 3, \tag{4}$$

where p^i is the three-dimensional observable momentum. They conclude that any massive particle, having two time projections, *exists in two observable states*, entangled to each other: the positive mass state is in our world, while the negatively charged mass state is in the mirror world. Using the techniques of chronometric invariants, they find that there are three separate areas: our world (i.e. normal 4-D space-time), the mirror world, and a membrane which separates the two [47].

The flow of time is well defined mathematically in General Relativity. It is determined by the sign of the derivative of the coordinate time t with respect to the proper time $(dt/d\tau)$. Using $w = c^2(1 - \sqrt{g_{00}})$ and $v_i = -c\frac{g_{0i}}{\sqrt{g_{00}}}$, Borissova and Rabounski derive the following quadratic equation:

$$\left(\frac{dt}{d\tau}\right)^2 - \frac{2 v_i v^i}{c^2\left(1 - \frac{w}{c^2}\right)} \frac{dt}{d\tau} + \frac{1}{\left(1 - \frac{w}{c^2}\right)^2} \left(\frac{1}{c^4} v_i v_k v^i v^k - 1\right) = 0, \tag{5}$$

the two roots of which are [48]:

$$\left(\frac{dt}{d\tau}\right)_{1,2} = \frac{1}{1 - \frac{w}{c^2}} \left(\frac{1}{c^2} v_i v^i \pm 1\right). \tag{6}$$

This equation has three possible solutions $dt/d\tau > 0$, $dt/d\tau < 0$, and $dt/d\tau = 0$. In our world, $dt/d\tau > 0$ and time flows from the past to the future. *In the mirror world* $dt/d\tau < 0$ *and so time flows in the opposite direction.* Between the two is a membrane where time has stopped $dt/d\tau = 0$. Thus the two worlds are separate, because of the membrane, but equal. So that to an Observer (in our world), time in the mirror world flows from the future to the past. A summary of their results is shown in Table 1 [49].

The membrane which separates the two worlds, has its own unique three-fold structure. On our world side and the

Table 1: Summary of Spacial Properties of Chronometric Invariant General Relativity.

Mass	Particles	Energies	Class of motion	Area	Time	Entropy
$m > 0$	massive particles	$E > 0$	move at sub-light speeds	our world	$dt > 0$	$\Delta S > 0$
$m = 0$	massless particles (photons)	$E > 0$	move at the speed of light	our world		
$m = 0$	light-like vortices	$E = 0$	moving and rotating at the speed of light	the membrane	$dt = 0$	
$m = 0$	massless particles (photons)	$E < 0$	move at the speed of light	the mirror world		
$m < 0$	massive particles	$E < 0$	move at sub-light speeds	the mirror world	$dt < 0$	$\Delta S < 0$

mirror world side, are streams of light-like particles (photons), moving at the speed of light, but with opposite energies and frequencies. Between the two in the membrane, time has stopped because $dt/d\tau = 0$, and so this region is a void which is purely spacial. However, in this void there are light-like vortices, previously unknown, which have zero relativistic masses (unlike photons which, although massless, have non-zero relativistic masses). These light-like vortices move and rotate at the speed of light, but have no energy because for them time has stopped — they are purely spacial.

In this theory, a mass-bearing particle has two time projections, one in each world, and exists in two observable states. Each particle is in effect a four dimensional dipole object, which exists in two states: in our world with positive mass and energy; in the mirror world with negative mass and energy (NB this negative mass state is not anti-matter, because the inertial mass of anti-matter is positive). However, they cannot "annihilate" or rather "nullify" (since the net energy is zero) because they are separated by the membrane. Furthermore our world and the mirror world have the same background space, and *the three-dimensional momentum remains positive in both sectors*. More details are given in the references above.

This theory of physically observable quantities, is normally referred as the "Chronometric Invariant Formalism of General Relativity". However, correcting for the Observer's reference frame in this way, changes the structure of space-time from 4D (3,1) to 5D (3,2) and so it is a major extension of General Relativity. We will refer to this extended theory as "Chronometric Invariant General Relativity" (CIGR), in this and related papers. However, words are important [21], so another name may be adopted. In CIGR, our world (normal 4-D space-time) and the mirror world have the same background space. So time in the mirror world is a macroscopic time dimension. Furthermore. mirror time is directed from the future to the past, so we would expect entropy in the mirror world *to be constant or decrease with our time*.

5 Photo Mirror Hypothesis

We make the hypothesis that light can switch matter into the mirror world state, by means of the Brittin and Gamow effect, because this reduces the entropy level which reverses the direction of time.

$$\text{normal}\,(x,t),\ \frac{dt}{d\tau} > 0 \quad \underset{\Delta S > 0}{\overset{\Delta S < 0}{\rightleftharpoons}} \quad \frac{dt}{d\tau} < 0,\ \text{mirror}\,(x,-t). \quad (7)$$

We predict this will occur locally where each photon interacts (in which case $\Delta Q = h\nu$ in equation 1). This reversal could be momentary or persistent depending on the phenomenon being observed. We call this the "photo-mirror hypothesis".

Note that when it occurs, this is a low energy effect for two reasons. Firstly according to CIGR, any massive particle exists in a 4-dimensional dipole state with positive mass and energy in our world and negative mass and energy in the mirror world. Since the mirror world state already exists, *it does not require any energy to produce it*. All that is required is the reversal of the direction of time *to reveal it*, which can be done by visible photons with energies of a few electron volts (equation 1). The author provides experimental evidence for this in a separate paper [8].

The reader may question why, if photons can switch space-time into the mirror world state, it has not been observed before. Firstly, the effect is subtle and occurs at very low energies. Secondly, physicists are so convinced that the second law of thermodynamics is absolute, that few have looked for the creation of order. Thirdly, it switches space-time into the mirror world where phenomena are less objective and so tend to get ignored or rejected (e.g. the magnetic monopoles above). Furthermore, any random processes which increase entropy will switch the direction of time back to normal (4-D space-time). Limitations of this are discussed below.

5.1 Explanation of Magnetic Monopoles

The explanation for these magnetic monopoles is that photons in the intense illumination, switch the direction of time experienced by the ferromagnetic particles (via the Brittin and Gamow effect), from normal 4D space-time into the mirror world space-time, where the magnetic monopoles exist and can be observed. Therefore the intense illumination does not "make magnetism" as Ehrenhaft claimed, but "reveals magnetic monopoles" in this other space-time.

This overcomes Dirac's objection to Ehrenhaft's monopoles, namely that magnetic monopoles would only be observed at high energies, because of the very strong force between pairs of them [14], in the following way. The monopoles are in mirror space-time where the masses are negative. Therefore the attractive force between two monopoles would cause them *to fly apart*, so dipoles would not form. Thus by switching the direction of time, light can reveal the monopoles at low energies.

Furthermore, Dirac also concludes that a monopole may be connected to a string extending to infinity. If the monopoles are in one space, and the dipole is in another, then the Dirac string between a monopole and the corresponding pole of the dipole, is naturally infinitely long. Therefore observation of monopoles in mirror space-time and of magnetic dipoles in normal 4-D space-time, provides a natural physical explanation for the infinite length of the Dirac string, and confirms this aspect of his theory. In view of these results, Ehrenhaft, Benedict and Leng, and Mikhailov really did observe Dirac monopoles at these very low energies.

6 Limitations

The photo-mirror hypothesis involves both quantum mechanics (the Brittin and Gamow effect) and the chronometric invariant formalism of General Relativity (CIGR), so it implies unification. But quantum mechanics and CIGR have not yet been unified, nor the standard model embedded therein, so there may be limitations. However the author has obtained *independent experimental evidence* for the photo-mirror effect, which justifies its usage above to explain the magnetic monopole data [8].

7 Conclusions

We have made the hypothesis that there may be phenomena which experiment can detect, but which are not completely objective, for example because they are not in normal 4-D space-time. Magnetic monopoles are an example of this, because they can only be detected under intense illumination, so that when the illumination is turned off, they cease to move as monopoles, and so do not seem to exist in their own right. However, if a phenomenon can be detected repeatedly (for example these magnetic monopoles), *we suggest it should be considered physically real.*

We have presented reproducible evidence for magnetic monopoles which appear to exist outside 4-D space-time. We conclude that the current method of experimental physics is flawed, because it limits observations to objective phenomena in 4-D space time. Phenomena beyond 4-D space-time, if they can be observed, are currently rejected. The solution is to relax the criterion of objectivity, and recognise reproducible phenomena as being physically real. This is especially the case if there is a theory for that phenomenon.

Several experimenters have observed more than 1600 magnetic monopoles under intense illumination, so they are reproducible. Mikhailov has determined that these monopoles have the charge predicted by Dirac: $\bar{g} = (3.27 \pm 0.16) \times 10^{-8}$ gauss $\times$ cm^2 = 0.99 g_{D} with an accuracy of $\pm 5\%$. Furthermore, he determined that this charge is quantised ($g = n g_{\mathrm{D}}$ with n = 1 to 5). This rules out Schwinger monopoles because $g_{\mathrm{S}} = 2 g_{\mathrm{D}}$ [30]. This also rules out pseudo-particles (instantons) because they would not be quantised, and certainly not with the Dirac charge [31]. We conclude that Dirac monopoles have been observed, but not in 4-D space-time because they are only observed when they are intensely illuminated.

To explain these monopoles, we combine the Brittin and Gamow effect and Chronometric Invariant General Relativity (CIGR) to make the photo-mirror hypothesis, namely that visible light lowers the entropy level and reverses the direction of time, thereby switching space-time into mirror space-time of CIGR, where time is directed from the future to the past. Therefore the photons of the intense illumination switch the ferromagnetic particles, via the photo-mirror hypothesis, into the mirror world space-time state, where the magnetic monopoles exist and are observed. In this way, the *intense illumination reveals magnetic monopoles in mirror space-time.*

Mirror space-time explains two aspects of Dirac's theory of monopoles: their observation at low energies, and the infinite length of the Dirac string. Firstly, we find the monopoles are in mirror space-time where the masses are negative. Therefore the attractive force between two monopoles would cause them to fly apart, so dipoles would not form. Thus by switching the direction of time, light can reveal the monopoles at low energies. Secondly, observation of magnetic monopoles only in mirror space-time and dipoles only in normal 4-D space-time, provides a natural physical explanation for the infinite length of the Dirac string.

This is evidence for phenomena beyond 4-D space-time. In effect, under certain circumstances, light gives us a window into another world. The photo-mirror hypothesis links a quantum mechanical effect (Brittin and Gamow) with General Relativity (CIGR), which implies unification.

Acknowledgements

The author thanks Dmitri Rabounski for helpful communications. An earlier version of this paper has been published as an e-preprint [50].

Submitted on November 21, 2024

References

1. Brittin W. and Gamow G. Negative entropy and photosynthesis. *Proc. of the Nat. Acad. of Sciences*, 1961, v. 47, 724.
2. Gell-Mann M. Some lessons from sixty years of theorising. *Int. J. Mod. Phys. A*, 2010, v. 25 (20), 3857–3861.
3. Ehrenhaft F. *Phys. Zeitschr.*, 1930, v. 31, 478.

4. Cox R.T., McIlwraith C.G. and Kurrelmeyer B. *Proc. Nat. Acad. Sci*, 1928, v. 14 (7), 544; Rubbia C., private communication.
5. McKellar A. *Publ. of the Dominion Astrophysical Observatory*, Vancouver, Canada, v. 7 (6), 251–272.
6. Shmaonov T.A. Methodology of absolute measurements for effective radiation temperature with lower equivalent temperature. *Apparatuses and Technics of Experiment*, 1957, v. 1, 83–86.
7. Einstein A., quoted by W. Heisenberg in *Physics and Beyond: Encounters and Conversations,* transl. by A. J. Pomerans, Harper & Row, New York, 1971.
8. Ellis R.J. Preliminary evidence for a second time dimension directed from the future to the past, and for unification. doi:10.5281/zenodo. 7347637.
9. Ellis R.J. Preliminary evidence for quarks and preons in mirror spacetime. doi:10.5281/zenodo.7671809.
10. Jaeckel J. and Ringwald A. *Ann. Rev. Nucl. Part. Sci.*, 2010, v. 60, 405.
11. Tanabashi M. et al. *Phys. Rev.*, 2018, D98, 030001.
12. Giacomelli G. et al. DFUB 2000-9 Bologna, arXiv: hep-ex/0005041.
13. Dirac P.A.M. *Proc. Roy. Soc.*, 1931, v. A133, 60.
14. Dirac P.A.M. *Phys. Rev.*, 1948, v. 74, 817.
15. Kragh H. Dirac: A Scientific Biography. Cambridge University Press, 1990, pp. 216–217.
16. Benedikt E.T. and Leng H.R. *Phys. Rev.*, 1947, v. 71, 454.
17. Ehrenhaft F. *Annales de Physique*, 1940, v. 11/13, 151.
18. Ehrenhaft F. and Banet L. *Nature*, 1941, v. 147, 297.
19. Ehrenhaft F. *Nature*, 1944, v. 154, 426.
20. Ehrenhaft F. *Phys. Rev.*, 1944, v. 65, 287.
21. The late V. L. Telegdi, private communication.
22. Dibner Library, Smithsonian, Washington DC, MSS 2898, Einstein to Ehrenhaft, 20 Feb. 1940.
23. Kemple T.E. The Magnetic Monopole. MSc Thesis, Univ. Missouri, School of Mines and Metallurgy, 1961, pp. 36–44 and references therein; scholarsmine.mst.edu/masters_theses/2765
24. Mikhailov V.F. *Phys. Lett.*, 1983, v. B130, 331.
25. Mikhailov V.F. *J. Phys. A*: *Math. Gen.*, 1985, v. 18, L903.
26. Mikhailov V.F. *Annales de la Fond. Louis de Broglie*, 1987, v. 12, 491.
27. Akers D. *Int. J. Theor. Phys.*, 1988, v. 27, 1019.
28. Mikhailov V.F. *J. Phys. A*: *Math. Gen.*, 1991, v. 24, 53.
29. Mikhailov V.F. On Interpretation of the Magnetic Charge Effect on Ferromagnetic Aerosols. Preprint, HEPI 88-05, Kazakh Academy of Sciences, Alma-Ata, 1988, see Figure 2.
30. Schwinger J. *Phys. Rev.*, 1966, v. 144, 1087–1093.
31. Mikhailov V.F. Experimental detection of Dirac's magnetic charge? *J. Phys. D*: *Applied Physics*, 1996, v. 29, 801–804.
32. Schrödinger E. What is Life? Cambridge University Press, 1944.
33. Prigogine I. *Bull. Acad. Roy. Belg. Cl. Sci.*, 1945, v. 31, 600.
34. Eddington A.S. The Nature of the Physical World. Cambridge University Press, 1928.
35. Bars I. Duality and hidden dimensions. *Frontiers in Quantum Field Theory*, World Scientific, Singapore, 1996, 52; arXiv: hep-th/9604200.
36. Vafa C. Evidence for F-Theory. *Nucl. Phys.*, 1996, v. B469, 403; arXiv: hep-th/9602022.
37. Köhn C. A solution to the cosmological constant problem in two time dimensions. *J. HEP, Grav. and Cosm.*, 2020, v. 6, 640–655.
38. Elsborg J. and Köhn C. Magnetic monopoles in two time dimensions. *Int. J. Modern Phys. A*, 2022, v. 37, 2250141.
39. Landau L.D. and Lifshitz E.M. The Classical Theory of Fields. The 4th final edition, Butterworth-Heinemann, 1980.
40. Zelmanov A.L. Chronometric invariants and the accompanying frames of reference in the General Theory of Relativity. *Soviet Physics Doklady*, 1956, v. 1, 227–230; Zelmanov A.L. On the relativistic theory of an anisotropic in-homogeneous Universe. *Proc. of 6th Soviet Conf. on the Problems of Cosmogony*, Nauka, Moscow, 1959, 144–174 (in Russian), see English transl. in *The Abraham Zelmanov Journal*, 2008, v. 1, 33–63.
41. Zelmanov A.L. Chronometric Invariants. English transl. of the 1944 Dissertation, Am. Res. Press, Rehoboth, 2006; see also Rabounski D. and Borissova D. Physical observables in General Relativity and the Zelmanov chronometric invariants. *Progress in Physics*, 2023, v. 19 (1), 3–29.
42. Cattaneo C. *Nuov. Cim.*, 1958, v. 10, 318–337.
43. Cattaneo C. *Nuov. Cim.*, 1959, v. 11, 733–735.
44. Cattaneo C. *Nuov. Cim.*, 1959, v. 13, 237–240.
45. Pollock M.D. Chronometric invariance and string theory. *Mod. Phys. Letts. A*, 2008, v. 23, 797–813.
46. Pollock M.D. Quantum gravity in the chronometrically invariant formalism of Zel'manov. IAEA-ICTP-90-69, 1990.
47. Borissova L. and Rabounski D. Fields, Vacuum, and the Mirror Universe. The 3rd revised edition, New Scientific Frontiers, London, 2023 (the 1st ed. published in 2001). See Chapters 1 and 6.
48. Rabounski D. and Borissova L. Particles Here and Beyond the Mirror. The 4th rev. edition, New Scientific Frontiers, London, 2023 (the 1st ed. published in 2001).
49. Borissova L. and Smarandache F. Positive, neutral and negative masscharges in General Relativity. *Progress in Physics*, 2006, v. 2 (3), 51–54.
50. Ellis R.J. I: Evidence for phenomena, including magnetic monopoles, beyond 4-D space-time, and theory thereof. arXiv: 2207.04916.

II: Preliminary Evidence for a Second Time Dimension Directed from the Future to the Past, and for Unification

Richard Ellis
Corpus Christi College (Alumnus), Oxford OX1 4JF, UK
E-mail: r.ellis@physics.oxon.org

Experiments are presented on the effects of visible light shining on water. To understand these, we note that Landau and others realised General Relativity was incomplete because it does not correct for the Observer's reference frame. When this is done for the general case,the chronometric invariant formalism of General Relativity (CIGR) predicts a second time dimension directed from the future to the past, and new phenomena at low (eV) energies. The initial objective was to test Brittin and Gamow's theory that sunlight lowers the entropy level at the Earth's surface. We detected this effect and found it persists for at least 10 months after exposure to sunlight (17 days after halogen light), *contrary to the second law of thermodynamics*. In a previous paper, the (photo-mirror) hypothesis was made that light can switch the arrow of time into the mirror world of CIGR, via the Brittin and Gamow effect. Experimental evidence is presented that visible photons switch small (0.2 to 1.5 microns) "quantized" regions of water into the mirror world state; and their brightness distributions match the energy spectrum of the halogen light source (χ^2/DF = 1.49 and 0.94 respectively) indicating causality. This is detailed evidence for the Brittin and Gamow effect. Furthermore, these domains persist (for 20 and 27 days respectively), which is evidence for the second time dimension, and there is evidence they are surrounded by the membrane also predicted by CIGR. This is also evidence for the photo-mirror hypothesis, which links Quantum Mechanics and Chronometric Invariant General Relativity, and so is preliminary experimental evidence for unification.

1 Introduction

Following on from Landau's work in the 1930s, Zelmanov developed the mathematical apparatus (chronometric invariants) to correct for the reference frame of the Observer in the general case. This was not published until 1956 [1], and confirmed by Cataneo. Since then Borissova and Rabounski have developed the chronometric invariant formalism of General Relativity (which we refer to as CIGR) further, and shown it predicts a more complex structure for space-time: 5D (3,2) [2]. In a previous paper we have made the (photo mirror) hypothesis that visible light can reverse the direction of the arrow of time into that of mirror space-time (predicted by CIGR), by lowering the entropy level via the Brittin and Gamow effect [3]. This provides the theoretical framework for understanding experiments which show evidence, presented below, for phenomena which violate the second law of thermodynamics.

The following experimental work investigates the photo mirror hypothesis, and finds evidence for this joint quantum mechanical-relativistic effect. which enables the second law of thermodynamics to be reversed, and for the reduced entropy levels to persist. This is made possible by mirror space-time, where time is directed from the future to the past. Murray Gell-Mann has said "I should like to emphasize ... the need to go against certain received ideas. ... Often they have a negative character and they amount to prohibitions of thinking along certain lines... Now and then, however, the only way to make progress is to defy one of these prohibitions that are uncritically accepted without good reason" [4].

One of these prohibitions is the second law of thermodynamics [5, 6]. There are several definitions of the second law. Two early ones by Carnot and Clausius, refer to heat engines [7, 8], which are not the subject of this paper. Furthermore, perpetual motion and similar devices are excluded [9]. Instead we focus on the statistical mechanical approach due to Boltzmann in 1877.

Briefly, in Maxwell's kinetic theory of an ideal gas, heat is due to the motion of the molecules. Each molecule can be in a number of different energy states ϵ_i, but can only be in one state at a time, so many states are empty. In a system of many molecules N, of which g_i could be in the state ϵ_i, but only some of them, N_i, are occupied, where $g_i \gg N_i$ and $N = \Sigma_i N_i$. In this degenerate system, there are several different configurations which all possess the same total energy and correspond to approximately the same temperature ($N_i \propto e^{-\epsilon_i/k_B T}$). The number of ways N_i indistinguishable molecules can be distributed amongst g_i energy states is $g_i^{N_i}/N_i!$. The number of ways a particular macrostate can be achieved is $\Omega = (g_1^{N_1}/N_1!) \times (g_2^{N_2}/N_2!) \ldots$, which increases rapidly with the degeneracy. Boltzmann showed that the entropy $S = k_B \ln \Omega$ where k_B is the Boltzmann constant, and the thermodynamic probability Ω is at its maximum at equilibrium [10]. Therefore the entropy is maximum at equilib-

rium, and is interpreted as a measure of statistical disorder of the system.

Thus the second law was formulated in the 19th century, is considered absolute, and is widely thought to lead to the "heat death" of the Universe. This is in effect a classical physics "Theory of Everything". It is true that (superficially) there is considerable evidence that entropy (of baryonic matter) tends to increase with time. However, baryonic matter makes up only about 4% of the Universe. The other 96% consists of dark matter and dark energy; and we do not know what these are, *nor what laws they obey*. So it is illogical to assume that the second law applies to them — it may or it may not. Therefore it is perfectly rational to look for processes which create order out of chaos. If an effect is found, then the problem is to understand the results theoretically, so as to facilitate more probing experiments.

This is not a general paper on the violation of the second law of thermodynamics. Our starting point is a little-known theory due to Brittin and Gamow (see equation (1) below). This predicts that sunlight shining on the Earth, pumps entropy out into space, thereby allowing negentropy (i.e. order) to accumulate on the Earth's surface. This appears to be the beginning of the food chain proposed by Schrödinger [11,12].

This paper is divided into three sections. In this first section, we present an exploratory experiment which provides evidence that visible light reverses the second law of thermodynamics by producing ordered states in an inanimate closed system (i.e. pure water), *which persist*. This persistence should not occur. Before we could investigate this in more detail experimentally, we needed a theoretical explanation for this persistence to guide the experimental work. This explanation comes from the little-known (chronometric invariant) extension of General Relativity (CIGR) mentioned above, which predicts a more complex structure for space-time. In particular it predicts a second time dimension directed from the future to the past and fundamental new phenomena at low energies. Details of this new theoretical approach, are presented in a previous paper and the references cited there [3].

Section II presents results of experiments to test this theoretical explanation. Section III presents conclusions, discussion, and predictions. We start by presenting the small exploratory experiment to test the Brittin and Gamow effect, which we did before this theoretical framework was developed.

1.1 Brittin and Gamow's Theory

Photons from the Sun's surface ($T_s \simeq 5,900^\circ$ K) come to the Earth ($T_e \simeq 300^\circ$ K), where they interact. Brittin and Gamow use the quantum theory of radiation to show that the net entropy change on the Earth's surface is [13]:

$$\Delta S = \Delta S_s - \Delta S_e = \frac{4}{3}\,\Delta Q\left(\frac{1}{T_s} - \frac{1}{T_e}\right), \qquad (1)$$

which is negative because $T_s > T_e$. They reason that this is not contrary to the second law of thermodynamics because it is simply due to the temperature gradient $T_s > T_e > T_{space}$. (NB A similar temperature gradient applies to light from a halogen lamp: $T_h > T_e > T_{space}$ since $T_h \simeq 3,000^\circ$ K.)

This quantum effect enables negative entropy to build up on the Earth's surface, *provided it can be stored* [14]. However, in the absence of a storage mechanism, any reduction in the entropy levels should dissipate as the (closed) system returns to equilibrium. Nevertheless, Brittin an Gamow calculate that photosynthesis has an efficiency of about 10% for capturing this negative entropy. So this is apparently not a purely physical theory because it relies upon plants (and hence biochemistry) to capture the negentropy. Does this mean that biochemistry alone enables plants to violate the second law? Or is there some underlying physical mechanism for storing the negative entropy, produced by visible light?

The focus of this paper is to test the above theory in inanimate systems, specifically in water, by looking for reductions of entropy levels which persist.

1.2 Theory of Exploratory Experiment

In order to investigate this, we have done the following simple experiment to test whether there is an *underlying physical storage mechanism.* 60% of the Earth's surface is covered by water, life is water-based, and plants are 70% water. So if there is a physical mechanism (i.e. not based on biochemistry) for storing this negative entropy, the most likely place to find it would be in water exposed to sunlight.

1.3 Entropy and Brownian Motion

We decided to expose a bowl of pure water to sunlight and later measure the Brownian motion of particles therein, to determine if there is any persistent entropy change. Brownian motion is a random walk which covers the whole of phase space. As is well known, the probability $\rho(x,t)$ of a suspended particle moving a distance x along the x-axis in time t is [15,16]

$$\rho(x,t) = \frac{e^{-x^2/4Dt}}{2\sqrt{\pi D t}}, \qquad (2)$$

where D is the diffusion constant. Diffusion takes place when a molecule moves to an unoccupied state, so that the more unoccupied states, the greater the diffusion. Entropy also increases when there are more unoccupied states, so that an increase in the diffusion constant implies an increase in entropy and vice versa. From the Fokker-Planck equation, the Boltzmann-Gibbs entropy $S = -k_B \int_{-\infty}^{+\infty} \rho(x,t)\ln\rho(x,t)\,dx$ where $\rho(x,t)$ is given by equation (2) above. Hence $S = -k_B(\ln(1/\sqrt{4\pi D t}) - 0.5)$ so that as the diffusion constant increases, so does the entropy. Conversely, if the entropy has been reduced then the probability $\rho(x,t)$ will become narrower.

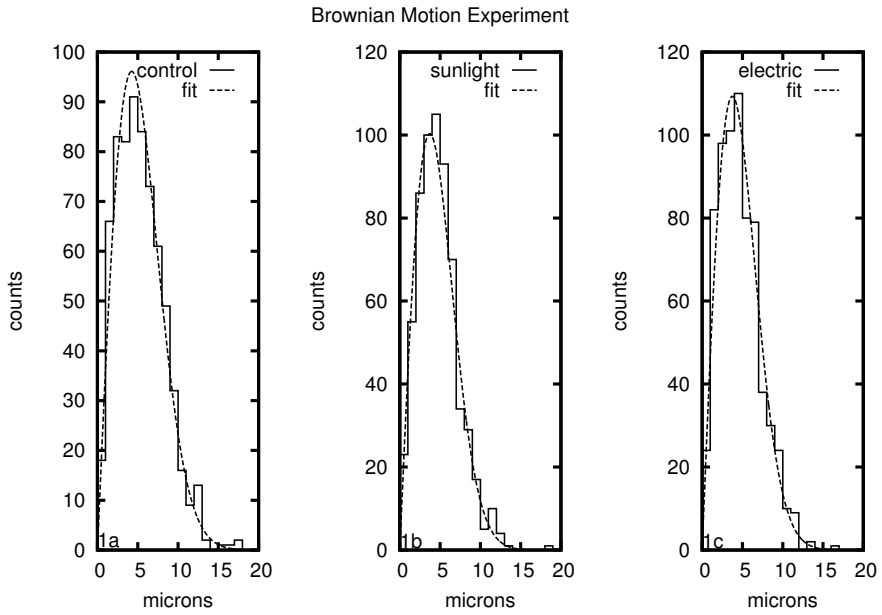

Fig. 1: Distribution of particle displacements every 10 seconds for a) non-irradiated distilled water = control; b) water measured 10 months after exposure to sunlight = signal 1; c) water measured 17 days after exposure to light from an halogen lamp = electric (i.e. signal 2). The dashed curves show the fits — see Table 1 for details. Both the sunlight and electric light samples are narrower than the non-irradiated control by 21% FWHM.

1.4 Details of Exploratory Experiment

Distilled water was exposed to sunlight for 8 days in August in the UK. Another sample was exposed to an halogen lamp ($T_h \simeq 3,000^\circ$ K) so as to receive a similar level of illumination. Both samples were bottled and stored in a box away from direct light, at room temperature which varied by a few °C at most. A third sample was taken directly from the amber Winchester supply bottle without any deliberate exposure to light and used as the control.

After storing the exposed samples, the Brownian motion measurements were made 10 months and 17 days later respectively, as follows. A few drops of the sample were placed on a microscope slide, 1 micron diamond particles were added, it was covered and viewed under a microscope (magnification ×1000), with a video attachment. The Brownian motion of the diamond particles was readily visible and recorded at room temperature.

1.5 Results of Exploratory Experiment

Diamond particles with a diameter of about 0.7 microns were selected for measurement. The distance $r = \sqrt{x^2 + y^2}$ moved in 10 seconds was measured. A number of particles were tracked for each sample, with a total of order 700 data points per sample. The distributions for the three samples are shown in Figure 1. There is little or no background and no long tails. Fits to the two-dimensional form of Einstein's theory are very good, as shown by the curves in the Figures, and the chi-squares per degree of freedom, shown in Table 1, are all close to 1. *So we have observed Brownian motion.*

The distributions of the solar and halogen (electric) samples, are *both narrower* than the non-irradiated control. The fits show that sunlight and halogen light have reduced the diffusion constant by about 23% and 22% respectively. (The difference $\delta = -0.01 \pm .029$ between these two signals is not statistically significant.) This translates into a reduction in the entropy by $4.7 \pm 0.7\%$ for water exposed to sunlight and $4.4 \pm 0.7\%$ for halogen light. These correspond to 6.5 and 6.2 standard deviations respectively, so this reduction in entropy is statistically significant. Therefore this is evidence for the Brittin and Gamow effect.

However, this reduction in entropy has *persisted*, despite the samples being closed systems in thermal equilibrium with their surroundings, for 10 months and 17 days respectively, which is far longer than the few hours to reach thermal equilibrium. *So there appears to be a physical mechanism for storing the negentropy.* What is this?

1.6 Discussion and Second Law

In the above experiments, most visible photons pass through the water because it is transparent. A few interact dynamically with water molecules, which can lower the entropy level locally by the Brittin and Gamow effect (see equation (3) below). Then according to the second law, as the water returns to thermal equilibrium, the entropy should return to the maximum. Pippard said that the second law is not violated under any circumstances [5]. Thus the fleeting kinematic effects of photons could not produce a persistant effect unless

Table 1: Exploratory experiment: Determination of Diffusion Constants and Entropy for water exposed to sunlight and halogen light.

Sample type or difference	χ^2/DF	Diffusion constant μm^2/sec	Entropy S $k_B = 1$	ΔS (signal — control)	$\Delta S/\sigma$ (No. of std. devn.)
Signal 1 = solarized water	1.13	$0.691^{+.019}_{-.021}$	$2.732^{+.014}_{-.015}$	$-4.7 \pm 0.7\%$	6.5
Control = non-irradiated water	0.91	$0.903^{+.023}_{-.026}$	$2.866^{+.013}_{-.015}$	—	—
Signal 2 = halogen light water	1.15	$0.701^{+.020}_{-.022}$	$2.739^{+.014}_{-.016}$	$-4.4 \pm 0.7\%$	6.2
δ = (signal 1 — signal 2)		$\delta = -0.01 \pm .029$			

there is some agency which causes or facilitates this persistence. Without such a mechanism, this persistence violates the second law.

In both experiments above (sunlight and halogen), it is just photons in and photons out. Photons are massless and travel at the speed of light, and cannot combine chemically with water. Therefore we rule out the so-called "memory of water" — see Appendix A for details. The interaction of photons with water is purely dynamical. Assuming that the water molecules move at random, one would expect the reductions in entropy to dissipate as the water returns to equilibrium. But this does not happen in the above experiment. There are two possible types of explanation for this. Either this effect is a property of water (e.g. due to its structure), or it is due to some external agency. It is generally accepted that water has some peculiar properties, some of which may be explained by its structure. Theories of the structure of water are summarised in Appendix B, where it is shown that *they do not explain the phenomena observed.* Therefore these isothermal entropy reductions must persist because there is some external agency which causes them too.

For example, when a magnetic field is applied to a perfect spin gas, the spins become aligned and the entropy decreases. This can occur at constant temperature, in which case both the energy levels and their populations change to correspond to the same Boltzmann distribution for that temperature [17]. In general an isothermal entropy change requires *both* the energy levels and their populations to change. However the above results, whilst they show an isothermal entropy decrease, cannot be so explained because there is no external field to entrain the water molecules. The Earth's gravity and magnetic fields would not do this, nor did they affect the control. Furthermore we present evidence below and in Appendix B, that the structure of water did not cause this persistence. So we need to find an alternative explanation.

There are two additional possibilities: either this simple experiment *and the others below*, are wrong, or there is something we don't know about the second law. In order to avoid theoretical bias, we decided to accept the experimental results at their face value and investigate an alternative (theoretical) solution.

One way to understand the above experiment is in terms of the arrow of time. Eddington noted that entropy tends to increase with time [6]. What happens when photons lower the entropy level, as observed above? Does the Brittin and Gamow effect reverse the arrow of time? There are three possibilities:

1. It does not affect the flow of time, in opposition to Eddington's hypothesis. Therefore the reduction in entropy would dissipate as the system returned to thermal equilibrium, contrary to the observations.

2. The direction of time is reversed momentarily, probably locally where the photon interacts, but returns to normal after the entropy has been reduced. However, the entropy would then increase as the system returned to equilibrium, contrary to the observations.

3. The direction of time is reversed locally *and this persists*. One possibility is that when a photon interacts, it switches the direction of the flow of time into another space-time, where time flows from the future to the past, if such a space-time exists. In this way, this effect would not violate the second law nor the arrow of time. Furthermore, this second type of space-time could provide the external agency required for this phenomenon to persist.

There is a version of General Relativity which predicts another space *where time flows from the future to the past*. We have discussed this in more detail in the theory paper referred to above [3]. However we give a brief summary here.

1.7 Chronometric Invariant General Relativity

In the 1930s, Landau pointed out that General Relativity is not complete because it does not allow for the Observer's reference frame [18]. Zelmanov correctly introduced the Observer using chronometric invariants [19, 20]. Borissova and Rabounski have shown that Chronometric Invariant General Relativity (CIGR) requires the existence of a second sector (mirror world) with a second time dimension directed from the future to the past [2,21,22]. The mirror world is separated from normal space-time by a membrane with three layers, but

shares the same space as normal space-time. We make the following deductions from this theory:

1. This second time dimension is a macroscopic one.

2. This second time dimension enables entropy levels to decrease with respect to our time, and therefore makes the second law of thermodynamics dual.

3. The membrane between the two worlds consists of 3 layers, 2 layers of photons (1 positive energy on the outside, the other negative on the inside) and a middle layer which is purely spacial with no time dimension, so photons cannot traverse is. It is thus opaque to photons and will reflect or scatter them.

4. We make the hypothesis that light, under certain circumstances, can switch space-time into the mirror world state, by means of the Brittin and Gamow effect, in which *light reduces the entropy level and so reverses the direction of time*. We call this the photo-mirror hypothesis [3].

The persistent decrease in the entropy of water exposed to sunlight and of that exposed to halogen light observed above, are preliminary evidence for the photo-mirror hypothesis.

1.8 Conclusions for Section I: Brownian Motion Experiment

1. Brownian motion has been observed in the above experiments.

2. Sunlight and halogen light both reduced the entropy levels in water by approximately the same amount within the errors. This reduction persisted (for at least 10 months and 17 days respectively), so there appears to be a physical mechanism for storing negentropy in water.

3. Theories of the structure of water do not explain this persistence. Therefore it must be due to some external agency.

4. We deduce that the external agency is probably a second space-time. For example, Chronometric Invariant General Relativity has a second macroscopic time dimension, which is directed from the future to the past.

5. We make the hypothesis that visible light can switch, via the Brittin and Gamow effect (when it lowers the entropy level), the direction of time into mirror space-time. We call this the photo-mirror hypothesis. The rest of this paper is directed to finding more specific evidence for this.

2 Light and Water

Light shining on pure water is a physical system. We decided to look for additional evidence for the Brittin and Gamow effect, for this hypothetical second time dimension and for the photo mirror hypothesis. To do this we exposed HPLC grade water to a 400 watt halogen lamp (1100 lux at surface of the water) and took regular samples for up to 6 days.

2.1 Viscometer Experiment

The statistical error in the exploratory experiment above goes as $1/\sqrt{M}$, where M is the number of observations, which makes it labour intensive to increase the precision. So for $M = 700$ the error is about 4%. There is another equation due to Einstein: $D = RT/6\pi N\eta a$ where R is the gas constant, η is the viscosity, a is the radius of the particle, and N is Avogadro's number; which shows that the diffusion constant D is inversely proportional to the viscosity. The advantage is that viscosity can normally be measured with a precision of about 0.1% using a capillary viscometer (in a constant temperature bath), with a stop watch.

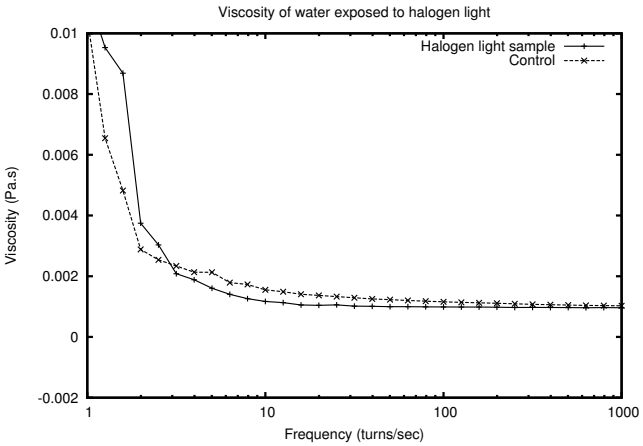

Fig. 2: This rheometer data shows the halogen sample has two components: at low turns per second the viscosity is above the control, and at higher tps it is below the control.

The viscometer used gave precise results for the *untreated* (i.e. not deliberately exposed to light) HPLC grade samples, which agreed with the known viscosity of water at 20° C with a precision of about 0.1% or better, as expected. However, results for all the halogen light *treated* samples tended to be less consistent, even if they had been exposed to halogen light for only a few hours. Repeated measurements of the same halogen light treated sample had a much wider spread, up to five times that for the control (i.e. untreated), despite attention to detail, such as cleansing between samples. (More details of the viscometer technique, are given in the following reference [23].) Despite these larger errors, all the viscosity measurements of treated water were significantly greater than that of untreated pure water, *implying that light lowers the diffusion constant and hence the entropy*, as originally observed. However, there was evidence that irradiated samples had two components, with different viscosities.

2.2 Rheometer Experiment

To investigate this possibility of two components, a sample was exposed to halogen light for 48 hours. Three days later, it was measured using a cone-and-plate rotation rheometer [24]. Distilled water was used as the control. The results are given in Figure 2. Note, the increase in the viscosity of distilled water below 10 turns per second (tps) is an instrumental effect. Nevertheless, the data shows that the water which has been exposed to halogen light, has two components, one with vis-

Fig. 3: The control sample of distilled water, examined using a novel microscope technique. It looks mainly black because there are no "structures" or domains to reflect the light, apart from a bit of noise (e.g. from ambient lighting).

cosity greater than that of the control at low tps, the other with viscosity less than that of the control at higher tps. So the water exposed to halogen light has two components. What are these?

2.3 Theory of light and water

Whilst Brittin and Gamow's theory (equation 1) is derived from the quantum theory of radiation, it is presented there in terms of the macroscopic energy flow from the Sun to the Earth, and then from the Earth to space. In this experiment, light from a halogen lamp shining onto a bowl of water, consists of individual photons. Water is transparent and so most photons pass straight through, and only occasionally does a photon interact with the water, so that ΔQ is replaced by the energy of that photon $h\nu$:

$$\delta S = \frac{4h\nu}{3}\left(\frac{1}{T_{s/h}} - \frac{1}{T_e}\right). \qquad (3)$$

This energy is radiated away by lower energy photons, and there is a small reduction in entropy δS locally in the water. Then by the photo-mirror hypothesis, a small region around this interaction would be switched into the mirror world state. According to CIGR, this will automatically be surrounded by the triple-layer membrane, since the two worlds are separated by this membrane. This enclosed mirror-world region could then persist in the water, because the momenta of molecules in the mirror state are still positive, and so will balance across the membrane. We will refer to these small mirror-world states as "domains", or in the case of images or software detection thereof, as "structures" or "sources".

2.4 Microscope Experiment

In order to make visible these otherwise hidden domains in water, we have used a novel microscope technique developed by Schweitzer [25]. This technique involves first examining the sample with normal illumination to see if it contains any bacteria, dust particles or other impurities. If the sample is clear (as expected for distilled water), then a drop of the water is allowed to evaporate whilst illuminated from the side, approximately orthogonal to the direction of view. When it is about 0.1 mm thick, hidden structures or domains, if present, become visible, provided that the side illumination and other conditions are correct (see Appendix C for details of this technique).

Quite why domains in bulk water are invisible, yet become visible when the thickness is less than about 0.1 mm, is not clear. Perhaps when the water becomes thin enough, the domain membranes become distorted and start to scatter the side illumination. The theory needs to be worked out in more detail. We just report the experimental facts.

Figure 3 shows the results using this technique, for the

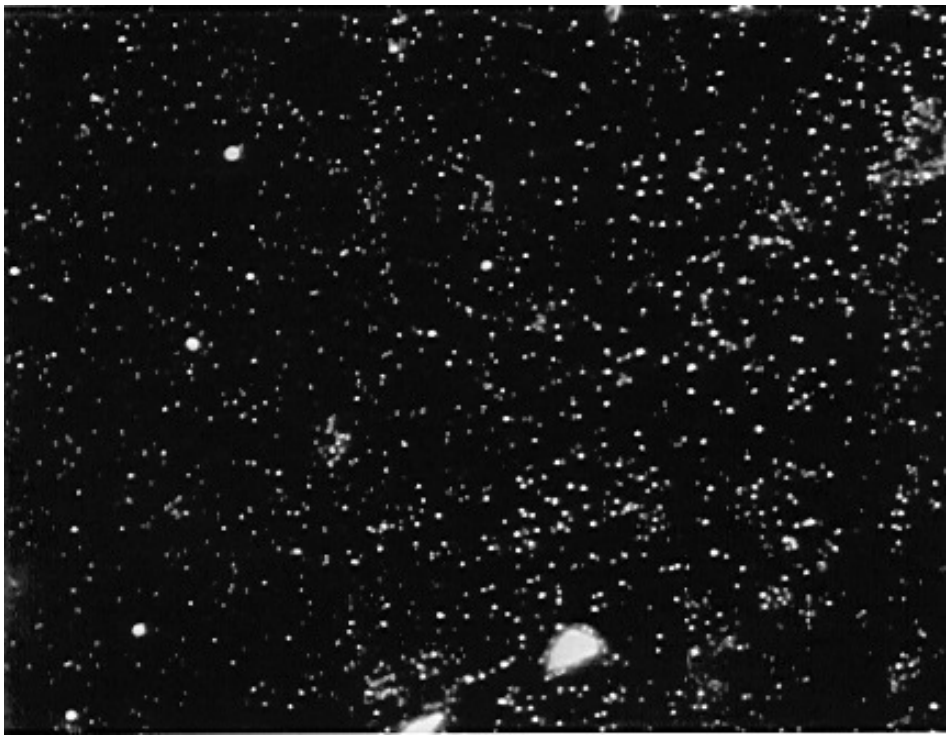

Fig. 4: Hidden domains in water exposed to halogen light for 37.5 hours, revealed by a novel microscope technique using side illumination. These domains are 0.2 to 1.5 microns in size, with a few exceptions.

control sample of distilled water (i.e. not HPLC grade) which has not been deliberately exposed to sunlight nor halogen light (although it may have been exposed to some ambient lighting during the experiment). The process of distillation randomises the water and so breaks up any "structures" or domains, so that this control sample looks mainly black because there are few "structures" or domains to scatter or reflect the light, apart from a bit of "noise".

Figure 4 shows the first sample, which had been exposed to a 500 Watt halogen lamp for 37.5 hours. Figure 5 shows the second sample which had been exposed to halogen light for 79.5 hours. These are the black and white versions of the original colour CCD images, which are also mainly black and white. There are no signs in the originals, of a range of colours, which could come from diffraction. We conclude that these domains are reflecting or scattering light (from the side illumination) into the microscope. The first image (figure 4) was recorded 20 days after exposure to halogen light, and the second (figure 5) 27 days after exposure. So the effect persists.

2.5 Analysis of Results of Microscope Experiment

In both images there are hundreds of white "sources" which are 0.2 to 1.5 microns across (apart from a few which have started to merge together), *independent of exposure time*. The existence of these 0.2 to 1.5 micron zones in the water suggest that halogen photons have interacted with the water according to equation (3). If these sources are so produced, then there should be some correlation between their size distribution and the energy spectrum of the photons which produced them. We investigate this and their persistence in more detail below.

These domains look like stars in the night sky, even though they are being observed with a microscope instead of a telescope. The appearance is so similar that we decided to use astronomy software to do pattern recognition on these images [26]. The software was run with the default parameters and found 1288 "sources" in the shorter exposure (figure 4) and 935 in the longer one (figure 5), which is a bit less because of the black regions in that image. The program calculates the isophotal flux which is defined as the sum of the pixel counts above backround of all the pixels in a particular "source" ($\sum_{i\in S} p_i$).

The histograms of the isophotal flux, or brightness, for the sources detected in the two images are shown in Figures 6 and 7 respectively, by solid lines. The selection criteria in the software for distinct sources affected the first two bins, so they are excluded. We have also plotted the spectrum of light from the halogen lamp, which has been converted from wavelengths to electron volts [27]. The halogen spectrum (broken line) falls away from the main peak quite quickly down to the secondary peak, and then decreases more slowly after that, matching the two measured brightness distributions well. This suggests the halogen photons have caused these sources. Furthermore, the brightness is independent of the exposure time, being depen-

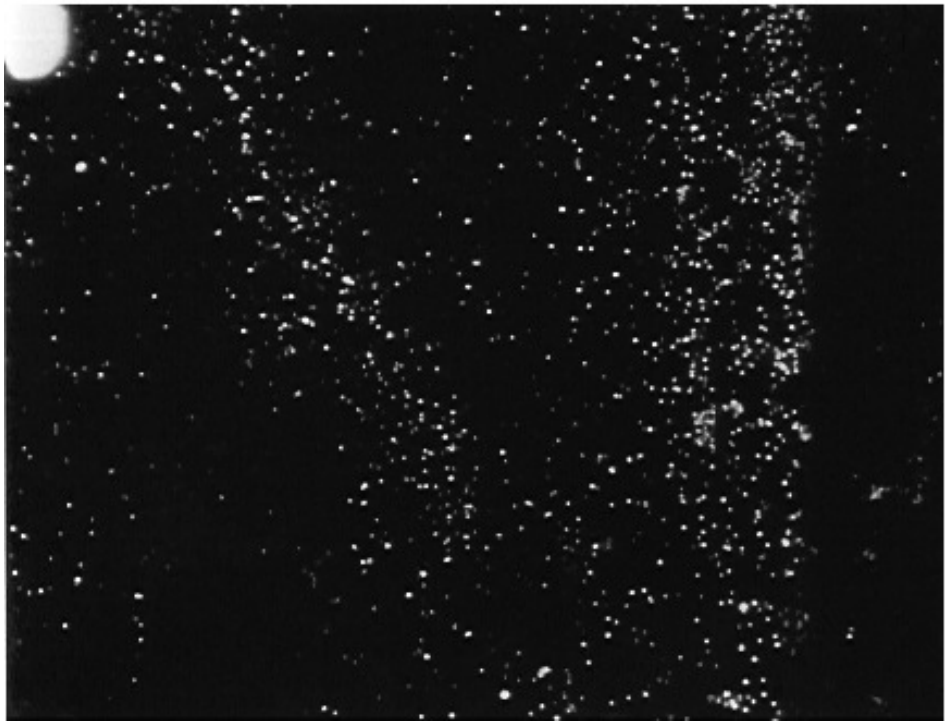

Fig. 5: Hidden domains in water exposed to halogen light for 79.5 hours, revealed by a novel microscope technique using side illumination. These are 0.2 to 1.5 microns in size.

dent on the photon energy, as predicted by equation 3.

We then fitted this spectrum to the data using just three parameters for the least squares fit: an x-axis offset because the photon energy corresponding to zero brightness is about 1.55 eV; an x-axis scaling parameter to convert from electron volts to brightness (counts); and a vertical scaling factor to convert from relative intensity to counts. The chi-squares per degree of freedom are 1.49 and 0.94 in Figures 6 and 7 respectively. So the two brightness distributions have the same shape as the halogen light spectrum, independent of the exposure time, as predicted by equation 3. This confirms that halogen photons have caused these domains via the Brittin and Gamow effect.

The problem with Figure 4 and 5 is that they are pictures. So although we see sources, we do not know if these are produced by the incident halogen photons, or by dust particles, or possibly even bacteria. The advantage of the astronomy software is that enables us to quantify the data and plot the brightness distributions and compare them with the halogen energy spectrum. We see in Figures 6 and 7 that they have almost the same shape, which is confirmed by the fits. Therefore these domains have been produced by halogen photons by the mechanism given in equation 3.

Furthermore, these mirror world domains are correlated with photons whose energies are quantised. Therefore we observe the "quantisation" of regions of water probably in mirror-space-time.

We then combined the two spectra. This is shown in Figure 8 and the chi-square per degree of freedom is 1.67. This is good evidence that the domains are being produced by the photons from the halogen lamp. Nothing material has changed — it is just photons in and photons out. But the state of the water has changed proportionately to the energy of the incident photon, and *the effect persists*.

2.6 Scattering from Surface or Volume of Domains

Do these domains reflect or scatter the side illumination from their surface or from their volume? According to equation 3 the decrease in entropy is proportional to the energy of the interacting photon. If the randomness of water is homogeneous, as one expects from the normal second law of thermodynamics, then the volume of the region generated with this reduced entropy δS will be proportional to the energy of the incident photon. Therefore if scattering is from the volume, then the brightness of these domains will be similar to that of the spectrum from the halogen lamp, as observed above.

However, it is probable that scattering comes from the surface for two reasons. Firstly because bulk water is transparent to the side illumination and appears black (e.g. Figure 3). If it scatters side illumination, then the water has changed in some way, for which there is no explanation, except perhaps CIGR. Secondly CIGR predicts there is a triple layer membrane around these domains which is impenetrable to photons, and therefore the scattering comes from the surface.

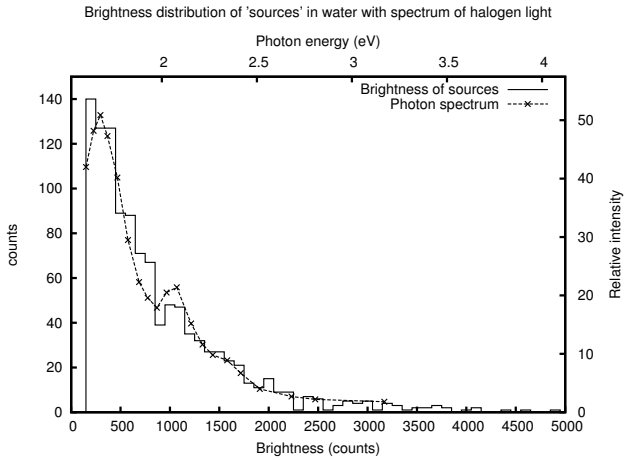

Fig. 6: Brightness distribution after exposure to halogen light for 37.5 hours, plus the spectrum of halogen light in eV. χ^2/DF of fit is 1.49.

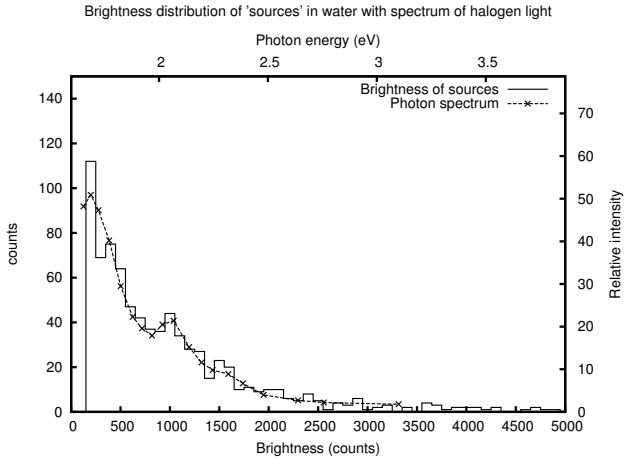

Fig. 7: Brightness distribution after 79.5 hours exposure to halogen light, with halogen spectrum. χ^2/DF of fit is 0.94.

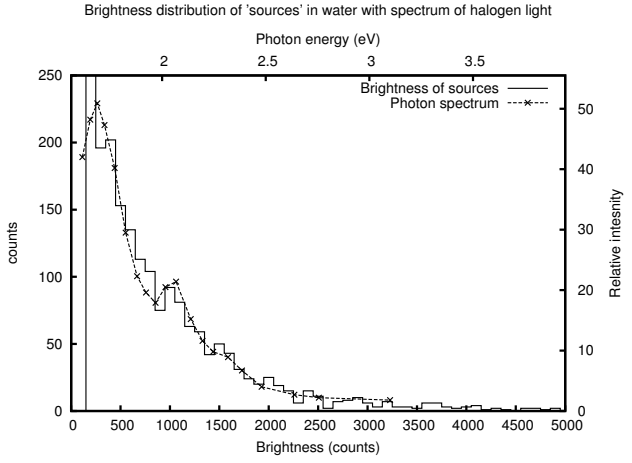

Fig. 8: Combined brightness distributions with halogen spectrum. χ^2 of fit is 1.67.

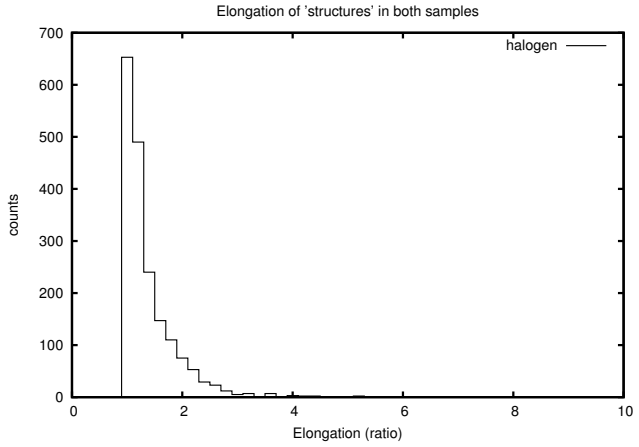

Fig. 9: Histogram of elongation (= major axis/minor axis) for both images.

We investigate the scattering as follows. In the absence of a complete unified theory of CIGR and Quantum Mechanics in water, we reason that these persistant domains probably have a stable shape, such as a spherical one or spheroidal one which is not too elongated. The source extraction software fits an ellipse to each "source" and calculates the major and minor axes, and their ratio, the "elongation", which is $\geqslant 1$. The distributions of the elongations for the two images, are very similar, so we have plotted them together in Figure 9. This is quite a narrow distribution: 74% have elongation less than 1.4. So most domains are only slightly elongated, as we expect for stable structures.

We now investigate the brightness distribution for different ranges of elongation El. Figure 10(a) shows the brightness distribution for elongation El < 1.2; 10(b) for the elongation in the range 1.2–1.4; and 10(c) for elongation El $\geqslant$ 1.4. We see that the more elongated domains tend to have higher brightness. We have shown above that brighter domains tend to be correlated with more energetic photons. Higher energy photons have higher momenta and will interact over longer distances in the water, and so reduce the entropy level in more elongated regions, as observed. This is evidence for this kinematic effect,

In Figure 10(a) (elongation < 1.2) only 5% of the total, have brightness greater than 1300 counts, whereas in 10(b) 20% have brightness greater than 1300, and in 10(c) 41% have brightness greater than 1300. So brighter domains are there in the data, but hardly any are detected in 10(a) with elongation < 1.2. Elongated domains must be in this sample, but with their longer axes pointing towards or away from the microscope, so that they do not appear elongated. If these hidden elongated domains were scattering and reflecting side illumination from their volume, then they would show up as brighter domains in 10(a). But they are not there in significant numbers, and so we conclude that they are scattering and/or reflecting the external light source from their surface, as predicted by CIGR.

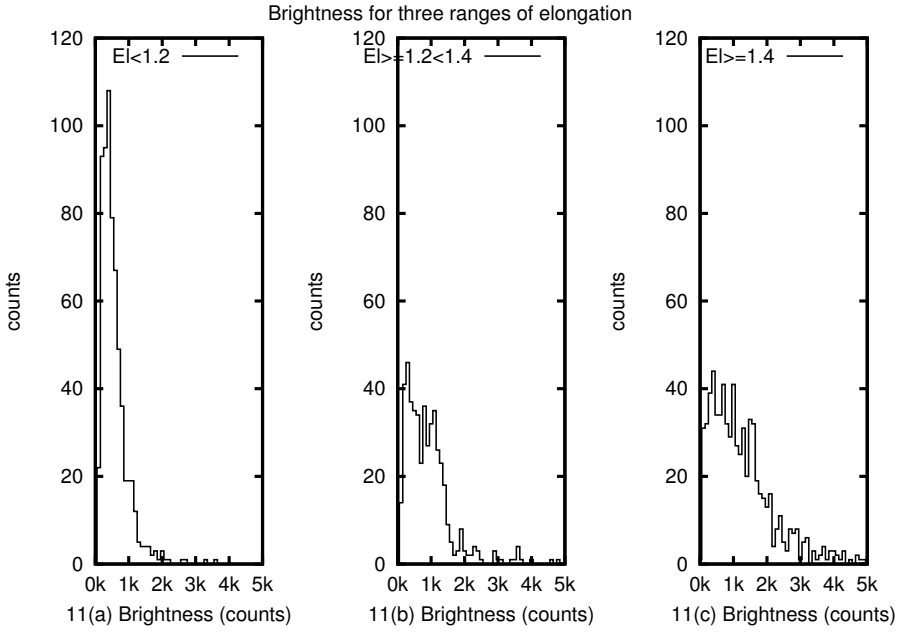

Fig. 10: Brightness distributions for elongation ratio: (a) less than 1.2; (b) in range 1.2-1.4; (c) greater than 1.4. Note the brighter domains are more elongated.

3 Conclusions

In the Brownian motion experiment, we observed reduced entropy levels which persisted, which could not be explained by the structure of water. More details are given in section 1.8: Conclusions for section 1.

We draw the following conclusions from the rheometer and microscope experiments:

1. Light shining on water increases the viscosity and this persists, which confirms the persistant reduction in entropy level previously observed in the exploratory Brownian motion experiment. However the spread in errors is much greater than that for water which has not been significantly exposed to visible light.

2. Measurements with a rheometer provide evidence that light from a halogen lamp produces two components in the water.

3. Water is transparent, so only a small fraction of the photons interact with it. Therefore, it is the small reductions in entropy produced (locally) by the interaction of individual photons (equation 3), which have to be detected,

4. Using a special microscope technique developed by Schweitzer, we have observed hidden domains in water previously exposed to halogen light (0.2 to 1.5 microns in size), which reflect or scatter side illumination, and which persist in time. These domains could be the second component observed in the rheometer experiment above.

5. The brightness distributions of these domains *match the energy spectrum of the halogen lamp well, suggesting that photons have caused these domains.* The brightness distributions are independent of the exposure times (c.f. Figures 6 and 7), as predicted by equation 3. We have previously shown that visible light lowers the entropy level of water. Furthermore, equation 3 predicts that these domains are low entropy regions created by individual photons interacting with the water, and the data confirms this. There are two samples, so this evidence for the Brittin and Gamow effect is reproducible.

6. These reduced entropy states persist for 20 and 27 days respectively, contrary to the normal second law of thermodynamics. The question is, what causes this persistence? Is it the structure of water, or some external agency such as mirror space-time? The most advanced theory of the structure of water at this time is coherent quantum electrodynamics (CQED), which predicts domains of about 100 nm determined by the internal energy levels of water. The domains observed in Figures 4 and 5 are $\times 2$ to $\times 15$ larger, and their brightness distributions shown in Figures 6 and 7, are determined by *the energies of the incident photons*, not the energy levels of water. Therefore they are a different phenomenon from that predicted by CQED. (The significance of this for CQED is discussed in Appendix B.) We therefore need a different theoretical explanation.

7. We conclude that this persistence is caused by some external agency. This could be the second time dimension in the mirror world of CIGR. If this is the case, then the domains will be surrounded by the triple layer membrane which we have predicted will scatter light.

8. We present evidence above that these domains scatter light from their surface (not their volume), which is evidence for the triple-layer membrane around them, predicted

by CIGR. These results are preliminary evidence for the second time dimension of mirror space-time, and the membrane predicted by CIGR.

9. Mirror space-time provides a physical mechanism for storing the negative entropy produced by the Brittin and Gamow effect, hence their persistence. Furthermore, these domains have an "inside" and an "outside" because they are surrounded by the membrane.

10. There is one problem with the above result. We have concluded that there is a second time dimension directed from the future to the past, without any direct evidence. For example, we have not sent a signal from the future to the past. However we have also concluded that the above phenomenon has an "inside" and an "outside", because of the membrane. Currently our instruments are located on the "outside" and therefore cannot make direct measurements on the "inside", where the second time dimension is predicted to exist. In the previous paper [3], we have shown that when phenomena occur outside normal 4-D space-time, then they may not be determined completely objectively by experiment. Nevertheless, *if they are reproducible, as above, then they should be considered physically real*. In addition to this, we present experimental evidence for a signal from the future to the past in a separate paper [28].

11. We have thus found evidence for a physical mechanism which reverses the second law of thermodynamics *and creates persistent ordered states*. Note that this occurs outside normal 4-D space-time, so that the second law continues to apply in 4-D space-time.

12. Together these results are evidence for the photo-mirror hypothesis. This effect depends upon Quantum Mechanics and CIGR and so is preliminary evidence for unification (see Appendix D).

3.1 Discussion

In the previous paper [3], we have used the photo-mirror hypothesis to explain the evidence for magnetic monopoles, which are observed only under intense illumination. The independent evidence above for the photo-mirror effect justifies this usage. There are however, two differences. The above results are due to single photons, whereas magnetic monopoles require intense illumination to reveal them. Furthermore, the above domains in water persist, whereas the monopoles disappear rapidly when the illumination is switched off. Both these could be due to the very strong interaction between monopoles. The theory needs to be worked out in more detail.

The chronometric invariant formalism of General Relativity, makes predictions about physically observable quantities which have been confirmed. However, General Relativity does not predict physically observable quantities. For example, it does not predict (as far as the author knows) Galileo's Principle (that objects with different masses have the same fall times) nor Newton's Law of Universal Gravitation. As a result there appear to be two theories of gravitation. Recently, however, the chronometric invariant formalism has been used to predict both Galileo's Principle and Newtom's Law [29]. So it is the more complete theory.

Furthermore, the evidence presented above for the second time dimension, is evidence for a 5th dimension, so space-time is 5-D (3,2). It is well-known that General Relativity is formulated in 4-D space-time. Therefore it seems to the author (an experimentalist) that the chronometric invariant formalism of General Relativity is actually a new theory, and so deserves its own name. The key point is that putting the Observer into General Relativity has changed the theory so much that the structure of space-time has changed. However this is not for the author to decide, and so for this current series of papers we will continue to refer to chronometric invairant General Relativity (CIGR). But a better name is desirable.

3.2 Predictions

In view of the above evidence for a unified phenomenon (the photo-mirror effect), we make the prediction that Quantum Mechanics can be unified with Chronometric Invariant General Relativity (CIGR), and the standard model embedded within it. The hidden sector of this hypothetical new unified theory would probably be based upon mirror space-time.

We have shown above that water detects individual photons interacting with it precisely, and that this can be explained by mirror space time. In effect the above techniques open a window into another world. We make the prediction that water is sensitive to other unusual phenomena occurring in mirror space-time. For example, it is possible that water can be used to detect some other new type of radiation which lowers entropy levels, if it exists [23].

Without mechanism(s) for the creation and storage of order, there can be no complexity [14]. So the above evidence for a mechanism for the creation of order, and a mechanism for its storage, is possibly the beginning of a theory of complexity, based on fundamental physics. The theory needs to be worked out in more detail.

The incorporation of the Observer into General Relativity (i.e. CIGR) requires a second time dimension, which automatically includes thermodynamics and complexity. Since these have been left out of many unified theories in the past, the unification of Quantum Mechanics with CIGR may well be the way to successful unification. The evidence for magnetic monopoles in mirror space-time [3], and for a new type of radiation in sunlight [23], support this conclusion.

4 Limitations

CIGR has not yet been properly unified with Quantum Mechanics yet, and so this may change some of its predictions, and clarify some of the details above.

Acknowledgements

We thank David Schweitzer for developing this microscope technique, for making measurements of samples we supplied, and providing the photo micrographs of same commercially. We also thank E. Bertin for making the astronomical source extraction software available via open source. We thank Brian Josephson for suggesting we do research into the physics of water as a detector. No Data is associated with this manuscript.

Appendix A: The "Memory of Water"

For completeness we mention the following. Some readers may think that the persistent effects observed above are due to the phenomenon known as the "memory of water". This may occur when a chemical substance is dissolved in water and then is serially diluted. However, there is no accepted explanation for this latter phenomenon, and so it is disputed. In the above experiments, photons are massless, and cannot be "dissolved" in water. Their interaction is purely dynamical. Nor was anything diluted — it is not even clear how one can dilute pure water. Therefore the above experiment of light shining on water, is investigating a completely different phenomenon from the "memory of water".

That being said, it is possible that mirror space-time may play a role in explaining the "memory of water". It is just that the structure of matter (e.g. the solute) is more complex than that of a photon, and its interaction with water also more complex. Therefore the phenomena of photons interacting with water reported in this paper, are different from the "memory of water".

Appendix B: Theories of Structure of Water

In the various experiments above, it is just photons in and photons out. So how can the decrease in entropy persist, if the water molecules move at random? This raises questions about the structure of water, so we consider theories of this. In 1891 Roentgen suggested that as ice melts, many of the less dense (ice floats) tetrahedral "ice molecules" persist intact in the liquid water as it warms. In this way, he tried to explain one of its more peculiar properties, namely that the density of water increases as its temperature is raised from 0° to a maximum at 4° C [30]. This approach was rejected by Bernal and Fowler for quantum mechanical reasons [31].

Another peculiarity of water is that in addition to the normal chemical bonds, water molecules also interact by the hydrogen bond, which is weaker and directional. Preparata states this is phenomenological in origin [32]. In 1950 Pople presented a quantum mechanical theory of the structure of water [33]. In 1951, Lennard-Jones and Pople showed that there may be a network of hydrogen bonds linking all the molecules together into one large molecule $(H_2O)_n$ [34]. The problem is that the water molecules move around and the hydrogen bonds, which are highly directional, make or break after a few picoseconds [35]. As the bonds make or break fluctuating EM fields are produced, and there is also the Earth's magnetic field, both of which Quantum Mechanics ignores, but quantum electrodynamics (QED) does not.

Preparata and del Giudice have solved the equations of QED for bulk matter and applied it to liquids, solids and water in particular [36]. This theory *replaces* the static picture of chemical bonds linking individual molecules together ("electrostatic meccano" or "erector set"), *with a dynamical interaction between groups of molecules spread over larger distances.* This theory, often referred to a coherent QED or CQED, is a new theory of condensed matter. Their approach is to consider water not to be "molten ice" but "condensed vapour" [37]. When this theory is applied to water, they find that the water molecules form two groups: coherent domains in which the molecules oscillate between the ground state and an excited state, and interstitial water which is random and surrounds these domains.

They predict that the excited state is at 12.07 eV (in the UV region), which produces domains of about 100 nm in extent, and that the radiation is trapped in these domains [38]. Enz agrees that the coherent domains probably exist, but questions whether their boundaries are precisely defined, so the radiation may not be completely trapped [39]. Whilst this theory explains a number of indirect experimental results, there has not been any direct experimental confirmation of these domains in water, nor has any UV radiation been detected leaking out. Therefore this theory has not been proven strictly to be correct.

Furthermore, the results of the experiments above, do not provide any direct evidence to support this theory. For example, Figure 3 does not show any sign of the predicted 100 nm domains in the control sample of distilled water (condensed from vapour). But the microscope experiment was not designed to detect these and so the resolution may not have been good enough. Instead, the domains observed in Figures 4 and 5 are $\times 2$ to $\times 15$ times larger. Furthermore *their size distribution is determined by the energies of the incident photons, not by the internal energy levels of water.* So the phenomena observed are completely different from those predicted by CQED. But this does not necessarily rule out CQED.

CQED predicts coherent domains surrounded by interstitial water which is random. If an incident photon, with an energy of 1 to 3 eV, interacts with a coherent domain of $\approx 10^7$ water molecules oscillating between the ground state and 12.07 eV, then it might be scattered away with little effect on the entropy of that 100 nm domain. However, if it interacts with the interstitial water, then it could lower the entropy level by the Brittin and Gamow effect. *But that reduction would not persist because the interstitial water is random. So even if this is the correct theory of water, then mirror space-time of CIGR is required to explain the observed results.*

Whilst these results do not prove CQED wrong, it does not provide any support for it. Furthermore CQED is clearly

incomplete because it does not include the mirror space-time of CIGR. In fact it is likely that the correct theory of water will be based upon Quantum Mechanics unified with CIGR.

Appendix C: Details of Microscope Technique

The microscope technique used to take the black and white images shown above, was developed by David Schweitzer. The technique requires a good quality high-powered microscope (e.g. a Nikon optifot), with a phase contrast lens and dark filter, a light source, fluorescence adaptor, video camera with CCD image sensor, computer with video card, software and printer. The technique involves first examining the sample with normal illumination to see if it contains any bacteria, dust particles or other impurities. If the sample is clear, as expected for distilled water, then a drop of the water is placed onto a microscope slide and allowed to evaporate at ambient temperature. (If the rate of evaporation is too slow, a gentle source of heat may be applied.) Whilst it is evaporating, it is illuminated horizontally from the side (we call this "side illumination"), the temperature of the light source is adjusted (a reddish white light was used), and it is observed vertically from above. (NB This is not the same as dark-field microscopy.) Schweitzer has found that if there are hidden "structures" present in the water, then these reflect light and become visible when the thickness of the water film has decreased to about 0.1 mm (possibly because of distortion), and the illumination, magnification and other settings are correct. The images shown above, were taken with the solarizing filter phase contrast 4, the Table tilted by 1.95° and microscope magnification of ×1000.

The random walk (Brownian motion) experiment at the beginning of this paper and the black and white images were all obtained using distilled water and exposure was to a 500 watt halogen lamp at 80 cms, which gave 1100 lux at the surface of the water. The viscosity measurements were made with HPLC grade water and a 400 watt halogen lamp (equivalent to 500 watts) also at 80 cms. The software used for the pattern recognition and source extraction was SExtractor version 2.25.0 by E. Bertin.

Appendix D: Unification

"Unification" is a project in physics which dates back to Einstein, who was convinced there is one set of equations which describe the whole Universe. So he spent the last 30 years of his life trying to unify the two main theories of physics, Quantum Mechanics and General Relativity, in order to develop the final theory. However the process of unification dates from before Einstein. For example before Newton's theory of gravity, it was thought that the laws of motion of a projectile through the air above the Earth's surface, were different from those of planets in the heavens. Newton's theory provided a unified explanation of terrestrial and celestial gravitation. (Note that the derivation of Newton's theory from CIGR, mentioned above, links CIGR to this first step towards unification.) Then before Maxwell, electricity and magnetism were thought to be completely different phenomena. Maxwell's equations unified the two into electromagnetism. After Einstein in the 1960s, electromagnetism was unified with the weak nuclear interaction (which causes beta-decay) in the electro-weak interaction, which led to the discovery of the W- and Z-bosons.

However, the unification of General Relativity and Quantum Mechanics has stalled, despite herculean efforts (e.g. quantum gravity; string theory; loop quantum gravity, and so on) [40]. In a sense the problem is simple. Quantum mechanics is a "digital" theory of ultra-small phenomena, whilst General Relativity is an analogue theory of large scale phenomena. About the only place where the two might come together is at the event horizon of a black hole, which cannot be easily studied in the laboratory. However, putting the Observer into General Relativity introduces low energy, small scale phenomena, such as thermodynamics, where CIGR and Quantum Mechanics can come together. The above evidence for the photo-mirror effect is highly significant, because it depends upon Quantum Mechanics and CIGR, and so is experimental evidence for unification.

Submitted on November 28, 2024

References

1. Zelmanov A.L. Chronometric invariants and the accompanying frames of reference in the General Theory of Relativity. *Soviet Physics Doklady*, 1956, v. 1, 227–230.
2. Borissova L. and Rabounski D. Fields, Vacuum, and the Mirror Universe. The 3rd revised edition, New Scientific Frontiers, London, 2023 (the 1st ed. published in 2001), Chapters 1 and 6.
3. Ellis R.J. Evidence for Phenomena, including Magnetic Monopoles, Beyond 4-D Space-Time, and Theory Thereof. doi:10.5281/zenodo.7344117; arXiv: 2207.04916.
4. Gell-Mann M. Some lessons from sixty years of theorising. *Int. J. Mod. Phys. A*, 2010, v. 25 (20), 3857–3861.
5. Pippard A.B. Elements of Chemical Thermodynamics for Advanced Students of Physics. Cambridge University Press, 1960, p. 100.
6. Eddington A.S. The Nature of the Physical World. Cambridge University Press, 1928.
7. Carnot S. Réflexions sur la puissance motrice du feu et sur les machines propres à développer cette puissance (Reflections on the Motive Power of Fire and on Machines Fitted to Develop that Power), Bachelier, Paris, 1824.
8. Clausius R. *Annalen der Physik und Chemie*, 1854, v.93 (12), 481–506.
9. Capek V. and Sheenan D. On Challenges to the Second Law of Thermodynamics: Theory and Experiment. Springer, Berlin/Heidelberg, 2005; Special Issue: Quantum Limits to the Second Law of Thermodynamics, *Entropy*, March 2004, v. 6 (1), 1–232; First Int. Conf. on Quantum Limits to the Second Law, *AIP Conf. Proc.*, 2002, v. 643 (1), 3–500; Second law of Thermodynamics: Status and Challenges, *AIP Conf. Proc.*, v. 1411 (1), 1–356.
10. Boltzmann L. *Wissenschaftliche Abhandlungen*, v. I, II and III, Barth, Leipzig, 1909; reissued, Chelsea, New York, 1969; Flamm D. Ludwig Boltzmann — A Pioneer of Modern Physics. arxiv: physics/9710007; Transl. of L. Boltzmann's paper "On the Relationship between the Second Fundamental Theorem of the Mechanical Theory of Heat and

Probability Calculations Regarding the Conditions for Thermal Equilibrium", *Sitzungber. Kais. Akad. Wiss. Wien Math. Naturwiss. Classe*, 1877, v. 76, 373–435, by K. Sharp and F. Matschinsky, *Entropy*, 2015, v. 17 (4), 1971–3009.

11. Schrödinger E. What is Life? Cambridge University Press, 1944.
12. Prigogine I. *Bull. Acad. Roy. Belg. Cl. Sci.*, 1945, v. 31, 600; see also Nicolis G. and Prigogine I. Self-Organization in Nonequilibrium Systems. John Wiley and Sons, New York, 1977.
13. Brittin W. and Gamow G. Negative entropy and photosynthesis. *Proc. of the Nat. Acad. of Sciences*, 1961, v. 47, 724. N.B. There is a sign error in equation (14) in this reference, which has been corrected.
14. Gell-Mann M. What is complexity? *Complexity*, 1995, v. 1 (1), 16–19.
15. Einstein A. *Annalen der Physik*, 1906, v. 19, 289.
16. Ming Chen Wang and Uhlenbeck G.E. *Rev. Mod. Phys.*, 1945, v. 17, 323–342.
17. Careri G. Order and Disorder in Matter. Benjamin/Cummings, CA, 1984, Chapter 1, Box 1.E.
18. Landau L.D. and Lifshitz E.M. The Classical Theory of Fields. The 4th final edition, Butterworth-Heinemann, 1980.
19. Zelmanov A.L. Chronometric invariants and the accompanying frames of reference in the General Theory of Relativity. *Soviet Physics Doklady*, 1956, v. 1, 227–230; Zelmanov A.L. On the relativistic theory of an anisotropic in-homogeneous Universe. *Proc. of 6th Soviet Conf. on the Problems of Cosmogony*, Nauka, Moscow, 1959, 144–174 (in Russian), see English transl. in *The Abraham Zelmanov Journal*, 2008, v. 1, 33–63.
20. Zelmanov A.L. Chronometric Invariants. English transl. of the 1944 Dissertation, Am. Res. Press, Rehoboth, 2006.
21. Borissova L. and Smarandache F. Positive, neutral and negative mass-charges in General Relativity. *Progress in Physics*, 2006, v. 2 (3), 51–54.
22. Rabounski D. and Borissova D. Physical observables in General Relativity and the Zelmanov chronometric invariants. *Progress in Physics*, 2023, v. 19 (1), 3–29.
23. Ellis R.J. Preliminary evidence for a new type of radiation in sunlight. doi:10.5281/zenodo.7347703.
24. Maxwell T. National Physical Laboratory, Teddington, UK.
25. David Schweitzer, private researcher, London, UK.
26. Ishamir L. and Johnston K. recommended SExtractor by E. Bertin, and AstroimageJ.
27. http://www.mtholyoke.edu/m̃peterso/classes/–phys301/projects2001/awgachor/awgachor.htm
28. Ellis R.J. A new approach to unification: the living universe hypothesis. doi:10.5281/zenodo.11478276.
29. Borissova L. and Rabounski D. Galileo's Principle and the origin of gravitation according to General Relativity. *Progress in Physics*, 2024, v. 20 (2), 69–78.
30. Roentgen W.C. Ice and water molecules. *Wied. Ann.*, 1891, v. 45, 91.
31. Bernal J.D. and Fowler R.H. *J. Chem. Phys.*, 1933, v. 1, 515.
32. Preparata G. QED Coherence in Matter. World Scientific, Singapore, 1995, p. 196.
33. Pople J.A. A theory of the structure of water. *Proc. Roy. Soc.* (*London*), 1950, v. A202, 323; ibid. 1951, v. A205, 163; *J. Chem. Phys.*, 1953, v. 21, 2234.
34. Lennard-Jones J. and Pople J.A. Molecular association in liquids. *Proc. Roy. Soc.* (*London*), 1951, v. A205, 155.
35. Bertolini D. et al. *J. Chem. Phys.*, 1989, v. 91, 1179–1190; Fernandez-Serra M.V. and Artacho E. arxiv.org: cond-mat/05073193.
36. Preparata G. QED Coherence in Matter. World Scientific, Singapore, 1995, see Chapter 10.
37. Bono I., Del Giudice E., Gamberale L., and Henry M. Emergence of the coherent structure of liquid water. *Water*, 2012, v. 4, 510–532.
38. Arani R., Bono I., Del Giudice E., and Preparata G. QED coherence and the thermodynamics of water. *Int. J. Mod. Phys. B*, 1995, v. 9, 1813–1841.
39. Enz C.P. *Helv. Phys. Acta*, 1997, v. 70, 141.
40. Smolin L. The Trouble with Physics: The Rise of String Theory, the Fall of a Science, and What Comes Next. Houghton Mifflin, Boston, N.Y., 2006.

Progress in Physics is an American scientifc journal on advanced studies in physics, registered with the Library of Congress (DC, USA): ISSN 1555-5534 (print version) and ISSN 1555-5615 (online version). The journal is peer reviewed.

Electronic version of this journal: http://progress-in-physics.com